PALAEOBIOLOGY OF SILURIAN TRILOBITES FROM NORTH GREENLAND

by

HELEN ELIZABETH HUGHES

A thesis submitted to
The University of Birmingham
for the degree of
DOCTOR OF PHILOSOPHY

School of Geography, Earth and Envrionmental Sciences
The University of Birmingham
November 2010

ABSTRACT

The Telychian (Llandovery, Silurian) reefs of North Greenland yield extensive collections of diverse and remarkably well preserved trilobites. The collections comprise 36 named trilobite species (32 new), and 30 under open nomenclature. These are assigned to 32 genera (six new). Members of the Scutelluidae (10 new species, four new genera), Illaenidae (one new species), Proetidae (10 new species, two new genera), Aulacopleuridae, Scharyiidae (three new species), Brachymetopidae, Harpetidae, Cheiruridae (three new species), Encrinuridae (two new species), Calymenidae, Phacopidae, Lichidae (two new species), and Odontopleuridae (one new species) are represented. Aspects of phylogenetic relationships within the Scutelluidae and Illaenidae are problematical because of the high number of effaced taxa. Selected effaced genera are analysed using cladistics, confirming the polyphyletic nature of effacement. Counts of trilobite sclerites from thirteen reef localities are analysed using cluster and correspondence analyses to identify trilobite associations, and taphonomic signatures. Seven trilobite associations are identified: Scutelluid-Illaenimorph; Scutelluid; Scutelluid-Cheirurid; Scutelluid-Harpetid; Proetid; Encrinurid; Illaenimorph. These can be encompassed within the previously defined Illaenid-Cheirurid ‘Community’. Trilobites are predominantly associated with a cement-rich microbial lithofacies deposited between storm- and fair-weather wave base. The variable distribution of taxa within the reefs is partly a reflection of intense hydrodynamic sorting in reef environments.

ACKNOWLEDGEMENTS

Firstly, I would like to thank my supervisors Alan Thomas and Phil Lane. Having collected so much wonderful material from North Greenland, they trusted this to me at risk of hammer and drill. I have been provided with all the advice, support, discussion and patience that I could ask for. Dr R.M. Owens is thanked for examining the thesis. This work was funded by a NERC PhD studentship (Grant No: NER/S/A/2006/14052). Additionally, SYNTHESYS funding (DK-TAF-4376 and DK-TAF-312) enabled two trips to examine further collections of trilobites in Copenhagen, and the Philip Scanlan Award enabled conference attendance in Spain.

I thank Drs R.M. Owens, D.J. Siveter, and D.J. Holloway for their comments on the proetaceans, Calymenidae and Scutelluidae respectively. Sten Lennart Jakobsen photographed the *Periostrix* pygidia originally figured by Teichert. Phil Jardine, Drs I. Sansom and J. Wheeley provided comments and advice on Chapter 4.

Thanks are given to Aruna Mistry, Paul Hands, Richard Greswell and Jon Clatworthy. They have helped me not only with all manner of practicalities along the way, but have always been friendly faces. To those of the dinobird office, particularly to Andy S, Andy R, Leyla and Sarah. Of course to Lil , who took me in and nutured me with coffee and friendship, and to Rob, who shared in this whilst adding some cider along the way. To Don Mikulic and John the Quarry man who showed me the little critters of North America, and to all at Copenhagen, particularly to Maria and to Christian, who kindly shared his knowledge of the Peel Collection.

Special thanks are given to Mum and Dad, Pete, Ali and the Stonefold massif, Karen, Jim, Jake and Lara (what will Auntie Helen be a doctor of, is it just trilobites?). And finally to Paul, who is always there to remind me that I am

‘living the dream’.

‘Censure would be his due who should be perpetually heaping up of natural collections, without design of building a structure of philosophy out of them, or advancing some propositions that might turn to the benefit and advantage of the world. This is in reality the true and only proper end of collections, of observations, and natural history.’

John Woodward, 1729.

TABLE OF CONTENTS

LIST OF FIGURES

LIST OF PLATES

LIST OF TABLES

CHAPTER ONE

INTRODUCTION

THE Telychian (Llandovery, Silurian) reefs of North Greenland are unusually well preserved and exposed, and provide valuable insights into palaeobiological and sedimentological processes during the early Silurian. Reconnaissance geological mapping of North Greenland in the 1970s and 1980s resulted in extensive collections of palaeontological samples from the reefs (Text-fig. 1.1A). This material includes thousands of remarkably well preserved trilobites, organisms which were both abundant and diverse in the reef environments. The study of Silurian trilobites has progressed greatly over the last four decades (see Chapter 2, Section 2.1.1 for a history of study). Silurian trilobite faunas from North Greenland have previously been little studied however, largely because of the remote location of the area. Trilobites comprised key components of many early Palaeozoic ecosystems, including the Greenland reefs. Given the diverse range of trilobite morphology, they are excellent subjects for phylogenetic studies and understanding invertebrate evolution. Their relatively rapid post-mortem disarticulation makes them ideal for taphonomic studies also. Additionally, the collections provide an opportunity to study the reef lithofacies, aiding palaeoenvironmental interpretation.

Detailed taxonomic accounts of the trilobite faunas are presented in Chapter 2, where representatives of the Scutelluidae, Illaenidae, Proetidae, Aulacopleuridae, Brachymetopidae, Harpetidae, Cheururidae, Encrinuridae, Calymenidae, Phacopidae, Lichidae, and Odontopleuridae are described. Of these families, the relationships between some genera of the Scutelluidae and Illaenidae are particularly problematical

due to a condition termed effacement, which results in the reduced distinctiveness or loss of the furrows characteristic of the trilobite exoskeleton. Effaced members of the Scutelluidae and Illaenidae are analysed using cladistics for the first time in Chapter 3, where the polyphyletic nature of effacement is confirmed. Chapter 4 incorprates lithofacies analysis and the identification of taphonomic attributes of the trilobite fauna, to provide a palaeoenvironmental context to the reefs of North Greenland. The principal conclusions resulting from this study are presented in Chapter 5.

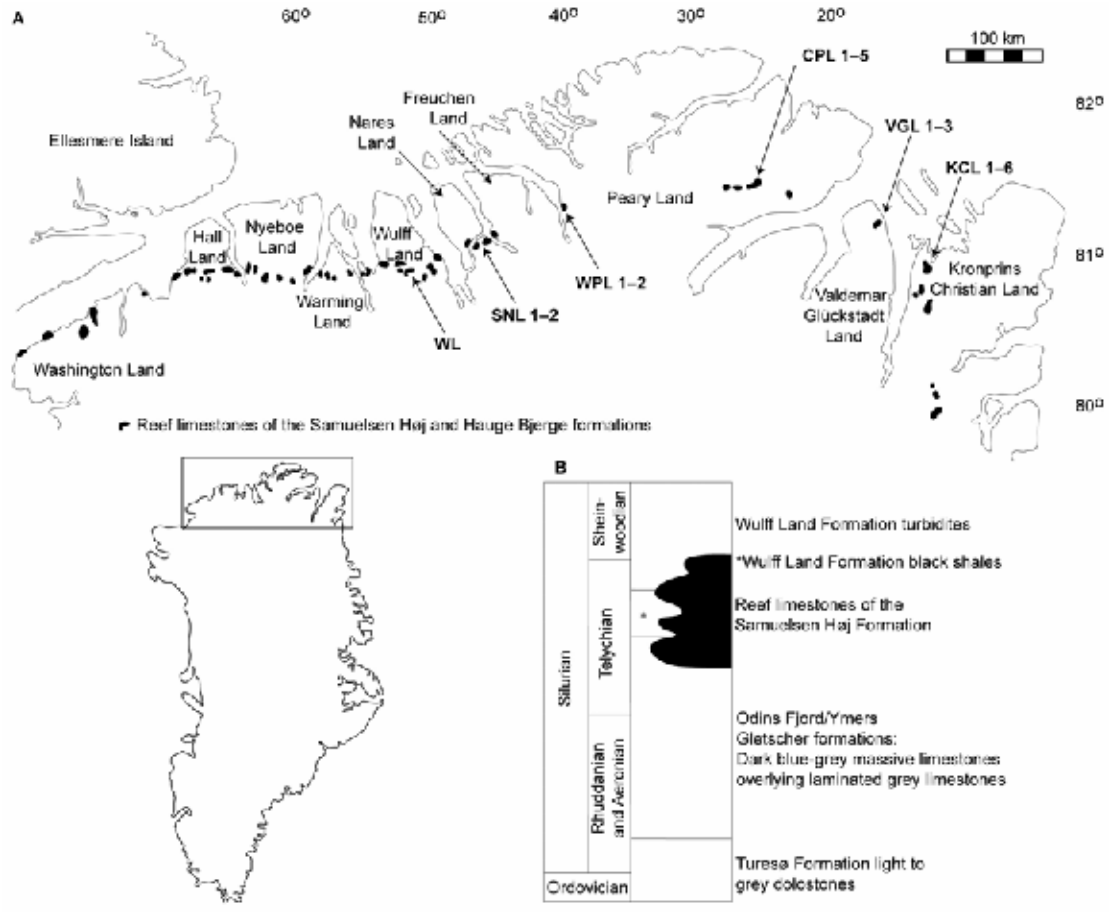

Text-fig. 1.1A. Map of North Greenland showing distribution of Silurian reefs (in black), adapted from Sønderholm and Harland (1989). Sample localities are indicated. **B.** Summary stratigraphy of central Peary Land showing the relationship of Telychian reefs to other stratigraphical units. Trilobites occur in the Samuelsen Høj and Odins Fjord formations and their time equivalents. For details of stratigraphical nomenclature see Hurst (1984), Sønderholm *et al*., (1987) and Peel and Sønderholm (1991).

1.1 STRATIGRAPHY AND GEOLOGICAL SETTING

North Greenland exposes a thick, east-west striking succession of Mesoproterozoic to Tertiary rocks. The Lower Palaeozoic strata exposed across North Greenland represent the sedimentary fill of the Franklinian Basin, which extends ~2000 km from the Canadian Arctic Islands to eastern North Greenland (Peel and Sonderhølm 1991). The Franklinian Basin formed part of the Laurentian passive margin of the Iapetus Ocean, and it is now widely agreed that Laurentia occupied an equatorial position throughout the early Palaeozoic, being largely contained between 30^{o} North and 30^{o} South (Scotese and McKerrow 1990; Torsvik *et al*. 1996; Harper *et al*. 1996; MacNiocaill *et al*. 1997; Cocks and Torsvik 2002; Fortey and Cocks 2003). This is indicated by both palaeomagnetic and zoogeographic data (Smith and Rasmussen 2008). A world palaeogeography for the early Silurian is shown in Text-fig. 1.2.

During the Ordovician and Lower Silurian, carbonate platform sedimentation dominated the Franklinian Basin. Different lithostratigraphical names are given to units of similar lithofacies and ages occurring across North Greenland. The summary which follows uses the terminology of Hurst (1984) which is applied to strata between Kronprins Christian Land and central Peary Land (Eastern North Greenland). The lower Llandovery comprises variable grey and dark grey limestones and dolostones, displaying varying degrees of silicification belonging to the Turesø, Ymers Gletscher and Odins Fjord formations. These pass upwards into Telychian argillaceous limestones and black shales of the Wulff Land Formation. Reefs are associated with these strata (Text-fig. 1.1B). The reefs are thought to have been initiated due to relative sea level rise (Hurst 1980), by means of either eustatic or continental transgression, shelf and basin subsidence related to synsedimentary faulting, or both.

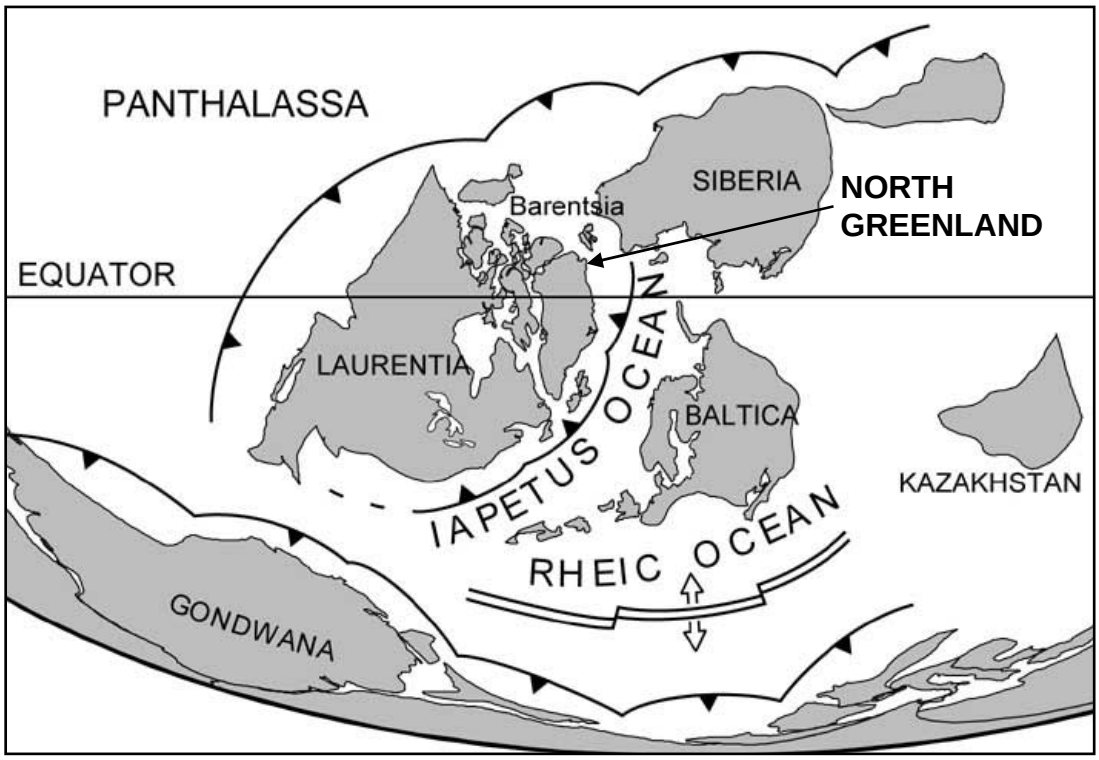

Text-fig. 1.2. World palaeogeography for the early Silurian (440 Ma), adapted from Scotese (2002).

The reefs form a roughly west-east trending belt (Text-fig. 1.1A). Dawes (1971, 1976) first reported the reefs to cover a distance of ~300 km, from Washington Land in the west to the Victoria Fjord region in the east. However, reefs are now known to extend across the whole of North Greenland (850 km), from Washington Land in the west to Kronprins Christian Land in the east (Sønderholm and Harland 1989). The most southerly located reef in this belt was recognised in 1994–1995, in the south of Kronprins Christian Land (Smith *et al*. 2004). Reefs are variable in size; Lane and Thomas (1979) recorded a maximum thickness of 300m, which, due to the onlapping nature of the overlying graptolitic shales and surrounding turbidites, is interpreted as original relief.

The reefs are represented by the Samuelsen Høj Formation in Kronprins Christian Land, Valdemar Glückstadt Land, and central Peary Land, and by the Hauge

Bjerge Formation in western Peary Land, south Nares Land, and Wulff Land. Thin sections were made from samples from all localities, and there are no significant differences in the reef lithofacies, other than a slightly greater amount of dolomite in those of the Hauge Bjerge Formation. These formations have been little studied with respect to their sedimentology and petrography. Mayr (1976) originally described two of the Peary Land reefs, followed by Christie and Peel (1977), Lane and Thomas (1979) and Mabillard (1980). Lane and Thomas (1979) described the dominant reef lithofacies as white to light grey crinoidal and stromatoporoidal bioclastic limestone. Bedding was described as massive in the core rocks and highly variable in the outer parts, and depositional dips were found to radiate outwards from the reef cores. The dominant fossil groups recorded were stromatoporoids and crinoid fragments, with pockets of other fossils including brachiopods, rugose corals, tabulate corals, trilobites, gastropods, cephalopods, rostroconchs and bivalves.

Field notebooks from Christie's 1974 expedition to Børglum Elv, Peary Land, describe the Samuelsen Høj Formation as a mixture of algal-coral limestones which were originally cavernous, and subsequently in-filled with crystalline carbonate and bioclastic material. Fossils, although distributed throughout, were particularly rich in these pockets, and most trilobites occur in such concentrations. Christie also described algal, coral and crinoid debris banks sloping off the reefs, dipping away from the centre of the reef with dips of up to 40^{o}, creating a domal form. These grainstone facies also yield trilobite faunas, although less concentrated than in the core rocks.

Hurst (1980) produced a preliminary account of the Silurian carbonate shelf across North Greenland. Later (Hurst 1984) he concentrated on the Samuelsen Høj Formation, providing a brief description and interpretation of the reef lithofacies which constituted thickly bedded to massive, very light grey to white limestone,

comprising three main lithofacies; lime mudstones with irregular large cavities, approaching a stromatactis form; incipient boundstones, comprising bryozoans and encrusting blue-green algae; and bioclastic floatstone (predominately comprising tabular and bulbous stromatoporoids) and rudstone (dominated by crinoids). These were interpreted as being deposited in fairly high-energy environments well within the euphotic zone. Fibrous calcite infills to cavities were interpreted as being suggestive of early submarine lithification.

Foundering of the platform from late Llandovery times onwards was due to loading by thrust sheets, and the platform carbonate deposition was replaced by turbidite deposition (Hurst and Surlyk 1982; Higgins *et al.* 1991; Smith and Rasmussen 2008) resulting in the termination of the reefs and so, at their stratigraphically highest points, reefs of the Samuelsen Høj Formation are surrounded by sand-rich turbidite deposits (Dawes 1976).

All material was collected from the Samuelsen Høj/Hauge Bjerge formations, except for that from Wulff Land which was collected from contemporaneous strata between reefs (the Djævlekløften Fomation, the time equivalent of the Odins Fjord Formation).

1.2 AGE OF THE FAUNAS

The accurate dating of the reef limestones is hampered by a lack of conodonts in their lithofacies. However, in eastern North Greenland, condonts have been collected from the Odins Fjord Formation which belong to the *celloni* Biozone (Aldridge 1979), and Armstrong (1990) recoded *celloni* as the youngest fauna from the reefs. The *celloni* Biozone lies within the upper but not uppermost Telychian, and is equivalent to the

lower *spiralis* Biozone (Ogg *et al*. 2008). All material here is considered Telychian in age.

1.3 LOCALITY INFORMATION

Bulk rock samples are distinguished by their 'GGU' numbers which directly relate to the collection localities. GGU samples from the same reef localities were grouped together and given an abbreviated locality, and a number to distinguish between reefs, e.g. WPL1 denotes western Peary Land, reef 1. Details of the GGU numbers concerned are given below, and collection localities shown in Text-fig. 1.1A.

Reef limestones from western Peary Land (WPL2), central Peary Land, Kronprins Christian Land and Valdemar Glückstadt Land are housed at the Lapworth Museum, University of Birmingham, with particularly well preserved specimens bearing 'BIRUG' numbers. Further collections from western Peary Land (WPL1), Wulff Land, and south Nares Land comprise the Peel Collection, and are housed in the Geological Museum, Natural History Museum of Denmark, Copenhagen. All type and figured specimen numbers are prefixed with 'MGUH', and are housed in the Geological Museum, Natural History Museum of Denmark, Copenhagen.

Wulff Land

WL. GGU 298504–298506. Collected by JSP (Dr J. S. Peel), 1985, from the inter-reef Djævlekløften Formation. GGU map sheet 81V3.

South Nares Land

SNL1. GGU 298930. Collected by JSP, 1985. 'East of Peel Camp 6 from sides of main mound'.

SNL2. GGU 298924. Collected by JSP, 1985. ‘Downslope main valley of Peel Camp 6’.

Western Peary Land

WPL1. GGU 301314, 301318–9, 301323–6. Collected by JSP, 1985. ‘South east side of JP Koch Fjord’.

WPL2. GGU 198833–6, 198838, 198842–6. Collected by JMH (Dr J. M. Hurst), 1978. ‘JP Koch Fjord’.

Central Peary Land

CPL1. GGU 198115–6, 198226. Collected by ATT (Dr A. T. Thomas) and PDL (Dr P. D. Lane), 1978. GGU map reference 27Y UM 7573.

CPL2. GGU 198135–198223. Collected by ATT and PDL, 1978. GGU map reference 27Y UM 7572. GGU 274645. Collected PDL, 1980. ‘Main mound, slope of hill at southern extremity of southeast limb.

CPL3. 198225. Collected by ATT, 1978. GGU map reference 27Y UM 804 679.

CPL4. GGU 274654. Collected by PDL, 1980. ‘Loose material from ‘Mab’s mound’’.

CPL5. GGU 274689. Collected by HAA (Dr H. A. Armstrong) and PDL, 1980. ‘*In-situ* and loose material from ‘sigmoid mound’’.

Valdemar Glükstadt Land

VGL1. GGU 275038. Collected by PDL and JSP, 1980. ‘*In-situ* and loose material from near Lane/Peel Camp 14’.

VGL2. GGU 275044. Collected by PDL, 1980. ‘*In-situ* material from 10 km south of Lane/Peel Camp 14’.

VGL3. GGU 275049. Collected by PDL and JSP, 1980. '*In-situ* and loose material from 3 km west of Lane/Peel Camp 14'.

Kronprins Christian Land

KCL1. GGU 275015. Collected by HAA and JSP, 1980. 'Reef rock near Peel/Armstrong Camp 11'.

KCL2. GGU 225793. Collected by JSP, 1979.

KCL3. GGU 275021. Collected by TW, 1980. 'Mound collection near Peel/Armstrong Camp 11'.

KCL4. GGU 274996. Collected by PDL and JSP, 1980. 'Vertical reef, 1 km southeast of Lane/Peel Camp 8'.

KCL5. GGU 274774. Collected by PDL, 1980. 'Large mound mass 1 km west of Lane/Peel camp12'.

KCL6. GGU 274788. Collected by PDL, 1980. '1 km north of Lane/Peel Camp 8'.

1.4 AIMS AND OBJECTIVES

The overall aim of this project is to provide a detailed palaeobiological and palaeoenvironmental account of existing collections of trilobites and their associated lithofacies, from the Silurian reefs of North Greenland. The more specific objectives are as follows:

1) To provide taxonomic descriptions of new trilobite taxa to assess the diversity of trilobites within the reefs.
2) To apply cladistic methods in order to investigate the phylogenetic relationships of effaced taxa belonging to the families Scutelluidae and Illaenidae.

3) To use multivariate analyses to identify trilobite associations and taphonomic signatures.
4) To analyse the associated lithofacies to aid understanding of the palaeoenvironmental context.

CHAPTER TWO

TRILOBITES FROM THE SILURIAN REEFS OF NORTH GREENLAND

Summary: Varied and well preserved trilobite faunas are described from the Telychian (Llandovery, Silurian) reefs of North Greenland. The faunas, collected between Kronprins Christian Land in the east and Wulff Land some 600 km further west, comprise 36 named species (32 new), and 30 under open nomenclature. These are assigned to 32 genera (six new). Members of the Scutelluidae (10 new species, four new genera), Illaenidae (one new species), Proetidae (10 new species, two new genera), Aulacopleuridae, Scharyiidae (three new species), Brachymetopidae, Harpetidae, Cheiruridae (three new species), Encrinuridae (two new species), Calymenidae, Phacopidae, Lichidae (two new species), and Odontopleuridae (one new species) are represented. The large number of new taxa reflects the lack of sampling of Silurian reef trilobite biotas. In the north Greenland reefs, trilobites occur predominantly in a cement-rich microbial lithofacies deposited between storm- and fair-weather wave base, the fossils being concentrated in cavities and depressions on the reef surface. Several associations are recognised, which can be encompassed within the previously defined and long-ranging Illaenid-Cheirurid ‘Community’: the fauna have particularly close affinities with other Telychian Laurentian faunas described from similar environments. Species are not evenly distributed across the reef belt however, and this smaller-scale variation is likely age-related, possibly reflecting the gradual foundering of the carbonate platform from east to west.

2.1 INTRODUCTION

FOR many years, Silurian trilobites were less intensively studied than those from other Palaeozoic systems. There are notable 19th Century contributions to the field, notably the works of Murchison's *Silurian System* (1839) and his revised studies (1854, 1859, 1867, 1872), Barrande (1846a, 1846b; 1850, 1852, 1868, 1872), Hawle and Corda (1847), Salter (1848, 1849, 1853, 1857, 1864a, 1864b–1883, 1868), and Hall (e.g. 1852, 1863, 1864a, 1846b, 1867, 1870, 1879) who was the first to consider the Silurian reef faunas of the Great Lakes region in the USA. Later, Weller (1907) further addressed the trilobite faunas of the Chicago area. Over the last 40 years there have been additional major studies focussed on faunas from Canada (mid- and north Laurentia; e.g. Perry and Chatterton 1977, Norford 1994, Adrain and Edgecombe 1997, Chatterton and Perry 1983, 1984, Adrain 2003, Chatterton and Ludvigsen 2004, Adrain and Tetreault 2005), the USA (mid-Laurentia; e.g. Campbell 1967, Whittington and Campbell 1967, Holloway 1980), Britain (Avalonia; e.g. Thomas 1978, 1981, Howells 1982, Curtis and Lane 1997, 1998) and Australia (North Gondwana; e.g. Chatterton 1971, Chatterton and Campbell 1980, Holloway 1994, Holloway and Lane 1998, Edgecombe and Sherwin 2001, Sandford and Holloway 2006) have begun to shed light on the evolutionary and palaeoenvironmental relationships of Silurian trilobites and of their distribution in time and space.

The faunas described here are from the Telychian reefs of North Greenland (Text-fig. 1.1) and were collected during the North Greenland reconnaissance geological mapping programme of the Geological Survey of Greenland (at the time GGU, now merged with DGU to form GEUS) in the 1970s and 1980s. Palaeontological samples were taken from when and where was practicable, rather than as part of a systematic sampling programme. The reef tract, which is exposed

across North Greenland represents the oldest large-scale reef development in the Silurian, and includes the most extensive of the late Llandovery reef-complexes (Copper and Brunton 1991). The reefs have yielded thousands of predominantly disarticulated calcitic trilobite sclerites which are dominated by scutelluids. These sclerites, like the reefs themselves, are remarkably well preserved, providing the most significant trilobite collections so far from any early Silurian reefs. The faunas of the Great Lakes area are predominantly both younger (Wenlock) and pervasively dolomitized.

The distribution of Silurian trilobite faunas is strongly related to lithofacies (Männil 1982a, 1982b, Chlupáč 1987, Thomas 1979, Mikulic 1981, 1999, Thomas and Lane 1999). The trilobites from the North Greenland reefs are predominantly associated with a cement-rich microbial lithofacies, and were deposited between storm- and fair-weather wave base, in cavities and depressions within the reef surface (see Chapter 4). The faunas found belong to the Illaenid-Cheirurid Community (Fortey 1975), an umbrella term used to denote recurrent groups of trilobites thought to have lived together. The term community, in its biological sense, cannot be applied strictly to fossil assemblages as it refers to populations of organisms actually alive at a particular time, but is used here in accordance with palaeontological convention to denote the broader, sometimes long-ranging, associations of trilobites recognised from similar palaeoenvironments.

The large number of new species described here reflects the lack of sampling of Silurian reef environments, both in North Greenland and elsewhere. The financial and logistical constraints of conducting fieldwork in such a remote area has restricted collecting along the North Greenland reef belt, which includes the most significant exposures of Telychian reefs anywhere in the world. Other Telychian reefs are also

most prevalent in inaccessible regions, other areas of the Arctic for example, and the Altai Mountains, Siberia. Previous works on trilobite taxa from the same age and similar lithofacies are few (Norford 1973, Norford 1981, Ludvigsen and Tripp 1990 (unnamed shallow-water limestones of the Illtyd Range), Adrain *et al*. 1995, Chatterton and Ludvigsen 2004), with other significant studies of Telychian trilobite faunas predominantly concerning those from deeper-water lithofacies (Chatterton and Perry 1983, 1984, Ludvigsen and Tripp 1990 (basinal sediments of the Road River Formation), Norford 1994).

2.1.1 Previous work

The first palaeontological work from North Greenland to consider its Silurian trilobite faunas, was that of Poulsen (1934), who studied the fossils collected by Dr Lauge Koch during the Second Thule Expedition (1916–1918) and the Danish Jubilee Expedition (1920–1923). The material available to him was from the Upper Rhuddanian/Aeronian Cape Schuchert Formation, Washington Land, and contained representatives of the Harpetidae, Aulacopleuridae, Proetidae, Odontopleuridae, Scutelluidae, Cheiruridae, and Encrinuridae. Most of the taxa are not congeneric with the material described here, and this probably reflects both the older age of the Formation and its lithofacies, which Hurst (1980) documented as being dominated by bituminous cherty lime mudstones. However, the fauna compares very strongly with that described by Ludvigsen and Tripp (1990) from the relatively deep, dark grey argillaceous lime mudstone lithofacies of the early Silurian Road River Formation at Prongs Creek, Yukon Peninsula. Teichert (1937) studied collections resulting from the fifth Thule Expedition (1921–24). In addition to his study of Arctic Canada faunas, he described what is now the type species of *Periostrix* gen. nov., *P.*

magnifica, from the Telychian Offley Island Formation, St George Fjord, North Greenland.

Over thirty years then passed until material collected from Kronprins Christian Land (Northeast Greenland) during the Lauge Koch Expeditions, was studied by Lane (1972). The material was collected from repetitive sequences of dolostones, limestones and shales then thought to belong to the Centrum Limestone and Dolomite, and the Drommebjerg Limestone. These stratigraphical terms are no longer in use, and were employed at a time before the effects of multiple thrusting (Smith and Rasmussen 2008) were recognised in the area. The material probably comes from the Samuelsen Høj Formation. New species of scutelluids, harpetids, cheirurids and lichids were described, as well as previously known species of calymenids, odontopleurids, proetids, aulacopleurids and illaenids. Lane discussed the similarities between his fauna and others, particularly those of the Niagaran ('middle' Silurian) reefs of the Great Lakes, New York, the Lower Devonian Koněprusy Limestone of the Czech Republic and the Middle Devonian limestones from South Devon, England. He noted that trilobite faunas might be expected to show a greater overall similarity within pure limestone rocks of different ages, than in rocks of variable lithofacies of the same age. Ten genera, including three species described from Lane's study, are represented here.

Expeditions in the 1960s (Operation Grant Land) and the 1970s to 1980s (geological mapping project of GGU) resulted in the collection of numerous fossiliferous samples available for study. Material from the Telychian Odins Fjord Formation in Peary Land was studied by Lane (1988), and from a more northerly locality by Thomas (1994). No taxa from the two localities are congeneric, but when compared to a sample collected from Wulff Land studied in the present work (from

the time equivalent of the Odins Fjord Formation, the Djævlekløften Formation) broader similarities are evident. The Odins Fjord and Djævlekløften formations are the only Silurian formations from North Greenland yielding members of the Phacopidae and the Pterygometopidae (Lane 1988), reflecting the difference between the bottom-dwelling faunas of the Odins Fjord and Djævlekløften formations, and the reef faunas of the Samuelsen Høj Formation.

Trilobite faunas from western North Greenland were studied by: Norford (1973) who described species of *Scotoharpes* from the Offley Island Formation, in Kap Tyson and Kap Schuchert; Lane (1979) from the Cape Schuchert Formation in Washington Land; Lane and Owens (1982) from blocks derived from the Telychian Pentamerus Bjerg Formation in Washington Land; Lane (1984) from the Telychian Offley Island and Hauge Bjerge formations in Hall Land and Nyeboe Land; Lane and Siveter (1991) from the Telychian Offley Island Formation, Kap Tyson, Hall Land. Of these, the material from Lane (1984) and Lane and Owens (1982) compares most closely with the faunas studied here, with five and six congeneric taxa respectively. This is a reflection of their similar age and lithofacies. The fauna studied by Lane and Siveter (1991), is unusual as it is dominated by *Calymene*. It is found in the time equivalent to the Odins Fjord and Djævlekløften formations, further demonstrating the faunal differences between level-bottom and reef environments.

2.2 MATERIALS AND METHODS

The trilobites are predominantly preserved as internal moulds. As the cuticle generally adheres to the external mould, it is often lost with the matrix during preparation with a pneumatic air pen. Specimens were painted with Indian ink (unless otherwise stated) and lightly coated in ammonium chloride sublimate before photography, to produce

maximum contrast. Photographs were taken with a Cannon EOS 40D, with dorsal views taken in palpebral view (cranidia and cephala) and extended view (pygidia).

2.2.1 Taxonomic disclaimer

Names of new taxa included in this thesis are not published validly under the rules of the ICZN. It is anticipated that most of the taxa will be formally published in the acknowledged literature, and the names given in this work will be retained where possible.

2.3 SYSTEMATIC PALAEONTOLOGY

2.3.1 Terminology

Terminology used is that set out in the *Treatise* (Kaesler 1997), except as outlined below. The scutelluid librigenae may have two peripheral furrows (Text-fig. 2.1A), here termed the *inner* and *outer librigenal furrows*. The fixigenal equivalents of these are the anterolateral border furrow for the outer furrow, and the fixigenal inner furrow for the inner furrow. The area between these furrows may be concave, and this is referred to as the '*anterolateral concave zone*'. Other terms applied to scutelluids are: '*holcos'* (Helbert and Lane *in* Helbert *et al*. 1982); '*cusp'* (Curtis and Lane 1997); '*anterolateral internal pit'*, '*lunette'* and '*omphalus'* (Holloway and Lane 1998); '*median node in lateral glabellar furrow S1'* (Whittington 1999). Proetid terminology includes '*intramarginal zone'* employed by Owens (2006, p. 119) to describe a flat band between the border and epiborder furrows, as seen in *Winiskia*. Additionally, the term '*preocular fixigenal furrow'* is introduced to describe a transversely trending furrow within the fixigena which is adaxially confluent with the preglabellar furrow,

as seen in *Airophryus* gen. nov. The 'border furrow' of Campbell (1977) is comparable to the preocular fixigenal furrow. Study of the doublure of *Airophrys* is required to confirm the homology of these structures, however. Lateral glabellar muscle impressions and furrows in front of occipital impressions and furrows are preceded with 'S' and 'L' respectively, and are numbered from the posterior S1/L1. Terminology of points on the facial suture follows that of Richter and Richter (1949, p. 68; Text-fig. 2.1B). Terminology used for encrinurids follows usage by Edgecombe and Chatterton (1993, p. 77) where PL = preglabellar lateral lobe, referring to the swelling on the lateral part of the anterior border of the cranidium.

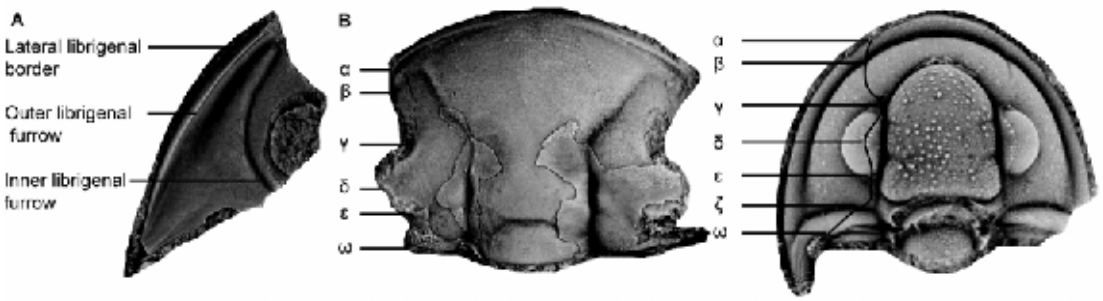

Text-fig. 2.1A. Specimen of *Aboskes anachoretes* with terminology of scutelluid librigenal furrows and border. **B.** Cranidium of *Ekwanoscutellum agmen* (left) and cephalon of *Owensus arktoperates* (right) with terminology applied to different points along the facial suture (based on Richter and Richter 1949).

2.3.2 Genus and specific characters

The new taxa described here mostly belong to the Scutelluidae and Proetidae. It is important to recognise the principal characters used to distinguish taxa both at a generic and specific level, for consistency in future description of similar taxa. The characters considered of prime importance in the specific and generic diagnosis of these new taxa are discussed below.

2.3.2.1 Scutelluidae

Lane and Thomas (1983) comprehensively reviewed the Scutelluina, detailing the morphological characters used in classification. Whittington (1999) further discussed the morphology and classification of the group. Holloway and Lane (1998) noted the importance of characters used in their study of effaced scutelluids from New South Wales. They believed exoskeletal convexity, rostral plate morphology, presence or absence of an omphalus and anterolateral internal pit, and thoracic morphology (axial width, distance between axial furrow and fulcrum) to be of most importance in diagnosing genera of effaced scutelluids.

Effacement has variably affected this family, and the taxa described here represent both non-effaced and effaced (illaenimorph) forms. The effects of effacement reduce the number of diagnostic characters. The difficulty in recognising meaningful characters has resulted in generic and species diagnoses of effaced scutelluids often comprising largely higher level taxonomic characters e.g. *Failleana* (Chatterton and Ludvigsen 2004, p. 37) and *Paracybantyx* (Ludvigsen and Tripp 1990, p.8).

Non-effaced scutelluids. Cephalic characters are most commonly required to distinguish between species and genera of non-effaced scutelluids. At both genus and species level the most useful distinguishing characters are: cephalic outline shape; convexity; size, shape and depth of the lateral glabellar muscle impressions. At genus level, the extent of the anterior border and preglabellar furrow, position of the lateral glabellar muscle impressions, course of the axial furrows and presence or absence and position of the inner librigenal furrow and related anterolateral concave zone, are important.

Non-effaced scutelluid genera predominantly exhibit very similar pygidial characters, and different species may have virtually identical pygidia: *Jungosulcus anaphalantos* and *J. ventricosus*, for example. In rare cases, for example *Opoa adamsi* and *O. limatula*, the pygidia may appear very different in overall morphology, but the axial characters remain similar. All of the non-effaced scutelluids described here share seven pairs of pleural ribs and a median rib, and a pygidial doublure with well developed terrace ridges which become progressively more scalloped towards margins. Pygidial characters deemed particularly important at a generic level are: pygidial length to width ratio; size, shape and inflation of the pygidial axis; position of maximum width of the pygidium (particularly to distinguish *Meroperix*); amount of bifurcation exhibited by median rib, although this can be variably expressed in populations of *Jungosulcus* and *Periostrix*. Sculpture and degree of effacement exhibited by both cephala and pygidia vary at species level.

Effaced scutelluids. The following cephalic characters are deemed most taxonomically informative at both genus and species level: length to width ratios; shape, size and depth of impression of lateral glabellar muscle impressions and lunettes; convexity. At genus level, the presence or absence of a complete and pronounced anterior border, course of the axial furrows, position of glabellar muscle impressions, size and position of the palpebral lobe, and the presence or absence of genal spines, are important. Caution should be exercised with the use of the sagittal carina on the cephalon, as this is variable within populations. In addition, the presence of cuticle can obscure the omphalus, cranidial axial furrows, lateral glabellar muscle impressions, and the occipital node.

The pygidia of effaced scutelluid taxa present particularly few characters, in addition, characters such as the presence or absence and relative sagittal length of the pygidial posterior carina, and paired muscle impressions on the pygidium can vary with preservation, and length to width ratios have been shown to vary with specimen size. The overall convexity, expression of the holcos, and the length and width of the articulating facet are useful at genus level.

Ontogeny. Ontogenetic stages of effaced scutelluids are best known from *Failleana calva* (Ludvigsen and Chatterton 1980). In addition, Holloway and Lane (1998) described ontogenetic stages for *Bumastella specula*, *Liolalax olibros* and *Excetra iotops*. The ontogeny of *Ligiscus diana* sp. nov. shows similarities with *E. iotops*. The most common ontogenetic changes observed within effaced scutelluids are: length of visual surface and palpebral lobe relatively decreases, and pygidial length to width ratio increases with growth. Gradual effacement with growth may be reflected through: loss of the genal spine, an increase in convexity, shallowing of axial furrows, and loss of the occipital furrow. Non-effaced scutelluids may also exhibit effacement with growth, for example, *Jungosulcus anaphalantos* exhibits gradual effacement of the anteriormost lateral glabellar muscle impressions, and *Ekwanoscutellum agmen*, of the median portion of the anterior border. Additionally, as with effaced scutelluids, an increase of the pygidial length to width ratio with growth is seen in *E. agmen* and *Periostrix magnifica*.

2.3.2.2 Proetidae

Owens (1973*a*, p. 6) provided a brief history of classification of the Proetidae. He noted the following characters to be of prime importance in classification: the type of

rostral plate; lateral profile of pygidial pleural ribs, for which the terms imbricate, flat-topped, and scalloped were introduced (see Owens, 1973*a*, text-fig. 2, p. 5); presence or absence of a preannulus. In subfamily diagnoses some or all of the following characters were used in his 1973 monograph: shape of the glabella and nature of the glabellar furrows; presence or absence of a preglabellar field and tropidium; presence or absence of a panderian opening at the base of the genal spine; the number of thoracic segments; the number of pygidial axial rings; type of surface sculpture. Šnajdr (1980, p. 28) presented unified criteria for classification at a generic level, with reference to the works of Ormiston (1967), Alberti (1969), Pillet (1972), Owens (197*3a*, *b*), and Fortey and Owens (1975). The following discussion draws on some of his main themes, with comments based on the current study.

Particular glabellar shapes characterize proetid families, with more specific variations in glabellar shape and convexity being generically diagnostic, as noted by Šnajdr. Both Owens (1973*a*) and Šnajdr considered the morphology and positioning of the lateral glabellar muscle impressions to be of subordinate importance as a generic character, showing no great differentiation between different genera in a subfamily. Species of *Winiskia* described below demonstrate that depth of these impressions can significantly vary between closely related species. Šnajdr considered the overall occipital ring morphology, position of the occipital node and occipital spine, and presence of lateral lobes to be of prime importance at a generic level. Relative proportions of the occipital ring and the presence or absence and position of an occipital node were found most useful at specific level here: for example, the placement of the occipital node is characteristic of different species of *Dalarnepeltis*. The length and depth of border furrows, and the course of facial sutures, are useful characters at a generic level, also as noted by Šnajdr. Additionally, the presence of an

intramarginal zone serves to distinguish the genus *Winiskia*, and the preocular fixigenal furrow to distinguish the genus *Airophyrus*. The morphology of the anterior border is variable at a specific level. Šnajdr remarked that the length (sag.) of the preglabellar field is characteristic of particular genera and of higher taxonomic levels, and this has proved a valuable distinguishing character here. There is some variation at a specific level, as seen in the species of *Winiskia* described below.

Šnajdr recognised that the size, vaulting and general outline of the pygidium varies only slightly within a genus. In genera with fewer than 8 axial rings, the number of rings and character of the terminal piece are important generic characters. In genera with 8 or more axial rings, the number of rings can vary within a very narrow range in representatives of the same species. Šnajdr also recognised the shape of the axial rings, the shape of the anterior and posterior pleural bands, the presence or absence of pleural spines and their shape, and the presence or absence of a pygidial border as important generic characters. Here, the morphology of the pleural ribs, including degree of inflation of both anterior and posterior pleural bands, the pygidial axial width relative to pygidial width, and the length:width ratio of pygidium were found to be useful generic characters. The morphology of the pleural ribs and axial rings, and the presence or absence of a pygidial border, were useful at a specific level.

Order CORYNEXOCHIDA Kobayashi, 1935

Suborder ILLAENINA Jaanusson *in* Moore, 1959

2.3.3 Family SCUTELLUIDAE Richter and Richter, 1955

Remarks. The composition of this family has a complex history. The Family Scutelluidae has sometimes been regarded as a junior synonym of Styginidae (e.g. Holloway and Lane 1998, Lane and Thomas 1983). Holloway's (2007) analysis of these taxa demonstrated the separation of the two. The family is here subdivided informally into non-effaced and effaced forms. This is convenient for purposes of description and comparison, and is consistant with the cladistic analysis shown in Chapter 3 (Text-fig. 3.3), that confirms that a range of highly effaced taxa are scutelluids rather than illaenids.

Non-effaced Scutelluidae

Genus ABOSKES gen. nov.

Derivation of name. Greek, *aboskes*, hungry, alluding to the narrow posterior part of the glabella. Gender masculine.

Type species. By original designation; *Aboskes anachoretes* gen. et sp. nov. from the Telychian Samuelsen Høj Formation, central Peary Land, North Greenland.

Diagnosis. Scutelluid with low convexity glabella; glabella narrow (tr.) in its posterior half, there comprising quarter of total cephalic width. Pronounced anterior border extending across whole anterior margin. S2 placed directly anterior of S1. Well impressed inner librigenal furrow following line of visual surface.

Remarks. The extremely narrow posterior half of the glabella distinguishes *Aboskes* from all other scutelluids. The very pronounced anterior border is also distinctive.

Aboskes anachoretes gen. et sp. nov.

Plate 1, figures 1–4

Derivation of name. Greek, *anachoretes*, one who has retired from the world, a hermit or recluse. The genus is represented by one individual. Gender masculine.

Holotype. MGUH1 (Pl. 1, figs 1–4) cephalon; GGU 198225 (CPL3).

Diagnosis. As for genus.

Description. Cephalon semicircular, 1.5 times as long (sag.) as wide. Portion of glabella between occipital furrow and S1 highest. Cranidium of approximately equal width posteriorly and anteriorly, slightly wider across β–β than δ–δ. Width (tr.) across palpebral lobes at δ–δ roughly equal to sagittal length of cranidium; width (tr.) across γ–γ roughly four-fifths cranidial sagittal length. Glabella parallel sided in its posterior half; anterior of S1 expands (tr.) rapidly forwards from exsagittal line at 45 degrees. Facial suture running parallel to this. Axial furrow with angular change in course at

point of glabellar greatest lateral expansion. Glabella widest at anterior end of axial furrow, there approximately 2.5 times wider than posteriorly. Occipital ring greatly expanded sagittally where it is over twice as long (sag.) as abaxially. Occipital muscle impression relatively wide (tr.), comprising one-third posterior glabellar width (tr.). Pronounced anterior border longer (sag.) than preglabellar furrow (Pl. 1, fig. 1). Latter slightly longer abaxially. S1 reniform, well impressed, posterior end opposite anterior of lunette, anterior end placed where axial furrow changes course, connected to axial furrow. S2 close to S1, less well impressed, elongate, not connected to axial furrow. S3 not impressed. Glabella completely covered with discontinuous terrace ridges, medially trending transversely; abaxially, directed posteriorly near intersection with axial furrow.

Fixigena with similar convexity to glabella. Palpebral lobe prominent, but not forming highest point of cephalon; posterior end opposite occipital furrow, anterior end opposite posterior of S1. Eye ridge trending anteriorly toward mid-point of anterior portion of axial furrow, almost vertical. Complete covering of short discontinuous terrace ridges trending variably obliquely and transversely.

Librigena with very pronounced lateral border and well impressed outer librigenal furrow; both narrow (tr.) posteriorly. Inner librigenal furrow placed roughly equidistant from visual surface and outer librigenal furrow at its midpoint (exsag.). Visual surface comprising roughly one-third total cephalic sagittal length (without genal spine). Genal spine comprising approximately one-third entire length (exsag.) of entire librigena. Complete covering of short discontinuous terrace ridges trending obliquely (Pl. 1, fig. 4).

Remarks. Initially, the cranidial morphology of *A. anachoretes* appears most similar to that of *Opoa limatula* sp. nov. (Pl. 5, figs 2–15), particularly the glabellar furrows. However the glabella of *O. limatula* is much wider (tr.) posteriorly, and more forwardly expanded leaving only a weak anterior border medially. *O. limatula* also has a greater convexity. The pronounced anterior border of *A. anachoretes* is reminiscent of '*Scutellum' rochesterense* (Whiteaves; see Howell and Sanford 1946, p. 69, fig. 46b) from the Middle Silurian Irondequoit Formation, Rochester, New York. A fragmentary cranidium from the Telychian Offley Island Formation; *?Ekwanoscutellum* (Lane and Siveter 1991, fig. 2d), is tentatively assigned to *Aboskes anachoretes*; it has a continuous and prominent anterior border, and the trend of the axial furrows is comparable.

Occurrence and distribution. Central Peary Land (CP3).

Genus EKWANOSCUTELLUM Přibyl and Vaněk, 1971

Type species. By original designation; *Bronteus ekwanensis* Whiteaves, 1904, from the Telychian–?early Wenlock Attawapiskat Formation, Ekwan River, Ontario, Canada.

Diagnosis. After Norford (1981, p. 4): scutelluid with anterior border and preglabellar furrows only present laterally. Glabella narrowest at cranidial midlength after which it displays a strong angularity and expands rapidly forwards to twice that width. Occipital impression and S1 large and well impressed, S2 and S3 much weaker and smaller, may not be visible. Librigena with inner furrow anteriorly converging with

outer furrow; terminating in a genal spine comprising over one-fifth total cephalic sagittal length. Pygidium with length subequal to width, and with maximum width in anterior quarter of pygidial sagittal length; vaulted, with axis roughly one-quarter sagittal length of pygidium. Median rib bifid for roughly its posterior half.

Remarks. Norford (1981) redescribed and refigured Whiteaves' original material. Comparisons of *E. ekwanensis* were made with both *Meroperix* and *Opoa*. Norford noted that the lack of sculpture of *Ekwanoscutellum* may be a generic feature. This study however demonstrates that sculpture does not hold more than specific significance for scutelluid taxa, for example, *Opoa limatula* sp. nov. exhibits a very different sculpture from the type species of *Opoa*, *O. adamsi*.

Meroperix shares most similarities with *Ekwanoscutellum*, particularly in overall cranidial shape, the positions of the lateral glabellar muscle impressions, and the lack of a preglabellar furrow and anterior border medially. The most important differences are: S3 is larger than S2 in *Ekwanoscutellum*, whereas the reverse is true for *Meroperix*; *Ekwanoscutellum* has a broader anterolateral border furrow; the *Meroperix* pygidium is about twice as wide as long and that of *Ekwanoscutellum* is variably subequal to width; the pygidium of *Ekwanoscutellum* is more convex than that of *Meroperix*, which is virtually flat; the pygidial axis of *Ekwanoscutellum* comprises one-quarter of the entire pygidial length whereas the pygidial axis of *Meroperix* is proportionally shorter, comprising one-fifth of the entire pygidial length; *Ekwanoscutellum* is characterised by its large maximum size, whereas *Meroperix* specimens reach much smaller maximum sagittal lengths.

Norford (1981) was not confident in assigning *Bronteus laphami* Whitfield, 1882 (p. 310, pl. 22, figs 1–4) from the Wenlock of Wisconsin, North America, to

Ekwanoscutellum. He noted that the species was essentially described from its pygidia and recognised the importance of the description of cranidial morphology to assign it to the genus. I have studied material from the type and figured collection in the Smithsonian Institute, Washington: a fragmentary cranidium (Text-fig. 2.2A) of *Bronteus laphami* processes all the distinguishing characters of *Ekwanoscutellum* – the medial lack of an anterior border and preglabellar furrow, combined with the course of the axial furrows and the effacement of S2 and S3 are all characteristic. A fragmentary pygidium (Text-fig. 2.2B) and a pygidial negative (Text-fig. 2.2C) demonstrate proportions which are characteristics of *Ekwanoscutellum*. I can therefore confidently assign *Bronteus laphami* to *Ekwanoscutellum*. *?Ekwanoscutellum* Lane and Siveter, 1991, fig. 2d is tentatively assigned to *Aboskes anachoretes* (gen. et sp. nov).

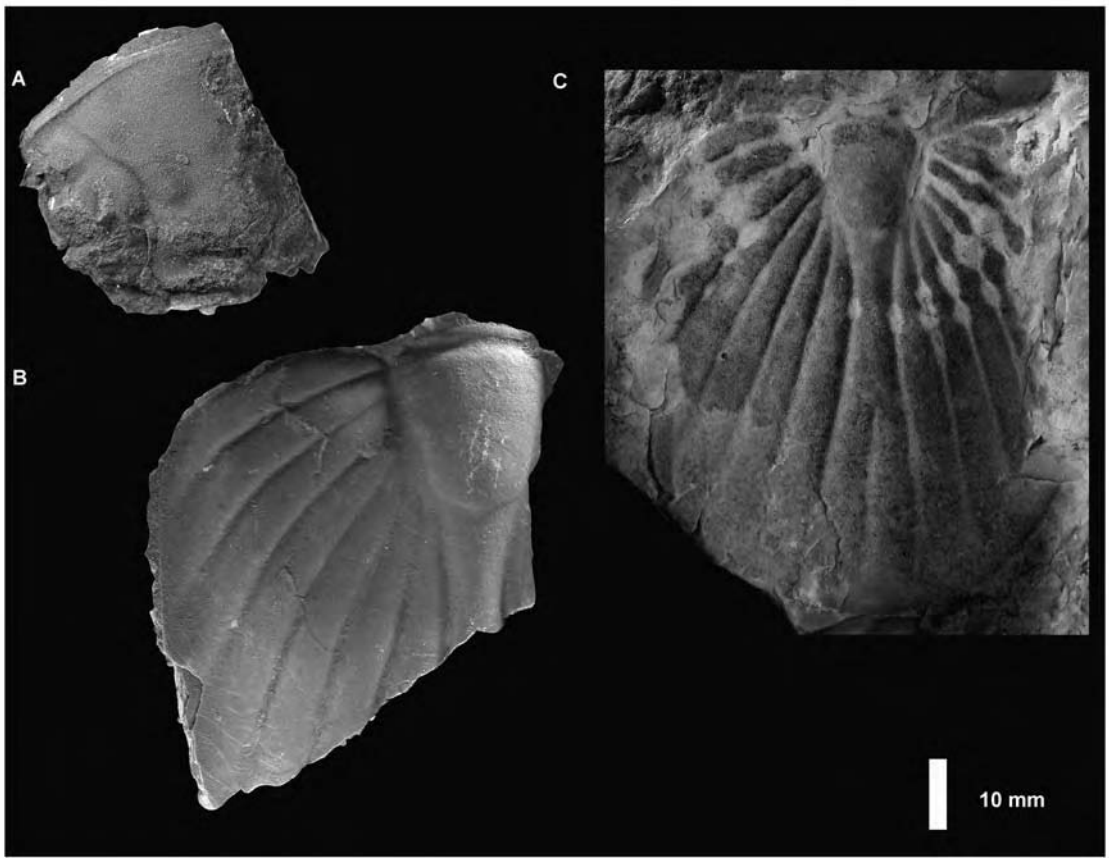

Text-fig. 2.2. *Ekwanoscutellum laphami* (Whitfield, 1882). Wenlock, Racine Formation, Kewaunee Co., Wisconsin. USNM numbers indicate specimens belong to the type and figured collection, Smithsonian Institute, Washington. **A.** Fragmentary cranidium USNM 135947; **B.** Fragmentary pygidia. USNM 135953; **C**. Pygidial negative. USNM 137042. All are syntypes.

Ekwanoscutellum agmen sp. nov.

Plate 1, figures 5–14; Plate 2, figures 1–20

Derivation of name. Latin, *agmen*, army on the march, multitude, crowd, train. This is the most abundant species described here.

Holotype. MGUH2 (Pl. 1, figs 5–7) cranidium; GGU 274689 (CPL5).

Figured paratypes. Locality CPL2: MGUH4, MGUH8 cranidia; MGUH12 librigena; MGUH14 rostral plate; MGUH18 thoracic segment; MGUH21–22, MGUH24–25 pygidia. Locality CPL4: MGUH15 hypostome; MGUH19 pygidium. Locality CPL5: MGUH6 cranidium; MGUH10–11 librigenae; MGUH13 rostral plate; MGUH17 thoracic segment; MGUH23 pygidium. Locality VGL1: MGUH5, MGUH7 cranidia. Locality KCL1: MGUH3, MBUH9 cranidia; MGUH16 hypostome; MGUH26 pygidium. Locality KCL3:MGUH20 pygidium.

Diagnosis. Ekwanoscutellum with librigena relatively narrow (tr.) anteriorly; both pygidium and pygidial axis a little wider (tr.) than long (sag.); pygidial maximum width (tr.) opposite midpoint to posterior of axis; posterior half of pygidial axis commonly ‘pinched’; slight marginal pygidial concavity.

Description. Cranidium of approximately equal width posteriorly between fulcral sockets as at anteriorly between anterolateral margins; wider across β–β than δ–δ. Width (tr.) across palpebral lobes at δ–δ greater than sagittal length of cranidium (83% as long as wide; range = 74–90%; n = 11); width (tr.) across γ–γ roughly equal to cranidial sagittal length. Maximum height in anterior part of glabella. Glabella parallel-sided for its posterior half, but for a slight inflexion opposite lunettes. Axial furrows well impressed. Anterior end of S1 50% total cranidial sagittal length from posterior margin (range = 45–53%; n = 16). Axial furrows there suddenly change course, diverging strongly at 35–50 degrees (n = 8) continuing in a straight line to intersect with the anterolateral border furrow. There, glabella 2.27 times wider than at its narrowest part (range = 2.10–2.53; n = 11). Occipital ring approximately twice as long sagittally as exsagittally. Well impressed occipital furrow and oval occipital

impressions connected to axial furrow. Occipital ring length (sag.) 34% of width (tr.) (range = 30–37%; n = 14). Narrow anterior border and preglabellar furrow best developed anterolaterally at least until point anterior of posterior portion of the axial furrows, fading medially where replaced by terrace ridges. S1 extending from anterior of lunettes to point where axial furrows change course, sagittally oval with a median node, connected to axial furrow. S2 and S3 effaced, rarely visible; S2 smallest, transversely oval, separated from but close to S1; S3 approaching size of S1 but weaker, the least well impressed of the muscle impressions, transversely oval. S2 and S3 close to, but not connected to axial furrows. Muscle impressions placed further from sagittal line anteriorly (Pl. 1, fig. 13). Sculpture comprising terrace ridges; covering anterior of glabella where prominent, continuous, non-anastomosing, roughly parallel to anterior margin, trending transversely. Fainter, transversely trending terrace ridges on fixigena. Largest cranidial sagittal length measured 30 mm.

Fixigena gently convex, palpebral lobe forming highest point of cranidium, posterior of which lies opposite midpoint of occipital impressions, extending forwards to posterior of S1. Palpebral lobe located 30% total cranidial sagittal length from posterior border (range = 28–32%; n = 10). Eye ridge intersecting axial furrow opposite S3. Lunette oval, placed between anterior of occipital muscle impression and posterior of S1. Anterolateral concave zone longer (exsag.) than anterolateral border.

Librigena with large, crescentic and strongly raised visual surface. Outer librigenal furrow separated from lateral border, most so at its midlength (exsag.), terminating at pronounced genal spine; broad and well impressed anteriorly, narrowing and shallowing posteriorly (Pl. 2, figs 1–2). Inner librigenal furrow well impressed, converging towards outer librigenal furrow anteriorly. Completely covered in transversely trending, persistent, regularly spaced terrace ridges which locally

anastomose and become increasingly well impressed posteriorly. Doublure with terrace ridges mirroring direction of epiborder and lateral border furrows (Pl. 2, fig. 3).

Rostral plate attributed to genus longer than wide; connective sutures diverging at 50–60 degrees, with slightly curved paths. Prominent, continuous terrace ridges trend transversely over entire rostral plate (Pl. 2, figs 4–5).

Hypostome of typical '*Scutellum*-type' (Lane and Thomas 1983, text-fig. 4 c); subtriangular, with posterior margin terminating in blunted point. Short (sag., exsag.) posterior lobe of middle body, prominent maculae, narrow border. Total sagittal length 62% of width (tr.) across anterior wings (range = 57–67%; n = 4). Prominent terrace ridges cover entire hypostome, trending in a 'U-shape'.

Thoracic segments all disarticulated. Axial ring at least one-third width (tr.) of whole segment. Articulating half ring roughly half length (sag.) of axial ring; well impressed axial furrow; covered in transversely trending continuous terrace ridges. Both axial ring and articulating half ring convex; pleural region flatter with thin, raised border anteriorly, and obliquely trending terrace ridges. Strongly curved backwards and terminating in a spine.

Pygidium an anteriorly truncated ellipse with smoothly curved margins, averaging 82% as long (sag.) as wide (tr.) (range = 59–96%; n = 19); when plotted, the pygidial transverse width = 1.094 pygidial sagittal length + 1.5568 (see remarks for discussion and Text-fig. 2.3A). Axis with maximum convexity anteriorly; a blunted triangle; commonly pinched inwards halfway along length; anteriorly expanded (tr.), there averaging 83% as long (sag.) as wide (tr.) (range = 53–103%; n = 42); when plotted, the pygidial axis transverse width = 1.1444 pygidial axis sagittal length + 0.2652 (see remarks for discussion and Text-fig. 2.3B). Locally displaying a

faint trilobation, and with very well impressed axial furrows. Axis constitutes 23% total pygidial sagittal width (range = 16–30%; n = 21); when plotted, the pygidial axis sagittal length = 0.208 pygidial sagittal length + 0.4819 (see remarks for discussion and Text-fig. 2.3C). Adaxial half of pleural region gently convex. Pleural ribs slightly sigmoidal. Median rib at posterior margin is twice width (tr.) of lateral pleural ribs. All pleural ribs transversely convex. Pleural furrows well impressed proximally, becoming fainter distally; both furrows and ribs gradually widen marginally. Sculpture of faint to prominent non-anastomosing terrace ridges, trending transversely across ribs; abaxially on axis they are deflected anteriorly, trending transversely. Doublure extending just over half pygidial sagittal length, with well impressed ribs and furrows mirroring the dorsal surface. Well developed terrace ridges become increasingly scalloped towards margins (Pl. 2, fig 19). Maximum pygidial sagittal length measured 68.09 mm.

Variation not accounted for by ontogeny.

1. Anterior course of axial furrows ranges from a straight line (Pl. 1, fig. 9) to sigmoidal (Pl. 1, fig. 13); to some extent cuticle has the effect of smoothing out the course of the axial furrow.
2. Pygidial axis may be straight-sided (Pl. 2, fig. 11) or ‘pinched’ inwards (Pl. 2, fig. 18).
3. Amount of marginal concavity to pygidia.

A cranidium from Kronprins Christian Land (MGUH9; Pl. 1, fig. 14) is identical to specimens of *E. agmen* in all respects other than possessing a complete anterior border. It is included in *E. agmen*; the occurrence of this in a single specimen does not require amending the generic diagnosis.

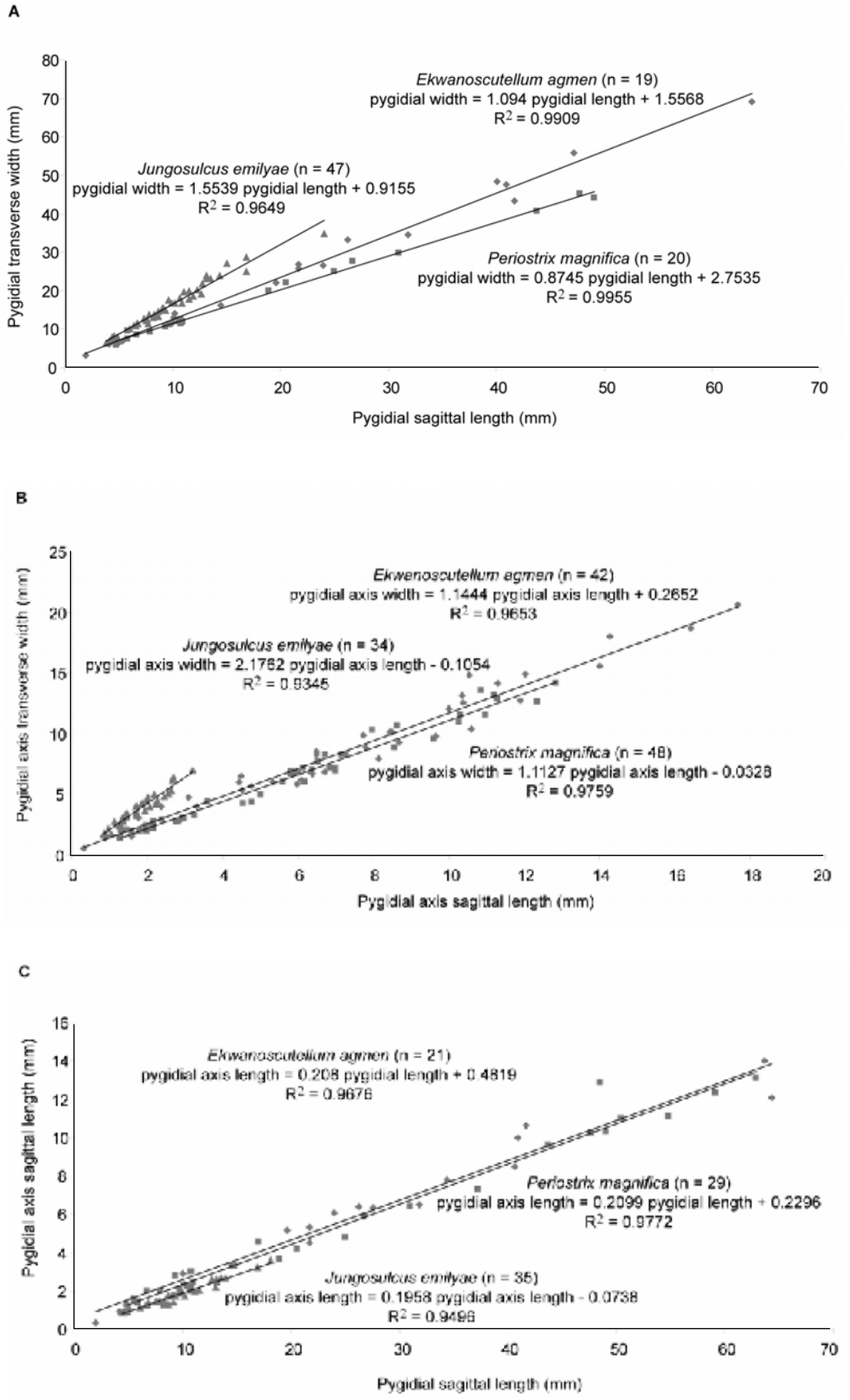

Text-fig. 2.3. Major axis regression for *Ekwanoscutellum agmen*, *Jungosulcus emilyae* and *Periostrix magnifica* of **A.** pygidial transverse widths against pygidial sagittal lengths. **B.** pygidial axial transverse widths against pygidial axial sagittal lengths. **C.** pygidial axial sagittal lengths against pygidial sagittal lengths.

Ontogeny. Important changes with growth of this species are as follows:

1. Gradual effacement of medial portion of anterior border and preglabellar furrow.
2. Pygidia become proportionally longer with growth; pygidial sagittal lengths average 74% of pygidial transverse width in the five smallest specimens, compared to 88% in the five largest specimens.

Remarks. The large sagittal lengths of pygidia of this species are characteristic of *Ekwanoscutellum*. The course of the cranidial axial furrows, proportion of the anterior margin with an anterior border and preglabellar furrow, the anterior position of the maximum width of the pygidia, the shape and relative length of the pygidial axis, and the morphology of the pygidial ribs and furrows make this species most similar to *E. ekwanensis*. The main differences from *E. ekwanensis* are: anterior portion of the fixigena is relatively narrower (tr.); median part of the occipital ring is more expanded; pygidium is a little wider than long, whereas the opposite is true for *E. ekwanensis*; lateral pygidial margins straighter, maintaining maximum width for longer; pygidial axial furrows straighter in *E. ekwanensis*.

Reduced major axis regression has been used previously to estimate the sagittal length of *Ekwanoscutellum* pygidia when, due to fragmentation, only the sagittal length of the axis is measurable (Westrop and Rudkin 1999). Plotting pygidial axis versus pygidial sagittal lengths, which show a linear relationship, gives a reasonable estimation of total pygidial length. Here, reduced major axis regression has been employed to investigate its use in identification of scutelluid species (Text-fig. 2.3). Pygidial length was plotted against pygidial width, pygidial axial length against pygidial axial width, and pygidial axial length against pygidial length for taxa with a

reasonable sample size: *E. agmen*, *Jungosulcus emilyae* and *Periostrix magnifica.* The resulting straight line equations for pygidial width against pygidial length clearly distinguish *E. agmen* from *P. magnifica* and *J. emilyae*. The straight line equations for axial width against axial length are extremely similar for *E. agmen* from *P. magnifica*, and only serve to distinguish *E. agmen* from *J. emilyae.* The plots of pygidial axial length against pygidial length are extremely similar for the three species despite the obvious differences in overall pygidial morphology.

Occurrence and distribution. Central Peary Land (CPL1–5), Valdemar Glückstadt Land (VGL1) and Kronprins Christian Land (KCL1, 3, 5).

Genus JUNGOSULCUS gen. nov.

Type species. By original designation; *Jungosulcus emilyae* sp. nov. from the Telychian Samuelsen Høj Formation, central Peary Land, North Greenland.

Other species. Jungosulcus anaphalantos sp. nov. from the Telychian Samuelsen Høj Formation, south Nares Land, North Greenland.
Jungosulcus ventricosus sp. nov. from the Telychian Samuelsen Høj Formation, Valdemar Glückstadt Land, North Greenland.

Derivation of name. Combination of Latin, *jungo*, unite or connect, and Latin, *sulcus*, furrow or groove. Reference to the proximal merging of pygidial ribs five, six and seven, and their associated pleural furrows. Gender masculine.

Diagnosis. Scutelluid with glabella expanding anteriorly for most of its course; long (sag.) anterior border and furrow laterally. Pygidium about two-thirds as long (sag.) as wide (tr.) anteriorly; axis almost twice as wide (tr.) anteriorly as long (sag.), with clear trilobation visible in larger specimens; median rib either bifid or with median carina, or both; lateral pygidial ribs five, six and seven merge prior to intersection with axial furrow.

Remarks. The distinctly trilobed axis of larger specimens, and the merging of pygidial ribs five, six and seven before intersecting the pygidial axis, distinguish *Jungosulcus* from any other scutelluid.

Jungosulcus emilyae gen. et sp. nov.

Plate 3, figures 1–15; Text-fig. 2.4A

Derivation of name. For Emily Thomas, who died suddenly while this work was in progress.

Holotype. MGUH27 (Pl. 3, figs 1–3) cranidium; GGU locality 274689 (CP3).

Figured paratypes. Locality CPL5: MGUH27–31 cranidia; MGUH32 eye; MGUH33 librigena; MGUH34–37 pygidia.

Diagnosis. Jungosulcus with all lateral glabellar muscle impressions deeply impressed; exsagittally connected S1 and S2; pronounced anterolateral border; cranidial axial furrows shallowing anteriorly, terminating as shallow impressions at

fixigenal equivalent of librigenal inner furrow; occipital impressions not connected to axial furrow; median pygidial rib bifid for at least the posterior quarter of its length (sag.).

Description. Cranidium subelliptical; of approximately equal width posteriorly between fulcral sockets as at anteriorly between anterolateral margins; width across β–β and δ–δ roughly equal. Width (tr.) across γ–γ subequal to cranidial sagittal length, 75% as long (sag.) as wide (tr.) across δ–δ (range = 67–85%; n = 20). Maximum height in glabella at level of S3. From posterior margin, axial furrows converge anteriorly for a very short distance (until a point just posterior of S1, at which the glabella is at its narrowest point), lunettes positioned there. Axial furrows continue anteriorly with a smooth trajectory; diverging forwards; remaining well impressed until they become shallower between S2 and S3. Axial furrows terminating at fixigenal equivalent of the librigenal inner furrow; glabella widest there; 2.4 times wider (tr.) than at its narrowest (range = 2.1–2.8; n = 6). S1 adjacent to axial furrow; shallowest and largest of lateral glabellar muscle impressions; comma-shaped; exsagittally connected to S2 via a narrow furrow. Abaxial of this connecting furrow is an obvious node, bounded by the connecting and axial furrows. S2 less than half the size of S1, subcircular and very deeply impressed; located further from axial furrow than S1. S3 similar in size, shape and depth of impression to S2; located at same distance from S2 as S2 is from S1; similar distance from axial furrow as S2. Anterior cephalic margins raised laterally forming a prominent anterolateral border (Pl. 3, figs 1–3); medially this is replaced by transversely trending, continuous terrace ridges. Posterior to shallow anterior border furrow is a concave zone longer (exsag.) than anterolateral border, and bounded posteriorly by a deeper furrow which corresponds

to the inner librigenal furrow. Occipital ring less convex than glabella and longest medially where almost twice as long (sag.) as abaxially; comprising 20% total cranidial sagittal length (range = 14–24%; n = 21). Occipital furrow broad and deeply impressed, abaxially terminating as subcircular occipital impressions.

Fixigena with raised palpebral lobe forming highest point. Lunettes oval, located in posterior half of palpebral lobe. Eye ridge meeting axial furrow between S2 and S3. Long anterolateral border furrow.

Librigena subtriangular and largely flat. Outer librigenal furrow becoming deeper and wider towards anterior of librigena. Inner librigenal furrow shallower, less distinct and sweeping around visual surface.

Pygidium an anteriorly truncated ellipse; 61% as long (sag.) as wide (tr.) (range = 55–69%; n = 47); when plotted, the pygidial transverse width = 1.5539 pygidial sagittal length + 0.9155 (see remarks for discussion and Text-fig. 2.3A) with maximum width very close to anterior margin, about midlength (exsag.) of first pleural rib. Axis triangular, terminating posteriorly in a sharply pointed tip; 48% as long (sag.) as wide (tr.) (range = 42–54%; n = 34); when plotted, the pygidial axis transverse width = 2.1762 pygidial axis sagittal length – 0.1054 (see remarks for discussion and Text-fig. 2.3B) comprising 19% total sagittal length of pygidium (range = 15–21%; n = 35); when plotted, the pygidial axis sagittal length = 0.1958 pygidial sagittal length – 0.0738 (see remarks for *E. agmen* for discussion and Text-fig. 2.3C); well impressed axial furrows. Pleural region gently vaulted in adaxial half, concave marginally. Median rib always bifid for at least one-quarter of its length (sag.), but amount of bifurcation is variable: longer bifurcation less distinct anteriorly (Pl. 3, fig. 11). Faint median carina may be present anterior of bifurcation (Pl. 3, fig. 13). Median rib twice width of pleural ribs where it reaches posterior margin. Clearly

impressed and almost straight pleural furrows; both furrows and ribs widen towards margins, furrows deeper anteriorly. Ribs with low transverse convexity and furrows terminating very close to margin or reaching it. Pleural region with closely spaced terrace ridges trending transversely across each rib. Doublure very broad, almost three quarters total pygidial sagittal length; ribs and furrows mirror those on ventral surface and bear persistent terrace ridges which become increasingly scalloped marginally. Maximum pygidial sagittal length measured 34.46 mm.

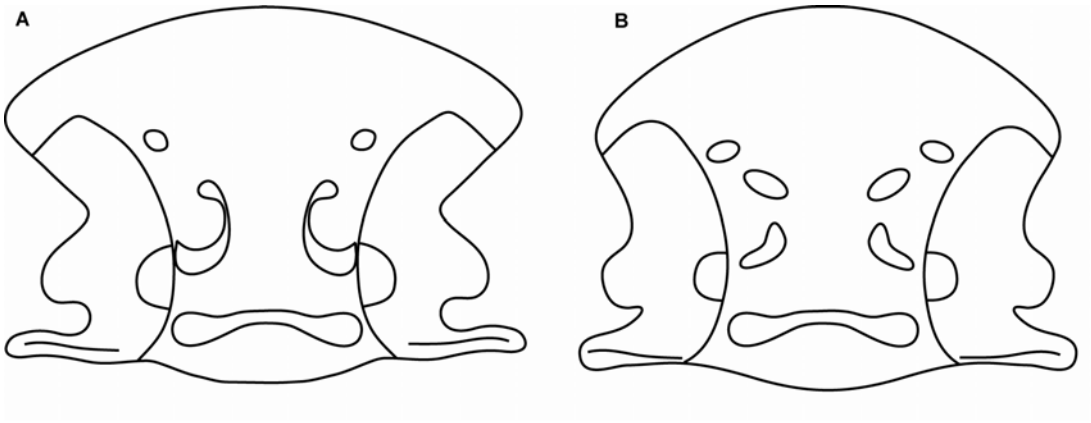

Text-fig. 2.4. Line drawings of cranidia of **A.** *Jungosulcus emilyae* and **B.** *Jungosulcus anaphalantos*, highlighting morphological differences between the two species.

Remarks. Jungosulcus emilyae shares similarities with *Kosovopeltis*. The type species of *Kosovopeltis*, *K. svobodai* Šnajdr, 1958 from the Ludlow Kopanina Formation, Czech Republic, figured by Šnajdr 1960 (pl. 2, figs 3–6; pl. 3, figs 1–16, 18–26; pl. 4, figs 1–2) has a similar cranidial morphology to *J. emilyae*. In particular, the shape of the anterior margin, course of the axial furrows, and position of the lateral glabellar muscle impressions are comparable. The most obvious difference between the two cranidia is the shape of the lateral glabellar muscle impressions, with S2 and S3 in *J. emilyae* subcircular (Text-fig. 2.4A), as opposed to the transversely elongate S2 and

S3 of *K. svobodai*. Additionally, *J. emilyae* exhibits an exsagittally connected S1 and S2. The pygidia of *J. emilyae* and *K. svobodai* are similar also, especially in their outline and form of the pygidial axis. In *K. svobodai* the pygidial axis constitutes more of the entire pygidial length, and the median rib lacks a clear bifurcation. *J. emilyae* also shares cranidial similarities with *Decoroscutellum.* The cranidium of the type species of *Decoroscutellum*, *D. haidingeri* Šnajdr, 1958, from the Ludlow Kopanina Formation, Czech Republic, figured by Šnajdr 1960 (pl. 5, figs 10–12, 14; pl. 6, figs 5–12) has a similar anterior marginal shape, and course of the axial furrows. The lateral glabellar muscle impressions are similarly deeply impressed and positioned, but S2 and S3 are slightly more transversely elongate in *D. haidingeri*. The resulting straight line equations for pygidial width against pygidial length, and for pygidial axial width against pygididal axial length, clearly distinguish *J. emilyae* from *E. agmen* and *P. magnifica*. The width of both the pygidial axis and the pygidium of *J. emilyae* increase at a faster rate with increasing length than for *E. agmen* and *P. magnifica* (Text-fig. 2.3).

Occurrence and distribution. Central Peary Land (CPL1, CP3).

Jungosulcus anaphalantos gen. et sp. nov.

Plate 4, figures 1–13; Text-fig. 2.4B

Derivation of name. Greek, *anaphalantos*, with bald forehead, alluding to the gradual effacement of the anteriormost lateral glabellar muscle impressions with growth.

Holotype. MGUH38 (Pl. 4, figs 1–3) cranidium; GGU locality 298930 (SNL1).

Figured paratypes. Locality SNL1: MGUH39–41 cranidia; MGUH42 librigena; MGUH43 hypostome; MGUH44–49 pygidia.

Diagnosis. Jungosulcus with anterior lateral glabellar muscle impressions increasingly effaced with growth; cranidial axial furrows terminating at anterolateral border furrow; occipital impressions not connected to axial furrow; median pygidial rib bifid only on smaller specimens, replaced by carina in larger ones.

Description. Cranidium subelliptical; a little wider (tr.) posteriorly between fulcral sockets as at anteriorly between anterolateral margins. Width across β–β and δ–δ roughly equal; width (tr.) across γ–γ subequal to cranidial sagittal length. Cranidium 82% as long (sag.) as wide (tr.) across palpebral lobes (δ–δ), (range = 71–92%; n = 11); maximum height of glabella at level of S3. From posterior margin, axial furrows converge anteriorly until just posterior of S1 where lunettes positioned. Axial furrows continue anteriorly with a smooth trajectory; diverging forwards remaining well impressed until they become shallower between S2 and S3; intersecting anterolateral border, where they have a similar depth of impression to anterolateral border. Glabella almost twice as wide (tr.) there than at its narrowest point (average = 1.9 times; range = 1.7–2.0; n = 12). S1 adjacent to axial furrow; most deeply impressed and largest of lateral glabellar muscle impressions; comma-shaped. S2 and S3 shallow and increasingly effaced in larger specimens; S2 subequal in size to S1, an obliquely directed ellipse; S3 the smallest impression, a transversely directed ellipse. S2 located roughly equidistant between S1 and S3, and is furthest from the axial furrow. Anterior cephalic margin not significantly raised, bounded by moderately impressed anterolateral border furrow. Shallow furrow present just anterior of eye ridge,

corresponding to librigenal inner furrow. Occipital ring with lower convexity than glabella and longest medially where almost twice as long (sag.) as abaxially; comprising 21% total cranidial sagittal length (range = 18–24%; n = 14). Occipital furrow broad, less impressed than axial furrow; abaxially terminating at subcircular occipital impressions.

Raised palpebral lobe forming highest point of fixigena; lunettes oval, weakly impressed, located opposite posterior half of palpebral lobe. Eye ridge meeting axial furrow between S2 and S3.

Cranidial sculpture strongest anterior of anterolateral border furrows, there comprising transversely trending, fairly continuous terrace ridges; weaker, less continuous, and more closely spaced transversely trending terrace ridges present elsewhere on cranidia, these are strongest on occipital ring where they are medially bowed anteriorly. Some pitting evident on fixigena.

Librigena subtriangular and of low convexity. Deepest furrow bounding eye; outer and inner librigenal furrows very shallow. Lateral margins slightly raised, most so anteriorly, forming lateral border. Sculpture of transversely trending, fairly continuous terrace ridges.

Hypostome of typical shield-shaped scutelluid type. 78% as long (sag.) as wide (tr.) across anterior wings. Anterior lobe of middle body subcircular; posterior lobe short (sag., exsag.), not inflated. Prominent maculae bounded by deep middle furrow; better impressed than border furrows. Posterior border longest (sag.) adaxially; lateral borders narrower (tr.) than this posterior of shoulders. Hypostome except for maculae covered in pronounced, continuous terrace ridges which trend roughly transversely across middle body, and run parallel with border furrows on lateral and posterior borders.

Pygidium is very similar to *J. emilyae* so that description is best achieved by supplying measurements to compare proportions and noting points of difference. Pygidium 64% as long (sag.) as wide (tr.) (range = 60–69%; n = 12); axis 44% as long (sag.) as wide (tr.) (range = 38–50%; n = 24); axis comprising 18% total sagittal length of pygidia (range = 16–21%; n = 12); only smaller specimens have a median rib which is bifid, and this is only posteriorly and for a small proportion of its length (Pl. 4, fig. 10). Median carina is always present. Maximum pygidial sagittal length measured 17.5 mm.

Ontogeny. J. anaphalantos exhibits gradual effacement of anteriormost glabellar muscle impressions with increasing size (Pl. 4, fig. 5), accompanied by loss of bifurcation of the median pygidial rib (Pl. 4, fig. 12).

Remarks. J. anaphalantos is close to *J. emilyae*, especially in terms of pygidial morphology, only substantially differing by the loss of bifurcation of the median rib with growth. As such, the principal distinguishing characters all relate to the cephalon (Text-fig. 2.4 contains line drawings of the cranidia of the two species for comparison) with *J. anaphalantos* differing from *J. emilyae* as follows: the cranidium is longer (tr.) relative to its width (tr.) and less expanded (tr.) anteriorly; the axial furrows clearly intersect the anterolateral border furrow, and do not fade before meeting it as in *J. emilyae*; glabella is not as expanded anteriorly; the lateral glabellar muscle impressions shallow anteriorly, whereas the reverse is true for *J. emilyae*; and S1 and S2 are not exsagittally linked. In these respects, *J. emilyae* seems more derived than *J. anaphalantos.*

Occurrence and distribution. South Nares Land (SNL1).

Jungosulcus ventricosus gen. et sp. nov.

Plate 4, figures 14–20

Derivation of name. Latin, *ventricosus*, potbellied, bulging. This is the most convex species of *Jungosulcus*.

Holotype. MGUH48 (Pl. 4, fig. 14) cranidium; GGU locality 275038 (VGL1).

Figured paratypes. Locality VGL1: MGUH48–49 cranidia; MGUH50–51 pygidia.

Diagnosis. Convex species of *Jungosulcus* with S2 and S3 effaced; axial furrows maintaining depth of impression throughout course; occipital furrows well impressed, connected to axial furrows; pygidial median rib proximally merged to lateral pleural ribs five, six and seven.

Description. Cranidium subelliptical; slightly wider (tr.) posteriorly between fulcral sockets than anteriorly between anterolateral margins, width across β–β and δ–δ of roughly equal. Width (tr.) across γ–γ roughly equal to cranidial sagittal length. Cranidium just over four-fifths as long (sag.) as wide (tr.) across palpebral lobes at δ–δ. Maximum height in anterior portion of glabella. Axial furrows well impressed, terminating at short (exsag.) anterolateral concave zone; anterolateral border furrow not clearly demarcated. From posterior margin, axial furrows converge anteriorly until intersection with lunettes (roughly two-thirds total cranidial sagittal length from

anterior margin) where they are deflected adaxially; anterior of lunettes, diverging anteriorly with a smooth trajectory and maintaining depth of impression. Glabella roughly twice as wide (tr.) anteriorly as at narrowest point. S1 close to but not connected to axial furrow; moderately impressed, bowl-shaped under median node (Pl. 4, figs 14–15). S2 and S3 effaced. Anterolateral border shorter (exsag.) than anterolateral concave zone; medially, anterior cranidial margins not raised; terrace ridges present for roughly most anterior 20% of total cranidial sagittal length. Terrace ridges strongest and continuous anteriorly, becoming more broken and then fading posteriorly. Occipital ring convex, longest sagittally where comprises 18% (n = 2) total cranidial sagittal length. Occipital node at midpoint of occipital ring length (sag.). Occipital furrows abaxially widening at occipital impressions. Occipital ring bears transversely trending, irregular and discontinuous terrace ridges.

Lunettes subcircular, extending from posterior of palpebral lobe, shorter (exsag.) than palpebral lobe. Eye ridge strong. Regularly spaced, discontinuous terrace ridges trend transversely across fixigena.

Librigena subtriangular and of low convexity. Inner and outer librigenal furrows equally well impressed, increasingly so anteriorly. Outer furrow wider (tr.) than inner furrow which sweeps around visual surface, anteriorly converging towards outer furrow. Short (exsag.), broad (tr.) genal spine present. Transversely trending terrace ridges.

Pygidium a truncated ellipse, 65% as long (sag.) as wide (tr.) (range = 63–70%; n = 8). Maximum pygidial width at anterior of first pleural rib. Axis triangular with well impressed axial furrows. Axis 47% as long (sag.) as wide (tr.) (range = 42–54%; n = 8), comprising 18% total pygidial length (sag.) (range = 15–21%; n = 8). In lateral view, pygidium smoothly convex; maximum convexity approximately halfway

along sagittal length. Median rib roughly twice width (tr.) of lateral pleural ribs at posterior margin. Pleural furrows clearly impressed, deepest anteriorly. Ribs transversely convex; wider towards margin, which they intersect. Sculpture comprising regularly spaced, transversely trending terrace ridges; mostly continuous across individual pleural ribs and axis. Doublure extending a little over two-thirds total pygidial sagittal length. Ribs and furrows mirror those on the ventral surface, covered in persistent terrace ridges which become increasingly scalloped marginally. Maximum pygidial sagittal length measured 12.39 mm.

Remarks. J. ventricosus differs from both *J. emilyae* and *J. anaphalantos* in: a more convex cranidium and pygidium; axial furrows maintaining depth of impression throughout course; shorter (exsag.) anterolateral border; glabella more anteriorly expanded, so the cephalon is slightly longer (sag.) relative to width (tr.); greater convexity of pygidial pleural ribs; maximum pygidial width located at anterior, as opposed to midlength of first pleural rib; median pygidial rib merged to lateral pleural ribs five, six and seven. In addition, *J. emilyae* and *J. anaphalantos* both appear to lack an occipital node, although this is possibly preservational.

Occurrence and distribution. Valdemar Glückstadt Land (VG1).

Genus MEROPERIX Lane, 1972

Type species. By original designation; *Meroperix ataphrus* Lane, 1972 (p. 343, pl. 60, figs 1–12), from the Telychian Samuelsen Høj Formation of Kronpins Christians Land, eastern North Greenland. Latitude and longitude 22^{o} 20’ W, 80^{o} 13’N.

Diagnosis. After Lane (1972, p. 343): scutelluid with glabella narrowing forward over posterior half; anterior border and preglabellar furrow laterally distinct and very short (exsag.) not present over medial three-fifths of frontal lobe. Pygidium of low convexity, axis about twice as wide (tr.) as long (sag.), occupying about one-fith pygidial sagittal length; seven pairs of weakly convex pleural ribs and median rib wholly bifid in large holaspides; only the posterior three-fiths bifid in smaller specimens.

Meroperix ataphrus Lane 1972

Plate 5, Figure 1

Figured material. MGUH52 pygidium, GGU 275038 (VG1).

Remarks. A fragmentary pygidium is assigned to *Meroperix ataphrus*. The length to width ratio of approximately 2:3, low pygidial convexity, and transversely oval morphology, distinguish the specimen from *Ekwanoscutellum* despite the absence of the pygidial axis.

Occurrence and distribution. Valdemar Glückstadt Land (VGL1).

Genus OPOA Lane, 1972

Type species. By original designation; *Opoa adamsi* Lane, 1972 (p. 341, pl. 59, figs 1–10), from the Telychian Samuelsen Høj Formation of Kronpins Christians Land, eastern North Greenland. Latitude and longitude 22^{o} 20’ W, 80^{o} 13’N.

Diagnosis. After Lane (1972, p. 340): scutelluid with lateral glabellar muscle impressions adjacent to axial furrow; S1 largest and bordering S2; S3 closer to S2 than to the anterior border. Narrow anterior border and weak preglabellar furrow extend along whole frontal lobe, but best developed anterolaterally. Pygidium and pygidial axis both wider than long. Pygidial axis inflated, highly convex blunted triangle comprising one-fifth sagittal length of pygidium. Median rib bifid for most of its posterior half. Maximum convexity of pygidium halfway between axis and margins, creating a humpback profile.

Remarks. Lane proposed the genus based on cranidia and pygidia and stressed the distinguishing features to be the arrangement of the glabellar muscle impressions, the presence of an anterior medial pit and the distinctive honeycomb sculpture. Lane (1988, p. 96) noted that the sculptural features of *O. adamsi* are superficial and the most important distinguishing characters of the genus are those relating to the axis, particularly the position of the lateral glabellar muscle impressions.

As sculpture only has specific importance within this genus, it is not a suitable character upon which to identify specimens of *Opoa*, and as such it is removed from the diagnosis. Subsequent recognition of other characters from the original diagnosis in other scutelluid taxa here described, for example the anterior median depression, have resulted in the removal of these also.

Opoa regale (Fritz, 1964), Ludvigsen 1979, p. 69, fig. 46c, from Silurian glacial drift, Hudson Bay area, Northern Ontario, and *Opoa ostreata* Lane, 1988 (p. 95, pl. 1, figs 1–12) , from the Wenlock of Peary Land, Eastern North Greenland, are now placed in *Periostrix* gen. nov.

Norford, 1981, p. 7, pl. 1, 10–13, figured an *Opoa* sp. from the Telychian–?early Wenlock Attawapiskat Formation, Ontario. A fragmentary pygidium displays the characteristic inflated nature of the axis.

Opoa limatula sp. nov.

Plate 5, figures 2–15

Derivation of name. Latin, *limatulus*, somewhat filed, polished, smoothed, alluding to the lack of the tubercular sculpture as found in other species belonging to the genus.

1991 *Kosovopeltis allaarti* Lane; Lane and Siveter, p. 7, fig. 2a–b.

Holotype. MGUH53 (Pl. 5, figs 2–3) cranidium; GGU 274689 (CPL5).

Figured paratypes. Locality CPL5: MGUH55 cephalon; MGUH54, 56 cranidia; MGUH57–61 pygidia.

Diagnosis. Opoa with pygidial margins smoothly curved and a sculpture of terrace ridges.

Description. Cephalon semicircular; of roughly equal width posteriorly between fulcral sockets as at anteriorly between anterolateral margins; width across β–β and δ–δ roughly equal. Width (tr.) across γ–γ roughly equal to cranidial sagittal length. Cranidium just over four-fifths as long (sag.) as wide (tr.) across palpebral lobes at δ–δ, roughly 33% as high as long (sag.). Highest point of cranidium in anterior part of

glabella. Where preservation permits, subdued median carina apparent (Pl. 5, fig. 2). Cranidial sagittal length 88% width (tr.) across palpebral lobes (range = 77–99%; n = 5). Glabella parallel sided for its posterior 49% (range = 45–50%; n = 4); between S1 and S2, axial furrows suddenly change course and diverge rapidly forward at 44–47 degrees (n = 4) to an exsagittal line, reaching maximum width (tr.) where intersects anterolateral border furrow; there, glabella 2.14 times wider (tr.) than at its narrowest point (range = 2–2.2%; n = 5). Occipital ring highest posteriorly and longest sagittally, where 38% as long (sag.) as wide (tr.) (range = 37–40%; n = 4). Narrow (sag.), deeply impressed occipital furrow. Abaxially, occipital ring shortens (exsag.) to accommodate large occipital impression. Narrow (sag., exsag.) anterior border and preglabellar furrow extend along whole frontal lobe; both very weak medially. Abaxially, preglabellar furrow becomes deeper and wider. S1 most impressed of lateral glabellar muscle impressions; reniform, with median node. S2 in very close proximity to S1; sub-square. S3 transversely directed ellipse, further from S2 than S2 is to S1. S2 and S3 of comparable size. Whereas S1 is connected to axial furrow, S2 and S3 are distinct from it (Pl. 5, figs 4–5). Sculpture of persistent terrace ridges; following curvature of anterior margin, trending transversely, most pronounced along anterior of glabella, fading posterior of S2. Largest cranidial sagittal length measured 12.13 mm.

Fixigena with palpebral lobe extending from anterior of occipital muscle impression to posterior of S1; lunette from opposite anterior of occipital muscle impression to posterior of S1. Eye ridge trending towards axial furrow near S3. Sculpture of terrace ridges trending transversely.

Librigena with narrow outer librigenal furrow most pronounced anteriorly. Outer librigenal furrow shallow, continuing through to short genal spine. Inner

librigenal furrow deeply impressed, gently converging towards outer librigenal furrow anteriorly.

Pygidium an anteriorly truncated ellipse with smoothly curved margins, 86% as long (sag.) as wide (tr.) (range = 80–96%; n = 6). Axis faintly trilobed, with well impressed axial furrows. Axis comprising 21% entire sagittal length of pygidium (range = 20–24%; n = 7). Anterior (maximum) width of axis 71% its sagittal length (range = 58–77%; n = 6). Pleural region slopes upwards (tr. and sag.) abaxially, until a point approximately half way from the margins, from which it slopes downwards (tr. and sag.) abaxially. At posterior margin, bifid median rib is twice width of pleural ribs at margins. Pleural ribs smoothly transversely convex. Pleural furrows and ribs widen towards margin; furrows fainter approaching margin. Sculpture of transversely trending, short terrace ridges covering pleural region and axis. Doublure extending half way to axis, with well impressed ribs and furrows mirroring dorsal surface. Well developed terrace ridges become increasingly scalloped towards margins. Maximum pygidial sagittal length measured 24.5 mm.

Remarks. The type species of *Opoa*, *O. adamsi*, is a very distinctive scutelluid, particularly because of its honeycomb sculpture and scalloped pygidial outline. These features are superficial, however. Similarities in shape and arrangement of the glabellar muscle impressions, and the inflation and form of the pygidial axis, are deemed particularly important in diagnosing *O. limatula*. The shape of the glabella, and the relative proportions of both the pygidia and axis, are considered important diagnostic features also. *O. limatula*, as well as lacking the distinctive sculpture and pygidial outline of *O. adamsi*, differs in the absence of an anterior medial pit. The specimen referred to as *Kosovopeltis allaarti* by Lane and Siveter (1991, fig. 2a-b) is

recognised as *O. limatula* due to the inflated nature of the pygidial axis and the proportions of both the pygidium and pygidial axis.

Occurrence and distribution. Central Peary Land (CPL5) and Kronprins Christian Land (KCL1).

Opoa sp.

Plate 5, figures 16–19

Figured material. MGUH62–63 pygidia, GGU 275015 (KCL1).

Description. Margins smoothly curved; pygidium 0.88 times as long (sag.) as wide (tr.); pygidial height roughly 21% of length (sag.) with axis and vaulted part of pleural region highest points. Axis roughly as long (sag.) as wide (tr.) at most anterior point, and one-quarter entire sagittal length of pygidium. Axial furrows well impressed. Pleural region sloping upwards (tr. and sag.) abaxially towards anterior for anteriormost half, posterior of this slopes downwards (tr. and sag.) abaxially. Median rib bifid posteriorly for roughly 40% of its entire length (sag.). Furrows and ribs both widen and shallow towards margins, which they intersect. Sculpture of pronounced, irregularly spaced turbercles covering entire pygidium. Doublure extending under half sagittal length, well impressed ribs and furrows and defined terrace ridges, becoming increasingly scalloped towards margins.

Remarks. The specimens are assigned to *Opoa* because of the inflated form of the axis and the humpback profile. Compared with the type species, *O.* sp. differs in having a

smoothly curved margin, not a scalloped one, and in the relatively longer (sag.) axis. The tubercles of *O.* sp. are reminiscent of *O. adamsi*, *O. regale* (Fritz, 1964) and *Opoa* sp. (Norford, 1981).

Occurrence and distribution. Kronprins Christian Land (KC1).

Genus PERIOSTRIX gen. nov.

Derivation of name. Contraction of Greek, *periosios*, immense, and Latin, *strix*, furrow, channel, groove, flute, alluding to the long (sag.) anterolateral concave zone of the genus. Gender feminine.

Type species. Designated herein; *Scutellum magnificum* Teichert, 1937, p. 148, pl. 21, fig. 6, from the Telychian Offley Island Formation, St. George Fjord, North Greenland.

Other species. Opoa ostreata Lane, 1988, from the Telychian Odins Fjord Formation of Peary Land, North Greenland.
Opoa regale (Fritz, 1964), Ludvigsen 1979, p. 69, fig. 46c, from Silurian clasts in glacial drift, Hudson Bay area, Northern Ontario.

Diagnosis. Scutelluid with lateral glabellar muscle impressions S1 and S2 adjacent; S1 connected to, and S2 and S3 close to, but separate from, axial furrow; narrow anterior border and preglabellar furrow strongest laterally; long (exsag.), well impressed anterolateral concave zone; pygidial length roughly equal to width and low

convexity lateral profile; pygidial axis flattened; median rib a little wider (tr.) than lateral pygidial ribs at intersection with margins, and faint bifurcation mostly confined to ventral surface.

Remarks. Teichert (1937, p. 148) proposed the species *Scutellum magnificum* based on a single pygidium (pl. 21, fig. 6, MGUH 4375) which is here designated the holotype (Pl. 6, fig. 16) from the Offley Island Formation (Telychian) from St. George Fjord, North Greenland. This pygidium is considered conspecific with material here described from western Peary Land: pygidial proportions, axial morphology and the non-bifid median rib are particularly comparable. The pygidium is covered in tubercles and is convex, features which are present ontogenetically in this species.

Teichert assigned another pygidium (pl. 21, fig. 5, MGUH 4374) from Kûk, mouth of Thomsen River, Duke of York Bay, northern Southampton Island to *Scutellum magnificum* with some uncertainty. I have studied the pygidium (Pl. 6, fig. 17), and although it is fragmentary, its proportions and sculpture confirm its assignment to *Periostrix magnifica*.

In cranidial morphology, particularly the arrangement of the glabellar muscle impressions, this genus is close to *Opoa*. The most notable cephalic differences are that the anterior border and furrow medially are weaker in *Periostrix*, and the anterolateral concave zone is longer (exsag.). The pygidium of *Periostrix* is proportionally longer than that of *Opoa*, is flatter in lateral profile, and lacks the inflated axis of *Opoa*. *Opoa regale* is assigned to *Periostrix* gen. nov. due to its long (sag.) anterolateral border, pygidium which is roughly as long as wide, and pygidial axis which does not display the inflation characteristic of *Opoa*.

Periostrix magnifica (Teichert, 1937)

Plate 6, figures 1–17; Plate 7, figures 1–8

1937 *Scutellum magnificum* Teichert, p. 148, pl. 21, fig. 6.

Holotype. MGUH 4375 (Pl. 6, fig. 16) pygidium; St. George Fjord.

Figured specimens. Locality WL: MGUH69 cephalon; MGUH65–66 cranidia; MGUH72 hypostome; MGUH77 pygidium. Locality WPL1: MGUH67–68 cranidia; MGUH70 rostral plate; MGUH71 librigena; MGUH73–75, 78 pygidia. Locality WPL2: MGUH64 cranidium; MGUH76 pygidium. Locality: Kûk, mouth of Thomsen River, Duke of York Bay, northern Southampton Island: MGUH 4374 pygidium.

Diagnosis. As for genus.

Description. Cephalon semicircular, almost twice as wide (tr.) as long (sag.) Highest point in anterior part of glabella. Cranidium of approximately equal width posteriorly and anteriorly, wider across β–β than δ–δ. Width (tr.) across palpebral lobes at δ–δ a little greater than sagittal length of cranidium (89% as long as wide; range = 81-97; n = 15); width (tr.) across γ–γ slightly less than cranidial sagittal length. Posterior half of glabella parallel-sided, anterior part expanding rapidly forward anterior of S1 at 35–40 degrees (n = 3). Anterior course of axial furrow smoothly curved, intercepting anterolateral border furrow where glabella is just over twice posterior width (tr.) (2.17 times wider than at its narrowest part (range = 2.01–2.53; n = 10). Facial suture positioned closer to axial furrow at α than at γ. Occipital ring 41% as long (sag.) as

wide (tr.) (range = 36–44%; n = 12); slopes forwards; just over twice as long sagittally as exsagittally. Occipital furrow strongly impressed; occipital impression large. Anterior border and preglabellar furrow variably expressed medially. Glabellar muscle impression S1 largest, most impressed, ovoid, with median node. S2 and S3 transversely elongate, of comparable size; S3 positioned further from S2 than S2 is from S1. All impressions adjacent to axial furrow. Sculpture comprises transversely trending terrace ridges following anterior margin convexity; only present anterior of lateral glabellar muscle impressions. Maximum cranidial sagittal length measured 32.72 mm.

Fixigena with palpebral lobe located between occipital furrow and S1. Lunettes oval, located between occipital furrow and S1. Eye ridge intersecting axial furrow near S3. Anterior portion of fixigena with transversely trending terrace ridges; posterior to eye ridge with pronounced elongate pits on internal moulds (Pl. 6, fig. 6) and irregular obliquely trending terrace ridges on external moulds (Pl. 6, fig. 1).

Librigena with prominent lateral border, narrowing (tr.) posteriorly. Outer furrow well impressed, wide (tr.); inner furrow sharply defined, directed in line with lateral border, so intersecting axial furrow at a distance from fixigenal equivalent of the outer furrow. Visual surface comprises roughly quarter of entire sagittal length of cephalon excluding genal spine. Librigena terminating in slender genal spine, comprising roughly 20% total cephalic sagittal length; terrace ridges converging towards tip of spine. Internal moulds with deeply impressed genal terrace ridge whorl on doublure (Pl. 6, fig. 14).

Rostral plate with slightly curved connective sutures diverging at 40–50 degrees. Sculpture of regularly spaced, continuous terrace ridges trending transversely.

Hypostome typical for the subfamily; subtriangular, with posterior margin terminating in blunted point. Total sagittal length roughly 80% of width (tr.) across anterior wings; short posterior lobe of middle body; prominent maculae, with midpoint located about halfway along hypostome length; posterior border longer (sag.) than lateral border is wide (tr.). Prominent terrace ridges cover entire hypostome, medially trending transversely, abaxially following line of borders.

Pygidium an anteriorly truncated ellipse with smoothly curved margins, 92% as long as wide (range = 61–111%; n = 20); when plotted, the pygidial transverse width = 0.8745 pygidial sagittal length + 2.7535 (see remarks for discussion and Text-fig. 2.3A); with maximum width close to anterior margin. Pygidial axis a flattened, blunted triangle; 91% as long as wide (range = 67–109%; n = 48); when plotted, the pygidial axis transverse width = 1.1127 pygidial axis sagittal length - 0.0328 (see remarks for discussion and Text-fig. 2.3B), and comprising 23% entire pygidial sagittal length (range = 19–28%; n = 29); when plotted, the pygidial axis sagittal length = 0.2099 pygidial sagittal length + 0.2296 (see remarks for *E. agmen* for discussion and Text-fig. 2.3C); faintly trilobate; well impressed axial furrows. Pleural ribs with low transverse convexity, sigmoidal, widen towards margins, which they intersect. Pleural furrows narrow and distinct proximally, becoming slightly weaker and wider marginally. From axis, median rib narrowing for about one-third its length, after which it widens. Sculpture of weak, discontinuous terrace ridges present only near posterior and lateral margins. Pygidial doublure with prominent terrace ridges; progressively scalloped towards margins. Maximum pygidial sagittal length measured 59.06 mm.

Variation not accounted for by ontogeny.

1. The extent of the anterior border and preglabellar furrow is very variable and is not correlated with specimen size. They may be present for all, or as little as half of the anterior cranidial width (tr.). When a particularly well developed anterior border is present, a median anterior depression is apparent.
2. The median rib is most commonly non-bifid on the dorsal surface. Ventrally, either a faint ridge is present, or the terrace ridges on the doublure are distorted medially (Pl. 7, fig. 3); this is rarely expressed as a furrow on the dorsal surface as a true bifurcation (Pl. 7, fig. 5).

Ontogeny. Important changes with growth of this species are as follows:

1. Pygidia become progressively proportionally longer with growth; the smallest pygidia are a little wider than long; the larger pygidia are a little longer than wide (pygidial sagittal lengths average 78% of pygidial transverse width in the five smallest specimens, compared to 105% in the five largest specimens).
2. The pygidial axis becomes proportionally longer with respect to its width with growth; pygidial axis sagittal lengths average 79% of pygidial axis transverse width in the five smallest specimens, compared to 91% in the five largest specimens.
3. Smaller pygidia are convex (Pl. 7, fig. 8) and decrease in convexity with increasing size to eventually reach a flattened profile (Pl. 7, fig. 2). Cephala display a similar reduction in convexity with growth.
4. The gradual replacement of a sculpture comprising a complete covering of irregularly spaced turbecles (Pl. 7, figs 7–8), by terrace ridges present marginally (Pl. 7, fig. 3). This type of change in sculpture with ontogeny is

very common in scutelluids and is also well seen in material from the Silurian (Wenlock/Ludlow) of Orange, New South Wales, Australia (Dr P.D. Lane, pers. comm. 2009).

Remarks. P. magnifica is closest to *P. ostreata*. There are striking similarities in terms of cephalic morphology: the course of the axial furrows which terminate in a broad, anterolateral concave zone and the position of the lateral glabellar muscle impressions. The most obvious differences are the greater anterior and dorsal glabellar expansion of *P. ostreata*, resulting in a more convex glabella. The morphology of smaller pygidia belonging to *P. magnifica* is remarkably similar to *P. ostreata* specimens of comparable size in terms of their outline, ratios and axial morphology. The most obvious differences are the lack of bifurcation of the median rib in *P. ostreata*, and the relative widths of the median rib at the margins: that of *P. ostreata* is twice as wide as that of *P. magnifica*. The sculpture of *P. magnifica* shares the following ontogenetic similarities with *P. ostreata*: both have terrace ridges covering the cephalon which are shortest on the librigena, and the pygidia bears tubercles on the pleural regions and short terrace ridges on the margins.

The pygidium of *P. magnifica* resembles that of *Ekwanoscutellum* in terms of its relative proportions and large size; however, the lower convexity of the pygidium of *P. magnifica*, combined with a posteriorly narrower median rib, and significant changes in sculpture with ontogeny distinguish it. The resulting straight line equations for pygidial axial width against pygidial axial length of *P. magnifica* and *E. agmen*, are very similar for the two species (Text-fig. 2.3B). Conversely, the straight line equations for pygidial width against pygidial length show the width of the pygidium

to increase at a slower rate with increasing length for *P. magnifica* than for *E. agmen* (Text-fig. 2.3B).

Occurrence and distribution. Western Peary Land (WPL1–2), south Nares Land (SNL1–2) and Wulff Land (WL).

Genus aff. *Periostrix*

Plate 7, figures 9–14

Figured material. MGUH79–80 cranidia, MGUH81–82 pygidia, GGU 225793 (KCL2).

Description. Posterior half of glabella parallel-sided, slightly wider (tr.) across occipital ring. At anterior end of S1, axial furrow displays angular change in course, trending roughly 45 degrees from an exsagittal line; well impressed throughout course. Prominent anterior border, increasing in length (exsag., sag.) medially; anterior median depression present. Anterior border furrow progressively shallowing and lengthening (sag., exsag.) abaxially to form a long (exsag.) anterolateral concave zone; fixigenal equivalent of the inner librigenal furrow positioned further posteriorly than seen elsewhere and separated from anterolateral concave zone. S1 large, about same size as well impressed occipital impression. S2 about one-quarter the size of S1 and shallower; a transversely directed oval shape; positioned directly anterior of S1, not connected to axial furrow. S3 positioned much further anteriorly of S2, than S2 is of S1; similar in size to S2 and close to axial furrow. Lunettes oval, subequal in size to S1, positioned from occipital furrow to just posterior of S1. Eye ridge intersecting

axial furrow just anterior of S2. Sculpture of discontinuous, short, transversely trending terrace ridges; fixigena pitted.

Pygidia measuring 4.67 and 5.31 mm sagittal length, both 72% as long (sag.) as wide (tr.) with maximum width just anterior of first pleural furrow. Axis a blunted triangle, pinched inwards at roughly half length (exsag.); larger specimen with axis 61% as long (sag.) as wide (tr.), comprising 27% pygidial sagittal length; smaller specimen with axis 58% as long (sag.) as wide (tr.), comprising 25% pygidial sagittal length. Median rib with almost straight pleural furrows; bifid for roughly its posteriormost 40%, terminating near margins like lateral pleural ribs, where about twice the transverse width of lateral pleural ribs. Larger specimen (Pl. 7, figs 13–14) with sculpture predominantly tuberculate, except for faint terrace ridges near edges. Smaller specimen (Pl. 7, fig. 12) with well spaced terrace ridges transversely trending across whole pygidium.

Remarks. The cranidia differ from those of other scutelluids by the positioning of the fixigenal equivalent to the inner librigenal furrow, which is clearly separated from the anterolateral concave zone. In cephalic morphology, the material is close to *Periostrix*, particularly with respect to the position of the lateral glabellar muscle impressions, however, S1 is more deeply impressed than in *Periostrix*, and the axial furrows exhibit a more angular change in course upon the point of glabellar expansion. The pygidia are assigned to the cranidia on the basis of their co-occurrence, and the differences in pygidial axis proportions and sculpture displaced by the two specimens are likely ontogenetic. The pygidia have significantly different proportions from those of *Periostrix*; they are most comparable in this respect to

Meroperix, although the position of greatest pygidial width (tr.) is positioned slightly more anteriorly.

Occurrence and distribution. Kronprins Christian Land (KCL2).

Scutelluid gen. indet.

Plate 7, figures 15–17

Figured material. MGUH83 cephalon, MGUH84 cranidium, MGUH85 pygidium, GGU 301318 (WPL1).

Description. Cranidium and cephalon measuring 4.10 and 4.58 mm sagittal length respectively. Cephalon 41% as long (sag.) as wide (tr.) across widest point along genal spine. Glabella of low convexity; slightly wider (tr.) at posterior of occipital ring than at occipital furrow where narrowest; widest (tr.) at anterior of axial furrow, where about twice as wide as posteriorly at narrowest point. Glabellar furrows predominantly straight and with steady anterior expansion along entire length of the glabella. Glabellar muscle impressions are roughly equidistant; S1 connected to axial furrow, kidney-shaped with a median node, and is the largest impression; S2 and S3 more oval in form and directed transversely, with S2 slightly wider (exsag.) and S3 more transversely slit-like. Occipital ring rapidly expanding (sag.) adaxially; there 37% as long (sag.) as wide (tr.). Anterior cephalic margin straight (tr.). Anterolaterally, very long (exsag.) concave zone present. Librigena convex adaxial to strong inner librigenal furrow. Between inner librigenal furrow and outer librigenal furrow, librigena is concave; narrow (tr.) lateral border. Genal spine slender, long

(exsag.) comprising 37% of cephalic sagittal length. Entire cephalon covered in coarse, dense tubercles; transversely trending terrace ridges present along anterior margin.

Pygidium measuring 6.06 mm sagittal length, about three quarters as long (sag.) as wide (tr.). Axis a posteriorly blunted triangle, 70% as long (sag.) as wide (tr.); both trilobed (tr.) and segmented (sag.); comprising about one-quarter total pygidial sagittal length. Pleural ribs widening towards margins; median rib pinching inwards proximally, and bifid for about half its length (sag.). Doublure present for at least half of pygidial sagittal length; with terrace ridges suddenly changing from fairly straight, to scalloped towards margins. Dorsal sculpture similar to that of cephalon, with tubercles of similar size and density; tubercles, however, bear central pores.

Remarks. The cephalic proportions, low convexity, and almost straight anterior margin, suggest that this material belongs to a juvenile scutelluid. The shape and positions of the lateral glabellar muscle impressions do not resemble those of any of the larger scutelluids described here. The coarsely tuberculate sculpture is reminiscent of some species of *Opoa*, but this character can change significantly throughout ontogeny.

Occurrence and distribution. Western Peary Land (WPL1).

Effaced Scutelluidae

Genus CYBANTYX Lane and Thomas *in* Thomas, 1978

Type species. By original designation; *Cybantyx anaglyptos* Lane and Thomas, 1978 *in* Thomas, 1978, from the Much Wenlock Limestone Formation, Dudley, West Midlands, U.K.

Diagnosis. Emended from Lane and Thomas *in* Thomas (1978, p. 18) to include their description of lateral glabellar muscle impressions: effaced scutelluid with pronounced anterior border furrow and short sharply upturned anterior border. Cranidial length (sag.) roughly equals width (tr.) across palpebral lobes. Cranidium with four pairs of glabellar muscle impressions; with S1 and occipital impression close together; S1 largest, but only slightly larger than occipital impression; S2 smallest; S2 and S3 transversely elongate. Occipital node placed close to posterior margin. Axial furrow impressed posterior of well impressed omphalus. Omphalus with median granule. Small anterolateral internal pit. Rounded genal angle. Pygidium with sagittal carina posteriorly.

Remarks. Ludvigsen and Tripp (1990) erected the genus *Paracybantyx* to distinguish their species, *P. asulcatus* from *Cybantyx*, due to its lack of an anterior border and border furrow. *Paracybantyx* has since been considered a junior subjective synonym of *Failleana* (Curtis and Lane 1997).

Adrain *et al.* (1995) considered the distinguishing morphological character of *Paracybantyx* to be a rostral plate lacking a posterior lobe and dorsal flange, and on

this basis assigned their Alaskan species *P. occidentalis* Adrain *et al*. (1995, p. 730, fig. 3, 1–12, 14, fig. 4) to the genus. The problems with this are twofold: firstly, a rostral flange is an upwardly turned structure, and both *P. occidentalis and C. nebulosus* sp. nov. have evidence for this. It is not associated with a posteromedially convex lobe as seen in the type species of *Cybantyx, C. anaglyptos*; secondly, as Adrain *et al*. noted, the rostral plate of the type species of *Paracybantyx, P. asulcatus,* is unknown, and the lack of a posterior lobe and instead the presence of a dorsal flange in the species, is presumed from the occurrence of these features in other Wenlock-Ludlow northern Laurentian illaenimorphs. In addition to this, Adrain *et al*. questioned the use of the anterior border as a diagnostic apomorphy. Here it is considered a readily identifiable and taxonomically important character; when no anterior border is present, the anterior margin has a much greater ventrally directed convexity. Accordingly, *P. occidentalis* is placed in *Cybantyx*; it has a definite anterior border as opposed to the ventral curvature of the anterior margin in *P. asulcatus*; its cranidial convexity is more comparable with *C. anaglyptos* than *P. asulcatus*.

Cybantyx nebulosus sp. nov.

Plate 8, figures 1–15; Plate 9, figures 1–10

Derivation of name. Latin, *nebulosus,* misty, cloudy, dark, indefinite, alluding to the difficulty of establishing the affinities of the species and genus.

Holotype. MGUH87 (Pl. 8, figs 4–5) cephalon; GGU 275689 (CPL5).

Figured paratypes. Locality CPL5: MGUH86 articulated specimen; MGUH94 articulated cephalon and thorax; MGUH88, 90–91 cephala; MGUH89, 92 cranidia; MGUH93 librigena; MGUH95–96 rostral plates; MGUH97–101 pygidia.

Diagnosis. Cybantyx with a rostral flange, sagittal cephalic carina, and cranidium as long (sag.) as wide (tr.).

Description. Cephala and cranidia ranging in sagittal length from 2.87–14.96 mm. Cephalon semielliptical; 79% as high as long (sag.), with maximum convexity in palpebral view opposite anterior of palpebral lobe. Cephalon 60% as long (sag.) as wide (tr.) (range = 53–69%; n = 7). Sagittal carina on internal moulds, extending from occipital node and fading out before anterior margin. Anterior margin upturned forming thin, pronounced, rim-like anterior border, border furrow even narrower (sag.). Cranidium 98% as long (sag.) as wide (tr.) across palpebral lobes (range = 87–107%; n = 22). From posterior margin, axial furrow anteriorly curves adaxially, intersecting lunette; there, positioned 76% of width apart (tr.) at posterior margin (range = 68–81%; n = 17). Lunette opposite mid-point of palpebral lobe; exsagittally directed oval, very well impressed on internal moulds, obscured on external moulds. Anterior of lunette, axial furrow curves abaxially, becoming gradually closer to facial suture and terminating at omphalus, where positioned 154% of width apart (tr.) at lunettes (range = 140–169%; n = 15). On internal moulds, axial furrow distinct throughout course, best impressed between lunette and omphalus. Axial furrows largely effaced on external moulds. Omphalus circular, no median granule apparent, clear on internal moulds, much fainter externally. Omphalus placed closer to facial suture than anterior margin (Pl. 8, fig. 11). Anterolateral internal pit smaller than

omphalus, only visible on internal moulds; slightly closer to anterior margin than to omphalus and placed a little more adaxially. Occipital node pronounced on interior moulds, much fainter on external moulds.

Lateral glabellar muscle impressions variably expressed within population; only visible on internal moulds and rarely clear. Occipital impression resembles two conjoined ovals, larger than lunette, and extending from occipital node to posterior of lunette. S1 extending from mid-point of lunette to anterior margin of palpebral lobe. Small reniform impression between occipital impression and S1. Anteriorly, muscle impressions situated progressively further from the sagittal line (Pl. 8, fig. 7).

External mould with laterally continuous, non-anastomosing terrace ridges, evenly spaced, running parallel to anterior margin, strongest at anterior margin, not extending posterior of anterior of palpebral lobe. Palpebral lobe comprising roughly one-quarter entire sagittal length, gently rounded, following curvature of cranidium with same convexity.

Librigena smoothly convex, gently rounded genal angle. Thin border present anteriorly. Finely pitted throughout, terrace ridges present near margins. Terrace ridges strongest and most evenly spaced anteriorly; weaker and increasingly shorter around genal angle.

Rostral plate with low convexity; maximum convexity where upturned to meet anterior margin. Connective sutures very slightly curved, diverging greatly. Posteromedial embayment on internal moulds (Pl. 9, fig. 1), indicating presence of upwardly turned rostral flange. This feature hidden by cuticle with regularly spaced, strong, continuous terrace ridges running parallel to anterior margin.

Pygidia ranging in sagittal length from 2.12–17.09 mm. Pygidium 69% as high as long (sag.), with maximum convexity approximately halfway along sagittal

length (extended view). Bluntly triangular in shape. Pygidium averaging 82% as long as wide (range = 73–89%; n = 41); when plotted, the pygidial transverse width = 1.1535 pygidial sagittal length + 0.6654 (see remarks for discussion and Text-fig. 2.5). Sagittal carina variably preserved; most commonly just over half sagittal length of pygidium, but may be absent or present for most of sagittal length. Holcos well developed; best developed anterolaterally. Abaxial end of articulating facet located roughly one-third total pygidial length (sag.) from anterior margin (medially). Pair of swellings on internal moulds, representing muscle impressions, rarely preserved (Pl. 9, fig. 3); located equidistant from the sagittal line, opposite abaxial end of articulating facet. Cuticle obscures sagittal carina, with irregular, discontinuous terrace ridges trending transversely. Terrace ridges strongest at margins. Doublure approximately 25% sagittal length pygidium and constant thickness.

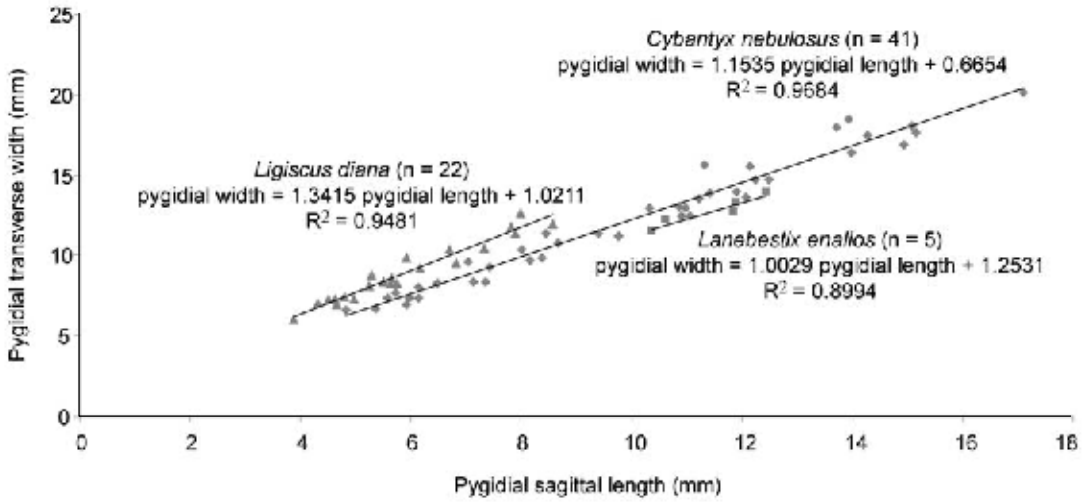

Text-fig. 2.5. Major axis regression of pygidial transverse widths against pygidial sagittal lengths.for *Cybantyx nebulosus*, *Lanebestix enalios* and *Ligiscus diana*.

Ontogeny. The pygidium of *C. nebulosus* becomes progressively longer with growth; pygidial sagittal lengths average 78% of pygidial transverse width in the five smallest specimens, compared to 85% in the five largest specimens.

Remarks. The size, shape and positions of the lateral glabellar muscle impressions of *C. nebulosus* are strikingly similar to those of the type species, *C. anaglyptos.* The small reniform impression situated between the occipital impression and S1 of *C. nebulosus* (Pl. 8, fig. 7), is intermediate between the separated occipital impression and S1 of *Cybantyx* and the conjoined form of *Bumastus*. The presence of a pronounced anterior border, well developed omphalus and sagittal pygidial carina, also reflect the generic placement for *C. nebulosus*.

The main differences between *C. nebulosus* and *C. anaglyptos* (Lane and Thomas, 1978 *in* Thomas, 1978, pl. 5, figs 1–8, text-fig. 3) are: the cephalon of *C. nebulosus* is roughly as long as wide, in *C. anaglyptos* it is 1.5 times as wide as long; the rostral plate of *C. nebulosus* bears a posteromedial embayment, presumably indicating the presence of an upwardly turned rostral flange, whereas the rostral plate of *C. anaglyptos* bears a broad-based rounded posteromedian projection; the pygidium of *C. nebulosus* is 82% as long as wide, whereas the pygidium of *C. anaglyptos* measures as long (sag.) as it is wide (tr.).

The cephalic morphology of *C. nebulosus* is most comparable to *C. occidentalis,* the main distinguishing features being: the cranidium of *C. nebulosus* is roughly as long (sag.) as wide (tr.) across palpebral lobes, in *C. occidentalis,* it is only 84% as long as wide; the lunettes of *C. nebulosus* are more compact and circular in form (in *C. occidentalis*, they are very elongate, comprising a greater exsagittal length), additionally the lunettes of *C. nebulosus* are positioned roughly at the

palpebral lobe midpoint, whereas those of *C. occidentalis* are positioned further posteriorly; the omphalus of *C. nebulosus* does not appear to have a median granule but this could be preservational.

The pygidium of *C. nebulosus* is typically illaenimorph and shows strong similarities to a variety of species, particularly to *C. occidentalis*, which is similar in length- to width- ratio. The main differences from *C. occidentalis* are that the abaxial end of the pygidial articulating facet of *C. nebulosus* is positioned further posteriorly, there is a wider (tr.) holcos, and *C. occidentalis* lacks a sagittal carina (possibly preservational).

As with the non-effaced scutelluids, reduced major axis regression has been employed to investigate its potential for the identification of effaced species (Text-fig. 2.5). Pygidial width was plotted against pygidial length for taxa with a reasonable sample size: *C. nebulosus* and *Ligiscus diana*. *Lanebestix enalios* is included also, although only five data points are available, the pygidia are superficially very similar to those of *C. nebulosus*. The resulting straight line equations for pygidial width against pygidial length clearly distinguish *C. nebulosus* from *L. diana*; pygidial width increases with length at a slower rate than for *L. diana*. Different straight line equations initially suggest that there are differences from *L. enalios* also, although more data are required to confirm this.

Occurrence and distribution. Central Peary Land (CPL1–5).

Cybantyx sp.

Plate 9, figures 11–16

Figured material. GGU 301319 (WPL1): MGUH102–103 cranidia; MGUH106 pygidium. GGU 301318 (WPL1): MGUH104 librigena; MGUH105 pygidium.

Description. Cranidia measuring 17.8 and 24.72 mm sagittal length; about as long (sag.) as wide (tr.) across palpebral lobes; about 54% as high as long (sag.), and with maximum convexity opposite palpebral lobe. Anterior margin upturned forming thin, pronounced, rim-like anterior border, and narrower (sag.) border furrow. Axial furrows distinct throughout course; from posterior margin, axial furrows converge strongly forwards until posterior end of palpebral lobe. From there, converging more subtly forwards until point just anterior of palpebral lobe, where furrows suddenly change course and diverge strongly forwards until intersecting omphalus which is sharply defined with no internal granule. Glabella at lunettes 74% width at posterior margin; glabella at omphalus 131% width opposite lunettes. Anterolateral internal pit present at about half distance between omphalus and internal margin, adaxial of omphalus. Lunettes oval (exsag.), extending for at least half length (exsag.) of palpebral lobe. Posteriormost lateral glabellar muscle impressions faintly impressed on one cranidium (Pl. 9, fig. 11–12): occipital impression extending from near posterior margin until posterior of lunettes; S1 oval (exsag.), extending from midpoint of lunettes to anterior end of palpebral lobe. Palpebral lobe comprising about 23% cranidial sagittal length. Terrace ridges present on anterior border.

Librigena with smoothly rounded genal angle; lateral border present, fading posteriorly approaching genal angle. Sculpture of fairly evenly spaced pits everywhere except lateral border which bears continuous, distinct terrace ridges.

Pygidium averaging 84% as long as wide (range = 83–87%; n = 3). Pygidial sagittal lengths ranging from 17.46–25.44 mm; pygidium about 24% as high as long (sag.), with maximum convexity approximately halfway along sagittal length (extended view). A blunted triangular shape. Very weak holcos.

Remarks. The cranidia and pygidia of *C.* sp. are both larger than the numerous cranidia and pygidia of *C. nebulosus* described. The axial furrows of *C.* sp are better impressed and begin to diverge forwards more anteriorly than in *C. nebulosus*, exhibiting a more sudden change in course; the glabella is slightly less anteriorly expanded; the lunettes are longer (exsag.) and the holcos is less well developed.

Detailed comparison of *C.* sp. and other species of *Cybantyx* is not appropriate given the limited material available for description, and the high variability of characters such as the sagittal carina and occipital node in any given population, as is demonstrated by *C. nebulosus*. As such, the material is left under open nomenclature.

Occurrence and distribution. Western Peary Land (WPL1–2) and south Nares Land (SNL2).

Genus LANEBESTIX gen. nov.

Derivation of name. For Dr P. D. Lane, studier of smooth trilobites, and who collected much of this material. Greek, *bestia*, beast, arbitrarily combined in the style of *Litotix.* Gender masculine.

Type species. By original designation; *Lanebestix enalios* sp. nov. from the Telychian Samuelsen Høj Formation, Valdemar Glückstadt Land, North Greenland.

Diagnosis. Effaced scutelluid with cephalon of lower convexity than pygidium, with a pronounced anterior border and short genal spine. Eye comprising roughly one-quarter total sagittal cephalic length (excluding genal spines) and placed its own sagittal length from posterior of cephalon. Pygidium 90% as long (sag.) as wide (tr.).

Remarks. The combination of a low convexity cephalon with short genal spines and a pronounced anterior border distinguish *Lanebestix* from other illaenimorphs. The eye is relatively short and is placed further anteriorly than in other illaenimorph taxa. The cephalon is less effaced than the pygidium; it is of lower convexity than the pygidium and possesses a short genal spine which has not been reduced to a rounded form as in most illaenimorph taxa.

Lanebestix enalios gen. et sp. nov.

Plate 10, figures 1–16

Derivation of name. Greek, *enalios*, in, on, of the sea, alluding to its streamlined morphology.

Holotype. MGUH107 (Pl. 10, figs 1–4) cephalon; GGU 275038 (VGL1).

Figured paratypes. Locality VGL1: MGUH108–110 cephala; MGUH111–114 pygidia.

Diagnosis. As for genus.

Description. Cephala, excluding genal spine, ranging in sagittal length from 9.78–10.51 mm. Cephalon with smoothly rounded anterior margin, 63% as high as long (sag.) excluding genal spine, with maximum convexity opposite anterior of palpebral lobe in palpebral view. Cephalon 76% as long (sag.) excluding genal spines as wide (tr.) (range = 74–78%; n = 2); 85% as long (sag.) including genal spine as wide (tr.) (range = 83–86%; n = 2). Faint sagittal carina. Anterior margin upturned forming thin, pronounced, rim-like anterior border, even narrower border furrow; anterior border increasingly upturned marginally between facial sutures. Cranidium 93% as wide (tr.) as long (sag.) across palpebral lobes (range = 91–95%; n = 4). From posterior margin, axial furrows converge anteriorly to intersect lunette; there, axial furrows are 67% width apart (tr.) that they are at the posterior margin (range = 58–73%; n = 3). Lunette oval, less well impressed on external moulds; extending from just posterior of posterior end of palpebral lobe to just posterior of anterior end of palpebral lobe. Axial furrows smoothly diverging anterior of lunette; terminating at omphalus where glabella is 138% width (tr.) at lunettes (range = 131–145%; n = 3) Omphalus very distinct on internal moulds, still distinguishable on external moulds; circular with a clear median granule. Anterolateral internal pit clear on internal moulds, slightly closer to anterior border than to omphalus, and a little adaxial of omphalus. Occipital node pronounced on both internal and external moulds, approximately one tenth total sagittal length of cranidium away from posterior margin.

S1 largest glabellar muscle impression, oval (elongated exsag.), extending from midpoint of lunette to anterior of palpebral lobe. S2 smallest, transversely oval, slightly anterior of palpebral lobe. S3 a little larger than S2, transversely oval, slightly

posterior of omphalus. S2 closer to S1 than S3; S1 and S2 equidistant from sagittal line; S3 slightly further abaxially.

Sculpture of pronounced, subequally spaced, continuous terrace ridges over roughly anteriormost quarter of cranidium. Cuticle pitted elsewhere.

Palpebral lobe comprising roughly one-quarter of total cranidial sagittal length. Librigena with greatest convexity medially; lateral margins with rim, this becoming more pronounced anteriorly. Terminating in short, stout genal spine with maximum convexity medially. Genal spine comprising roughly 15% of total cephalic sagittal length. Anterior border an upturned rim; very thin (sag.) border furrow. Pronounced terrace ridges branching from posterior of genal spine and short terrace ridges trending obliquely from librigena lateral margin. Remainder of librigena and area between terrace ridges covered in fairly evenly spaced pits.

Rostral plate of low convexity; maximum convexity where upturned to meet anterior margin. Connective sutures with slight curvature, diverging strongly. Only specimen showing ventral view, an external mould with slight posteromedial embayment, possibly indicating presence of a rostral flange. Fairly regularly spaced, continuous, transversely trending terrace ridges run parallel to anterior margin; a few short, fainter terrace ridges present between these.

Pygidia ranging in sagittal length from 10.37–12.45 mm. Pygidium posteriorly smoothly rounded, 54% as high as long (sag.) and maximum convexity approximately halfway along sagittal length (in extended view). Length (sag.) 90% of width (tr.) (range = 87–93%; n = 5) when plotted, the pygidial transverse width = 1.0029 pygidial sagittal length + 1.2531 (see remarks for discussion and Text-fig. 2.5). Posterior sagittal carina variably preserved; can be present for 65% total sagittal pygidial length. Holcos only defined anterolaterally. Abaxial end of articulating facet

located roughly one-quarter total pygidial length (sag.) from anterior margin. A single pygidium (Pl. 10. figs 10–11) exhibits a pair of dark muscle impressions, located equidistant from sagittal line, anterior of articulating facet, close to anterior margin. Sculpture of terrace ridges; strongest near margins, trending transversely, discontinuous, fairly regularly spaced. Clearly pitted between terrace ridges. Doublure extending 30% (range = 26–32%; n = 3) total pygidial sagittal length, of constant thickness. Doublure bearing well defined terrace ridges; more regular and continuous posteriorly.

Remarks. The genal spines of *Lanebestix enalios* resembles those of both *Litotix armata* (Hall, 1864) and *Ligiscus* (Lane and Owens, 1982). However, the cephalon is less convex than either of these genera and in this way is comparable with *Failleana*. The size, shape and positions of the lateral glabellar muscle impressions hold most resemblance to those of *Cybantyx nebulosus*, and the pronounced anterior border, curvature of the anterior margin, and relative proportions of both the cephalon and cranidium are reminiscent of *C. nebulosus*, also.

The pygidium of *Lanebestix enalios* is of typical illaenimorph form. The most useful distinguishing characters are the convexity and length to width ratio, and in these respects the pygidium of *Lanebestix* is most similar to those pygidia of: *Paracybantyx asulcatus* (Ludvigsen and Tripp, 1990, p. 8-9, pl. 1, figs 10-11, 13-15); *Paracybantyx occidentalis* (Adrain *et al*., 1995, p. 730, fig. 3, 5-8); *Bumastus* sp. (of Lane 1984, p. pl. 4, figs 10a–10c); goldillaenid gen. et sp. indet. 2. (of Lane 1972, p. 347, pl. 62, figs 10a–c, 13, 14a–b) and *C. nebulosus*.

The resulting straight line equations for pygidial width against pygidial length, initially suggest that the pygidia of *L. enalios* can be differentiated from those of *C.*

nebulosus using this method; pygidial width appears to increase with length at a slower rate than for *C. nebulosus* and *L. diana*.

Occurrence and distribution. Valdemar Glückstadt Land (VGL1).

Genus LIGISCUS Lane and Owens, 1982

Type species. By original designation; *Ligiscus arcanus* Lane and Owens, 1982, p. 46-48, fig. 3, pl. 3, figs 4-8, from the Upper Rhuddanian/Aeronian Cape Schuchert Formation, Washington Land, western North Greenland.

Diagnosis. Modified from Lane and Owens (1982, p. 46), to reflect specific differences in the strength of cephalic axial furrows, and subsequent fuller description of pygidia. Effaced scutelluid with axial furrows in dorsal view diverging backwards a little over the posterior one-sixth of their course, diverging more strongly forwards over anterior one-third. S1 largest muscle impression, longer (exsag.) than wide (tr.); S2 smaller and very close to S1; S3 smallest and remote. Visual surface large and inflated, about one-third sagittal length of the cranidium, reaching from mid-occipital impression to anterior of lateral muscle impression. Occipital node far back on glabella, close to posterior margin. Anterior section of facial suture runs less obliquely outwards than the axial furrow. Rostral plate with posteromedial elevation, about three times wider (tr.) than long (sag.). Convex pygidium with pentagonal to triangular axis. First pygidial furrow most deeply impressed.

Remarks. Ligiscus is a remarkable morphological intermediate between a scutelluid and an illaenimorph. This is particularly apparent with respect to the pygidium; it is of high convexity and has a holcos, both characteristic of illaenimorph taxa. It retains pleural ribs and furrows however, and has a doublure with scalloped-shaped terrace ridges, features characteristic of scutelluids. In addition, effacement occurs gradually through ontogeny, mirroring that occurring within the family as a whole; juvenile specimens strongly resemble scutelluids, with more illaenimorph characters appearing with growth.

Ligiscus diana sp. nov.

Plate 11, figures 1–22

Derivation of name. Latin, *Diana*, goddess of the chase and the moon, alluding to the cephalon which resembles a crescent moon. Noun in apposition.

Holotype. MGUH115 (Pl. 11, figs 1–2) cephalon; GGU 275044 (VGL2).

Figured paratypes. Locality VGL1: MGUH117 cephalon; MGUH118, 120 cranidia; MGUH125–127 pygidia. Locality VGL2: MGUH116 cephalon; MGUH119, 121 cranidia; MGUH122 librigena; MGUH123 hypostome; MGUH124, 128–129 pygidia.

Diagnosis. Ligiscus with non-bifid median rib, shield-shaped pygidial axis and well developed articulating facet.

Description. Cephala ranging in sagittal length from 1.8–7.34 mm. Cephalon semicircular, 53% as high as long (sag.) excluding genal spine, with maximum convexity opposite midpoint of palpebral lobe in palpebral view. Cephalon roughly two-thirds (64%) as long (sag.) as wide (tr.) (range = 60–69%; n = 3). Cranidium 91% as long (sag.) as wide (tr.) across midpoint of palpebral lobes (range = 87–96%; n = 25). Axial furrows subparallel alongside palpebral lobes; diverging posteriorly to intersect posterior margin so that axial furrows are 86% width apart (tr.) at lunettes, as at posterior margin (range = 80–95%; n = 25). Anterior of palpebral lobes, axial furrows diverge strongly forwards, fading before anterior margin; strongest on internal moulds. Lunette visible only on internal mould; extending from midpoint of palpebral lobe to just anterior of palpebral lobe. Occipital node can be obscured by cuticle. Midpoint of palpebral lobe approximately two-thirds of total cephalic sagittal length from anterior margin. Anterior of axial furrows, cranidium has well defined terrace ridges following curvature of margin, mostly continuous, fairly evenly spaced (Pl. 11, fig. 9).

Librigena with narrow (tr.) lateral border and border furrow; terminating in short genal spine. Sparse terrace ridges originating from posterior of visual surface.

Hypostome attributed to species with median body transversely oval, anterior wing anteriorly directed, large relative to whole hypostome, maculae small, pronounced. Covered with strong, continuous terrace ridges arranged in a ‘u-shape’ (Pl. 11, fig. 14).

Pygidia ranging in sagittal length from 3.73–8.57. Pygidium semicircular, 55% as high as long (sag.), with maximum convexity approximately halfway along sagittal length (in extended view). 66% as long (sag.) as wide (tr.) (range = 60–71%; n = 22) when plotted, the pygidial transverse width = 1.3415 pygidial sagittal length +

1.0211 (see remarks for discussion and Text-fig. 2.5). Pygidium highly inflated in pleural region, sloping rapidly posteriorly from mid-point of pleural region; very slightly upturned at margins. Axis with faint trilobation, clearest on internal moulds (Pl. 11, fig. 17); roughly as wide as long, comprising 33% of total sagittal length (range = 31–38%; n = 10) and 22% of total transverse width anteriorly (range = 18–28%; n = 10). Variably effaced, increasingly so with increasing size. Articulating half-ring short (sag.), convex, medially bowed anteriorly. Seven pairs of pleural ribs, non-bifid median rib roughly twice as wide as pleural ribs at posterior margin. First pleural rib most convex, demarcated by deep pleural furrow not affected by effacement, anteriorly developed into articulating facet. Remaining pleural ribs and median rib only slightly convex; all ribs widening towards margin. Pleural furrows deepest where they intersect margin, shallowing anteriorly. Pleural region variably effaced; most effaced medially resulting in loss of rib convexity and shallowing of pleural furrows. Sculpture of transversely trending continuous terrace ridges; strongest on articulating facet, less strong across the axis and the margins, weakest medially. Doublure not commonly exposed; extending for at least one-quarter total sagittal length and bearing scalloped shaped terrace ridges (Pl. 11, fig. 22).

Ontogeny. Important changes with growth of this species are as follows:

1. Cranidial axial furrow intersects with narrow anterior border in smaller specimens (Pl. 11, fig. 4); in larger specimens, axial furrows fade before anterior margin accompanied by loss of border (Pl. 11, fig. 8).
2. Occipital ring and furrow only present on specimens up to 3.5 mm long (sag.) (Pl. 11, fig. 12).

3. Cephala less than 3 mm long (sag.) have at least 2 pairs of nodes medially, presumably relating to glabellar muscular impressions (Pl. 11, fig. 12).
4. Proportionally longer (sag.) palpebral lobe in smaller specimens (Pl. 11, figs 4–5).
5. Gradual effacement of pygidial axis with growth.
6. Pygidial articulating facet increasingly well developed in larger specimens (Pl. 11, fig. 22).

Remarks. The cephalon of *L. diana* differs from the type species, *L. arcanus* in its smoothly rounded anterior cranidial margin, lacking the anteromedial angulation shown by *L. arcanus*. The glabella is less forwardly expanded than the type species and lacks a median carina. Both *L. diana* and *L. arcanus* differ from *L. smithi* in that specimens of comparable size have axial furrows which do not intersect the anterior section of the facial suture as they do in *L. smithi* (Adrain *et al*., 1995, p. 726, figs 2.1–2.2, 2.4–2.15, 3.13, 3.15–3.16).

The pygidium of *L. arcanus* is known from one incomplete specimen which is effaced abaxially leaving only five discernable pleural furrows and ribs. The pygidium of *L. diana* has a slightly greater length to width ratio than *L. arcanus*. The pygidial axes of both species are comparable in both shape and length relative to the whole pygidium. The pygidium of *L. smithi* has a similar length to width ratio to *L. diana*, but differs in having a bifid median rib and the pygidial axis is wider than long and more triangular in shape, compared to an axis as long as wide and more pentagonal in *L. diana*.

Holloway and Lane (1998) erected the genus *Excetra*, commenting on some cephalic similarities to both *L. arcanus* and *L. smithi*. The type species, *E. iotops*, shares common ontogenetic characteristics with the cephalon of *L. diana*, with smaller specimens having: increased depth of axial furrow, particularly anteriorly; presence of occipital furrow; relatively longer (exsag.) palpebral lobe. Larger cephala of the two species are not similar.

The resulting straight line equations (Text-fig. 2.5) for pygidial width against pygidial length, clearly distinguish *L. diana* from *C. nebulosus* and initially suggest differences from *L. enalios* using this method; pygidial width increases with length at a faster rate than for *C. nebulosus* and *L. enalios*.

Occurrence and distribution. Central Peary Land (CPL1–2), Kronprins Christian Land (KCL1, 4–5) and Valdemar Glückstadt Land (VGL1–2).

Genus LIOLALAX Holloway and Lane, 1999

[nom. nov. *pro Lalax* (Hamilton, 1990) *non* Holloway and Lane, 1998].

Type species. By original designation: *Lalax olibros* Hollway and Lane, 1998, p. 878, pl. 4, figs 11–12, 14–16, 19–20; pl. 5, figs 1–23; pl. 6, figs 9, 13, 16, 18. From the mid–late Wenlock to Ludlow Mirrabooka Formation, Orange District, New South Wales.

Diagnosis. From Holloway and Lane (1998, p. 877): effaced scutelluid with cephalon strongly convex (sag.), curvature in sagittal plane subtending more then 90 degrees,

height in lateral profile greater than or equal to sagittal length. Omphalus and anterolateral internal pit present. Axial furrow diverging moderately behind and immediately in front of lunette, dying out anteriorly behind omphalus. Eye large, situated less than its own length from posterior cephalic margin; socle not strongly convex (tr.). Posterior branch of facial suture strongly diverging backwards; anterior branch diverging moderately forwards. Genal angle broadly rounded. Rostral plate subtriangular, gently convex (sag., exsag.) over anterior 70% and gently concave in posterior part, without upturned posterior flange; connective suture meeting hypostomal suture close to sagittal line; vincular furrow present across posterior edge of doublure. Thorax with very wide, gently arched axis comprising 60–70% segment width (tr.); axial furrow weak; fulcrum situated very close to axial furrow; pleurae abaxial of fulcrum almost continuous in slope with lateral part of axial rings. Pygidium moderately convex (sag., exsag.) lenticular in dorsal view, maximum width just in front of mid-length; anteriormost pleural furrow and holcos very weak or not defined. Terrace ridges present over most of dorsal surface of cephalon and pygidium.

Remarks. Holloway and Lane (1998) noted the similarities of the genus to *Cybantyx*, particularly in the presence of an omphalus and anterolateral internal pit, and rostral plate outline. The two genera were distinguished (Holloway and Lane, 1998) on the basis of the presence of an upturned rim on the anterior and lateral cephalic border of *Cybantyx*; the lunette positioned slightly further forwards in *Cybantyx*, and a better impressed axial furrow anteriorly; facial suture of *Cybantyx* converging weakly in front of palpebral lobe instead of diverging (as demonstrated by *C. nebulosus*, this is species-specific and not diagnostic of the genus); posterior of rostral plate not concave (sag.) in *Cybantyx*; longer pygidial length of *Cybantyx.*

Liolalax naresi sp. nov.

Plate 12, figures 1–9

Derivation of name. For George S. Nares, who led the British Arctic Expedition in 1875–76 and proved that the Arctic Basin was inaccessible because of ice cover. This material was collected from south Nares land.

Holotype. MGUH130 (Pl. 12, figs 1–3) cranidium; GGU 298930 (SNL1).

Figured paratypes. Locality SNL1: MGUH131 cranidium; MGUH132 rostral plate; MGUH133–135 pygidia.

Diagnosis. Liolalax with weakly impressed lunettes; cranidium about 69% as long (sag.) as wide (tr.); pygidium about 65% as long (sag.) as wide (tr.); doublure present for about a third of pygidial sagittal length; dorsal terrace ridges confined to anterior of cranidium and anterolateral margins of pygidium.

Description. Complete cranidium measuring 5.67 mm (sag. length); 69% as long (sag.) as wide (tr.) across palpebral lobes (n = 1), about 19% as high as long (sag.) and maximum convexity opposite anterior of palpebral lobe in palpebral view. Axial furrow at posterior margin just abaxial of axial furrow at lunettes, which are very shallow and elongate (exsag.); glabella there comprising 45% cranidial transverse width across palpebral lobe midpoint. Anterior to this, axial furrows smoothly diverging forwards until fading anterior of palpebral lobe. Axial furrows shallow throughout course. Omphalus only clear on internal moulds (Pl. 12, fig. 4), where it is

circular with no median granule apparent, and positioned much closer to facial sutures than to anterior margin, and just posterior to anteriormost glabellar muscle impressions. Anterolateral internal pit present close to anterior margin, and just adaxial to omphalus, only visible on internal moulds. S3 only impressions visible with limited material, and only impressed on internal moulds, they are transversely elongate (Pl. 12, fig. 4). Palpebral lobe comprising about 36% total cranidial sagittal length, mid-point positioned about one-third total cranidial sagittal length from posterior margin; posterior end very close to posterior margin. Cranidial sculpture clear on external moulds (Pl. 12, figs 1–3), comprising strongly raised, fairly continuous, unanastomosing terrace ridges present for anteriormost 30%, these terminating at lateral margin anteriorly, and posteriorly becoming more removed from lateral margin. Terrace ridges weakly impressed on internal moulds.

Rostral plate behind connective sutures concealed by cuticle; bearing numerous transversely trending terrace ridges.

Pygidia ranging in sagittal length from 6.06–8.52 mm; about 19% as high as long (sag.); 65% as long (sag.) as wide (tr.) (n = 3; 62–68%). A weak sagittal carina visible on one internal mould (Pl. 12, figs 7–8). Articulating facet narrow (exsag.), located about 20% total pygidial length (sag.) from anterior margin (medially). Terrace ridges only present approaching anterolateral margins, from which they radiate; weaker than those on cranidium. Doublure comprising 34% pygidial sagittal length and of constant thickness; bearing about 12 concentric terrace ridges.

Both cranidial and pygidial cuticle are remarkably thick for size of specimens.

Remarks. The long (exsag.) palpebral lobe and the presence of an omphalus, readily distinguish the material from species of *Bumastus* Murchison, 1839. *L. naresi* is most

similar to the type species, *L. olibros*, particularly with respect to cranidial proportions. *L. naresi* differs as follows: the lunettes are much weaker; cranidial terrace ridges confined to anterior of cranidium, whereas they are also present posteriorly on *L. olibros*; pygidium wider (tr.), of lower convexity overall, and with greatest convexity anteriorly, not posteriorly, doublure twice as long.

Lateral glabellar muscle scars have been described from cranidia of *L. lens* (Holloway and Lane 1998) from the Silurian Mirrabooka Formation, New South Wales. The S3 of *L. lens* is sub-circular, as opposed to the transversely elongated form seen in *L. naresi*; both are similarly positioned in front of the omphalus however.

Occurrence and distribution. South Nares Land (SNL1).

Liolalax? sp.

Plate 12, figures 10–12

Figured material. GGU 275015 (KCL1): MGUH136 cephalon.

Description. A cephalon measuring 9.62 mm, and cranidium measuring 10.59 mm, are both fragmentary and preserved as internal moulds. Cephalon almost twice as wide (tr.) as long (sag.) and 79% as high as long (sag.). Maximum convexity opposite anterior of palpebral lobe in palpebral view. Cranidium about three quarters as long (sag.) as wide (tr.) across palpebral lobes. Anterior margin smoothly curved ventrally. Weak, wide (tr.) axial furrows, diverging rapidly for a short distance anterior of lunette, and terminating at omphalus, which has a clear median granule. Anterolateral

internal pit positioned closer to anterior margin than omphalus, and a little adaxially. Occipital impression and S1 both large, unclear; S2 and S3 much smaller, transversely elongate; muscle impressions situated further from the sagittal line anteriorly. Lunette elongate, about two-thirds length (exsag.) of palpebral lobe.

Palpebral lobe comprising roughly one-third total cranidial sagittal length; midpoint situated about 30% total cranidial sagittal length from posterior border.

Librigena gently rounded with terrace ridges trending exsagittally.

Remarks. These specimens are tentatively assigned to *Liolalax* on the basis of the combination of the following characters: ventrally curved anterior margin, lacking rim; presence of omphalus and anterolateral internal pit; long (exsag.) palpebral lobe; rounded genal angle. The palpebral lobe is however, positioned slightly further from the posterior margin, and is slightly shorter (exsag.) than in other members of the genus. Additionally, the axial furrows are better impressed than in species of *Liolalax*; this could reflect the preservation as an internal mould.

Occurrence and distribution. Kronprins Christian Land (KC1) and Valdemar Glückstadt Land (VG1).

2.3.4 Family ILLAENIDAE Hawle and Corda, 1847

Genus STENOPAREIA Holm, 1886

Type species. By orginal designation; *Illaenus linnarssonii* Holm, 1882, from the Ordovician of Dalarne, Sweden.

Diagnosis. Modified from Curtis and Lane (1997, p. 18) to accommodate variations in degree of effacement of axial furrows: illaenine with cephalon strongly convex longitudinally, pygidium smaller and flatter than cephalon. Cranidial axial furrows visible posterior of lunette, may be present but shallow for a little distance in front. Eyes small, and placed far back. Hypostome subquadrate with small triangular anterior wings. Thorax with nine segments. Anterior sagittal margin of pygidial doublure modified, usually into cusps. Exoskeletal surface with terrace ridges; doublural surfaces with prominent terrace ridges.

Remarks. As with all illaenimorph taxa, the effaced nature of *Stenopareia* can significantly hamper description and identification at a specific level. The use of the number of cusps on the pygidial doublure to distinguish species, as recognised by Jaanusson (1954, p. 574; 1957, p. 109) and Curtis and Lane (1997, p. 19) is particularly useful.

Stenopareia persica sp. nov.

Plate 12, figures 13–15; Plate 13, figures 1–13

Derivation of name. Latin, *persica*, peach. Noun in apposition.

Holotype. MGUH137 (Pl. 12, figs 13–15) cranidium; GGU 275049 (VGL3).

Figured paratypes. Locality CPL5: MGUH138–139 cranidia; MGUH140–141 librigenae; MGUH142 rostral plate; MGUH145 pygidium. Locality VGL1: MGUH143 pygidium. Locality CPL2: MGUH144 pygidium.

Diagnosis. Stenopareia reaching large sagittal lengths, with individual cranidial sagittal lengths in excess of 60 mm; axial furrows only diverging posteriorly behind palpebral lobe; anterolateral cephalic margin rim-like; pygidium with well developed, strongly upturned articulating facet and a single cusp.

Description. Cranidia measuring from 7.73–68.35 mm sagittal length. 59% as high as long (sag.) with maximum convexity about halfway between palpebral lobe and anterior margin. 91% as long (sag.) as wide (tr.) across palpebral lobes (range = 85–97%; n = 6). Anterior margin with short (sag.) upturned rim-like border (Pl. 12, fig. 15) and much shorter (sag.) border furrow. From posterior margin, axial furrows converging anteriorly until point opposite posterior end of palpebral lobe. From there, furrows are sub-parallel until anterior of lunettes; latter shallow, exsagittally elongated, and placed opposite anterior half of palpebral lobe. Glabellar width at lunettes 92% that at posterior margin (range = 85–99%; n = 8). Anterior to lunettes, axial furrows smoothly diverging forwards at roughly 20 degrees from an exsagittal line, fading roughly halfway between palpebral lobe and anterior margin. No lateral glabellar muscle impressions preserved. Palpebral lobe comprising on average 16% cranidial sagittal length (range = 16–23%; n = 6), and positioned on average 26% cranidial sagittal length, from posterior border (range = 25–29%; n = 5). Sculpture of fairly regularly spaced and continuous, non-anastomosing and transversely trending terrace ridges approaching anterior margin of cranidium.

Librigena most convex posterolaterally. Lateral margins with rim like that of anterior cranidial border. Genal angle well rounded. Where preservation permits, short, discontinuous terrace ridges present laterally. Doublure with distinct vincular groove increasingly positioned further from margins posteriorly.

Rostral plate most convex (sag., tr.) medially; connective sutures slightly curved and diverging at about 30 degrees from an exsagittal line. Eleven or 12 prominent terrace ridges, trending transversely.

Pygidium sagittal lengths measuring from 8.31–48.83 mm; about 31% as high as long (sag.) and maximum convexity about one-third pygidial sagittal length from posterior margin; 68% as long (sag.) as wide (tr.) (range = 59–73%; n = 5). Median arch comprising 36% (range = 32–39%; n = 5) maximum pygidial width (tr.); expanded anteriorly, forming a smoothly curved outline. Doublure comprising 19% (n = 1) total pygidial sagittal length (excluding cusp); with distinct, continuous terrace ridges.

Ontogeny. The pygidia display the change from a more polygonal outline to a more semicircular one during growth, noted to occur in *S. grandis* (Billings, 1859), by Chatterton and Ludvigsen (2004). The articulating facet in smaller specimens comprises a much greater proportion of pygidial length (Pl. 13, figs 12–13), with the abaxial end placed opposite 44% pygidial length from anterior margin medially (sag.), this decreasing to 25% in larger specimens (Pl. 13, figs 8–11). This change of proportions is also seen in *S. grandis* (Chatterton and Ludvigsen 2004, p. 17, pl. 1, figs 10–11; pl. 2, figs 4–5, 11–16; pl. 3, figs 5–8) and *S. somnifer* (Lane 1979, p. 14, pl. 1, figs 17, 19–23, 25; pl. 2, figs 10, 13; pl. 3, figs 1–2, plate 5, fig. 3), making it useful in identification of juvenile specimens.

Remarks. S. persica is comparable to *S. grandis* in terms of its large maximum size; Chatterton and Ludvigsen (2004) note that *S. grandis* can exceed sagittal lengths of 100 mm. Both taxa also possess a single cusp. The cranidium of *S. persica* is very

distinctive for the genus, and is readily differentiated from that of *S. grandis* and all other species of *Stenopareia* in the possession of a *Cybantyx*-like upturned rim on the anterolateral cephalic margins. Additionally, the axial furrows are less effaced anteriorly, and converge anteriorly for a much greater proportion of their course.

Occurrence and distribution. Central Peary Land (CPL2, 4–5) and Valdemar Glückstadt Land (VGL1–2).

Stenopareia cf. *grandis* (Billings, 1859)

Plate 14, figures 1–3

Figured material. GGU 298506 (WL): MGUH146 cranidium. GGU 301318 (WPL1): MGUH147 pygidium.

*Description.*Cephala and cranidia with sagittal lengths measuring from 5.3–20.01 mm; cranidia 84% as long (sag.) as wide (tr.) across palpebral lobes (range = 83–85%; n = 3); cephala 67% as long (sag.) as wide (tr.) at widest point opposite palpebral lobes. Axial furrows from posterior margin, converging anteriorly until intersection with lunettes which are faint and placed opposite palpebral lobes; effaced anterior of this. Socle-like swelling under middle of eye. Anterior margin with about eight distinct and continuous terrace ridges trending transversely. Terrace ridges also visible on posterior of cephalon, between axial furrows; fairly continuous, irregular; trending transversely but bowed medially.

Pygidium sagittal lengths measuring from 9.25–16.34 mm; 65% as long (sag.) as wide (tr.) (range = 62–69%; n = 5). Median arch with a fairly straight anterior

margin; comprising 38% maximum pygidial width (tr.). One pygidium with pair of exsagittally directed oval muscle scars situated opposite mid-length of articulated facets (Pl. 14, fig. 3).

Remarks. The cephalon has a socle-like swelling under the middle of the eye, as seen in *S. grandis* (Chatterton and Ludvigsen 2004, p. 17, pls 1–2) and the pygidial length:width ratios agree. However, the lunettes are positioned opposite the palpebral lobe, not anterior of it, and the pygidial median arch occupies a slightly smaller proportion of the total pygidial width. For these reasons, the material is assigned as *S.* cf. *grandis.*

Occurrence and distribution. Wulff Land (WL), western Peary Land (WPL1–2) and south Nares Land (SNL2).

Stenopareia sp.

Plate 14, figures 4–8

Figured material. GGU 275049 (VGL3): MGUH148 cranidium; MGUH149–150 pygidia.

Remarks. Fragmentary cranidia and pygidia from Valdemar Glückstadt Land are closest to *S.* cf. *grandis* but differ as follows: cranidia are 97% as long (sag.) as wide (tr.) (n = 2) as opposed to 84%; pygidia are 57% as long (sag.) as wide (tr.) (n = 2) as opposed to 65%; pygidial axial furrows are deeper; pygidial terrace ridges are stronger, are strongly bowed forwards medially, and become more discontinuous

laterally. Given the limited material and lack of distinguishing characters, the material is kept under open nomenclature.

Occurrence and distribution. Valdemar Glückstadt Land (VGL3).

Order PROETIDA Fortey and Owens, 1975

Superfamily PROETOIDEA Hawle and Corda, 1847

2.3.5 Family PROETIDAE Hawle and Corda, 1847

Subfamily PROETINAE Hawle and Corda, 1847

Genus PROETUS Steininger, 1831

Type species. By original designation; *Calymmene concinna* Dalman, 1827, from the Wenlock Mulde Marl, Djupvik, Gotland, Sweden.

Diagnosis. After Thomas (1978, p. 36): proetine with preglabellar field typically absent or short (sag.); lateral glabellar muscle impressions usually weak; pygidium subsemicircular in outline; axis with 6–12 rings and rounded posteriorly, pleural areas with 4–6 pairs of pleural ribs.

Proetus? *confluens* sp. nov.

Plate 14, figures 9–15; Plate 15, figures 1–3

Derivation of name. Latin, *confluens*, place where two streams meet, alluding to the medially confluent preglabellar and anterior border furrows.

Holotype. MGUH151 (Pl. 14, figs 9–11) cephalon; GGU 198225 (CPL3).

Figured paratypes. Locality CPL3: MGUH152 cephalon; MGUH153–154 cranidia; MGUH155 articulated pygidium and thorax; MGUH156 articulated cephalon and thorax.

Diagnosis. Proetus? with glabella longer (sag.) than wide; short (sag.) preglabellar field only present abaxial to medially confluent preglabellar and anterior border furrows; posteriorly expanded anterior border; granular sculpture coarsest on glabella and occipital ring. Pygidium with anteriorly wide (tr.) and strongly tapering pygidial axis with at least 6 axial rings; at least 5 inflated pleural ribs, all extending to pygidial margin.

Description. Cephala and cranidia raging in sagittal length (excluding genal spine) from 2.96–3.95 mm (n = 9). Cephala averaging 76% as long (sag.) as wide (tr.) (range = 66–84%; n = 3). Glabella conical, pre-occipital part averaging 80% as wide (tr.) as long (sag.) (range = 75–87%; n = 8). Maximum width posteriorly, gradually tapering to a sub-triangular blunted point anteriorly. Axial furrows equally moderately impressed throughout their course. Lateral glabellar muscle impressions shallow, delineated by smooth areas lacking tubercles, all connected to axial furrow. S1 abaxially placed opposite midpoint of palpebral lobe (δ). From there, running posteriorly at an angle of roughly 55 degrees from an exsagittal line for about half its course, after which narrowing posteriorly and directed at a much lower angle, terminating prior to occipital furrow. Faint auxiliary impression present just adaxial of the mid-length of S1. S2 placed opposite anterior end of palpebral lobe (γ) abaxially,

running posteriorly at an angle of roughly 65 degrees from an exsagittal line, widening adaxially. S3 the weakest impression, not always visible. S3 closer to S2 than S2 is to S1, running roughly parallel to S2. Glabella densely covered in coarse granules (except for muscle impressions), fairly evenly sized and spaced. Sculpture slightly subdued towards anterior of glabella. Occipital ring slightly wider (tr.) than posterior of pre-occipital glabella and slightly longer (sag.) than anterior border. Slightly convex anteriorly, and very gently sloping anteriorly. Occipital furrow deep. Lateral occipital lobes clear, ovate and inflated. Occipital node situated very slightly posterior to mid-point (sag.) of occipital ring. Occipital ring covered in granules which are slightly finer than on glabella. Facial suture from γ to β diverging from an exsagittal line at roughly 12 degrees. γ positioned slightly further from axial furrow than ε. Posterior branch not clear. Palpebral lobe extends from just anterior of occipital lobe to a point opposite S2. Anterior border pronounced and convex (sag.) with numerous parallel terrace ridges. Preglabellar and deep anterior border furrows are confluent medially so that short (sag.) preglabellar field is only present abaxial to this point. Anterior border expanded posteriorly at this point, partly infilling furrowed area. Fixigena and preglabellar field with granules, similar density but more subdued than those on glabella and occipital ring.

Eye comprising roughly one-third total sagittal length of cephalon excluding genal spine. Eye socle narrow with impressed parallel furrows, retaining roughly equal thickness along length of eye. Librigena convex, similar granular sculpture to fixigena and preglabellar field. Lateral border slightly wider (tr.) than expanded anterior border length (sag.), and with numerous sub-parallel terrace ridges. Posterior border with terrace ridges abaxial to ω. Posterior and lateral borders bearing numerous terrace ridges join to run down genal spine as a median grove, terminating

before tip where terrace ridges become confluent. Genal spine roughly quarter sagittal cranidial length.

Only posterior part of thorax known, axis gradually tapering, on average forming roughly 40% of entire thoracic width (tr.), and with deep axial furrow. Axial rings roughly equal length exsagittally and sagittally. Intra-annular furrow present. Posterior pleural bands markedly longer (exsag.) than anterior pleural bands, pleural tips rounded. Pleural furrow long (exsag.), incised, abaxially terminated where truncated by posterior edge of articulating facet. Axis and pleurae with similar granular sculpture.

Pygidium almost twice as wide (tr.) as long (sag.). Anterior width of axis roughly 40% anterior pygidial width (tr.) and axis comprising roughly 70% its total sagittal length. Axis tapering rapidly for its posterior half, terminating in a sub triangular tip. Axial furrows well impressed throughout course. Six discernible axial rings and a terminal piece. Paired apodemal impressions present on anteriormost 4 axial rings. Anterior 5 pleural ribs visible, posterior to this effaced. Both anterior and posterior bands equally inflated with a scalloped profile. Interpleural and pleural furrows equally well impressed, terminating at narrow pygidial border.

Remarks. Granular sculpture is not a character typical of *Proetus*, but it is seen in species such as *P. granulatus* Lindström (1885, p. 81, pl. XIV, fig 13) from the Silurian of Gotland (refigured by Owens 1973, pl. 2, fig. 3) which shares similarly well impressed lateral glabellar muscle impressions. Such a well impressed lateral glabellar muscle impressions are not characteristic of *Proetus* either, but it should be noted that the local absence of sculpture makes the impressions more conspicuous. *P. granulatus* also exhibits distinct terrace ridges on the cephalic anterior and lateral

borders, as seen in *P*? *confluens.* Despite the similarities in sculpture, the cephala are readily distinguished by their different glabellar outlines and greater anterior expansion of the anterior glabellar lobe in *P. granulatus*. The semicircular pygidium with a pygidial axis that is wide (tr.) relative to the pleural areas, and which tapers strongly, seen in *P*? *confluens*, are characteristic of the genus. The extension of pleural and interpleural furrows to the pygidial margin is not characteristic of *Proetus*, and for this reason, *P.*? *confluens* is referred to *Proetus* with some doubt.

Occurrence and distribution. Central Peary Land (CPL3).

Genus AIROPHRYS gen. nov.

Derivation of name. Contraction of Greek, *airo*, raise, lift, and Greek, *ophrys*, brow, eyebrow, alluding to the fancied resemblance of the preocular fixigenal furrows to a pair of raised eyebrows. Gender feminine.

*Type species.*By original designation; *Airophrys balios* from the Telychian Samuelsen Høj Formation, Valdemar Glückstadt Land, North Greenland.

Other species. Cyphoproetus sp. (Lane 1972, p. 349, pl. 61, figs 4a–4b), from the Telychian Samuelsen Høj Formation of Kronpins Christians Land, eastern North Greenland.

Airophrys sp. from the Telychian Samuelsen Høj Formation, central Peary Land, North Greenland.

Diagnosis. Proetine with glabella roughly as long as wide and strongly tapering anteriorly; anterior border with a flattened profile, distinct anterior border furrow; preocular fixigenal furrow present. Pygidium with six axial rings and a terminal piece, four pleural ribs, and no border. Pygidial axial rings and pleural ribs all inflated. Sculpture of unevenly sized and spaced granules.

Remarks. The preocular fixigenal furrow is seen in *Airophrys* sp. herein, and *Cyphoproetus* sp. (Lane 1972, p. 349, pl. 61, figs 4a–4b), from the Telychian Samuelsen Høj Formation of Kronprins Christian Land, eastern North Greenland. As such, these are included in *Airophrys.*

Airophrys balios gen. et sp. nov.

Plate 15, figures 4–8

Derivation of name. Greek, *balios*, spotted, dappled, piebald, alluding to the tuberculate sculpture.

Holotype. MGUH157 (Pl. 15, figs 4–8) cranidium; GGU 275038 (VGL1).

Figured paratypes. Locality VGL1: MGUH158 pygidium.

Diagnosis. As for genus.

Description. Glabella conical, tapering strongly forwards to a very gently rounded anterior. Pre-occipital glabella as long (sag.) as wide (tr.) posteriorly. S1 deep,

trending at roughly 40 degrees from exsagittal line, anterior end placed very close to but separate from axial furrow, posteriorly terminating at occipital furrow. L1 subtriangular, a little longer (exsag.) than wide (tr.), exsagittally comprising just over one-third total glabellar length. S2 and S3 equally well impressed, closer to one another than S1 is to S2; both connected to axial furrow and trending sub-parallel to one another at roughly 75 degrees to an exsagittal line. S3 slightly shorter than S2. Occipital ring as wide (tr.) as posterior of pre-occipital glabella, mostly incomplete. Length (sag.) of preglabellar field comprising roughly 15% total sagittal length of cranidium. Preglabellar field sloping anteriorly to meet anterior border furrow, which is longer (sag.) medially than abaxially, and well defined. Preocular fixigenal furrow present. Between this and the anterior border furrow is an anteriorly sloping area which adaxially becomes the preglabellar field. Anterior border with a flattened profile. Facial suture from γ to β initially diverging from exsagittal line at roughly 35 degrees. Unevenly spaced granules covering entire cranidium, coarsest on preglabellar field, finest on anterior border.

Pygidium roughly twice as wide as long (sag. length = 51% tr. width). Anterior width of axis comprising 36% total anterior width (tr.) of pygidium. Axis comprising 81% total sagittal length of pygidium, bluntly rounded posteriorly. Axial furrow well impressed throughout course. Six axial rings and a terminal piece. Posteriorly, axial ring furrows not connected adaxially. Paired subcircular apodemal pits connected to anterior most 5 anterior ring furrows. Four pleural ribs and an anterior band. Anterior band and anterior pleural band of first rib proportionally slightly wider (exsag.) than other pleural ribs. Interpleural furrows more deeply impressed than pleural furrows which increase in depth towards pygidial margins,

terminating shortly before margins. No distinct pygidial border. Complete covering of coarse, unevenly sized and spaced granules.

Remarks. Airophrys balios resembles *Cyphoproetus*, the genus which is probably most closely related: the deeply incised S1 defining a prominent L1, pygidial morphology with a scalloped profile to the pleural ribs and granular sculpture. Distinguishing characters of *Airophrys balios* are: the very strongly tapering and anteriorly narrower (tr.) frontal glabellar lobe, giving a very different glabellar outline; anterior border with a distinctly flattened profile; defined anterior border furrow; presence of a preocular fixigenal furrow; inflated pygidial axial rings and pleural ribs.

Occurrence and distribution. Valdemar Glückstadt Land (VGL1).

Airophrys sp.

Plate 15, figures 9–13

Figured material. GGU 198226 (CPL1): MGUH163 cephalon; MGUH159–160 cranidia; MGUH161–162 libriginae.

Remarks. Fragmentary material comprising a cephalon, two cranidia and three librigenae from central Peary Land are assigned to *Airophrys*. These fragments are found in association and share a similar coarsely granular sculpture. Determinable characters are: glabella conical, pre-occipital part roughly as long (sag.) as wide (tr. posteriorly); deep S1, posteriorly terminating at occipital furrow, and defined L1; well

impressed S2, trending roughly 75 degrees from an exsagittal line; posteriorly placed occipital node; short (tr.) preglabellar field with preocular fixigenal furrow; flattened lateral border, a little wider (tr.) than lateral border furrow; distinct eye socle, anteriorly and posteriorly expanded (Pl. 15, fig. 11); genal spine extending for roughly one-third the exsagittal length of remaining librigena; coarsely granular sculpture, with granules smaller and sparser on flattened lateral border and border furrow.

The material has a similar glabellar morphology to *Airophrys balios*; the pre-occipital glabella is as long (sag.) as wide (tr.) in both *A.* sp. and *A. balios*. Additionally, both species have a preocular fixigenal furrow. *A.* sp. differs from *A. balios* by having inflated glabellar lobes, and a more coarsely granular sculpture on the glabella.

Occurrence and distribution. Central Peary Land (CPL1).

Genus CYPHOPROETUS Kegel, 1927

Type species. Subsequently designated by Přibyl 1946, p. 15; *Cyphaspis depressa* Barrande, 1846, p. 60; from the Wenlock Liteň Formation, Lištice, near Beroun, Prague district, Czech Republic.

Diagnosis. The following diagnosis is based on that of Thomas (1978, p. 40), emended to allow for the variable position of the occipital node: proetine with glabella with deep S1 defining prominent L1; lateral occipital lobes typically present. Preglabellar field, if present, shorter (sag.) than anterior border; lateral cephalic

margin commonly incurved at base of genal spine. Thorax of 9–10 segments. Pygidium without border; axis with 5–8 rings, pleural areas with 3–6 pairs of pleural ribs.

Cyphoproetus peeli sp. nov.

Plate 15, figures 14–18

Derivation of name. For Professor J. S. Peel, who collected much of this material.

Holotype. MGUH164 (Pl. 15, figs 14–15) cranidium; GGU 274689 (CPL5).

Figured paratypes. Locality CPL5: MGUH165, 167 cranidia. Locality CPL2: MGUH166 cranidium.

Diagnosis. Cyphoproetus with S1 forming subtriangular incision anteriorly and not connected to axial furrow; preglabellar field shorter (sag.) than anterior border; effaced lateral occipital lobes, posteriorly placed occipital node; sculpture comprising both terrace ridges and granules.

Description. Cranidia of low convexity (sag. and tr.), ranging in sagittal length from 2.13–2.38 mm. Glabella pear-shaped, bluntly rounded anteriorly, pre-occipital part roughly 90% as long (sag.) as wide (tr.) (n = 4). S1 prominent, not connected to axial furrow; terminating forwardly in a deeply incised obliquely directed subtriangular incision, shallowing posteriorly to meet occipital furrow. L1 slightly longer than wide, comprising roughly one-quarter total sagittal length of glabella, posteriorly exsagittaly

expanded, there forming widest (tr.) part of glabella. S2 and S3 connected to axial furrow, closer together than S1 is to S2. S2 deeper than S3. S2 directed between 65 and 85 degrees posteriorly and S3 between 75 and 85 degrees anteriorly. Occipital ring over twice as long medially as abaxially; as wide (tr.) as glabella at position of L1. Occipital node positioned near posterior margin, lateral occipital lobes effaced. Preglabellar field slightly shorter (sag.) than anterior border. Anterior border furrow about equal in length (sag.) to preglabellar field, shallowing anteriorly. Strongly raised and smoothly convex anterior border, roughly twice as wide (sag.) as occipital ring. Glabellar and occipital ring with scrobiculae trending transversely. Preglabellar field and fixigenae with sparse, coarse granules.

Remarks. The glabellar morphology and well developed L1 are typical of the genus. The absence of a tropidium or tropidial ridges distinguish *C. peeli* from *Warburgella*, although these characters may be weakly expressed in some *Warburgella* species, as in *W. scutterdinensis*. The cranidia are closest to those of *C. svartoensis* Owen (1981, p. 25, pl. 6, figs 3-6) from the Ordovician (Ashgill, late Rawtheyan) of the Oslo Distict, Norway. Both species have poorly developed occipital lobes, posteriorly situated occipital nodes, and subtriangular form of S1, which is not connected to the axial furrow. The cranidium of *C. peeli* differs from *C. svartoensis* in having a more elongate glabella, and a shorter (sag.) preglabellar field. Although both species share a combination of both scrobiculate and granular sculpture, the granules of *C. svartoensis* are transversely elongate and situated on both the glabella and preglabellar field. The granules of *C. peeli* are coarser, and only situated on the preglabellar field and fixigenae.

Occurrence and distribution. Central Peary Land (CPL2, 5).

Cyphoproetus sp.

Plate 15, figure 19

Figured material. GGU 298924 (SNL2): MGUH168 cranidium.

Remarks. A single cranidium measuring 3.56 mm has the following distinguishing characters: tongue-shaped glabella, pre-occipital part 89% as wide (tr. posteriorly) as long (sag.); S1 the only visible glabellar muscle impression, and not connected to either axial or occipital furrows; intramarginal zone prominent and long (sag.), anteriorly shallowing; preglabellar field about same length (sag.) as anterior border; anterior border with prominent terrace ridges anteriorly; posteriorly positioned occipital node.

The deep S1 is characteristic of *Cyphoproetus.* The glabellar morphology and effaced S2 and S3 distinguish this cephala from those assigned to *C. peeli*, and *C.* sp. is not directly comparable to any described *Cyphoproetus* species.

Occurrence and distribution. South Nares Land (SNL1).

Genus OWENSUS gen. nov.

Derivation of name. For Dr R. M. Owens, studier of proetoideans, arbitrarily combined in the style of *Proetus*. Gender masculine.

Type species. Owensus arktoperates from the Telychian Samuelsen Høj Formation, central Peary Land, North Greenland.

Diagnosis. Proetine with highly convex cephalon, preglabellar field convex longitudinally and comprising over one-third sagittal length of glabella; glabella parallel sided between S1 and S2, forked S1, occipital ring anteriorly expanded medially; 10 thoracic segments; pygidium with 7 axial rings and 5 pleural ribs with inflated anterior pleural bands; pleural and interpleural furrows well impressed and all extending to margin; axial region covered in coarse granules.

Owensus arktoperates gen. et sp. nov.

Plate 16, figures 1–15

Derivation of name. Contraction of Greek, *arktous*, northern, and Greek, *perates*, wanderer. Noun in apposition.

Holotype. MGUH169 (Pl. 16, figs 1–2) articulated specimen; GGU 274689 (CPL5).

Figured paratypes. Locality CPL2: MGUH174 cephalon. Locality CPL3: MGUH173 cranidium. Locality CPL5: MGUH171 articulated cephalon and thorax; MGUH170 cephalon; MGUH172 cranidium; MGUH175 librigena; MGUH176–177 articulated pygidia and thoraxes.

Diagnosis. As for genus.

Description. Cephala and cranidia range in sagittal length from 1.91–4.88 mm, cephala averaging 74% as long (sag.) as wide (tr.) (range = 64–89%; n = 38). Glabella broad, conical, pre-occipital part averaging 84% as wide (tr.) as long (sag.) (range = 65–101%; n = 57). Maximum glabellar width in posterior half of inflated L1, subparallel between S1 and S3, anterior to this tapering forwards to form a smoothly rounded point. Axial furrows well impressed. Glabellar muscle impressions all connected to axial furrow, S1 to S3 progressively weaker. S1 well impressed, abaxial end placed opposite halfway between δ and ε, from there running posteriorly at roughly 40 degrees from an exsagittal line, terminating as a fork well before occipital furrow. S2 and S3 close together; abaxially S2 is just posterior of γ and S3 just anterior of it. S2 runs posteriorly at roughly 70 degrees, and S3 at roughly 80 degrees from an exsagittal line. S3 most visible on internal moulds (Pl. 16, fig. 6). Glabella densely covered in unevenly sized and spaced coarse granules. Occipital ring as wide (tr.) as posterior of pre-occipital glabella; convex forwards adaxially, where roughly twice as long (sag.) as abaxially. Medially, occipital ring is longer (sag.) than anterior border; anterior slope more gradual than posterior slope. Occipital furrow deep. Small ovate lateral lobe defined by shallow furrow. Pronounced occipital node situated closer to anterior than to posterior of occipital ring. Granular sculpture similar to glabella. Facial suture from γ to β initially diverging from an exsagittal line at 20–30 degrees, halfway along course changing direction to run in an almost exsagittal line. γ and ε equally very close to axial furrow, and from ζ to ε running close to and almost parallel with axial furrow. Palpebral lobe situated half its exsagittal length from posterior border furrow, comprising roughly 40% total glabellar sagittal length (more in the very smallest specimens). Posterior of palpebral lobe situated opposite anterior half of L1, and anterior situated just in front of S3, at point where glabella begins to

taper. Length of preglabellar field on average 21% total sagittal length of cranidia (range = 15–27%; n = 57), steeply sloping anteriorly to meet deep, narrow (tr.) anterior border furrow. Anterior border pronounced, convex (sag.) and with about 4 sub-parallel terrace ridges. Fixigena and preglabellar field with scattered granules, much sparser and more subdued than on glabella and occipital ring.

Narrow eye socle retaining equal width along its length, with lower and upper margins defined by furrows, of which the lower is shallower and wider (tr.). Librigena with similar convexity to preglabellar field, and sparsely granular sculpture like fixigena and preglabellar field. Lateral border of similar width (tr.) to anterior border length (sag.), of similar convexity and bearing about 4 terrace ridges. Posterior border with no terrace ridges, long (exsag.) abaxial of ω, rapidly narrowing adaxial of ω. Lateral and posterior border furrows deep, joining to run down genal spine as a median groove, but terminating before tip of genal spine. Genal spine roughly half sagittal length of cranidium, extending back to sixth thoracic segment and with numerous terrace ridges trending roughly sagittally.

Thorax of 10 segments. Axis anteriorly comprising almost half total width (tr.) of thorax, tapering posteriorly to roughly one-third total width. Last ring roughly 70% width (tr.) of first ring. Axial rings slightly longer exsagittally than sagittally. Intra-annular furrow present. Axial furrow deep. Axis with sparse granules, similar to those on librigena. Nearly flat-topped pleurae with anterior and posterior pleural bands roughly equal in length (exsag.). Pleural furrows incised, longest (exsag.) at mid-width, terminating abaxially before tips of pleurae which are bluntly rounded. Fulcrum located roughly half way (tr.) across pleura. Pleurae lacking granules.

Pygidium 47% as long (sag.) as wide (tr.) (range = 43–50%; n = 6). Anterior width of axis comprising on average 31% total anterior width (tr.) of pygidium (range

= 21–36%; n = 6). Axis comprising on average 85% total sagittal length of pygidium (range = 79–90%; n = 3), bluntly rounded posteriorly. Axial furrow well impressed, slightly shallower around posterior of axis. Seven axial rings and a terminal piece, axial ring furrows becoming progressively shallower posteriorly. Paired, well impressed subcircular apodemal pits obvious on anterior most 5 axial rings, with the most anterior 2 connected to the anterior ring furrow, posterior to this placed increasingly centrally (exsag.) on axial rings. Five discernible pleural ribs and an anterior band. Anterior pleural bands strongly inflated, posterior bands weakly inflated. Interpleural and pleural furrows equally well impressed. Furrows terminate abruptly at narrow pygidial border, bearing irregular terrace ridges.

Remarks. The combination of characters displayed by *O. arktoperates*: high convexity cephalon; presence of a long (sag.) preglabellar field; granular sculpture much more pronounced in axial region; pygidium with inflated anterior pleural bands and with pleural and intepleural furrows extending to the margin, serve to distinguish it from all other proetine genera.

The long (sag.) preglabellar field with convex lateral profile of *O. arktoperates* is characteristic of some lower Devonian genera (*Podoliproetus* Šnajdr, 1978, p. 92, *Unguliproetus* Erben, 1951, p. 95 and *Pragoproetus* Šnajdr, 1977, with emended diagnosis in Šnajdr 1980, p. 98), but *O. arktoperates* has a proportionately shorter (sag.) anterior border. The pygidium of *O. arktoperates* is distinct in that all of the pleural and interpleural furrows extend to the margin. R.M. Owens (pers. comm. 2010) suggested that *O. arktoperates* could be derived from *Proetus ainae* from the Boda Limestone Formation (Ashgill), Dalarna, Sweden (Owens 1973, p. 122, fig 1, A–F, H–L) which was transferred to *Astroproetus* by Owens (2006, p. 135). *O.*

arktoperates certainly shares most pygidial characters with *A. ainae*, although the pygidium of *A. ainae* is proportionally slightly longer, and has significantly shallower pleural and interpleural furrows. The cranidia are less similar, although the glabellar outlines are comparable. *O. arktoperates* has a longer (sag.) preglabellar field, better defined anterior border furrow and L1, and granular sculpture present.

A single pygidium referred to *Proetus (Lacunoporaspis)* sp. from the Cape Schuchert Formation (Rhuddanian/Aeronian, B1, Idwian stage or slightly older), Washington Land, North Greenland (Lane 1979, p. 17, plate 3, fig. 3), is likely congeneric. The pygidium displays the following characters considered diagnostic of the genus: 7 axial rings and 5 pleural ribs; inflated anterior pleural bands; well impressed pleural and interpleural furrows which all extend to pygidial margins. Lane's pygidium has a wider axis (tr. relative to width of anterior of pygidium) than that of *O. arktoperates*.

Occurrence and distribution. Central Peary Land (CPL2–5).

Subfamily CRASSIPROETINAE Osmólska, 1970

Remarks. Owens (2006) revised the subfamily Crassiproetinae, including the genera *Astroproetus, Boliviproetus, Crassiproetus, Dechenellurus, Elimaproetus, Mannopyge, Monodechenella, Raerinproetus, Thebanaspis* and *Winiskia* which he regarded as a monophyletic group, likely derived from the Proetinae during the Ordovician.

Genus ASTROPROETUS Begg, 1939

Type species. By original designation; *Proetus (Astroproetus) reedi* Begg, 1939, p. 37, from the Ordovician Upper Drummuck Group (Ashgill Series, Rawtheyan Stage), Lady Burn, near Girvan, Scotland.

Diagnosis. After Owens (2006, p. 135): crassiproetine with glabella conical; preglabellar field as long (sag.) or longer than anterior border; transversely elongate lateral occipital lobes; pygidial axis narrow (tr.) relative to pygidial width, with 7–8 rings; pleural fields with 5–6 pairs of ribs; no pygidial border.

Remarks. Lütke (1990, p. 46) noted the close relationship between *Astroproetus* and *Thebanaspis*. This relationship was confirmed by Owens (2006, p. 135) and *Astroproetus* was included in the Crassiproetinae rather than the Tropidocoryphinae, to which it was assigned previously.

Astroproetus franklini sp. nov.

Plate 17, figures 1-9

Derivation of name. For Sir John Franklin, who lead an ill-fated expedition to the high Arctic in 1845. All of the material here was collected from the Franklinian Basin.

Holotype. MGUH178 (Pl. 17, figs 1–2) cephalon; GGU 198226 (CPL1).

Figured paratypes. Locality CPL1: MGUH182 librigina; MGUH183 cranidium. Locality CPL2: MGUH179 cranidium; MGUH180 cephalon. Locality VGL1: MGUH181 cephalon.

Diagnosis. Astroproetus with glabella longer than wide, preglabellar field roughly one-third sagittal length of cranidia. Anterior and lateral borders and genal spine bearing at least 4 distinct terrace ridges; fine, scattered granules elsewhere.

Description. Cephalon semicircular, averaging 60% as long (sag. excluding genal spines) as wide (tr. at widest point) (range = 52–65%; n = 3). Glabella conical, anteriorly tapering anterior of S2 to a sub-triangulate form ; pre-occipital part slightly longer (sag.) than wide (tr.) with maximum width posteriorly. Well impressed axial furrows throughout course. Lateral glabellar muscle impressions impressed on internal mould, with S1 running from axial furrow at roughly 60 degrees from an exsagittal line for about half its course, after which at a much lower angle, terminating prior to occipital furrow. S2 running sub parallel to and for the same distance as the first half of S1. Occipital ring slightly wider (tr.) than posterior of pre-occipital glabella. Occipital furrow deep, becoming longer (exsag.) abaxially. Convex forwards adaxially where slightly longer (sag.) than anterior border. Occipital lobes weakly defined anteriorly; ovoid. Pronounced occipital node situated closer to anterior margin of occipital ring. Facial suture from γ to β initially diverging from an exsagittal line at roughly 40 degrees. γ and ε equally very close to axial furrow. Posterior branch from ε to ζ directed smoothly away from axial furrow. Palpebral lobe comprising roughly one-third total sagittal length cranidium; posterior end positioned just anterior of occipital furrow. Palpebral width averaging 60% cranidial sagittal length (range = 57–

63%; n = 3). Preglabellar field longer (sag.) than anterior border; length of preglabellar field roughly one-third sagittal length of cranidium. Anterior border furrow deep. Pronounced anterior and lateral borders bearing at least 4 distinctive, regularly spaced terrace ridges. Sculpture of fine, scattered granules, except on anterior border.

Eye socle narrow; upper and lower margins incised, retaining equal thickness along eye. Lateral border furrower wider (tr.) than anterior border furrow length (sag.) and shallowing posteriorly. Lateral border of similar width (tr.) to anterior border length (sag.), of similar convexity and bearing about 4 terrace ridges. Posterior border narrower than lateral border, and lacking terrace ridges. Lateral and posterior borders joining to run down genal spine as a median groove, terminating prior to tip of genal spine. Genal spine with at least 4 terrace ridges, and extending for over half sagittal length cranidium. Sculpture of fine scattered granules except on borders and genal spine.

Remarks. The glabellar morphology, tapering to a sub-triangular point anteriorly, is characteristic of *Astroproetus*, as exemplified by *A. interjectus* (Reed, 1935, figured by Owens 1973*a*, pl. 11, figs 13–15, pl. 12, figs 1a–b), *A. scoticus* (Reed, 1941, figured by Owens 1973*a*, pl. 11, figs 5–8, 10) and *A. achabae* (Chatterton and Ludvigsen, 2004, pl. 74, figs 2, 4, 6, 8, 9). These species all have a shorter (sag.) preglabellar field than that of *A. franklini*. *A. franklini*. differs from the type species *A. reedi*, in the following: glabella longer (sag.) than wide (tr.), rather than as wide (tr.) or a little wider than long (sag.); longer preglabellar field; granular sculpture and distinct terrace ridges on cephalic borders (the apparent absence of these in *A. reedi* could be preservational).

The glabellar morphology, pronounced anterior border bearing four terrace ridges, and the granular sculpture are reminiscent of *Scharyia*? sp. of Lane (1972, p. 352, pl. 61, fig. 12) from the Telychian Samuelsen Høj Formation of Kronprins Christian Land, eastern North Greenland. Species of *Astroproetus* typically have very faint lateral glabellar muscle impression, S1 and S2 are clear on one of the cranidia of *A. franklini* (pl. 17, fig. 3), as this is an internal mould. A wetted cranidium of *A. achabae* (Chatterton and Ludvigsen, 2004, pl. 74, fig. 9) shows a similar S1 and S2 morphology to that of *A. franklini*.

Occurrence and distribution. Central Peary Land (CPL1, 2) and Valdemar Glückstadt Land (VGL1).

Astroproetus sp.

Plate 17, figures 10-12

Figured material. GGU 274996 (KCL4): MGUH184 cephalon.

Remarks. The fragmentary nature of the specimen and its preservation as an internal mould enable only limited description. Distinguishable characters are as follows: cephalon 60% as long (sag.) as wide (tr.); glabella conical, tapering anteriorly to a sub-triangular point, of low convexity (tr.), with a granular sculpture preserved posteriorly; posterior of palpebral lobe positioned just anterior of occipital furrow; preglabellar field comprising 35% total cranidial sagittal length; anterior border roughly half sagittal length of preglabellar field and with at least 3 terrace ridges; narrow eye socle gradually expanding anteriorly; lateral border of comparable width

(tr.) to anterior border length (sag.) and with 4 terrace ridges; posterior border longer (exsag.) adaxial to ω; Lateral and posterior border furrows joining to run down genal spine bearing numerous terrace ridges.

The sub-triangular anterior of the glabella, long (sag.) preglabellar field, and anterior border with distinct terrace ridges are similar to *Astroproetus franklini*, and the cranidium is considered congeneric.

Occurrence and distribution. Kronprins Christian Land (KCL4).

Genus THEBANASPIS Lütke, 1990

Type species. By original designation; *Thebanaspis thebana* Lütke, 1990. From the Silurian (Llandovery, Rhuddanian) Edgewood Formation, Thebes, Illinois, USA.

Diagnosis. From Owens (2006, p. 132): crassiproetine with glabella ovate, bluntly acuminate anteriorly; occipital ring with weakly defined, transversely ovate to elongate lateral lobe; short preglabellar field, shorter (sag.) than anterior border; no intramarginal zone; pygidium with comparatively narrow axis with 8-10 rings; pleural areas with 5-7 pairs of ribs, the anteriormost of which extend close to margin, and with more posterior ribs terminating at inner edge of border; anterior pleural bands not inflated distally.

Remarks. Owens (2006, p. 129) considered *Thebanaspis* to have derived from *Astroproetus*. He noted that *Thebanaspis* can be distinguished by a broader, more ovate glabella, a shorter preglabellar field, and a longer subparabolic pygidium with

more axial rings and pleural ribs. The cranidial differences are obvious between the *Thebanaspis* sp. and *Astroproetus* species (pl. 17, figs 1–12) described here.

Thebanaspis sp.

Plate 17, figures 13–16

Figured material. GGU 301326 (WPL1): MGUH185 cranidium. GGU 298506 (WL): MGUH186 cranidium.

Description: Cranidia with sagittal lengths 7.52 and 8.5 mm. Pre-occipital glabella roughly 87% as wide (tr.) as long (sag.) and almost straight sided for posterior three-quarters. Lateral glabellar muscle impressions effaced. Axial furrows well impressed. Preglabellar field roughly two fifths length (sag.) of anterior border. Anterior border furrow well impressed. Occipital ring shorter (sag.) than anterior border. Facial suture from γ to β diverging from an exsagittal line at roughly 35 degrees. Midpoint of palpebral lobe (δ) located roughly one-third entire glabellar length (sag.) from occipital furrow.

Remarks. The cranidia display the subacuminate frontal glabellar lobe and short preglabellar field characteristic of *Thebanaspis. Thebanaspis* sp. differs from the type species, *T. thebana* most notably by having a relatively longer (sag.) glabella with straighter, more parallel-sided axial furrows posteriorly. Additionally, the lateral glabellar impressions are more effaced than those of *T. thebana*.

Occurrence and distribution. Wulff Land (WL) and western Peary Land (WPL1).

Genus WINISKIA Norford, 1981

Type species. By orginal designation; *Winiskia perryi* Norford, 1981. From the Telychian–?early Wenlock Attawapiskat Formation, Ekwan River, Ontario, Canada.

Diagnosis. Modified from Owens (2006, p. 132) to allow for presence or absence of a pygidial border: crassiproetine with elongate, tapering glabella; lateral occipital lobes; preglabellar field very short (sag.) or absent; intramarginal zone present; pygidium ranges from 60–80% as long (sag.) as wide (tr.), with 8–10 (?+) axial rings plus terminal piece and 6–8 pairs of pleural ribs.

Remarks. Owens (2006, p. 132), noted the close relationship between *Winiskia* and *Thebanaspis.* The genera may be distinguished by the presence of an intramarginal zone in *Winiskia*, accompanied by a more elongate glabella.

Winiskia eruga sp. nov.

Plate 18, figures 1–9

Derivation of name. Latin, *erugo*, clear of wrinkles, smooth, alluding to the loss of characters by effacement.

Holotype. MGUH187 (Pl. 18, figs 1–2) cranidium; GGU 274654 (CPL4).

Figured paratypes. Locality CPL3: MGUH188 librigena; MGUH189 thoracic segment; MGUH191 articulated pygidium and partial thorax; MGUH192 pygidium. Locality KCL3: MGUH190 librigena.

Diagnosis. Highly effaced species of *Winiskia* with glabella strongly tapering anteriorly and intramarginal zone narrow anteriorly. Sculpture of faint pits present on lateral border. Pygidium with upturned borders.

Description. Pre-occipital glabella roughly 75% as wide (tr.) posteriorly as long (sag.); conical, tapering strongly anteriorly to a blunted point. Lateral glabellar muscle impressions effaced. Midpoint of palpebral lobe situated one-third entire glabellar sagittal length from occipital furrow. Axial furrows well impressed throughout course. Occipital ring a little wider (sag.) than posterior of pre-occipital glabella, occipital furrow deep medially, shallowing abaxially. Occipital ring equally long (sag.) abaxially and adaxially (roughly twice sagittal length of anterior border). Lateral occipital lobes ovoid, transversely elongate, and largely effaced. Extremely short (sag.) preglabellar field present. Anterior border with similar course to anterior of glabella, abaxially trending posteriorly at angle of roughly 70 degrees from sagittal line. Intramarginal zone narrow medially, rapidly increasing in length (exsag.) abaxially.

Narrow eye socle with well incised lower furrow. Lateral border with two raised terrace ridges marginally. Intramarginal zone sharply defined at both border and epiborder furrows, wide (tr.) and shallow. Lateral border faintly pitted adaxial of terrace ridges. Posterior border furrow deeper than lateral epiborder furrow both

furrows join to run down genal spine which comprises at least one-quarter entire length (exsag.) of librigena.

Axial regions of thorax very convex transversely. Articulating half ring roughly half the length (sag.) of axial ring. Pleural furrow trending transversely, well defined for over half width (tr.) of pleura.

Pygidium 73% as long (sag.) as wide (tr.) (n = 1). Axis straight-sided and conical; smoothly rounded and tapering posteriorly. Raised area tapering posterior of axis. Anteriorly, axis comprising 38% entire pygidial exsagittal length (n = 1). Axis comprising on average 87% total pygidial sagittal length (n = 2). Anterior most 6 axial rings visible, posterior to this highly effaced; exact number indeterminable but possibly 9 or 10, with a terminal piece. First axial ring raised relative to others; slightly convex sagittally as well as transversely, other rings flattened sagittally. Anterior pleural band clear, number of pleural ribs estimated as 7, but very faint as interpleural furrows become increasingly effaced posteriorly. Very shallow pleural furrows visible on anteriormost ribs; posterior to this, effaced. Pleural ribs intersect borders. Borders broad, especially posteriorly; smoothly concave.

Remarks. The cranidia are assigned to this species on the basis of their effaced exoskeleton, the lack of sculpture being a diagnostic character of the pygidia. The cranidium of *W. eruga* differs from the type species *W. perryi*, and other *Winiskia* species in the narrow nature of the intramarginal zone anteriorly. The principal differences between the cranidia of *W. eruga* and *W. perryi*, are the more bluntly rounded frontal glabellar lobe of *W. perryi* which extends into the intramarginal zone (the cranidium of *W. eruga* retains a short (sag.) preglabellar field). The morphology

of the glabella of *W. eruga* is most comparable with that of *W.* sp. 1 (Owens 2006, p. 133, fig. 7. 8a–b); they both taper strongly anteriorly.

The pygidium of *W. eruga* is relatively wider (tr.), and more effaced than that of the type species; axial rings and pleural and interpleural furrows are less clear, and it lacks a distinct postaxial ridge. The pygidium instead, has similar proportions to *W. lissa* (Owens, 2006, p. 133, fig. 7. 5–7.7). *W. eruga* differs from *W. lissa* in its greater degree of effacement: in some specimens the pleural ribs are almost invisible. In addition, *W. eruga* has a more upturned margin, and the posterior of the axis of *W. eruga* is not sharply defined as in *W. lissa*: there is a raised area posterior of the pygidial axis in *W. eruga*, probably representing effacement of a post-axial ridge.

Occurrence and distribution. Central Peary Land (CPL3–4) and Kronprins Christian Land (KCL3, 5).

Winiskia leptomedia sp. nov.

Plate 18, figures 10–16

Derivation of name. Contraction of Greek, *leptos*, thin, fine, small, slender, subtle, delicate, and Latin, *medius*, middle, alluding to the narrow pygidial axis.

Holotype. MGUH193 (Pl. 18, figs 10–11) cranidium; GGU 275015 (KCL1).

Figured paratypes. Locality KCL1: MGUH194 cranidium; MGUH195–196 pygidia.

Diagnosis. Winiskia with short (sag. and exsag.) occipital ring; intramarginal zone subequal (sag.) to anterior border; pygidial axis comprising under one-third pygidial transverse width anteriorly.

Description. Glabella conical, pre occipital part 74% as wide (tr.) at widest point opposite palpebral lobes, as long (sag.). Tapering forwards strongly in anterior 30% of glabella, to a blunted point. S1–S3 largely effaced; faint impressions trend from axial furrows between 40 and 50 degrees from exsagittal line. Occipital ring wider (tr.) than posterior of pre-occipital glabella, roughly equal in transverse width to part of glabella opposite palpebral lobes, and comprising 11% total glabellar sagittal length. Equal length medially (sag.) and at axial furrows (exsag.), and occipital node placed sagittally midway across occipital ring. Anterior border convex, a little longer (sag.) than intramarginal zone. Extremely short (sag.) preglabellar field present. Midpoint of palpebral lobe situated a little over one-third pre-occipital glabellar length (sag.) from occipital furrow.

Pygidium averaging 65% as long (sag.) as wide (tr.) (range = 60–70%; n = 4). Axis straight sided and conical; smoothly rounded and tapering posteriorly. Raised postaxial ridge tapering posterior of axis. Anteriorly, axis averaging 28% entire pygidial exsagittal length (range = 27–30%; n = 4). Axis comprising on average 88% total pygidial sagittal length (range = 86–90%; n = 4). Axial rings highly effaced medially and posteriorly; exact number indeterminable, possibly 9 with a terminal piece. Axial rings sagittally flattened. Anterior pleural band with deeply incised furrows. Anteriormost pleural ribs distinguishable; posterior of this effaced. Number of ribs estimated as 7. Anteriormost pleural ribs with interpleural furrows deeper than pleural furrows. Pleural ribs intersecting smoothly concave margins.

Remarks. The pygidium of *W. leptomedia* is very similar to that of *W. eruga*. It is distinguished from *W. eruga* by its narrower pygidial axis (relative to pygidial transverse width). The cranidia of the two species are quite different: *W. eruga* has a posteriorly wider, more strongly tapering glabella, and shorter (sag.) intramarginal zone. The cranidia of *W. leptomedia* has a similar glabellar outline to both the type species *W. perryi* (which has no preglabellar field), and *W. lissa*. It is distinguishable from these cranidia by a more posteriorly placed palpebral lobe, and differs from all other *Winiskia* cranidia by its short (sag. and exsag.) occipital ring.

Occurrence and distribution. Kronprins Christian Land (KCL1).

Winiskia lipopyga sp. nov.

Plate 18, figures 17–20

Derivation of name. Contraction of Greek, *lipos*, fat, and Greek, *pyge*, rump, buttocks, alluding to the convexity of the pygidium.

Holotype. MGUH197 (Pl. 18, figs 17–18) pygidium; GGU 274689 (CPL5).

Figured paratypes. Locality CPL4: MGUH199 pygidium. Locality CPL5: MGUH198 pygidium.

Diagnosis. Winiskia with a very convex pygidium, post-axial ridge, and a finely pitted sculpture.

Description. Pygidium averaging 62% as long (sag.) as wide (tr.) (range = 60–65%; n = 3). Axis straight-sided and conical; smoothly rounded posteriorly, with a post-axial ridge. Anteriorly, axis averaging 34% entire pygidial exsagittal length (range = 30–37%; n = 4). Axis comprising on average 83% total pygidial sagittal length (range = 83%; n = 3). Ten axial rings and a terminal piece. Axial rings well impressed anteriorly, more effaced posteriorly and medially. Axial ring furrows slightly sigmoidal. First axial ring raised relative to others; slightly convex sagittally as well as transversely, other rings flattened sagittally. Seven pleural ribs and an anterior pleural band. Interpleural furrows are mostly well impressed; strongest anteriorly, becoming effaced near posterior of pygidium. Pleural ribs intersect margins. Margins broad, especially posteriorly; smoothly concave. Entire surface of pygidium very finely pitted.

Remarks. The pygidium of *W. lipopyga* is similar to that of *W. eruga*. *W. lipopyga* is distinguished by: greater axial and pleural region convexity; more pronounced axial ring and interpleural furrows; anterior of axis relatively wider; presence of a clear post-axial ridge; exoskeleton finely pitted, rather than smooth.

W. lipopyga also resembles the pygidium of *W.* sp. 1 of Owens (2006). Both are highly convex, with interpleural furrows widening near the margins, show a similar degree of effacement, and have sigmoidal axial ring furrows. *W. lipopyga* differs from *W.* sp. 1 in its shorter pygidium (62% as long (tr.) as wide (exsag.) compared to nearly 80% as long as wide in *W.* sp. 1), upturned pygidial margins, and post-axial ridge.

Occurrence and distribution. Central Peary Land (CPL4 –5).

Winiskia stickta sp. nov.

Plate 19, figures 1–11

Derivation of name. Greek, *sticktos*, punctured, spotted, dappled, alluding to the pitted sculpture.

Holotype. MGUH200 (Pl. 19, figs 1–2) cranidium; 198214 (CPL2).

Figured paratypes. Locality CPL2: MGUH201 cranidium; MGUH202 librigena; MGUH203 hypostome; MGUH204–207 pygidia.

Diagnosis. Winiskia with a broad and deep intramarginal zone, visible glabellar muscle impressions, and pronounced pygidial border; pitted sculpture, with pits largest and deepest within intramarginal zone and pygidial border.

Description. Pre-occipital glabella 86% as wide (tr.) as long (sag.) (n = 2); conical, bluntly rounded anteriorly. Glabellar furrows S1 and S2 weak but visible, both in contact with axial furrow which is inflated adaxially at these contacts. Both S1 and S2 steeply inclined, S1 forked. Occipital ring roughly equal in width (tr.) to posterior of pre-occipital glabella, medially longer (sag.) than at axial furrows (exsag.), and comprising 17% total glabellar sagittal length (n = 2). Occipital furrow well impressed, occipital lobes less so but still conspicuous. Occipital node faint, situated sagittally midway across occipital ring. Narrow preglabellar field. Anterior border gently convex sagittally. Intramarginal zone longer (sag.) than anterior border, and with distinct pits; finer pits covering all other parts of cranidium.

Librigena with lower margins of eye socle deeply incised. Lateral border with two raised terrace ridges marginally. Intramarginal zone sharpest at border furrow, deep and wide (tr.) Posterior border longer (exsag.) than width (tr.) of lateral border; posterior border furrow deeper than lateral epiborder furrow. Posterior and lateral border furrows join to run down genal spine (length unknown). Entire librigena finely pitted, pits larger and deeper in intramarginal zone.

Hypostome roughly 78% as long (sag.) as wide (tr.) across anterior wings, with width across shoulders 69% width across anterior wings. Anterior wings subrectangular; roughly twice as long (exsag.) as wide (tr.). Narrow (tr.) lateral border. Middle body very convex (sag. and tr.), very slender; roughly twice as long (sag.) as wide (tr.). Anterior lobe not anteriorly expanded (tr.), with lateral border furrows subparallel. Middle furrow significantly weaker than deep lateral border furrow; trending posteriorly roughly 25 degrees from exsagittal line, enclosing very narrow (tr.) maculae. Middle furrow joining lateral border furrow roughly one-third total middle body length (sag.) from posterior of middle body. Anterior lobe of middle body with terrace ridges trending from lateral border and middle furrows, converging anteriorly. Medially, where middle body lacks terrace ridges, fine pits similar to those on dorsal exoskeleton occur.

Pygidium averaging 65% as long (sag.) as wide (tr.) (range = 59–70%; n = 6). Axis straight-sided and conical; smoothly rounded posteriorly and with a post-axial ridge. Anteriorly, axis averaging 29% entire pygidial exsagittal length (range = 28–29%; n = 5). Axis comprising on average 79% total pygidial sagittal length (range = 75–82%; n = 6). 9 axial rings and a terminal piece. Axial rings slightly convex, those of well preserved specimens each with paired shallow, subcircular muscle impressions positioned close to the axial furrow, mid-length (exsag.) of axial rings.

Axial ring furrows well impressed. Seven pleural ribs and an anterior pleural band. Interpleural furrows well impressed. Faint pleural furrows locally visible on anteriormost pleural ribs. Pleural ribs terminate at pronounced pygidial border. Sculpture of fine pits, increasing in size and depth towards border.

Remarks. *W. stickta* is the least effaced of the *Winiskia* species described here. The pygidium of *W. stickta* is most similar to *W. sextaria* (Owens, 2006, p. 133, figs 7.1–7.3) in terms of the depth of both axial and pleural ribs and the presence of a pygidial border. The pygidium of *W. sextaria* is relatively slightly longer (sag.) than that of *W. stickta* (70% as long as wide as opposed to 65% in *W. stickta*) and has an extra axial ring and pleural rib. The pygidial border of *W. stickta* is more pronounced than in *W. sextaria*. The cranidium of *W. stickta* differs from that of *W. eruga* and *W. sextaria* in having a slightly longer (sag.) preglabellar field, blunter glabellar anterior, less effaced glabellar muscle impressions, a wider intramarginal zone, and pitted sculpture.

The associated hypostome (Pl. 19, figs 5–6) represents the only described *Winiskia* hypostome: it is comparable with that of *Hedstroemia delicata* (Hedström, 1923), figured by Owens (2006, fig. 1.15-17c), also included in the Crassiproetinae. The position at which the middle furrow meets the lateral border furrow, convexity of the middle body, and the position and trend of terrace ridges and fine pitting, are particularly similar. The *Winiskia* hypostome lacks the slight anterior expansion shown by the hypostome of *H. delicata* and has the middle furrow directed at a lower angle posteriorly, resulting in more slender maculae.

A distinctive feature of the species from the Llandovery of North Greenland and the Telychian–?early Wenlock Attawapiskat Formation, Ontario (as shown by *W.*

perryi), is the presence either of a tapering raised area posterior of the pygidial axis or a post-axial ridge. By contrast, forms from the Llandovery of Sweden and Norway described and figured by Owens (2006) have the pygidial axis sharply defined posteriorly. The three *Winiskia* pygidia described and figured by Owens (2006, fig. 7), each strongly resemble one of the new Greenland taxa. Owens's taxa show the same kind of variation as the Greenland taxa, particularly with respect to the degree of effacement, and relative width (tr.) of pygidial axis to total pygidial width.

Occurrence and distribution. Central Peary Land (CPL2).

Subfamily TROPIDOCORYPHINAE Přibyl, 1946

Genus DALARNEPELTIS Přibyl and Vaněk, 1978

Type species. By original designation; *Decoroproetus campanulatus* Owens, 1973b, from the Upper Ordovician Boda Limestone, Sweden.

Diagnosis. Modified after Přibyl and Vaněk (1978, p. 166): tropidocoryphine with a subrectangular, waisted glabella with frontal glabellar lobe displaying an almost straight anterior margin; S1 deeply impressed, isolating oval L1; S2 and S3 visible but weaker than S1; preglabellar field short (sag.) or absent; occipital ring wider (tr.) than pre-occipital glabella, with weakly defined occipital lobes; pygidium with 7–9 axial rings, becoming increasingly effaced posteriorly, and 4–8 pairs of pleural ribs.

Remarks. *Dalarnepeltis* was originally considered to be a subgenus of *Decoroproetus* Přibyl, 1946*b*, by Přibyl and Vaněk, 1978. Here, sufficient differences from *Decoroproetus* are recognised for *Dalarnepeltis* to be considered a genus, particularly given the distinctive glabellar morphology. *Decoroproetus narbonnei* Chatterton and Ludvigsen (2004, p. 70, pl. 78, figs 10–17. pl. 84, figs 14-15), from the Aeronian Goéland Member of the Jupiter Formation, Anticosti Island, Québec, Canada, and *Decoroproetus dewingi* Chatterton and Ludvigsen (2004, p. 71, pl. 78, figs 1-7, 9), from the Telychian Ferrum or Pavillon Member of the Jupiter Formation, Anticosti Island, Québec, Canada, share remarkably similar glabellar morphologies, position and depth of impression of the lateral glabellar muscle impressions, and scrobiculate sculpture, with the type species of *Dalarnepeltis, D. campanulatus*, and *D. brevifrons* described below. As such, these species should be included in *Dalarnepeltis*. The genus shows a trend towards the shortening of the preglabellar field, which is virtually lost in *D. dewingi*, and *D. brevifrons*.

Dalarnepeltis brevifrons sp. nov.

Plate 19, figures 12–17

Derivation of name. Contraction of Latin, *brevis*, short, and Latin, *frons*, brow, forehead, alluding to the extremely short preglabellar field. Noun in apposition.

Holotype. MGUH208 (Pl. 19, figs 12–13) cephalon with two articulated thoracic segments; GGU 274654 (CPL4).

Figured paratypes. Locality CPL1: MGUH209–10 pygidia. Locality CPL4: MGUH211 pygidium.

Diagnosis. Dalarnepeltis with cephalon with extremely short preglabellar field, shallow anterior and border furrows, and δ placed opposite anterior of S1. Pygidium with eight or nine axial rings, and distinct postaxial ridge; eight strongly imbricate pleural ribs.

Description. Cephalon almost twice as wide (tr.) as long (sag.). Pre-occipital glabella almost as wide (tr.) as long (sag.), maximum width near anterior of L1. Axial furrows well impressed; from anterior of L1 converging anteriorly until S2, then diverging until near front of glabella. S1 deepest anteriorly, terminating prior to axial furrow; posteriorly narrowing and shallowing, very shallow where intersecting occipital furrow. L1 comprising roughly one-third total glabellar sagittal length. S2 and S3 equally weakly impressed, both connected to axial furrow. S2 directed roughly transversely and S3 directed anteriorly at roughly 45 degrees, both for a short distance. S2 placed opposite γ, S3 half the distance from S2 as S2 is from S1. Occipital ring slightly wider (tr.) than widest point of glabella, longer (sag.) than anterior border. Lateral occipital lobes only expressed anteriorly. Occipital node midlength on occipital ring. Occipital furrow deep, trending transversely for most of width. Facial suture from γ to β diverging from exsagittal line at 15 degrees. Facial suture between α and β, directed strongly adaxially; γ and ε almost in contact with axial furrow. Palpebral lobe comprising just over one-quarter total cephalic sagittal length. Posterior of palpebral lobe located just anterior of occipital furrow; anterior

end located opposite S2. Anterior border furrow very shallow, anterior border weakly sagittally convex.

Librigena gently convex. Narrow eye socle with equal thickness along length; margins defined by deep upper furrow, and shallower lower furrow. Lateral border of similar width (tr.) to anterior border length (sag.) and very gently convex. Posterior border furrow markedly deeper than anterior and lateral border furrows, joining with lateral border furrow to run down genal spine. Genal spine length unknown. Posterior border shorter (exsag.) adaxially than lateral border width (tr.); becoming longer (exsag.) abaxially.

Scrobiculate sculpture covering entire cephalon. Glabella and occipital ring with most pronounced sculpture, where scrobiculae are convex forward medially.

Pygidium on average 59% as long (sag.) as wide (tr.) (range = 50–65%; n = 3). Anterior width of axis comprising on average 30% of total anterior width (tr.) of pygidium (range = 25–34%; n = 3). Axis on average 88% total sagittal length of pygidium (range = 87–89%; n = 3), sharply tapering to a sub-triangular posterior. Axial furrow moderately impressed; weaker around posterior of axis. Axial ring furrows becoming very shallow posteriorly. Eight strongly imbricate pleural ribs. Interpleural and pleural furrows both moderately impressed and intersecting pygidial margins; no pygidial border.

Remarks. D. brevifrons has the most effaced anterior and lateral border furrows, and the most anteriorly positioned palpebral lobe of all *Dalarnepeltis* species. The near loss of the preglabellar field in *D. brevifrons*, is shared with *D. dewingi*; these cranidia are readily differentiated by the presence of coarse granules interrupting the

scrobiculae in *D. dewingi* however, which also has a more anteriorly positioned occipital node.

The pygidium of *D. brevifrons* differs from all other species of *Dalarnepeltis* in possessing a distinct post-axial ridge: other species exhibit a raised area tapering posterior of the axis (as seen in *Winiskia eruga*), which could represent effaced post-axial ridges. *D. brevifrons* also exhibits a greater number of axial rings and pleural ribs than the other three species. The morphology of the pleural ribs, being highly imbricate, is particularly similar to those of *D. campanulatus*.

Occurrence and distribution. Central Peary Land (CPL1, 4).

Tropidocoryphine gen. et sp. indet.

Plate 20, figures 1–3

Figured material. GGU 198186 (CPL2): MGUH212 pygidium. GGU 198201 (CPL2): MGUH213 pygidium.

Description. Pygidium roughly twice as wide (exsag.) as long (tr.). Number of axial rings estimated as 6 or 7, with paired apodemal pits visible on anterior most rings. Axis roughly 80% entire pygidial sagittal length, posteriorly bluntly rounded. Axial furrow well impressed, although less so around posterior of axis. Four pleural ribs and an anterior band. Anterior pleural bands inflated and with coarse scattered granules, posterior pleural bands not inflated and with fewer granules. Interpleural and pleural furrows equally impressed, shallower in posteriormost ribs. Pygidial margins concave, adaxial to a narrow pygidial border.

Remarks. The imbrication of the pleural ribs is typical of the subfamily, however, the pygidial morphology is not characteristic of any described genus.

Occurrence and distribution. Central Peary Land (CPL2).

Superfamily AULACOPLEUROIDEA Angelin, 1854

2.3.6 Family AULACOPLEURIDAE Angelin, 1854

Aulacopleurid cf. *Songkania* Chang, 1974

Plate 20, fig. 4

Figured material. GGU 275038 (VGL1): MGUH214 cephalon.

Remarks. A single fragmentary cephalon from Valdemar Glückstadt Land has the following distinguishing characters: subquadrate glabella; isolated L1; short, almost transverse S2; long preglabellar field; long (sag.) anterior border furrow. The glabella morphology and length of the preglabellar field are reminiscent of *Songkania*.

Occurrence and distribution. Valdemar Glückstadt Land (VGL1).

2.3.7 Family SCHARYIIDAE Osmólska, 1957

Diagnosis. From Owens and Fortey (2009, p. 1215): aulacopleuroideans with triangular or subtriangular glabella, with or without prominent, isolated L1; long

(exsag.) palpebral lobe; more derived taxa with cedariiform postocular facial suture; thorax with 6–9 segments; pygidium isopygous or subisopygous, with elongate, conical axis with 5–10 rings; 4 –6 pleural ribs.

Remarks. Owens and Hammann (1990) included only *Scharyia* in the subfamily Scharyiinae, and assigned the subfamily to the Family Brachymetopidae. They reassigned *Panarchaeogonus* Öpik, 1937, to the family Aulacopleuridae, based on the following characters: isolated L1; over 10 thoracic segments; short, transverse pygidium. Adrain and Chatterton (1993) argued that an isolated L1 is a condition general to the Aulacopleuroidea, that the only species of *Panarchaeogonus* for which the number of thoracic segments is known, does in fact contain nine (*P. trigodus* Warburg, 1925) and that although poorly known, the pygidium of *Panarchaeogonus* is quite long relative to its width, like that of *Scharyia* but unlike that of aulacopleurids. Adrain and Chatterton (1993) returned to the shared characters of *Scharyia* and *Panarchaeogonus* recognised by Owens (1974), and considered these genuinely indicative of relationship: triangulate glabella; large palpebral lobe; position of the eye; occipital ring morphology. Adrain and Chatterton (1993) therefore considered the Scharyiidae as a separate Aulacopleuroidean family, including the genera *Scharyia*, *Panarchaeogonus* and also, *Niuchangella* (Chang, 1974) which they found to have affinities to *Panarchaeogonus*. Owens and Fortey (2009) accepted that *Panarchaeogonus* shares more characters with *Scharyia* than believed by Owens *in* Owens and Hammann (1990), and noted that the two genera are linked particularly by their pygidial proportions which also differentiate them from other members of the family.

Jell and Adrain (2003, p. 479) included the following genera in the Scharyiidae: *Scharyia* Přibyl, 1946*b*; *Lasarchopyge* Chatterton, Edgecombe, Waisfeld and Vaccari, 1998; *Panarchaeogonus* Öpik, 1937; *Niuchangella* Chang, 1974. Owens and Fortey (2009, p. 1215) described new species of *Lasarchopyge* from the Upper Ordovician of Arctic Russia, which share the following characters with *Scharyia*, supporting inclusion of both genera within the same family: glabella without isolated L1; cedariiform postocular facial suture; length and segmentation of the pygidium.

The affinities of *Proscharyia* Peng 1990, pl. 19, figs 7-15, from the Tremadoc Madaoyu Formation, north-western Hunan, remain unresolved. The genus was proposed as a member of the Scharyiinae by Peng (1990) and Adrain and Fortey (1997), and as forming a clade at family level with *Scharyia* and *Panarchaeogonus*, by Adrain and Kloc (1997). The species was listed as a questionable bathyurid by Jell and Adrain (2003, pp. 431, 467).

The concept of the Scharyiidae as defined by Jell and Adrain (2003, p. 479) and Owens and Fortey (2009), is accepted here.

Genus SCHARYIA Přibyl, 1946*b*

Type species. By original designation; *Proetus micropygus* Hawle and Corda, 1847, from the Kopanina Formation, Ludlow, Prague district, Czech Republic.

Diagnosis. After Owens (1974, p. 688): aulacopleuridine with glabella triangulate; occipital ring of almost constant length sagittally and exsagittally, without lateral lobes; preglabellar field weakly convex in longitudinal section; facial suture

cedariiform; thorax of 6 segments; pygidial axis conical with 5–9 rings with narrow (tr.) crescentic half rings, pleural areas with 4–6 pairs of ribs; small granule on adaxial end of each thoracic and pygidial pleural band.

Scharyia lobarga sp. nov.

Plate 20, figures 5–7

Derivation of name. Contraction of Latin, *lobus*, a rounded projection or protuberance, and Latin, *margo*, brink, border, alluding to the inflated lobes on the pygidial margin.

Holotype. MGUH215 (Pl. 20, figs 5–6) pygidium; GGU 198226 (CPL1).

Figured paratypes. Locality CPL1: MGUH216 pygidium.

Diagnosis. Scharyia with inflated lobes on pygidial margin, evenly increasing in size posteriorly. Posterior pleural bands with distinct granule abaxially as well as adaxially.

Description. Pygidium averaging 77% as long (sag.) as wide (tr.) (range = 72–82%; n = 5). Pygidial sagittal length ranging from 1.96 mm to 3.08 mm. Axis conical and straight-sided, comprising on average 70% entire sagittal length of pygidium (range = 51–86%; n = 5). Anteriorly, axial width comprising about one-third (34%, range = 32–35%, n = 5) entire pygidial transverse width. Axis with seven axial rings and a terminal piece. Depth of impression of ring furrows increases towards deeply

impressed axial furrow. Axial rings increasingly convex anteriorly. Anterior pleural band and five furrowed ribs curved strongly backwards. Both pleural and interpleural furrows well impressed. Pleural furrows increasing in depth distally, slightly shallower than interpleural furrows. Pleural furrows of ribs four and five do not reach axial furrow. Additional to the granule present on the adaxial end of each anterior pleural band, a larger granule is present on the abaxial end of each posterior pleural band. Distinct border with five pairs of inflated lobes and one terminal inflated lobe; both border and lobes smoothly increasing in size posteriorly. First pleural rib anterior to pleural furrow, distinctly connected to first lobe. This repeated but less obvious with remaining ribs. Deep border furrow. Entire pygidium with fine, scattered granules.

Remarks. See under remarks for *Scharyia deiropede* below.

Occurrence and distribution. Central Peary Land (CP1).

Scharyia deiropede sp. nov.

Plate 20, figures 8–10

Derivation of name. Greek, *deiropede*, collar, necklace, fancied resemblance of the marginal pygidial lobes to a necklace. Noun in apposition.

Holotype. MGUH217 (Pl. 20, figs 8–9) pygidium; GGU 198226 (CPL1).

Figured paratypes. Locality CPL1: MGUH218 pygidium.

Diagnosis. Scharyia with sigmoidal course to interpleural furrows. Inflated lobes on pygidial margin, with terminal lobe notably more inflated in comparison to other lobes.

Description. Pygidium averaging 75% as long (sag.) as wide (tr.) (range = 73–76%; n = 2). Pygidial sagittal length ranging from 3.47–3.60 mm. Axis conical and straight-sided, comprising roughly 70% entire sagittal length of pygidium. Anterior axial width comprising one-third (33%; n = 2) entire pygidial transverse width. Axis with 7 or 8 axial rings and a terminal piece. Depth of impression of ring furrows increases towards axial furrow which is deeply impressed. Axial rings increasingly convex anteriorly. Anterior pleural band and five furrowed ribs curved strongly backwards. Pleural furrows very shallow, increasing in depth distally. Interpleural furrows better impressed. Pleural furrows of ribs four and five do not reach axial furrow. Distinct border with five pairs of inflated lobes and one terminal inflated lobe; both border and lobes increasing in size posteriorly, with posteriormost lobe distinctly larger than all others. Deep border furrow. Entire pygidium covered in fine, scattered granules.

Remarks. The small granule on the adaxial end of each pleural band is diagnostic of the genus. The axial ring morphology, comprising what essentially appear to be failed half rings is also characteristic of *Scharyia*.

The pygidium of *S. deiropede* shares strong similarities with *S. lobarga* in overall morphology, most noticeably in the presence of inflated lobes on the border. *S. deiropede* differs from *S. lobarga* in the following: the course of the interpleural furrows is more sigmoidal; border lobes are significantly more inflated further posteriorly; both pleural and interpleural furrows are less well impressed; pleural ribs

are more distinct from the border; granular sculpture is both finer and more dense. *S. lobarga* has distinct granules abaxially on the posterior pleural bands, these may also be present in *S. deiropede*, with the feature obscured due to preservational effects.

The pygidia of *S. lobarga* and *S. deiropede* are closest to a single pygidium of *S.* sp. Lane (1972, p. 352, pl. 61, fig. 11), from the Telychian Samuelsen Høj Formation of Kronprins Christian Land, eastern North Greenland. Notable similarities are the pygidial length to width ratio, axis morphology, the border furrow becoming increasingly interrupted by ribs anteriorly, and the fine granular sculpture. *S. lobarga* and *S. deiropede* differ from *S.* sp. most obviously in the presence of pronounced inflated lobes of the pygidial border (although *S.* sp. does show very low swellings), the pleural furrows of ribs four and five do not reach the axial furrow, and both new species have a deeper border furrow.

A single pygidium assigned to *S.* sp. from the Telychian of the Holitna Group, Taylor Mountains, Southwestern Alaska (Adrain *et al.* 1995, p. 732, fig. 5. 15), possesses similarly inflated marginal lobes to *S. lobarga* and *S. deiropede*. These are more elongated and spine-like than the marginal lobes of both Greenland species. The Alaskan species is too poorly preserved to enable further comparison.

S. sp. B, represented by a single fragmentary pygidium, from the Ludlow Tamchi Regional Stage, Chaltash Formation, Shaly Sai, northern Nuratau Range, Uzbekistan (Ivanova *et al*. 2009, p. 730, fig. 10.2), also displays pronounced nodes on the pygidial border, but unlike the comparative swellings of *S. lobarga* and *S. deiropede*, these are clearly isolated. This pygidium also differs from those of *S. lobarga* and *S. deiropede* in having swollen abaxial ends of the anterior pleural bands.

Occurrence and distribution. Central Peary Land (CP1).

Scharyia unicorna sp. nov.

Plate 20, figures 11–13

Derivation of name. Contraction of Latin, *unicus*, sole, only, singular, and Latin, *cornus*, horn, alluding to the pygidial caudal spine.

Holotype. MGUH220 (Pl. 20, figs 12–13) pygidium; GGU 198226 (CPL1).

Figured paratypes. Locality CPL1: MGUH219 pygidium.

Diagnosis. Scharyia with long (sag.) caudal spine projecting from pygidium.

Description. Pygidium subtriangular, 82% as long (sag. excluding spine) as wide (tr.) (n = 2). Axis cone-shaped tapering to a point posteriorly. Axis comprising 79% total sagittal length of pygidium (n = 2). At anterior end, axis comprising 32% entire width of pygidium (n = 2). Eight axial rings and a terminal piece; rings furrows increasingly deep towards axial furrow. Axial rings increasingly convex anteriorly. Anterior pleural band and five furrowed ribs curved very strongly backwards. Furrows between pleural band and first pleural rib longest and most deeply impressed. Pleural furrows increasing in depth distally; shallower than interpleural furrows. Marginal inflection of pleural ribs creates appearance of border furrow; ribs inflated abaxial to this creating border. Post-axial ridge merging with border and extending into terminal spine. End of spine broken, but seems to comprise roughly one-quarter entire pygidial sagittal length. Entire pygidium covered in fine, scattered granules.

Remarks. This is the only species of *Scharyia* with a terminal pygidial spine, reminiscent of *Dalmanites*.

Occurrence and distribution. Central Peary Land (CP1).

2.3.8 Family BRACHYMETOPIDAE Prantl and Přibyl, 1951

Subfamily BRACHYMETOPINAE Prantl and Přibyl, 1951

Genus RADNORIA Owens and Thomas, 1975

Type species. By original designation; *Radnoria syrphetodes* Owens and Thomas, 1975 from the lower-middle Wenlock of the Welsh Boderland and South Wales, UK.

Diagnosis. After Owens and Thomas (1975, p. 812): brachymetopine with preglabellar field concave or flat in longitudinal section; shallow depression crosses its posterior part and inner part of fixed and free cheeks, running parallel to margin; glabella comprising up to two-thirds of total cephalic sagittal length; anterior branch of facial suture diverges at 60–90 degrees from an exsagittal line through γ; pygidial axis with 10–13 rings, pleural areas with 6–7 pairs of ribs; latter with flat-topped profile or with posterior pleural band elevated above anterior; dorsal surface smooth or with fine pits and sporadic granules.

Remarks. Owens and Thomas (1975) regarded their new genus *Radnoria* to show similarities to both members of the subfamily Warburgellinae and the family

Brachymetopidae. As such, they placed the Warburgellinae in the Brachymetopidae rather than the Proetidae, to which it had been previously assigned.

Following suggestions by Lütke (1980, p. 118), Owens and Hammann (1990, p. 239) recognised that characters shared by *Radnoria* and *Prantlia* should be interpreted in terms of convergence. Species of *Prantlia* described since Owens and Thomas (1975) show characters such as a 'tube-like' cephalic doublure and a rostral plate with backwardly connective sutures; these are uncharacteristic of the genus. Furthermore, Owens and Hammann recognised that *Prantlia* and other Warburgellines described since Owens and Thomas (1975) show significant differences from *Radnoria*, such as the presence of short, transverse S2 and S3, and palpebral lobe close to axial furrow. Owens and Hammann considered the Warburgellinae to have its origins in *Astroproetus*, as originally suggested by Owens (1973*a*, p. 65, p. 82) and returned to placement of the Warburgellinae in the family Proetidae.

Radnoria cf. *Radnoria triquetra* Owens and Thomas, 1975

Plate 20, figure 14

Figured material. GGU 275038 (VGL1): MGUH221 cranidium.

Remarks. A fragmentary cranidium from Valdemar Glückstadt Land is assigned to *Radnoria*, and shares the following characters with *R. triquetra* Owens and Thomas (1975, p. 816, pl. 96, figs 3–5), from the Wenlock (Homerian) Much Wenlock Limestone Formation, Nodular Beds, Wren's Nest Hill, Dudley, West Midlands, UK: triangular glabella, roughly as wide (tr. posteriorly) as long (sag.); L1 distinct; S2 and

S3 effaced; occipital lobe slightly wider (tr.) than glabella; lateral occipital lobes effaced; long (sag.) preglabellar field. *R.* sp differs from *R. triquetra* in having S1 less deeply incised posteriorly.

The occurrence of *Radnoria* is sporadic in the Ordovician and Silurian. It is mostly represented in collections by small numbers of specimens, with a known stratigraphic range of early Caradoc to late Wenlock (Owens and Hammann, 1990, p. 239). This specimen represents the second recorded occurrence of *Radnoria* in the Llandovery; it is also known from the Chintin Formation (Telychian *crenulata* Biozone to Sheinwoodian ~*murchisoni* Biozone), central Victoria, Australia (Sandford and Holloway, 2006, p. 216; table 1 and p. 218).

Occurrence and distribution. Valdemar Glückstadt Land (VGL1).

Order PTYCHOPARIIDA Swinnerton, 1915

Suborder HARPINA Whittington *in* Moore, 1959

2.3.9 Family HARPETIDAE Hawle and Corda, 1847

Genus SCOTOHARPES Lamont, 1948

Type species. By monotypy; *Scotoharpes domina* Lamont, 1948, p. 535, pl. 1, fig. 2; from the Upper Llandovery, Wether Law Linn Formation, North Esk Inlier, Scotland.

Diagnosis. After Norford (1973, p. 11): harpetid with cephalic central region convex, prolongations almost straight or curving adaxially; glabella subquadrate to suboval, longer than wide, transversely strongly convex; axial furrows commonly with two or

three pairs of very shallow pit-like areas between eye ridges; S1 narrow (tr.); small, triangular lateral glabellar lobes; preglabellar field with low axial mound; eye tubercles opposite front quarter of glabella; adaxial edge of gena separated from rear three-quarters of axial furrow by two depressed triangular areas separated by low gently convex semicircular ala and alar furrow; genal roll commonly with low axial mound, upper lamella strongly flexed at site of girder, girder meets lower rim some distance in front of tip of prolongation; gena and fringe with pits separated by smooth ramifying genal caecae branching from region of axial furrow just behind eye ridge; caecae radial on outer part of gena and fringe, cross inner margin of fringe, reach and cross smooth ridge of upper lamella that marks site of girder, in most species reaching rim in parts of brim; single rows of slightly coarser pits developed against girder and upper and lower rims; thorax with at least 17 segments, widest at fourth or fifth; axis narrow, strongly raised, pleurae with bluntly rounded tips; pygidium with strongly curved pleural furrows.

Scotoharpes loma (Lane, 1972)

Plate 20, figures 15–17

1972 *Selenoharpes loma* Lane, p. 353, pl. 62, figs 1–9.

Holotype. MMH 11357, cephalon, Lane, 1972, p. 353 pl. 62, figs 1a-b from the Telychian Samuelsen Høj Formation of Kronprins Christian Land, eastern North Greenland.

Diagnosis. From Lane (1972, p. 353): *Scotoharpes* with very convex glabella whose basal lobes protrude only slightly from its straight sides. Ala well defined, convex, standing above cheek lobe and well above posterior border furrow posteriorly. Preglabellar field very narrow (sag.); cheek roll medially with distinct convex swelling. Brim concave, widest anteriorly. Genal caecae indistinct on cheek lobe, very distinct on cheek roll and brim, reaching external rim; minute pits between caeca about 16 in number in the width of the cheek roll anteriorly, and about 40 in the brim in the same region.

Figured material. GGU 275015 (KCL1): MGUH222–223 cranidia.

Remarks. The medial swelling on the cheek roll is particularly characteristic of the species. The material here figured does not differ in any significant respect from the type and figured material (see Lane, 1972, p. 353 for full description). A fragmentary thorax (not figured) is typical of the genus.

Occurrence and distribution. Wulff Land (WL), south Nares Land (SNL2), western Peary Land (WPL1–2), central Peary Land (CPL5), Kronprins Christian Land (KCL1), Valdemar Glückstadt Land (VGL1).

Order PHACOPIDAE Salter, 1864b

Suborder CHEIRURINA Harrington and Leanza, 1957

2.3.10 Family CHEIRURIDAE Hawle and Corda, 1847

Subfamily CHEIRURINAE Hawle and Corda, 1847

Genus CHEIRURUS Beyrich, 1845

Type species. Subsequently designated by Barton 1916, p. 129; *Cheirurus insignis* Beyrich, 1845, p. 12, pl. [unnumbered], fig. 1; from the Wenlock Liteň Formation, Svatý Jan pod Skalou, Czech Republic.

Diagnosis. After Lane (1971, p. 11): cheirurine with glabella about one-third cephalic width at occipital ring or slightly less, expanding forward; S3 and S2 very gently curved back, of equal length, reaching about one-third way across glabella; basal glabellar lobe subtriangular and isolated; transversely about one-third width of glabella across L1. Anterior border and preglabellar furrow interrupted medially by posterior margin of L2; posterior branch of facial suture running from palpebral lobe slightly forward to lateral border furrow. Thorax of 11 segments. Pygidium with three pairs of radially disposed spines of either equal or slightly decreasing length backward, with in either case the anterior pair most curved back; axis with 3 rings and terminal piece.

Cheirurus falcatus sp. nov.

Plate 21, figs 1–18; Plate 22, figs 1–7

Derivation of name. Latin, *falcatus*, sickle-shaped, curved, alluding to the shape of the pygidial spines.

Holotype. MGUH235 (Pl. 22, figs 1–2) pygidium; GGU 274689 (CPL5).

Figured paratypes. Locality CPL2: MGUH224–225 cranidia; MGUH230 hypostome; MGUH233 thoracic segment; MGUH236–237 pygidia. Locality KCL5: MGUH226, 229 cephala. Locality CPL5: MGUH227 cranidium; MGUH228 glabella; MGUH231–232 hypostomes; MGUH234 thoracic segment; MGUH238 pygidium.

Diagnosis. Cheirurus with posterior of glabella comprising 30% cephalic transverse width; anterior part of glabella under 25% width of posterior part; S1 shallowing posteriorly; L1 comprising 30% transverse glabellar width; pygidial pleural spines decreasing in length backward.

Description. Cephala and cranidia ranging in sagittal length from 4.74–35.81 mm, averaging 57% as long (sag.) as wide (tr.) at posterior of lateral border (range = 56–58%; n = 5). Glabella almost straight sided, posterior part comprising 30% total transverse width of cranidia/cephalon (range = 28–32%; n = 6); gradually widening (tr.) towards frontal lobe where it is widest. Posterior of glabella averaging 79% of its anterior transverse width (range = 71–90%; n = 11). S1 deepest abaxially; firstly trending obliquely back from axial furrow, then much more steeply at which point it

narrows and shallows, reaching the occipital furrow as a shallow impression (depth of impression here variable and independent of size). L1 comprising roughly 30% total transverse glabellar width at this point. S2 and S3 anteriorly convex, trending sub-parallel to one another; longest (exsag.) at axial furrow, becoming shorter and weaker adaxially, terminating at roughly one-third transverse glabellar width. Abaxial position of lateral glabellar muscle impressions from occipital furrow (as percentage of preoccipital glabellar length (sag.) as follows: S1 on average 19% (range = 15–24%; n = 12); S2 on average 38% (range = 34–46%; n = 12); S3 on average 61% (range = 57–70%; n = 12). Hence S2 is located the same distance from S1 as S1 is from the occipital furrow, and S3 situated at a slightly greater distance than this from S2. Occipital ring anteriorly inflated medially so that abaxially it is between half and two-thirds the sagittal length. Occipital furrow of constant depth. Median occipital node situated roughly halfway (sag.) along occipital ring. Glabellar sculpture comprising small granules; very densely packed medially between glabellar lobes and on anterior part of frontal glabellar lobe. A few scattered slightly larger granules occur exsagittally between glabellar furrows. Anterior border gradually shortening (sag.), and anterior border/preglabellar furrow shallowing adaxially, to merge with frontal glabellar lobe medially. Palpebral lobe placed between S2 and S3. Eye ridge intersecting axial furrow just anterior of S3. Anterior branch of facial suture directed smoothly towards axial furrow, intersecting anterior border approximately at mid-length (sag.) of frontal lobe of glabella at a point very close to axial furrow. Posterior branch running in line with S2, intersecting lateral border opposite posterior half of L3. From there, directed slightly posteriorly until midway across lateral border, after which directed very steeply posteriorly, terminating at adaxial margin of lateral border opposite L2. Fixigena of low convexity between axial furrow and palpebral lobe,

adaxial to this sloping downwards more strongly. Lateral border width (tr.) greater than posterior border length (exsag.). Lateral and posterior border furrows equally well impressed. Genal spine slender, roughly one-third cephalic sagittal length. Sculpture of fixigena and librigena within borders, comprising unequally sized but rather equally spaced large, flat-bottomed pits which are sub-circular to oval in dorsal view. Lateral and posterior borders with small, densely packed granules.

Hypostome about 80% as long (sag.) as wide (tr.) across anterior of shoulders. Middle body smoothly convex (sag. and tr.); elongate, roughly two-thirds as long (sag.) as wide (tr. at widest point near anterior of middle body). Anterior lobe of middle body about four times as long (sag.) as posterior lobe, with maculae placed roughly 30% from posterior of hypostome and defined by a shallow middle furrow. Anterior and posterior margins of middle body smoothly rounded. Anterior border and shallow anterior border furrow continuous medially. Lateral and posterior border furrows deep; lateral border furrow becoming progressively wider (tr.) and slightly shallower anteriorly. Lateral border of constant width; posterior border laterally expanded with angular posterolateral corners. Entire hypostome very finely granulose; middle body additionally with larger widely-spaced scattered granules.

Axial ring about twice width (tr.) of inner portion of pleura. Articulating half-ring pronounced, almost as long (sag.) as axial ring. Articulating furrow shallow, particularly near apodemal pit. Axial furrow deep, sharp. Inner portion of pleura roughly 60% as long (exsag.) as wide (tr.); divided by deep pleural furrow into equally sized and shaped triangular anterior and posterior pleural bands. Outer portion of pleura curved backwards in most distal quarter, terminating in spinose tip.

Pygidium including spines roughly twice as wide (tr.) across tip of first pair of pleural spines as long (exsag.; taken to tip of last pair of pleural spines). Axis

triangular, averaging 68% as wide (tr. anteriorly) as long (sag. taken to terminal mucration as not defined posteriorly) (range = 65–76%; n = 6). Axis comprising 3 rings and a terminal piece. Axial rings increasingly convex (sag.) anteriorly. Terminal piece of axis continues posteriorly into short, rounded, terminal mucronation. Axial furrow well impressed. Three pairs of pleural spines; from anterior to posterior, each pair successively decreasing a little in length and increasingly backwardly projected. First pleural furrow resembling those of thoracic segments, but not connected to posterior of pleura. Second pleural furrow shorter than first, running from anterior of pleura and terminating at its mid-length (exsag.). Third pleural furrow running from near anterior of pleura for a very short distance. Sculpture, where preserved, granulose (Pl. 22, figs 1–2).

Ontogeny. A cephalon (MGUH229; Pl. 21, figs 9–11) is significantly smaller (3.74 mm sag. length) than the cranidia and cephala of the holotype and other paratypes (6.3–35.81 mm sag. length) and differs from these in the following: eye placed slightly more anteriorly, the posterior margin is placed opposite the posterior half of L3, and the anterior margin opposite posterior portion of frontal glabellar lobe; genal spine more abaxially deflected; glabella proportionally longer with respect to its width; S3 shorter than S2, rather than equal; confluence of lateral and posterior border furrows is angular, rather than rounded.

Remarks. The pygidium of *C. falcatus*, is very typical of the genus. The strength of the axial furrow, the similarity of the anteriormost pygidial pleurae to those of the thoracic segments, degree of terminal mucration, and pleural spines successively reducing in length posteriorly, are the most distinctive generic characters.

C. falcatus differs from the type species, *C. insignis*, and from most *Cheirurus* species, most notably in the morphology of S1 and L1; S1 shallows posteriorly and L1 comprises under one-third the glabellar width (tr.) in *C. falcatus*. In most *Cheirurus* species, L1 is more elongated and clearly isolated by strong S1 furrows. In this material, cephala and cranidia which are otherwise identical display a variation in the strength of S1 approaching the occipital furrow (e.g. Pl. 21, fig. 1 cf. fig. 4); this variation is independent of size and therefore is not attributed to ontogeny.

Occurrence and distribution. Central Peary Land (CPL1–5).

Genus PROROMMA Lane, 1971

Type species. By original designation; *Proromma bregmops* Lane, 1971, from the Lower Llandovery Skelgill Beds, Crummack Dale, near Austwick, Yorkshire.

Diagnosis. After Curtis and Lane (1997, p. 39): cheirurine with S1 impression not reaching, or weakly connected to occipital furrow. Eye extending from opposite posterior margin of frontal lobe to opposite mid-L3. Pygidium with three rings and terminal piece in the axis, the rings increasing in sagittal length posteriorly; two pairs of long, slender spines, some species with a small third posterior pair (sometimes represented by blunt projections of the posterior part of the posterior pleural portion of the pygidium); middle pair about two-thirds width and length of anterior pair.

Proromma? *parageia* sp. nov.

Plate 22, figs 8–14

Derivation of name. Greek, *parageios*, pertaining to shallow water. The genus is found elsewhere in deeper environments.

Holotype. MGUH239 (Pl. 22, figs 8–10) cranidium with two articulated thoracic segments; GGU 275038 (VGL1).

Figured paratypes. Locality CPL5: MGUH240 cephalon. Locality VGL1: MGUH241 cranidium. Locality KCL1: MGUH242 thoracic segment.

Diagnosis. Proromma? with glabella only slightly anteriorly expanded; S3 straight, extending for over one-third glabella width (tr.).

Description. Cephala and cranidia ranging in sagittal length from 3.71–8.5 mm, averaging 51% as long (sag.) as wide (tr.) at posterior of lateral border (range = 47–56%; n = 4). Glabella almost straight-sided, posterior part comprising 30% total transverse width of cranidia/cephalon (range = 29–32%; n = 3); gradually widening (tr.) towards frontal lobe where at its widest. Posterior of glabella averaging 88% anterior transverse width (range = 81–92%; n = 5). S1 well impressed and trending as a straight line posteriorly from axial furrow at 60–70 degrees from an exsagittal line, for one-third glabellar width (tr.). From there, abruptly shallowing to run almost exsagittally to connect with the occipital furrow. Depending on the faintness of this part of the furrow, L1 can appear fully or partially isolated. S2 well impressed,

trending as a straight line posteriorly from axial furrow at 70–80 degrees from an exsagittal line, for approximately one-third glabellar width (tr.). S3 well impressed, trending as a straight line posteriorly from axial furrow at roughly 60 degrees from an exsagittal line, for just over one-third glabellar transverse width. Abaxial position of lateral glabellar muscle impressions from occipital furrow (as percentage of preoccipital glabellar length (sag.) is: S1 on average 21% (range = 17–25%; n = 6); S2 on average 38% (range = 34–45%; n = 6); S3 on average 64% (range = 60–70%; n = 6). So that S2 is located slightly closer to S1 than S1 is from the occipital furrow, and that S3 is the most isolated impression. Occipital ring anteriorly inflated medially. Deep occipital furrow. Anterior border and preglabellar furrow absent medially. Posterior of palpebral lobe placed opposite mid-length of L3, anterior placed opposite S3. Anterior branch of facial suture directed smoothly towards axial furrow, intersecting anterior border in anterior portion of frontal lobe of glabella at a point close to axial furrow. Posterior branch running anterolaterally from posterior of palpebral lobe to intersect lateral border roughly midlength along L3. Fixigena at highest point in line (sag.) with palpebral lobe; smoothly sloping adaxial of this. Lateral border width (tr.) subequal to posterior border length (exsag.); lateral and posterior borders equally well impressed. Genal spine directed slightly adaxial to lateral border, extending for one-quarter cephalic sagittal length. Densely packed sub-circular to oval pits cover fixigena and librigena within borders.

Number of thoracic segments unknown. Axial ring width (tr.) forming roughly one-quarter entire thoracic segment width (tr.) and about twice the width (tr.) of inner portion of pleura. Articulating half-ring roughly two-thirds as long (sag.) as axial ring. Axial and pleural furrows deeply impressed. Inner portion of pleura roughly 58% as long (exsag.) as wide (tr.), divided by pleural furrow into equally sized triangular

anterior and posterior pleural bands. Outer portion of pleura curved backwards to terminate in spinose tip.

Remarks. The forwardly placed eye, and posteriorly effaced nature of S1 suggest that this species could belong to *Proromma*. Without knowledge of the pygidia, the generic assignment can not be confirmed, and it could be that the cephala represent a new genus of Cheiruridae. Known *Proromma* species are found in shelf edge facies, and are commonly associated with graptolite faunas.

Much *Proromma* material from the British Llandovery described by Lane (1971, p. 38) and Curtis and Lane (1997, p. 39) is distorted, impeding comparison. This is highlighted by the variation displayed by the lateral glabellar muscle impressions. No other *Proromma* species however, exhibits a perfectly straight S3, which runs at a lower angle and for a greater distance than S2. *P.*? *parageia* is also distinguished by having a glabella which is only 12% wider (tr.) anteriorly than posteriorly: other species display a greater anterior glabella expansion.

Occurrence and distribution. Central Peary Land (CPL5), Kronprins Christian Land (KCL1) and Valdemar Glückstadt Land (VGL1).

Genus RADIURUS Ramsköld, 1983

Type species. By original designation; *Radiurus phlogoideus* Ramsköld, 1983, from the Lower Visby Marl, Telychian (Llandovery), Norderstrand, Visby, Gotland, Sweden.

Diagnosis. Modified from Ramsköld (1983, p. 188), to account for differences in length between pairs of pygidial spines, and the lack of a pygidial mucration which all species exhibit: cheirurine with entire anterior border and preglabellar field; S3 and S2 reaching one-third to three-eighths across glabella. Pygidium with three pairs of radially disposed, equally spaced spines; axis terminating at posterior border.

Remarks. Lane (1971, p. 77) first remarked that Silurian cheirurids with radially disposed spines have their ancestry near '*Cheirurus'* [= *Radiurus*] *estonicus* and *Cheirurus*. The unspecialised features of *Radiurus* were also commented on by Rämskold (1983), Norford (1994) and Chatterton and Ludvigsen (2004). Norford (1994) suggested that from *Radiurus*, a more inflated frontal glabellar lobe and development of a small pygidial mucration would lead to *Cheirurus*, and forward relocation of the palpebral lobe and a pronounced pygidial axial mucration, to *Chiozoon* Lane, 1972. All three genera are found in North Greenland; comparison of *C. falcatus* (above), *R. pauli* (below), and *Chiozoon cowiei* Lane, 1972 from the Telychian Samuelsen Høj Formation of Kronprins Christian Land, reveal that despite comfortably falling into different genera, the taxa share the position of the palpebral lobe between S2 and S3, and have similarly shaped pygidial pleural spines (although differing in length). The principal distinguishing characters of the genera are the degree of terminal mucration, and the complete anterior border in *Radiurus*; the taxa are otherwise close.

Radiurus pauli sp. nov.

Plate 23, figs 1–17

Derivation of name. For my fiancé.

Holotype. MGUH251 (Pl. 23, figs 15–17) pygidium; GGU 298506 (WL).

Figured paratypes. Locality WL: MGUH243 cephalon; MGUH244–245 cranidium; MGUH247 hypostome; MGUH248 pygidium; MGUH249 thoracic segment. Locality SNL2: MGUH246 cranidium; MGUH250 pygidium.

Diagnosis. Radiurus with L2 shortest (exsag.) of lateral glabellar lobes; palpebral lobe placed between S2 and S3; pygidial pleural spines markedly decreasing in length posteriorly.

Description. Cephala and cranidia ranging up to 12.9 mm sagittal length, averaging 54% as long (sag.) as wide (tr.) at posterior of lateral border (range = 50–60%; n = 5). Glabella gradually expanding in width (tr.) anteriorly, with posterior of glabella averaging 90% of its widest point in frontal lobe, at intersection with anterior border (range = 77–100%; n = 10). Frontal glabellar lobe rounded; flattened and less anteriorly expanded in smaller specimens (Pl. 23, figs 1–2). S1 deepest abaxially; following smooth trajectory to intersect occipital furrow. L1 subtriangular, comprising roughly 30% total transverse glabellar width at this point. S2 and S3 anteriorly convex, trending subparallel to one another; longest (exsag.) at axial furrow, becoming shorter and weaker adaxially until both terminate at roughly 30%

glabellar transverse width. Abaxial position of lateral glabellar muscle impressions from occipital furrow (as percentage of preoccipital glabellar length (sag.) as follows: S1 on average 24% (range = 19–26%; n = 10); S2 on average 40% (range = 36–43%; n = 10); S3 on average 62% (range = 58–68%; n = 10). So that S2 is located closer to S1 than to S3. Occipital ring anteriorly inflated medially; occipital furrow of constant depth. Median occipital node situated roughly halfway (sag.) along occipital ring. Glabellar sculpture comprising small, scattered granules. Anterior border/preglabellar furrow shortest (sag.) and shallowest medially. Palpebral lobe placed between S2 and S3. Eye ridge intersecting axial furrow at abaxial end of S3. Anterior branches of facial suture smoothly converging anteriorly, intersecting anterior border at approximately mid-length (sag.) of frontal lobe of glabella, very close to axial furrow. Posterior branch running at same angle and in line to S2, intersecting lateral border opposite S2. From there, directed slightly posteriorly until midway across lateral border, after which directed very steeply posteriorly, terminating at adaxial margin of lateral border opposite S1. Fixigena convex, increasingly so abaxially. Lateral border of subequal width (tr.) to posterior border length (exsag.). Lateral and border furrow broader than posterior border furrow; furrows equally well impressed. Genal spine slender, roughly one-quarter cephalic sagittal length. Sculpture of fixigena and librigena within borders, comprising unequally sized and spaced pits; these subcircular to oval in dorsal view.

Hypostome about 80% as long (sag.) as wide (tr.) across anterior of shoulders. Middle body smoothly convex (sag. and tr.); ovoid, about 70% as long (sag.) as wide (tr.) at widest point near anterior of middle body. Anterior lobe of middle body about four times as long (sag.) as posterior lobe, with maculae placed roughly 35% from posterior of hypostome. Anterior and posterior margins of middle body smoothly

rounded. Anterior border and anterior border furrow continuous medially. Lateral and posterior border furrows deep; lateral border furrow progressively widening anteriorly. Lateral border pinched inwards, and so narrowest (tr.) opposite maculae; posterior border of constant width with gently rounded posterolateral corners. Fine granules where cuticle is present.

Axial ring about three times width (tr.) of inner portion of pleura. Articulating half-ring pronounced, almost as long (sag.) as axial ring. Articulating furrow shallow. Axial furrow deep, sharp. Inner portion of pleura almost as long (exsag.) as wide (tr.); divided by deep pleural furrow into equally sized and shaped triangular anterior and posterior pleural bands. Outer portion of pleura curved backwards, terminating in spinose tips.

Pygidium including spines 46% as wide (tr. across tip of first pair of pleural spines) as long (exsag.) taken to tip of last pair of pleural spines (range = 45–50%; n = 5). Axis triangular, averaging 86% as wide (tr.) anteriorly as long (sag.) (range = 83–90%; n = 4). Axis comprising 3 rings and a terminal piece. Axial rings increasingly convex (sag.) anteriorly. Terminal piece of axis connected abaxially to posteriormost axial ring; reaching posterior border but not extending past this. Axial furrow well impressed. Three pairs of pleural spines; from anterior to posterior pair, each pair successively decreasing in length and increasingly backwardly directed so that posteriormost pair are roughly half the length of the anteriormost pair from tip to connection with axial furrow. First pleural furrow like those of thoracic segments; second pleural furrow shorter than first, running from middle of pleura and terminating mid-length (exsag.) of pleura. Third pair of pleural spines without furrow.

Remarks. R. pauli differs from all other species of *Radiurus* in having a more anteriorly placed eye. The pygidium of *R. pauli* is close to that of the type species; *R. phlogoideus*, and *Cheirurus*? sp. Norford 1981 (subsequently assigned to *Radiurus* by Ramsköld, 1983) from the Telychian–?early Wenlock Attawapiskat Formation, Canada, with respect to its broad pleural spines. The pleural spines of these three species are markedly different from the slender forms displayed by *R. adraini* Chatterton and Ludvigsen, 2004, from the Telychian Jupiter Formation, Anticosti Island, Québec, Canada, and *R. avalanchensis* Chatterton and Perry, 1984, from the Llandovery Whittaker Formation (lower part of the *amorphognathoides* Biozone, Over and Chatterton, 1987), Mackenzie Mountains, Northwestern Canada. The pygidium of *R. pauli* is differentiated from all of the above species in having pairs of pleural spines which are progressively shorter posteriorly, so that the posteriormost pair is proportionally very short. Other *Radiurus* species have pleural spines of subequal length. The pygidial axial morphology of *R. pauli* is very similar to that of *R. phlogoideus*, particularly with respect to the morphology of the terminal piece, which is connected abaxially to the posteriormost axial ring. *R. phlogoideus* has a pair of tubercles on each pygidial axial ring, which are not present in *R. pauli*.

Occurrence and distribution. Wulff Land (WL), south Nares Land (SNL1–2) and western Peary Land (WPL1–2).

Subfamily ACANTHOPARYPHINAE Whittington and Evitt, 1954

Remarks. Adrain (1998) provided a history of study and conducted cladistic analysis of the Subfamily Acanthoparyphinae. All Silurian species were found to form a monophyletic group including the genera *Hyrokybe* Lane, 1972, *Parayoungia* Chatterton and Perry, 1984, and *Youngia* Lindström, 1885.

Genus HYROKYBE Lane, 1972

Type species. By original designation; *Hyrokybe pharanx* Lane, 1972, p. 357, pl. 64, figs 1-3 from the Telychian Samuelsen Høj Formation of Kronpins Christians Land, eastern North Greenland.

Diagnosis. From Adrain (1998, p. 707): acanthoparyphine with occipital spine very short and thornlike, separated from median occipital node; fixigena small posteriorly, protruding only slightly laterally in dorsal view; hypostomal suture fused in holaspid; posterior margin of hypostome posteriorly concave, with median cluster of small denticles.

Remarks. As with some other cheirurid genera, differentiating between *Hyrokybe* and *Youngia* is problematical when the hypostomal and pygidial morphology is not known. Cephalic characters at first thought to be diagnostic, for example the lack of S3 in the type species of *Hyrokybe*, were subsequently found unreliable. Chatterton and Perry (1984, p. 29) provided a diagnosis based on a number of species of *Hyrokybe* for which pygidia were also known. The diagnosis given here, as provided

by Adrain (1998) was composed following his cladistic analysis of the Acanthoparyphinae.

Hyrokybe pharanx Lane, 1972

Plate 24, figs 1–3

Figured material. MGUH252 cranidium, GGU 274689 (CPL5). MGUH253 cranidium, GGU 198137 (CPL2).

Remarks. The proportions of the glabella, the morphology of the lateral glabellar muscle impressions, which comprise a very distinct S1 connected to the axial furrow, very faint S2 and even fainter 3S (both of which are close to but isolated from the axial furrow), and the spacing and size of the granular sculpture, are all characteristic of the type species of *Hyrokybe*, *H. pharanx*. The hypostome and pygidium of the species are unknown.

Occurrence and distribution. Central Peary Land (CPL2, 5).

Hyrokybe? sp.

Plate 24, figs 4-12

Figured material. MGUH254 cephalon, GGU 274654 (CPL4). MGUH255 cranidium, GGU 274689 (CPL5). MGUH256–7 cranidia, GGU 274654 (CPL4).

Description. Glabella subcircular, as long (tr.) as wide (sag.) (n = 4). Pre-occipital glabella averaging 83% as long as wide (range = 76–89%; n = 5). Maximum width at mid-L1, anterior to this tapering smoothly forwards. Axial furrows well impressed. Lateral glabellar muscle impressions all connected to the axial furrow, although S2 shallows prior to furrow. Abaxial position of lateral glabellar muscle impressions from occipital furrow (as percentage of pre-occipital glabellar length (sag.) as follows: S1 on average 34% (range = 30–36%; n = 6); S2 on average 60% (range = 58–62%; n = 3); S3 on average 80% (range = 74–85%; n = 3). S1 deepest; S2 almost as deep as S1; S3 much shallower than S2. S1 running at angle of 60–80 degrees from axial furrow for roughly half its course; along this section a posteriorly convex deflection is present. Then directed posteriorly at angle of 35–45 degrees from exsagittal line, terminating before occipital furrow. S2 running subparallel to S1, for about half the length of S1. Occipital ring slightly expanded medially, only base of occipital spine preserved. Posterior margin of palpebral lobe placed opposite S1, posterior border of fixigena not preserved.

Librigena highly convex, with well impressed lateral border furrow.

Sculpture comprising scattered, poorly sorted, coarse granules; identical on pre-occipital glabella, occipital ring, fixigena and librigena.

Ontogeny. Two glabellae are significantly smaller than the others (MGUH257–257; Plate 24, figs 10–12) and differ from the larger ones as follows: glabella is more acorn-shaped, and shorter (sag.) relative to its width (tr.); lateral glabellar muscle impressions are more deeply impressed; S3 is positioned relatively more anteriorly.

Remarks. H.? sp. differs from *H. pharanx* most notably in the deeper S2 and S3, and the more densely packed granular sculpture. The material is close to *H. meliceris* from the Llandovery/Wenlock of Kap Schuchert, Washington Land, western North Greenland (Lane and Owens, 1982). Particular similarities are: morphology of the lateral glabellar muscle impressions; position of the palpebral lobe; convexity of the librigena; closely packed granular sculpture. *H.*? sp. has a more distinct S2, and this could account for its observed connection with the axial furrow (S2 is distinct from the axial furrow in *H. meliceris*), and the glabella of *H.*? sp. is relatively slightly longer (sag.) than that of *H. meliceris*.

Similarities in glabellar morphology, course and depth of impression of the lateral glabellar muscle impressions, and sculpture, are shared with *H.*? *globiceps* (Lindström, 1885, figured by Ramsköld 1983, pl. 26, figs 7, 10-11) from the Wenlock, Upper Visby Marl, Visby area, Gotland, Sweden. The two species are readily distinguished by the position of the palpebral lobe: the anterior margin of the palpebral lobe is situated opposite S1 in *H.*? *globiceps*, whereas the posterior margin is situated opposite S1 in *H.*? sp. Without further exoskeletal parts, certain attribution of this material to *Hyrokybe* as opposed to *Youngia* is not possible, and the material is not formally named. However, the path of S1 in lateral profile, with a posteriorly convex deflection about halfway up the glabella, is an apomorphic character state partly defining the node upon which the clade containing *H. julli, H. hadnagyi, H. lenzi, H. copelandi* and *H. youngi* is based in Adrain's (1998, figure 3, p. 701) analysis of the Acanthoparyphinae. The presence of this apomorphy, combined with the general similarities of *H.*? sp. to species of *Hyrokybe*, supports the provisional assignment to *Hyrokybe*.

Occurrence and distribution. Central Peary Land (CPL4–5).

Acanthoparyphinae gen. et sp. indet. 1

Plate 24, figs 13–14

Figured material. MGUH258 cephalon, GGU 198226 (CPL1).

Remarks. A single cranidium from central Peary Land is assigned to the Subfamily Acanthoparyphinae on the basis of its subcircular glabellar morphology with maximum width across basal lobes and granular sculpture. The cranidium differs from others described here, in having: a beehive-shaped glabella; the palpebral lobe much farther from axial furrow; lateral glabellar muscle impressions are all positioned closer to the occipital furrow, relative to pre-occipital glabella sagittal length; S1 is more effaced posteriorly, and so terminates farther from the occipital furrow; finer, more irregularly spaced granular sculpture.

The morphology of the glabella, and the eye positioned well away from the axial furrow, distinguish this cranidium from all other species of *Hyrokybe* and *Youngia*; its placement within the Acanthoparyphinae is uncertain.

Occurrence and distribution. Central Peary Land (CPL1).

Acanthoparyphinae gen. et sp. indet. 2

Plate 24, figs 15–17

Figured material. MGUH259 cranidium, GGU 274689 (CPL5).

Remarks. A subcircular, granulose pre-occipital glabella from central Peary Land is characteristic of the Subfamily Acanthoparyphinae. The fragment measures 4.35 mm, and is distinguished from all other Acanthoparyphinae here described by its coarser granular sculpture and presence of shallow S4 directed from anterior margin. Generic assignment is not possible based on such limited material.

Occurrence and distribution. Central Peary Land (CPL5).

Suborder PHACOPINA Struve *in* Moore, 1959

2.3.11 Family ENCRINURIDAE Angelin, 1854

Subfamily ENCRINURINAE Angelin, 1854

Genus DISTYRAX Lane, 1988

Type species. By original designation; *Distyrax peeli* Lane, 1988, from the Telychian Odins Fjord Formation, central Peary Land, North Greenland.

Diagnosis. From Edgecombe and Chatterton (1992, p. 53): encrinurine with tubercle abaxially along anterior edge of occipital ring; librigenal lateral border coarsely tuberculate, outer row of tubercles typically overhanging margin; hypostomal rhynchos short (sag.), blunt, weakly defined abaxially; anterior wings positioned relatively far forward; five free pairs of strongly turned-back pygidial pleural ribs; fifth rib pair at least partially enclosing sixth (or fused sixth and seventh) posteromedially; sixth pair parallels axis, bounded by very shallow or obsolete axial furrow.

Distyrax bibullus sp. nov.

Plate 25, figures 1–5

Derivation of name. Combination of Latin, *bi*, two, double, and Latin, *bulla*, bubble, knob, boss, alluding to the tubercles present abaxially along posterior, as well as anterior, edge of occipital ring.

Holotype. MGUH260 (Pl. 25, figs 1–3) cephalon; GGU 275015 (KCL1).

Figured paratypes. Locality KCL1: MGUH261 pygidium.

Diagnosis. Distyrax with tubercle present abaxially along posterior, as well as anterior, edge of occipital ring; tubercles present on pygidial axis and pleural ribs, the latter also densely pitted.

Description. Highly convex cephalon measuring 7.47 mm long (sag.). Pre-occipital glabella roughly as long (sag.) as wide (tr.) across PL; narrowest across L1. Deep axial furrow. L1–L4 tuberculate; L1 smallest and sub-rounded, L2–L3 largest and elongate in direction of axial furrow. L4 larger than L1, but smaller than L2–L3. Anterior to L4, axial furrow obscured, although PL is partially visible. Other pre-occipital glabellar tubercles comparable in size to that of L1, arranged asymmetrically, and with a narrow range of sizes. S1–S4 long (exsag.). No pseudoglabellar area and preglabellar furrow weak. Anterior border with tubercles similar in size and distribution to those on frontal glabellar lobe. Palpebral lobe roughly 20% total cranidial sagittal length; midpoint opposite posterior of S3; raised,

with tubercles aligned on raised area. Area immediately adjacent to palpebral lobe lacking tubercles. Fixigenal tubercles overhanging axial furrow larger than those on rest of fixigena, but smaller than lateral lobe tubercles; other fixigenal tubercles of similar size and density to those on glabella. Posterior border furrow deep and long (exsag.); posterior border increasing in length (exsag.) abaxially, bearing a single row of tubercles. Genal spine present, but broken near base. Lateral border narrower (tr.) than librigenal field, but at least twice as wide (tr.) as posterior border is long (exsag.) and slightly increasing in width (tr.) anteriorly. Two or three rows of tubercles on lateral border (excluding those overhanging abaxial margin). Lateral border furrow shallower than posterior border furrow.

Pygidium fragmentary, discernable characters are: high convexity; posterior of axis with ring furrows separated from axial furrow and absent medially; median tubercle present on every fourth ring; pleural furrows deep and longer (exsag.) abaxially; pleural ribs strongly pitted to the point where they become upturned abaxially; up to five randomly placed tubercles on each pleural rib, comparable in size to those on axis.

Remarks. Both the cephalic tuberculation patterns and pygidial morphology are characteristic of the genus. The posterior abaxial tubercle on the occipital ring of *D. bibullus*, and the combination of turbecles and densely pitted sculpture on the pygidial pleural ribs, are unique to the genus. Both cephalon and pygidium most resemble the type species, *D. peeli*, also from North Greenland. Notable differences are that *D. bibullus* has no pseudoglabellar area, its palpebral lobe is more anteriorly positioned, and the cephalic tubercles are smaller and more numerous.

Occurrence and distribution. Kronprins Christian Land (KCL1).

Distryax? sp.

Plate 25, figure 6

Figured material. MGUH262 cranidium, GGU 274689 (CPL5).

Remarks. A fragmentary cranidium from central Peary Land, with a sagittal length of 8.17 mm, is preserved as an internal mould, and has a similar glabellar morphology to *Distryax* sp. nov. It is also highly convex, and the eye occupies a similar position, but the sculpture is much more coarsely tuberculate. As no occipital ring or librigena is preserved, generic placement is tentative.

Occurrence and distribution. Central Peary Land (CPL5).

Genus PERRYUS Gass and Mikulic, 1982

Type species. By original designation; *Perryus severnensis* Gass and Mikulic, 1982, from the late Telychian–?early Wenlock Attawapiskat Formation, northern Ontario, Canada.

Diagnosis. Modified after Gass and Mikulic (1982, p. 591): encrinurine with cephalon with numerous low, closely spaced, asymmetrically arranged tubercles. L2 to L4 with subquadrate tubercles; L2 and L3 comprising two partially fused longitudinally directed tubercles. S1 to S3 transversely narrow and distinct. Sagittal cranidial

depression absent. Midpoint of palpebral lobe opposite L3 or S3. Lateral border of free cheek wide, with row of large tubercles against border furrow. Pygidium strongly vaulted with prominent rachis typically comprising 18–25 rings. Pleural lobes strongly sloping with 9–11 pairs of ribs. Sagittal groove absent. Exoskeleton granulate and perforate.

Remarks. A combination of characters displayed by the species of *Perryus* described here, and those of *P. bartletti* Edgecombe and Chatterton, 1992, and *P. palasso* Lane, 1988, have required some modification of the original diagnosis of Gass and Mikulic (1982). The consistently subquadrate morphology of L2 to L4, together with the partially fused nature of the tubercles of L2–L3, is considered particularly diagnostic; Edgecombe and Chatterton (1992) suggested that the broad librigenal border may be diagnostic, and this is supported here by its presence in *P. mikulici*. The transversely elongated nature of alternate tubercles on the lateral border is specific to *P. severnensis*, and so is removed. Other modifications relate to the presence of a genal spine in *P. palasso* and *P. bartletti*, compared with the rounded genal angle of the type species (although Edgecombe and Chatterton, 1992 noted that its presence in *P. bartletti* may be a juvenile character state), greater variation in the number of pygidial axial rings and pleural ribs, and variations in pygidial sculpture.

Perryus mikulici sp. nov.

Plate 25, figures 7–15; plate 26, figures 1–4

Derivation of name. For Dr D. G. Mikulic, geologist at the Illinois Geological Survey, who was an excellent guide to the Silurian of the Great Lakes area, U.S.A.

Holotype. MGUH263 (Pl. 25, figs 7–9) cephalon; GGU 275015 (KCL1).

Figured paratypes. Locality CPL5: MGUH264 cephalon with articulated thoracic segments; MGUH266, 268 cranidia; MGUH267 librigena; MGUH269 pygidium. Locality KCL1: MGUH265 cranidium with articulated thoracic segments. Locality KCL6: MGUH270 pygidium.

Diagnosis. Perryus with L4 comprising three partially fused longitudinally-directed tubercles, and PL a singular longitudinally directed tubercle; frontal glabellar lobe with subtriangulate anterior margin; glabellar tubercles markedly flattened, especially so medially; tubercles non-perforate; pygidial axis with 20–22 rings bearing subdued tubercles, and pleural regions with 11 pairs of ribs.

Description. Cephala and cranidia ranging in sagittal length from 4.89–13.25 mm; cranidial sagittal length two-thirds transverse width (average 68%, n = 7, range 60–78%). Maximum glabellar width roughly three-quarters total glabellar sagittal length from occipital furrow; pre-occipital glabella roughly 90% as wide (tr.) at this point as long (sag.). Axial furrows wide (tr.) and deep. L1 short (exsag.) and wide (tr.) with a singular longitudinally directed tubercle. Glabellar width across L1 exceeding width across L2; glabellar width (tr.) at PL just over twice that across L2. S1 distinct from occipital furrow; S1–S3 similar in length (exsag.) to their corresponding lateral lobes, narrow transversely, directed slightly anteromedially. Anterior margin of frontal glabellar lobe with about 14 tubercles aligned alongside clear preglabellar furrow, these increasing in size abaxially. Anterior border becoming longer (exsag.) abaxially, with tubercles similar in size and distribution to those on frontal glabellar lobe. Entire

pre-occipital glabella covered in unevenly sized and shaped, and irregularly distributed granulate tubercles. Tubercles are dorsally flattened, most so medially. Occipital ring as wide as glabella at point near posterior of L4; 30% as wide (tr.) as long (sag.), two-thirds as long (exsag.) abaxially, as medially; flattened in lateral profile. Occipital furrow long (sag.) and deep. Palpebral lobe 15–20% total cranidial sagittal length; palpebral furrow well incised. Midpoint of palpebral lobe opposite L3; about three tubercles occur between palpebral lobe and axial furrow. Distance between palpebral lobes subequal to sagittal cranidial length. Fixigena (excluding posterior border and palpebral lobe) covered in granulate tubercles, which are more equally sized than those covering the glabella, and less flattened. Areas between tubercles distinctly pitted. Deep posterior border furrow. Posterior border of roughly equal length (exsag.) until abaxial of palpebral lobe where it expands to form a rounded genal angle; granulose sculpture becoming faintly tuberculate near genal spine. Posterior branch of facial suture increasingly posteriorly directed across lateral border. Lateral border of constant transverse width, wider (tr.) than librigenal field and posterior border length (exsag.). At least eight large tubercles alongside deep lateral border furrow, and less distinct tubercles abaxial of these. Librigena with identical sculpture to fixigena. Connective sutures obscured.

Hypostome at least 80% as wide (tr.) across anterior wings, as long (sag.). Anterior wings representing maximum transverse width, located roughly one-quarter total hypostomal sagittal length back from anterior border. Middle body with maximum width (tr.) in anterior lobe, one-third total sagittal length from posterior of middle body (just anterior of maculae). There measuring 73% sagittal length of middle body, from which point middle body narrows forwards. Maculae obliquely elongate, located about 15% total sagittal length of middle body, from posterior

border of middle body. Rhynchos subquadrate, not projecting past hypostomal anterior border. Lateral margins of rhynchos gradually diverging and fading posteriorly, terminating completely by one-quarter sagittal length of middle body from anterior margin. Anterior border subtriangulate; shorter (sag.) than anterior border furrow. Posterior hypostomal margin incomplete, but posterior border forming at least 13% entire hypostome sagittal length. Sculpture of fine granules covering entire middle body and posterior border.

Anterior of thorax with axis forming about 40% total transverse width. Thoracic segments with no discernable sculpture.

Pygidial sagittal length ranging from 3.83–12.76 mm, averaging 97% as long as wide (n = 27; range = 88–110%). Axis comprising 41% total width of anterior of pygidium (n = 28; range = 33–50%). Axial rings medially with granulate sculpture and with irregular swellings, which in places are approaching tuberculate form. All rings longer sagittally than exsagittally, and ring furrows equally well impressed medially and abaxially. Axial furrow well impressed. Pleural region with ribs displaying a granulate sculpture. Pleural ribs terminating as bluntly rounded expansions; these increasingly upturned anteriorly. Posteriormost pair merged posteroventrally. Pleural furrows deep.

Remarks. P. mikulici is close to the type species of *Perryus*, *P. severnensis*. *P. mikulici* differs from *P. severnensis* by having a longer (sag.) glabella and cranidium, relative to their respective widths (tr.), and the glabellar frontal lobe is less semicircular in outline than that of *P. severnensis*. Additionally, the preglabellar furrow is visible throughout its course in *P. mikulici*, whereas it is only visible at the lateral extremities in *P. severnensis*. Internal moulds of *P. mikulici* (Pl. 25, figs 7–9,

13) show L4 to comprise three partially fused tubercles; the nature of L4 is difficult to ascertain in *P. severnensis* as is obscured by cuticle. The pygidial axial ring furrows of *P. mikulici* are medially deeper and longer (sag.) than in *P. severnensis*. There are also considerable differences in the nature of the sculpture. *P. mikulici* has a flatter lateral profile to its glabellar tubercles, and tubercles become medially effaced. Conversely, the pygidium bears a more pronounced sculpture; it is tuberculate in places, whereas there are no tubercles present in *P. severnensis*. Perforations are only present between tubercles on the genae in *P. mikulici*, whereas in *P. severnensis* these cover the entire body, and the tubercles themselves contain perforations.

Occurrence and distribution. Western Peary Land (WPL1), central Peary Land (CPL5) and Kronprins Christian Land (KCL1, 6).

Perryus cf. *P. palasso* Lane, 1988

Plate 26, figures 5–7

Figured material. MGUH271 cranidium, GGU 298924 (SNL2). MGUH272–273 pygidia, GGU 298506 (WL).

Remarks. Cranidia referable to *Perryus* from Wulff Land and south Nares Land, bear short genal spines. This, and the much reduced L1, are characters of *P. palasso* Lane, 1988, from Peary Land. The figured cranidium is almost twice as wide (tr.) as long (sag.), and the pre-occipital glabella is 92% as wide as long.

The pygidia are tentatively assigned to the cranidia on the basis of their association within the material. Nine pleural ribs are present and the pygidium is

slightly wider than long, as in *P. palasso*. They differ from other *Perryus* species, including *P. palasso*, in having about 16 axial rings: the genus typically contains 18–22. Unlike *P. palasso*, there are rows of tubercles on both axial rings and pleural ribs, and larger tubercles on five of the axial rings.

Occurrence and distribution. Wulff Land (WL) and south Nares Land (SNL2).

Perryus sp. 1

Plate 26, figures 8–12

Figured material. MGUH274 glabella, GGU 198221 (CPL2). MGUH275 cephalon, GGU 198206 (CPL2). MGUH276 pygidium, GGU 198214 (CPL2) dorsal view.

Remarks. The material is represented by internal moulds with little cuticle attached, and only limited description is possible. L2 and L3 comprise pairs of partially fused and longitudinally directed tubercles which are characterisitc of the genus. Tubercles where present exhibit the granulose form exhibited by most species of *Perryus*. Proportionally, the cephalon is similar to *P. mikulici* but has a distinct pseudoglabellar area, and tubercles are clear on the internal mould, which is not the case with *P. mikulici*. Pygidia are relatively wider than those of *P. mikulici*, and comprise nine pleural ribs and 18–20 axial rings, fewer than in *P. mikulici*. A new species is represented, but further material is required to name it.

Occurrence and distribution. Central Peary Land (CPL2).

Perryus sp. 2

Plate 26, figures 13–17

Figured material. MGUH277 cranidium, MGUH278 articulated pygidium and thorax, MGUH279 pygidium. GGU 274774 (KCL5).

Remarks. This cranidium has more strongly raised tubercles than those of *P. mikulici*. Associated pygidia exhibit further differences; they have fewer axial rings (18 compared to 20–22), and rows of clear tubercles are present on both axial rings and pleural ribs.

Occurrence and distribution. Kronprins Christian Land (KCL5).

Genus aff. *Perryus*

Plate 26, figures 18–21; plate 27, figures 1–4

Figured material. MGUH280 cranidium, MGUH281 cephalon, MGUH282–283 pygidia. GGU 198225 (CPL3).

Description. Cephala and cranidia ranging in sagittal length from 3.11–4.85 mm; cranidial sagittal length 64% of transverse width (n = 3, range 63–65%). Maximum glabellar width located roughly three-quarters distance from occipital furrow; pre-occipital glabella there roughly 85% as wide (tr.) as long (sag.). All lateral lobes bearing singular sub-rounded tubercles. L1 more longitudinally directed and with smaller tubercle than other lateral lobes. Tubercles on L2–L5 roughly equal in size,

and larger than other glabellar tubercles. Glabellar width across L1 subequal to width across L2; glabellar width (tr.) at PL roughly twice that across L2. PL comparable in size and shape with tubercles on L2–L5. S1 the most deeply incised, S2–S5 all long (exsag.). Anterior of frontal glabellar lobe smoothly sub-triangulate, with about 16 very irregularly sized tubercles alongside shallow preglabellar furrow. Anterior border becoming longer (exsag.) abaxially, with a greater abundance of smaller tubercles compared to rest of glabella. Entire pre-occipital glabella with randomly distributed, non-symmetrical, and very unequally sized, moderately inflated tubercles; tubercles sub-rounded and finely granulate. Occipital ring as wide as glabella near anterior of L4; 20% as wide (tr.) as long (sag.), medially expanded; sagittally and transversely convex. Occipital furrow deep.

Palpebral lobe with well incised furrows; roughly 20% total cranidial sagittal length, midpoint positioned opposite anterior of L3. Distance between palpebral lobes subequal to cranidial sagittal length. Fixigena (excluding posterior border and palpebral lobe) covered in granulate tubercles, as with glabella. Areas between tubercles distinctly pitted. Deep posterior border furrow. Posterior border progressively increasing in length (exsag.) towards blunted genal angle. Posterior border predominantly with granulose sculpture; about five unevenly sized tubercles placed adaxially around genal angle. Posterior branch of facial suture increasingly posteriorly directed across lateral border. Lateral border of constant transverse width, and at least twice as wide (tr.) as posterior border length (exsag.) and wider (tr.) than librigenal field. About ten large tubercles immediately adjacent to deep lateral border furrow; smaller tubercles abaxial of these, and granules instead of tubercles most abaxially. Librigena with identical sculpture to fixigena. Connective sutures obscured.

Pygidia ranging in sagittal length from 4.31–4.90 mm, non-mucronate, and 80% as long (sag.) as wide (tr.). Axis comprising 38% total anterior width of pygidium, with 15 clearly discernible axial rings. Axial rings medially slightly longer (sag.) than abaxially, bearing rows of tubercles, with about five larger tubercles medially placed. All rings longer sagittally than exsagittally, and ring furrows equally well impressed medially and abaxially. Axial furrow well impressed. Pleural region with 10 pairs pleural ribs, posteriormost pair merged posteroventrally. Pleural ribs gently convex, terminating as bluntly rounded expansions. Ribs with granulate sculpture and rows of tubercles, significantly more subdued than those on axial rings. Pleural furrows deep.

Remarks. The material shares some characters with the *Perryus* species decribed here: asymmetrically arranged and granulate tubercles; position of palpebral lobe opposite L3; lateral border wider (tr.) than librigenal field; pitted cheeks; pygidial proportions; posteroventrally merged posteriormost pleural ribs. The morphology of the lateral glabellar lobes is however quite different from *Perryus*, comprising individual sub-rounded tubercles as opposed to the diagnostic paired longitudinally fused-type.

Occurrence and distribution. Central Peary Land (CPL3).

variolaris plexus gen. indet. 1

Plate 27, figures 5–11

Figured material. GGU 274689 (CPL5): MGUH284 cranidium, MGUH286–287 pygidia. GGU 274996 (KCL4): MGUH285 cranidium.

Description. Pre-occipital glabella roughly as long (sag.) as wide (tr.). L1 very subdued or absent, L2–L4 larger than glabellar tubercles and themselves tuberculiform. Glabellar tubercles unevenly sized; tuberculation includes I-1, small ii-0, II-1 abaxial to I-1, iii-0, III-1,2 (III-2 partially merged with L3), IV-1,2,3 (IV-3 partially merged with L4). Much smaller, irregularly distributed tubercles present between these. Glabellar width (tr.) across L2 roughly half that across anterolateral extremities of frontal glabellar lobe. S0-3 short (exsag.). Midpoint of palpebral lobe placed opposite point between L2 and L3. Tubercles on fixigena comparable in distribution of size, with those of glabella. Posterior border consistently lengthening (exsag.) abaxially, and with 3 or 4 large tubercles posteriorly; elsewhere, granulose. Short, thorn-like genal spine.

Pygidium about 80% as long (sag.) as wide. Axis comprising about 36% pygidial sagittal width across widest point, with about 13 axial rings. Rows of tubercles along axial rings, with larger tubercles adaxially present on at least four axial rings. Sagittal depression present. Eight or nine pleural ribs, with posteriormost pair merged posteroventrally. Pleural ribs with rows of tubercles similar in size to the abaxial tubercles on axial rings. Deep pleural furrows.

Remarks. Generic assignment is difficult based on such limited material. The fragments show characters consistent with those of the *"Encrinurus"* [= *Balizoma*] *variolaris* plexus of Strusz (1980): enlarged tuberculiform lateral lobes anterior of L1; L1 reduced; complex glabellar tuberculation; genal spines small; subtriangular pygidium; tuberculate pleurae, last one or two recurved, loop-like; pygidium non-mucronate and lacking pygidial spine. The *variolaris* plexus has been well studied, including cladistically (Edgecombe and Ramsköld 1996, Adrain and Edgecombe

1995), and differentiation made between typical Llandovery taxa such as *Nucleurus* Ramsköld, 1986 and *Billevittia* Edgecombe and Ramsköld 1996, and post-Llandovery clades which include *Balizoma* Holloway, 1980 and *Struzia* Edgecombe, Ramsköld and Chatterton *in* Edgecombe and Chatterton, 1993. The material has characters in common with both Llandovery and post-Llandovery genera, and to avoid the assumption that it should fit into one of the Llandovery genera, it is left under open nomenclature.

Occurrence and distribution. Central Peary Land (CPL5) and Kronprins Christian Land (KCL4).

variolaris plexus gen. indet. 2

Plate 27, figures 12–20

Figured material. MGUH288–289 cranidia, MGUH290 glabella, MGUH291 librigena, MGUH292–293 pygidium. GGU 198226 (CPL1).

Remarks. Fragmentary cranidia, pygidia and free cheeks from central Peary Land, are all preserved as internal moulds. The cranidia are reminiscent of *variolaris* plexus gen. indet. 1, however have larger, more evenly sized, glabellar tubercles. The pygidia are also of similar proportions, and have the same number of axial rings and pleural ribs.

Occurrence and distribution. Central Peary Land (CPL1).

2.3.12 Family CALYMENIDAE Burmeister, 1843

Subfamily CALYMENINAE Burmeister, 1843

Genus CALYMENE Brongniart *in* Brongniart and Desmarest,1822

Type species. Calymene blumenbachii Brongniart *in* Desmarest, 1817, from the Wenlock (Homerian Stage) Much Wenlock Limestone Formation, Dudley, West Midlands, England, by subsequent designation of Shirley (1933, p. 53).

Remarks. Siveter (1985) reillustrated and revised the type species.

Calymene aff. *iladon* Lane and Siveter, 1991

Plate 28, figures 1–8

Figured material. MGUH294 cephalon, MGUH295 hypostome, MGUH296–297 pygidia. GGU 298506 (WL).

Description. Cranidium with sagittal length 2.3 mm; 57% as long (sag.) as wide (tr.). Glabella bell-shaped; 83% as wide (tr.) across L1, as long (sag.). Preoccipital glabella as wide (tr.) across L1, as long (sag.). Occipital ring comprising 20% total glabellar sagittal length. Very deeply incised S1, trending from an exsagittally directed line at 150 degrees. L2 roughly half length (exsag.) of L1 and joined to free cheek. S2 trending transversely, and S3 weak defining short (exsag.) L3. Anterior of glabella smoothly rounded. Preglabellar border furrow well defined, anterior border furrow less so. Preglabellar field short; of subequal length (sag.) to anterior border. Palpebral

lobe anteriorly placed. Librigena very convex (tr.). Complete covering in evenly spaced coarse granules.

Hypostome with narrow (tr.) lateral border, bifid posterior margin and weak macula. Middle body about twice as long (sag.) as wide (tr.); anterior lobe just over twice as long (sag.) as posterior lobe.

Pygidium measuring 3.8 mm sag. length; 87% as long (sag.) as wide (tr.). Axis comprising roughly half the width (tr.) of pygidium anteriorly. Seven or eight axial rings and a terminal piece. Axial rings expanded (sag.) medially. Inter-ring furrows increasing in depth and length (exsag.) towards axial furrow, which is well impressed except posteriorly. Steeply sloping pleural regions with six pairs of pleural ribs. Interpleural furrows deep, pleural furrows much shallower; pleural and interpleural furrows becoming effaced towards pygidial margins. Granular sculpture.

Remarks. The nature of the anterior border, and the connection of L2 to the fixigena, confirm the generic assignment of the cephalon. The cephalon is closest to *C. iladon*, and shares the following distinctive combination of characters with that species: glabella weakly bell-shaped; relatively short preglabellar area; forward positioning of the palpebral lobe; granular sculpture. Certain characters differ from *C. iladon*, but these could, to some extent, reflect the small size of the cephalon: fork of S1 with less distinctive intermediate lobe; L1 lobe distinctly more triangulate in form; weak L2-fixigena buttress. The pygidium is associated on the basis of its co-occurrence with the cephalon, but it is larger in size. The wide (tr.) axis distinguishes the pygidium from that of *C.* sp. 1, and it is also proportionally wider than that of *C. iladon*. The number of axial rings and pleural ribs, and the granular sculpture do however agree with *C. iladon*.

Adrain and Edgecombe (1997, p. 659) erected the genus *Arcticalymene* from the Wenlock Cape Phillips Formation, central Canadian Arctic. They noted that *C. iladon* and *C.* (s.l.) aff. *iladon* (Adrain *et al.,* 1995) are among the only calymenines with the coarseness of tuberculate sculpture seen in *Arcticalymeme*. Other cephalic synapomorphies are: eye placed far forwards; fixigena gently notched in front of L2 buttress; glabella weakly bell-shaped; cranidium posteriorly narrow.

Occurrence and distribution. Wulff Land (WL).

Calymene sp.

Plate 28, figures 9–18

Figured material. GGU 198185 (CPL2): MGUH298 cranidium. GGU 198223 (CPL2): MGUH300 cranidium, MGUH299 cranidium with articulated thoracic segments, MGUH303 pygidium with articulated thoracic segments. GGU 198214 (CPL2): MGUH302 pygidium. GGU 198196 (CPL2): MGUH301 pygidium.

Description. Cranidium 57% as long (sag.) as wide (tr.) (n = 2, range = 56–57%). Glabella weakly bell-shaped; 74% as wide (tr. across L1) as long (sag.) (n = 3, range = 69–79%). Preoccipital glabella averaging 87% as wide (tr. across L1) as long (sag.) (n = 4, range = 81–94%). Occipital ring narrower (tr.) than glabella at L1. L1 subquadrate, comprising about 20% entire glabellar sagittal length. Anterior of L1 forming widest point (tr.) of glabella. L2 papillate, connecting with buttress on fixed cheek. Exsagittal length of S2 roughly 70% that of L1. L3 transversely elongate, exsagittal length roughly 50% that of L2. S1 and S2 deep. Distinct intermediate lobe

located in fork of S1. Frontal lobe of glabella roughly 75% as wide as glabella across L1; projecting anterior of fixed cheeks, smoothly convex forwards. In lateral profile, glabella increasing sagittally convex anteriorly. Preglabellar and anterior border furrows not preserved. Glabella terminating well posterior of anterior border.

Midpoint of palpebral lobe placed opposite midpoint of L2; palpebral lobe is slightly longer (exsag.) than L2. Width (tr.) of cranidium at midpoint of palpebral lobe is roughly 1.8 times width of glabella at midpoint of L2. Posterior branch of facial suture distinguishable; running from palpebral lobe almost transversely for about half its length, then suddenly changing course to run at an angle of roughly 20 degrees from an exsagittal line. Sculpture of very unevenly sized and spaced granules.

Number of thoracic segments unknown. Axial rings gently convex (sag.) and roughly equal in length medially and at axial furrows. Articulating half-ring roughly half length of axial ring (sag.) Sculpture similar to that of cranidium; granules more evenly sized and have a smaller average size.

Pygidium 80% as long (sag.) as wide (tr.). Axis comprising 35% total width (tr.) of pygidium anteriorly. Total number of axial rings difficult to establish, probably seven or eight and a terminal piece. Axial rings expanded (sag.) medially. Inter-ring furrows increasing in depth towards well impressed axial furrow. Steeply sloping pleural regions. Interpleural furrows deep, pleural furrows much shallower and retaining depth of impression throughout course. Sculpture identical to that of axis.

Remarks. Description of *C.* sp. is constrained by the limited material, and the patchy nature of cuticle cover; however, the papillate L2 opposite a distinct buttress on the fixigena confirms the generic assignment. *C.* sp. differs from all other described species from the Silurian of North Greenland, of which *C. iladon* (Lane and Siveter,

1991) from the Telychian Offley Island Formation is the most complete known. *C. iladon* can be distinguished by having a very forwardly placed palpebral lobe though the species have very similar sculpture.

C. sp. (Lane, 1972, p. 359, pl. 64, figs. 6a–d, 7a–b) from the Telychian Samuelsen Høj Formation of Kronprins Christian Land, eastern North Greenland, has a more convex (sag.) glabella, with the frontal lobe almost overhanging the anterior border. His material was reassigned to *Arcticalymene* by Adrain and Edgecombe (1997). A fragmentary cranidium from south-eastern Hall Land on the northern slopes of Kayser Bjerg (Telychian Offley Island and Hauge Bjerge formations) (Lane 1984, p. 62, pl. 2, fig. 10) is thought to be conspecific with Lane's 1972 material (Lane and Siveter, 1991).

Occurrence and distribution. Central Peary Land (CPL1–2).

Calymene? sp.

Plate 28, figures 19–21

Figured material. MGUH304 cephalon, GGU 301318 (WPL1).

Description. Cranidium 64% as long (sag.) as wide (tr.). Glabella subrectangular; 75% as wide (tr.) across L1, as long (sag.). Preoccipital glabella 93% as wide (tr.) across L1, as long (sag.). Occipital ring comprising 16% total glabellar sagittal length. Anterior of L1 forming widest point (tr.) of glabella. Exsagittal length of S2 roughly 70% that of L1. L3 obliquely elongate, anteriorly weakly defined by shallow S3; S1 and S2 significantly deeper. Distinct intermediate lobe located in fork of S1. Frontal

lobe of glabella roughly 88% as wide (tr.) as glabella across L1; projecting anteriorly to fixed cheeks, anteriorly flattened. In lateral profile, glabella increasing sagittally convex anteriorly. Preglabellar and anterior border furrows not visible. Glabella terminating well posterior of anterior border. Anterior border dorsoventrally expanded.

Palpebral lobe roughly as long (exsag.) as L1; midpoint placed opposite posterior portion of L2. Cranidium at midpoint of palpebral lobe roughly twice as wide (tr.) as glabella there. Posterior branch of facial suture distinguishable; running from palpebral lobe almost transversely for about half its length, then suddenly changing course to run at roughly 20 degrees outwards from an exsagittal line. Sculpture of very unevenly sized and spaced granules.

Remarks. The cranidium is refered to *Calymene*? as matrix obscures the nature of the axial furrows and a connection between L2 and the fixigena cannot be confirmed. This matrix cannot be removed without damaging the specimen. The anterior border is particularly distinctive, being more dorsoventrally expanded and transversely arched than is typical for *Calymene*. The subrectangular glabellar morphology is also distinctive, and the cephalon has proportionally smaller lateral glabellar lobes than in *C.* sp. and *C.* aff. *iladon*. The anterior position of the eye, and the coarsely granular sculpture also agree with *Arcticalymeme*.

Occurrence and distribution. Western Peary Land (WPL1).

2.3.13 Family PHACOPIDAE Hawle and Corda, 1847

Subfamily PHACOPINAE Hawle and Corda, 1847

Genus ACERNASPIS Campbell, 1967

Type species. By original designation: *Phacops orestes* Billings, 1860, from the Llandovery Jupiter and Gun River Formations, Anticosti Island, Canada.

Diagnosis. From Campbell (1967, p. 32): phacopine with glabella only moderately convex in longitudinal profile, never with a vertical front wall, nor overhanging the anterior margin; length/width ratios of glabella 1 or greater; S1 not continuous, but with its inner end directed strongly forward; S2 and S3 moderately impressed; S3, but not S2, being connected to the axial furrow; strong incision into the occipital ring at the inner end of the occipital apodeme; axial furrow strong and straight on the flank of the glabella; preglabellar furrow weak; facial sutures continuous around anterior of cephalon and cutting across anterolateral corners of glabella; eye large; genal angle subrounded to pointed; dorsal surface covered with minute granules; anterior doublure long, and granulate, the granules not arranged in rows; vincular furrow continuous, moderately strong anteriorly, and notched laterally to receive the ends of the thoracic pleurae. Thoracic ring with an incision near the outer end, but without a lateral node. Pygidium with 6–8 rings, the posterior ones being poorly defined, and 5–6 pleurae; all pygidial furrows narrow and rather weak; thorax and pygidium either smooth or with minute granules.

Acernaspis? sp.

Plate 29, figures 1–3

Figured material. MGUH305 cephalon, GGU 298506 (WL).

Description. A single, fragmentary cephalon has a sagittal length of 7.88 mm. Pre-occipital glabella 87% as long (sag.) as wide (tr.) across widest point near anterior; expanding forwards at an angle of roughly 30 degrees, so that is 45% of maximum width (tr.) across L1. Small, node-like L1. Glabellar muscle impressions effaced; this could be preservational. Narrow (tr.) intercalating ring. Anterior margin of glabella smoothly rounded; preglabellar furrow clearly impressed both abaxially and medially. Palpebral lobe raised above fixigena, with defined rim and shallow palpebral furrow. Palpebral lobe comprising about one-third total cephalic sagittal length; posterior margin of palpebral lobe placed just anterior of L1, so remote from posterior border furrow. Visual surface with seven rows and sixteen files; lens formula: 234 34**4** 4**4**4 434 343 2; total 55 (pl. 29, fig. 3). Librigena fragmentary but highly convex.

Remarks. Lenses in bold are significantly smaller than others. The cephalon is closest to *Acernaspis*, particularly in terms of glabellar morphology including the narrow (tr.) intercalating ring. It does, however, share characters in common with *Ananaspis* Campell, 1967: the eye is close to axial furrows anteriorly, but is well separated from posterior border furrow posteriorly. The glabella is much more highly inflated in lateral profile than either *Acernaspis* or *Ananaspis*, and this convexity is also shown by the librigena. The cephalon could represent a new genus related to both *Acernaspis* and *Ananaspis*.

Occurrence and distribution. Wulff Land (WL).

Order LICHIDA Moore, 1959

2.3.14 Family LICHIDAE Hawle and Corda, 1847

Subfamily TROCHURINAE Phleger, 1936

Genus DICRANOGMUS Hawle and Corda, 1847

Type species. By monotypy; *Dicranogmus pustulatus* Hawle and Corda, 1847, from the Ludlow Kopanina Formation, Czech Republic.

Diagnosis. Cranidial features from Thomas and Holloway (1988, p. 230), and librigenal and pygidial features from Adrain (2003, p. 751), here modified to reflect the partial definition of the second and third ring furrows seen in some species: trochurine with strongly convex (sag., exsag.) glabella overhanging anterior border; in dorsal view, glabella wider across bullar lobes than long (sag.) and smoothly curved in outline anteriorly, median and bullar lobes there lacking independent convexity. Longitudinal furrows subparallel in front of S1, usually dying out approximately half way to front of bullar lobe, may extend behind S1 as poorly defined depressions not interrupting exoskeletal granulation. Maximum width of bullar lobe almost equal to width of median lobe. L1a usually clearly circumscribed; S1 may be present behind median lobe as weak, concave-forward depression not interrupting exoskeletal granulation and meeting occipital furrow on sagittal line; posterior and lateral librigenal border furrows shallow or effaced; genal spine broad and short; entire librigena with dense tuberculate sculpture matching that on cranidium; librigenal

lateral border with dorsal row of large tubercles; pygidium with anteriorly broad axis on which only the first segment and ring furrow are fully defined, second and ring furrow may be apparent abaxially; narrow and tapering subtriangular pygidial terminal piece set off from axis by abrupt change in slope; three sets of subtriangular to pointed border spines; first and second pygidial pleural and interpleural furrows fully defined; third defined only as minute proximal depression.

Dicranogmus pearyi sp. nov.

Plate 29, figures 4–13

Derivation of name. For Admiral Robert Edwin Peary, who carried out seven expeditions to North Greenland, reaching the North Pole in 1909, and for whom Peary Land was named, where this material was collected.

Holotype. MGUH306 (Pl. 29, figs 4–7) cephalon; GGU 274689 (CPL5).

Figured paratypes. Locality CPL5: MGUH307–308, hypostomes, MGUH309–310 pygidia.

Diagnosis. Dicranogmus with: glabellar tubercles becoming finer anteriorly; longitudinal furrows deflected abaxially, just anterior of palpebral lobe; faint posterior extension behind S1running almost exsagittally; hypostomal lateral border furrow continually diverging anteriorly throughout its course; almost intersecting hypostomal anterior margin; second and third pygidial axial ring furrows visible abaxially; postaxial band short (sag.), roughly one-third total pygidial axis length (sag.)

Description. Pre-occipital glabella on average 83% as long (sag.) as wide (tr.) across bullar lobes (n = 2; range = 80–87%). Longitudinal furrows visible for posteriormost 64% of pre-occipital glabella (n = 2; range = 63–66%). Moderately sized tubercles becoming finer towards anterior of glabella.

Hypostome subtrapezoidal, posterior border incomplete. Middle body averaging 65% as long (sag.) as wide (tr.) anteriorly (n = 2; 62–67%); middle body width (tr.) across middle furrow, at least half hypostomal width (tr.) across shoulders. Middle furrow running subtransversely, and impressed for one-quarter to one-third total transverse width of middle body at this point. Posterior border furrow curved posteriorly. Sculpture comprising elongated pits and striations, sparsely tuberculate around anterolateral borders of middle body.

Pygidium semicircular; 54% as long (sag.) as wide (tr.) (n = 1). Axis comprising 40% (n = 1) pygidial width (tr.) anteriorly; first axial ring demarcated by well impressed ring furrow; second ring furrow less well impressed than first, effaced in medial third of axial width; third axial ring furrow visible abaxially for less than this. Terminal piece inflated; postaxial band strongly triangulate, with furrows converging and almost meeting, not intersecting posterior pygidial margin. Interpleural furrow reaching margin on first pleural segment, fading on approach to margin on second rib. Sculpture of densely packed, unevenly sized tubercles.

Remarks. The high convexity glabella, anterior effacement of the longitudinal furrows, and lack of a deep pleural furrow on the posteriormost pygidial pleural segment, are particularly characteristic of the genus. *D. pearyi* is closest to *Dicranogmus*? sp. Lane and Owens, 1982 from blocks believed to have been derived from the Telychian Pentamerous Bjerg Formation, of Kap Schuchert, Washington

Land, western North Greenland. *D. pearyi* differs most noticeably by: longitudinal furrows more distinct; hypostomal sculpture with elongated pits and striations, and only sparsely tuberculate, whereas that of *Dicranogmus*? sp. is more tuberculate, especially on the lateral border; finer tubercles on both cephalon and pygidium, which are move evenly sized than those of a *Dicranogmus*? sp.

Occurrence and distribution. Central Peary Land (CPL3, 5).

Dicranogmus mabillardi sp. nov.

Plate 29, figures 14–16; Plate 30, figures 1–5

Derivation of name. For Dr J. E. Mabillard, material was collected from a reef informally known as ‘Mabs mound’.

Holotype. MGUH311 (Pl. 29, figs 14–15) cranidium; GGU 274654 (CPL4).

Figured paratypes. Locality CPL1: MGUH312 cranidium, MGUH313 hypostome, MGUH315–316 pygidia. Locality CPL2: MGUH314 pygidium.

Diagnosis. Dicranogmus with: glabellar tubercles becoming finer anteriorly; longitudinal furrows with a trichotomy of furrows posterior of S1 and most impressed anteriorly; second and third axial ring furrows visible abaxially.

Description. As for *D. pearyi*, other than: pre-occipital glabella relatively longer, on average 91% as long (sag.) as wide (tr.) across bullar lobes (n = 6; range = 87–96%);

longitudinal furrows sub-parallel, lacking the abaxial inflection seen in *D. pearyi*, and visible for posteriormost 72% of pre-occipital glabella (n = 6; range = 61–87%), so less effaced anteriorly; coarser tubercles; hypostomal lateral border furrow anteriorly curved adaxially, terminating prior to hypostomal anterior margin, so that short (exsag.) anterior border present abaxially; middle furrow running slightly posteromedially; sculpture tuberculate rather than striated and pitted; pygidial axis relatively narrower (tr.); terminal piece less inflated in lateral profile; postaxial band comprising a much greater sagittal length of pygidium; both first and second interpleural furrows do not reach pygidial margin; sculpture more finely tuberculate.

Remarks Dicranogmus? sp. Lane and Owens, 1982, *D. pearyi* and *D. mabillardi* represent the only *Dicranogmus* species from North Greenland with described cranidia, hypostomes, and pygidia. They differ from the Canadian Arctic species *D. skinneri* Perry and Chatterton, 1977 and *D. wynni* Adrain, 2003, by having: anteriorly reduced glabellar tubercles; better impressed hypostomal middle furrows; posterior border furrow curved posteriorly as opposed to running transversely with a slight anterior deflection; posterior border abaxially more posteriorly extended; second and third pygidial axial ring furrows are visible abaxially.

Occurrence and distribution. Central Peary Land (CPL1–2, 4).

Genus ACANTHOPYGE

Type species. By subsequent designation of Reed 1902, p. 60; *A. leuchtenbergii* Hawle and Corda, 1847, p. 144, pl. 1, figs. 5–7; from the Eifelian Acanthopyge Limestone, Czech Republic.

Diagnosis. From Thomas and Holloway (1988, p. 222): trochurine with strongly convex (sag., exsag.) glabella usually not overhanging anterior border; in dorsal view glabella approximately as wide across bullar lobes as long, median lobe typically projecting strongly in front of bullar lobe. Longitudinal furrow extending to occipital furrow but shallower behind S1 than in front, diverging strongly around front of bullar lobe. Medial portion of L1 very short (sagittal length less than that of occipital ring), depressed, and bearing a prominent tubercle. L1a not defined. S1 well impressed behind median glabellar lobe, commonly merging with occipital furrow on sagittal line. Posterior margin of cephalon with deep subgenal notch. Pygidium with two or three pairs of pleural furrows and three or four major pairs of marginal spines; major spines sometimes with secondary spines behind them; convex border may be weakly developed behind anterior pair of spines.

Acanthopyge? sp.

Plate 30, figures 6–8

Figured material. MGUH317–318 hypostomes. GGU 274689 (CPL5).

Description. Non-fragmentary hypostome (MGUH317; Pl. 30, figs 6–7) measures 10.10 mm maximum exsagittal length; middle body a little wider (tr.) across maculae than long (sag.); anterior margin moderately convex forwards; middle furrow shallow, indistinct and only present laterally; lateral border furrow with straight projection, deep; posterior border furrow longer (sag.) than lateral border width (tr.) and shallower, running subtransversely; posterior border incomplete; anterior lobe of middle body with very coarse, irregularly shaped and laterally elongated tubercles, smaller tubercles elsewhere.

Remarks. The hypostomal middle body has the characteristic proportions and effaced median furrow of a trochurinae. Its proportions and coarse sculpture are particularly reminiscent of *Acanthopyge*.

Occurrence and distribution. Central Peary Land (CPL5).

2.3.15 Family ODONTOPLEURIDAE Burmeister, 1843

Genus CERATOCEPHALA Warder, 1838

Type species. By monotypy; *Ceratocephala goniata* Warder, 1838, unnumbered text-fig. from the middle Silurian of Springfield, Ohio.

Diagnosis. From Thomas (1981, p. 93): odontopleurid with narrow (tr.) lateral glabellar lobes; occipital ring with posterior band and a pair of long, slender spines; palpebral lobe placed opposite S1, eye not prominently pedunculate. Ten thoracic

segments, pleurae unfurrowed, terminal spines blade-like and vertically directed. Pygidium with 1-4 pairs of lateral border spines and median spine. Axis with two or fewer rings.

Ceratocephala papilio sp. nov.

Plate 30, figures 9–16

Derivation of name. Latin, *papilio,* butterfly, the fancied resemblance of the glabella to a butterfly. Noun in apposition.

Holotype. MGUH319 (Pl. 30, figs 9–10) cephalon; GGU 274689 (CPL5).

Figured paratypes. Locality CPL1: MGUH321 cranidium. Locality CPL4: MGUH320 cranidium. Locality CPL5: MGUH323 pygidium. Locality KCL1: MGUH322 cranidium.

Diagnosis. Ceratocephala with median glabellar lobe expanded (tr.) at mid-length; median glabellar lobe medially swollen opposite anterior of L2; three marginal pygidial spines, lateral ones barbed; marginal pygidial spines separated by at least four secondary marginal spines and at least four secondary marginal spines lateral to them.

Description. Cranidia ranging in sagittal length from 2.09–6.76 mm, on average 65% as long (sag.) as wide (tr.) (range = 62–71%, n = 6). Glabellar sagittal length (including occipital ring) roughly equal to glabellar transverse width where widest

across anterior of L1. Median glabellar lobe more convex than lateral lobes, and additionally expanded (tr.) opposite S1, so widest at this point; narrowest (tr.) at S2. L1 roughly twice the size of L2 and fused abaxially to it; L3 distinct, narrow (exsag.), and anterolaterally directed. S2 much longer (exsag.) and deeper than S1, both running subparellel. Exsagittal furrows separate glabellar lateral lobes so that they are distinct from median body, these shallower than other glabellar furrows. Longitudinal furrow clearly separating lateral occipital lobes which are subequal in width (tr.) to L1; most deeply impressed on occipital ring. Occipital furrow deepest between occipital ring and L1, fading abaxially. Occipital ring with distinct occipital band and with three spine bases. At least one swelling on fixigena, opposite anterior part of L1. Posterior border furrows deeper than lateral border furrows. Entire cranidium with bimodal sculpture; smaller granules are numerous and scattered, larger tubercles are present as symmetrical pairs, centrally perforated, and probably representing spine bases.

Associated fragmentary pygidium with axis anteriorly comprising about 45% total width (tr.) across anterior of pygidium. Pygidial axis with two visible rings; first ring furrow deepest abaxially, fading medially; second ring furrow only impressed medially. Sculpture of centrally perforated tubercles which are more equal in size to one another than those of the cranidium; a pair of larger spine bases is present on two medially placed swellings on the first axial ring, and two pairs of spine bases on second axial ring, are slightly smaller and further abaxial to those on first axial ring. A spine base similar in size to those on the first axial ring, is also present at the same level, but abaxially to the well impressed axial furrow.

Ontogeny. The cranidia of *C. papilio* exhibit three main changes with growth: smaller specimens (MGUH321–322; Pl. 30, figs 12–14) have increasingly distally fused L1 and L2, these becoming more abaxially distinct in larger specimens (MGUH319–320; Pl. 30, figs 9–11); median glabellar lobe is increasingly swollen opposite L2 in larger specimens; in smaller specimens, the median spine base on the occipital ring is subequal in size to the ones abaxial to it; in larger specimens, the median spine base is reduced in size relative to those abaxially.

Remarks. Chatterton and Perry, 1983, noted that all *Ceratocephala* species from the Ordovician and early Silurian have three spined pygidia, and as such the pygidium is best compared to the pygidia of *Ceratocephala* species from the Llandovery Whittaker Formation, Mackenzie Mountains, Canada, such as *C. avalanchensis* Chatterton and Perry, 1983 (p. 48, pl. 31, figs 5–6, 9, 23–24; pl. 32, figs 7, 10, 15, 18–19, 21, 24; pl. 33, fig. 17; text-fig. 40) and *C. crawfordi* Chatterton and Perry, 1983 (p. 49, pl. 34, figs 18, 20–22, 26, 28, 30; text-fig. 42). These two species both have three pygidial border spines which are separated by over three marginal barbs, as is the condition seen in *C. papilio*.

The outline cranidial morphology is similar to that of *C. avalanchensis*, however, the cranidium is quite distinct from the Mackenzie Mountain species which have a less inflated (tr.) median glabellar lobe and no anterolateral swelling. These conditions are present in Ordovician species such as *C. laticapitata* Warburg, 1925 from the Boda Limestone, Kallholn, Siljan District, redescribed and figured by Bruton, 1966 (p. 24, pl. 4, figs 5–8; pl. 5, figs 6–8), and also Silurian species such as *C.* cf. *C. bicuspis* (Angelin, 1854) Lane and Owens, 1982, which is the only other *Ceratocephala* cephalon previously described from North Greenland. *C. papilio*

differs from *C. laticapitata* proportionally and sculpturally, and from *C.* cf *C. bicuspis* by having lateral glabellar lobes less confluent with the fixigena so that they are better defined abaxially.

Occurrence and distribution. Central Peary Land (CPL1–2, 4–5) and Kronprins Christian Land (KCL1).

Ceratocephala sp.

Plate 30, figures 17–19

Figured material. MGUH324 cephalon, MGUH325 hypostome. GGU 298506 (WL).

Description. A fragmentary cephalon is sufficiently similar to the cranidia of *C. papilio* to require only description of differences: L1 and L2 are not distally fused and are narrower (tr.) and more oval in form; glabella and fixigenal sculpture comprises a smooth range in size from granules to larger centrally perforated tubercles, as opposed to the bimodal form of *C. papilio*, and these are randomly distributed as opposed to the symmetrical form of *C. papilio*.

Additionally, the librigena exhibits the same sculpture as the glabella and fixigena, however, the tubercles are more organised, occurring in rows which are aligned with the lateral border. Lateral border with two rows of larger centrally perforated tubercles; lateral border narrower (tr.) and more convex posterior to maximum width (tr.) of librigena. Lateral border furrow wide (tr.) and shallow, bordered adaxially by a row of centrally perforated tubercles which increase in size posteriorly.

Associated hypostome measures 2.3 mm maximum exsagittal length; 60% as long (exsag.) along maximum length, as wide (tr.) across shoulders, there positioned roughly at hypostomal mid-length; middle body 60% as long (sag.) as wide (tr.); anterior margin running transversely; middle furrow deep, only present laterally where directed posteromedially; lateral border furrow deepest posterior to middle furrow, and deeper here than posterior border furrow; posterior border abaxially inflated posteriorly.

Remarks. Based on the limited material similarities are evident with *C. papilio*, and species such as *C. laticapitata*, which share the medially expanded median glabellar lobe and well defined lateral glabellar lobes.

Occurrence and distribution. Wulff Land (WL).

PLATES

EXPLANATION OF PLATE 1

Figs 1–4. *Aboskes anachoretes* gen. et sp. nov. MGUH1; holotype cephalon, GGU 198225 (CPL3); 1, dorsal, 2, lateral and 3, anterior views, 4, dorsal view of librigena.

Figs 5–14. *Ekwanoscutellum agmen* sp. nov. 5–7, MGUH2 holotype cranidium, GGU 274689 (CPL5). 5, dorsal, 6, anterior and 7, lateral views; 8, MGUH3 cranidium, GGU 275038 (VGL1) dorsal view; 9. MGUH4 cranidium, GGU 198186 (CPL2) dorsal view; 10. MGUH5 cranidium, GGU 275038 (VGL1) dorsal view; 11. MGUH6 cranidium, GGU 275689 (CPL5) dorsal view; 12. MGUH7 cranidium, GGU 275038 (VGL1) dorsal view; 13. MGUH8 cranidium (not blackened), GGU 198216 (CPL2) dorsal view; 14. MGUH9 cranidium, GGU 275015 (KCL1) dorsal view.

All scale bars = 10 mm.

PLATE 1

EXPLANATION OF PLATE 2

Figs 1–20. *Ekwanoscutellum agmen* sp. nov. 1, MGUH10 librigena, GGU 274689 (CPL5) dorsal view; 2, MGUH11 librigena, GGU 274689 (CPL5) dorsal view; 3, MGUH12 librigena, GGU 198186 (CPL2) dorsal view; 4, MGUH13 rostral plate, GGU 274689 (CPL5) ventral view; 5, MGUH14 rostral plate, GGU 198136 (CPL2) ventral view; 6, MGUH15 hypostome, GGU 274654 (CPL4) ventral view; 7–8, MGUH16 hypostome, GGU 275015 (KCL1) 7, ventral and 8, oblique lateral views; 9, MGUH17 thoracic segment, GGU 274689 (CPL5) dorsal view; 10, MGUH18 thoracic segment, GGU 198194 (CPL2) dorsal view; 11–12, MGUH19 pygidium, GGU 274654 (CPL4) 11, dorsal and 12, lateral views; 13–14, MGUH20 pygidium, GGU 275021 (KCL3) 13, dorsal and 14, lateral views; 15, MGUH21 pygidium, GGU 198216 (CPL2) dorsal view;16, MGUH22 pygidium with abnormal fifth pleural rib, GGU 198204 (CPL2) dorsal view; 17, MGUH23 pygidium, GGU 274689 (CPL5) dorsal view; 18, MGUH24 latex cast of pygidium, GGU 198216 (CPL2) dorsal view; 19, MGUH25 pygidium, GGU 198216 (CPL2) dorsal view; 20, MGUH26 pygidium, GGU 275015 (KCL1) dorsal view.

All scale bars = 10 mm.

PLATE 2

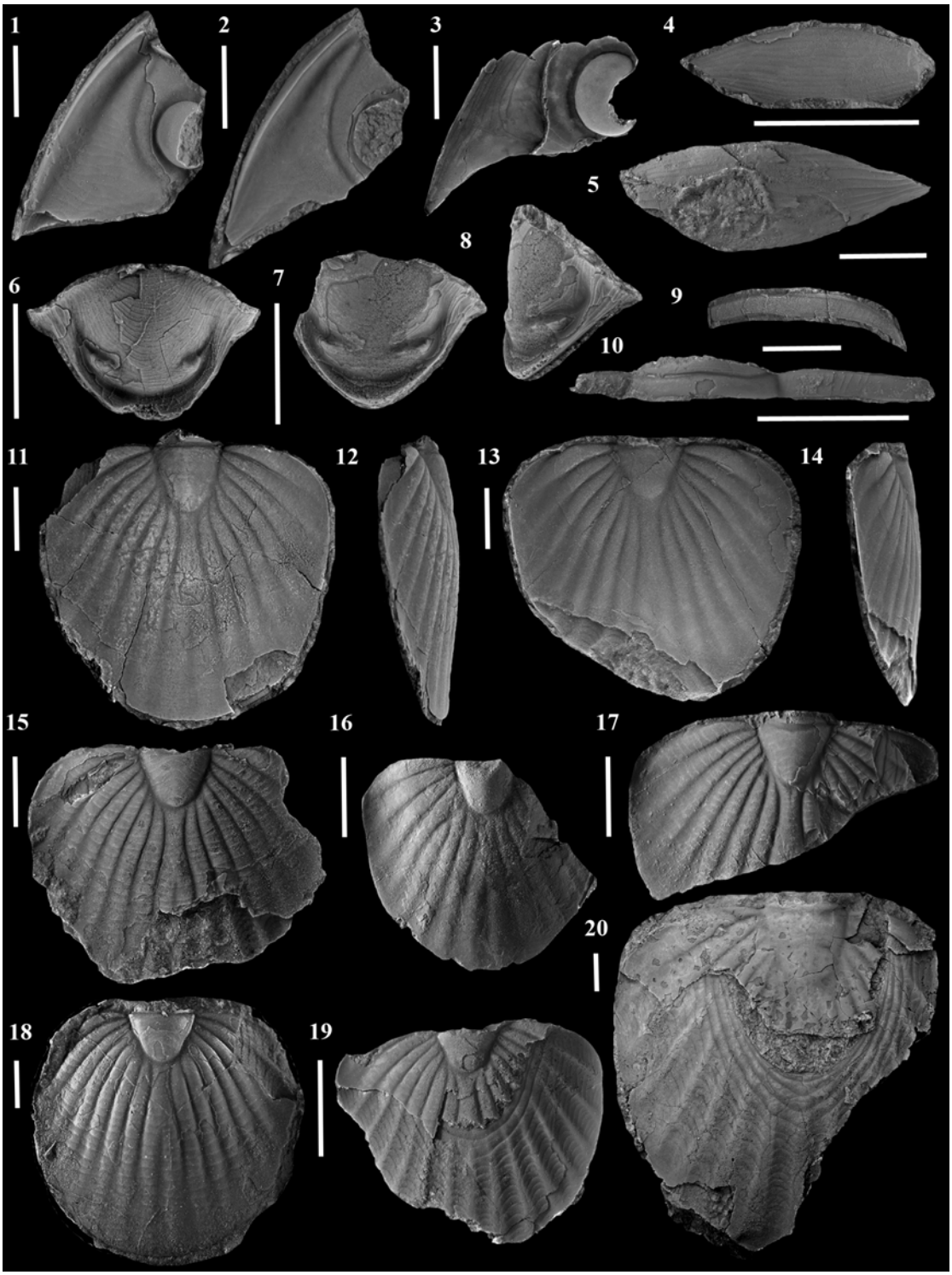

EXPLANATION OF PLATE 3

Figs 1–15. *Jungosulcus emilyae* gen. et sp. nov. 1–3, MGUH27 holotype cranidium, 1, dorsal, 2, anterior and 3, lateral views; 4–5, MGUH28 cranidium, 4, dorsal and 5, oblique lateral views; 6, MGUH29 cranidium, dorsal view; 7, MGUH30 cranidium, dorsal view; 8, MGUH31 cranidium, dorsal view; 9, MGUH32 close up of eye, dorsal view; 10, MGUH33 librigena, dorsal view; 11–12, MGUH34 pygidium, 11, dorsal and 12, oblique lateral views; 13, MGUH35 pygidium, dorsal view; 14, MGUH36 pygidium, dorsal view; 15, MGUH37 pygidium, dorsal view. All material from GGU 274689 (CPL5).

Figs 1–8 and 11–15, scale bars = 5 mm; Fig. 9, scale bar = 0.5 mm; Fig. 10, scale bar = 1 mm.

PLATE 3

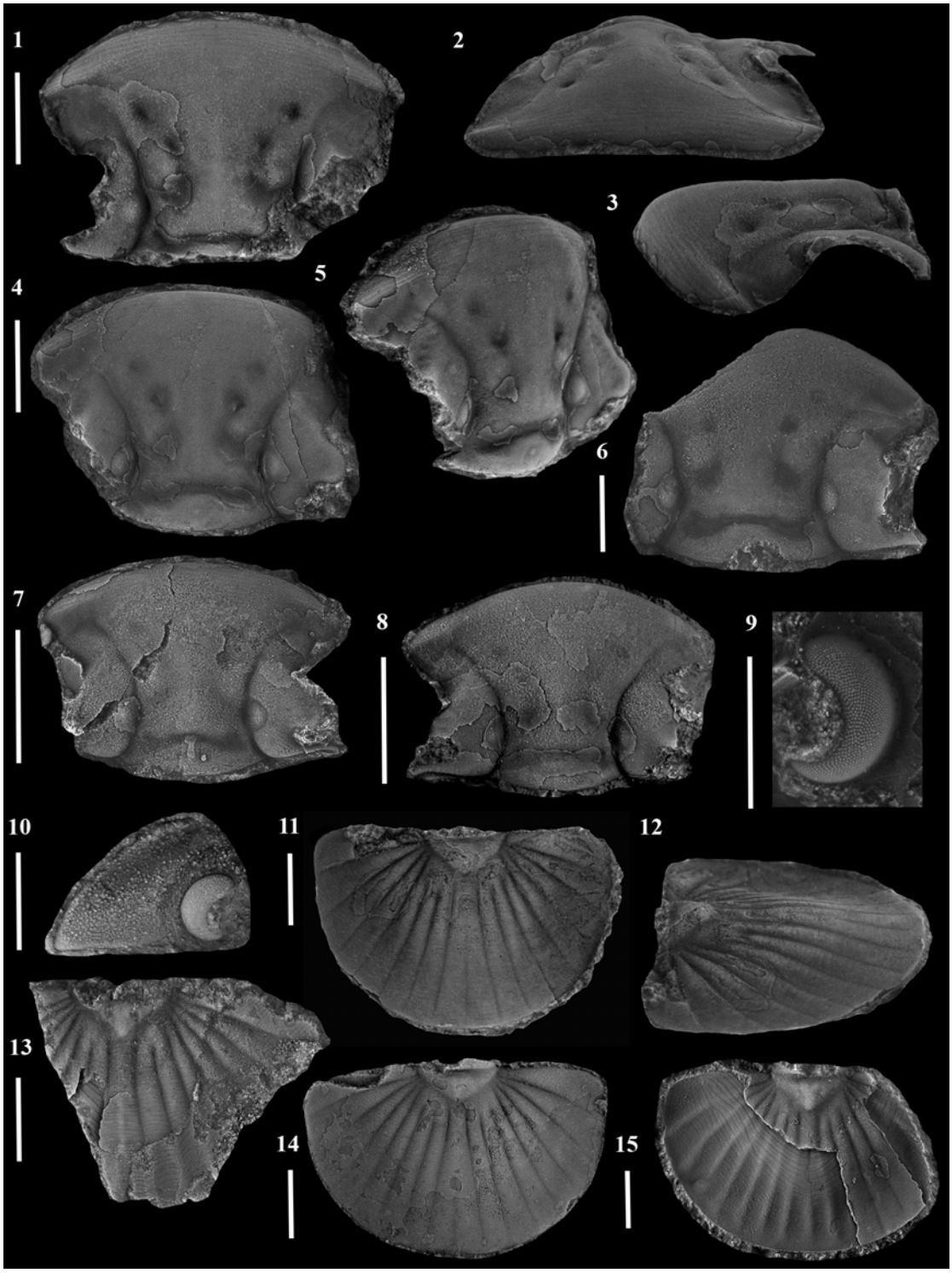

EXPLANATION OF PLATE 4

Figs 1–13. *Jungosulcus anaphalantos* gen. et sp. nov. 1–3, MGUH38 holotype cranidium, 1, dorsal, 2, lateral and 3, anterior views; 4, MGUH39 cranidium, dorsal view; 5, MGUH40 cranidium, dorsal view; 6, MGUH41 cranidium, dorsal view; 7, MGUH42 librigena, dorsal view; 8, MGUH43 hypostome, ventral view; 9, MGUH44 pygidium, dorsal view; 10, MGUH45 pygidium, dorsal view; 11, MGUH46 pygidium, dorsal view; 12–13, MGUH47 pygidium, 12, dorsal and 13, oblique lateral view. All material from GGU 298930 (SNL1).

Figs 14–20. *Jungosulcus ventricosus* gen. et sp. nov. 14, MGUH48 holotype cranidium, dorsal view; 15–17, MGUH49 cranidium, 15, dorsal, 16, anterior and 17, lateral views; 18–19, MGUH50 pygidium, 18, dorsal and 19, lateral views; 20, MGUH51 pygidium, dorsal view. All material from GGU 275038 (VGL1).

All scale bars = 5 mm.

PLATE 4

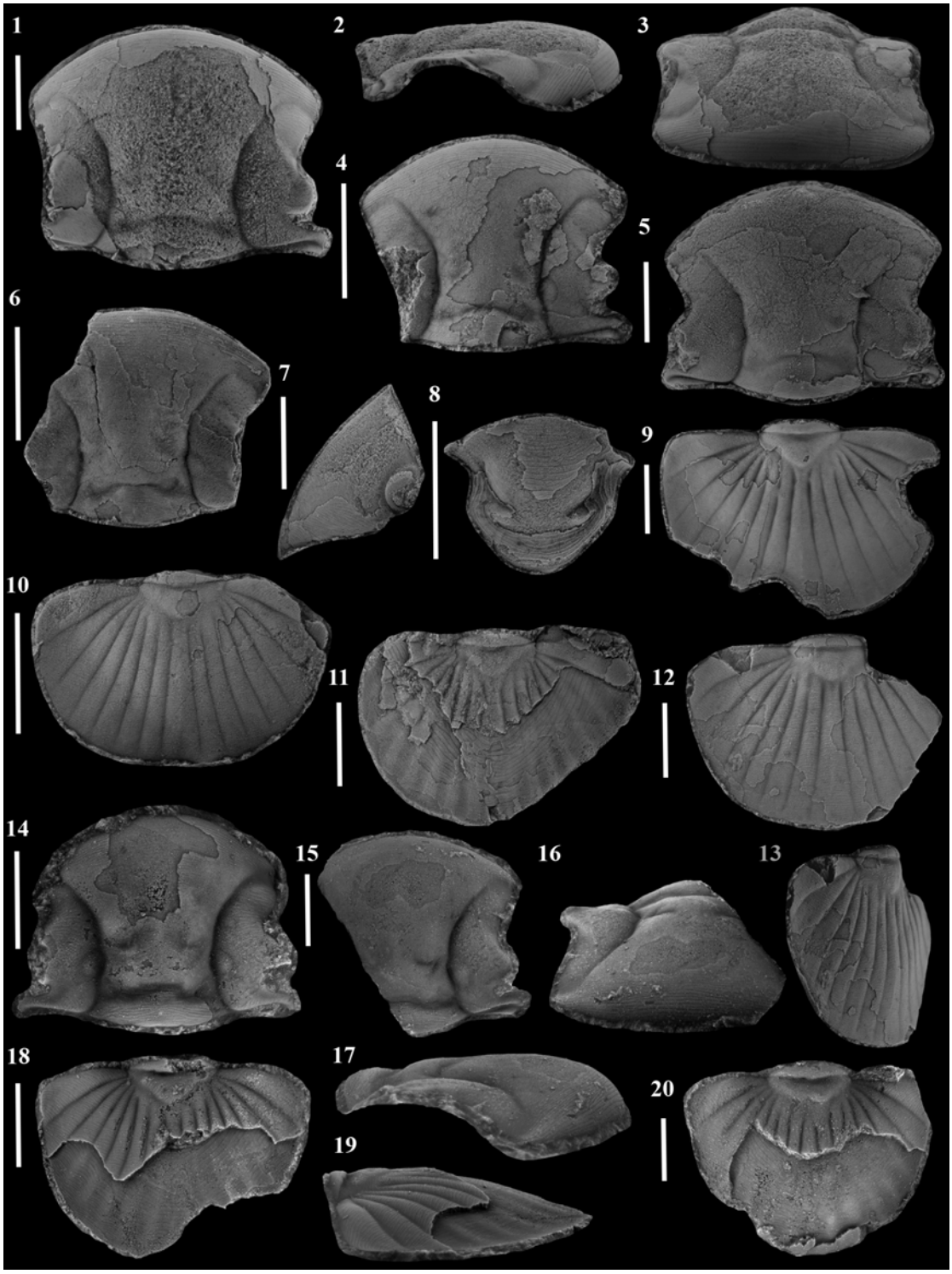

EXPLANATION OF PLATE 5

Fig. 1. *Meroperix ataphrus* Lane 1972, MGUH52 pygidium, dorsal view, GGU 275038 (VGL1)

Figs 2–15. *Opoa limatula* sp. nov. 2–3, MGUH53 holotype cranidium, 2, dorsal and 3, oblique lateral views; 4–5, MGUH54 cranidium, 4, dorsal and 5, lateral views; 6, MGUH55 cephalon, 7–8, MGUH56 cranidium, 7, dorsal and 8, anterior views; 9–10, MGUH57 pygidium, 9, dorsal and 10, oblique lateral views; 11, MGUH58 pygidium, dorsal view;12–13, MGUH59 pygidium, 12, dorsal and 13, lateral views; 14, MGUH60 pygidium, dorsal view; 15, MGUH61 pygidium, dorsal view. All material from GGU 274689 (CPL5).

Figs 16–19. *Opoa* sp.16–17, MGUH62 pygidium, 16, dorsal and 17, lateral views; 18–19, MGUH63 pygidium, 18, dorsal and 19, lateral views. Both pygidia from GGU 275015 (KCL1).

All scale bars = 5 mm.

PLATE 5

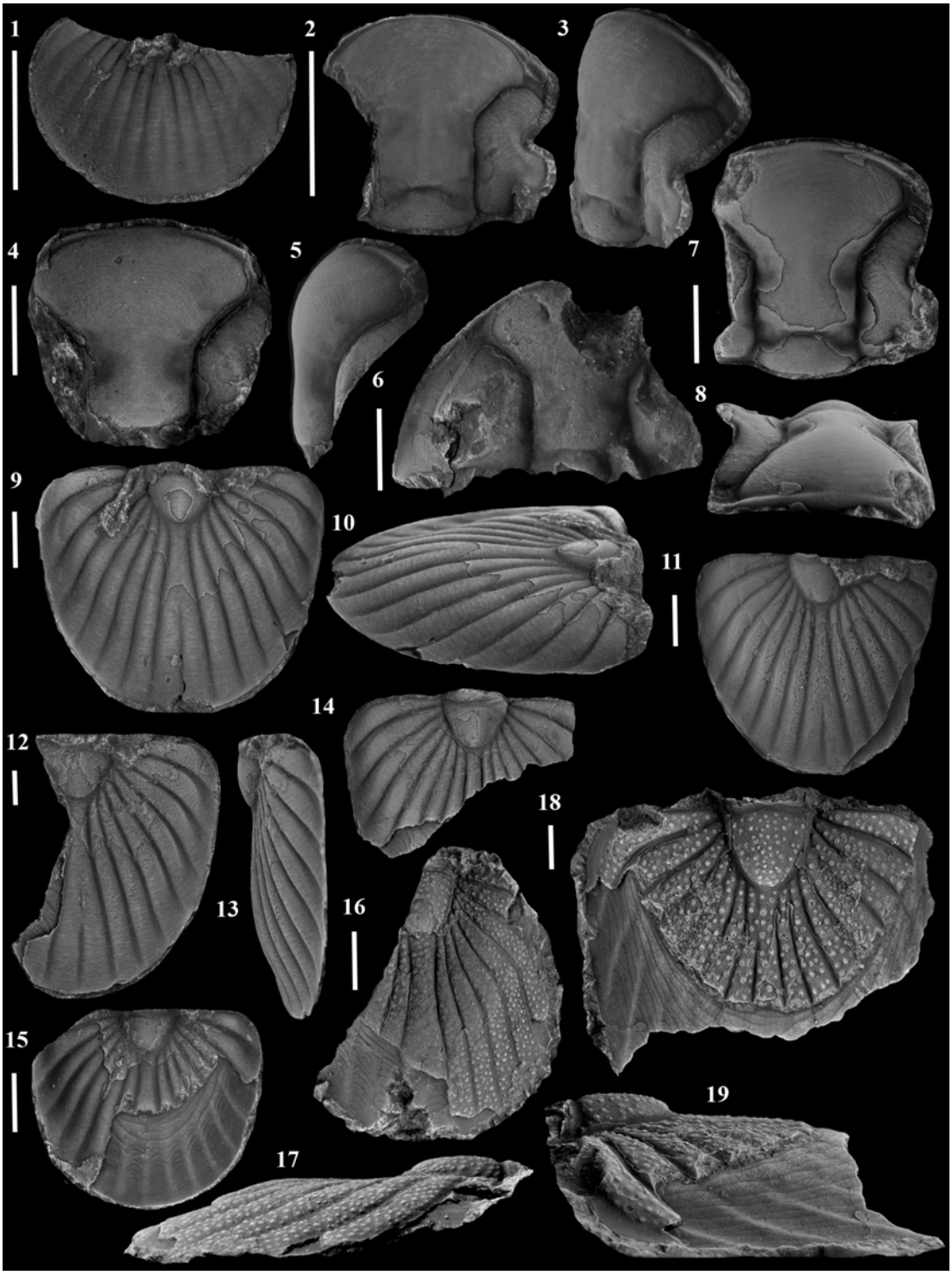

EXPLANATION OF PLATE 6

Figs 1–17. *Periostrix magnifica* (Teichert, 1937), 1–3, MGUH64 cranidium, GGU 198842 (WPL2) 1, dorsal, 2, oblique lateral and 3, anterior views; 4–5, MGUH65 cranidium, GGU 298504 (WL) 4, dorsal and 5, oblique lateral views; 6–7, MGUH66 cranidium, GGU 298504 (WL) 4, dorsal and 5, oblique lateral views; 8, MGUH67 cranidium, GGU 301326 (WPL1) dorsal view; 9, MGUH68 cranidium, GGU 301318 (WPL1) dorsal view; 10–12, MGUH69 cephalon, GGU 298506 (WL) 10, dorsal, 11, anterior and 12, lateral views; 13, MGUH70 rostral plate, GGU 301318 (WPL1) ventral view; 14, MGUH71 librigena doublure, GGU 301318 (WPL1) dorsal view; 15, MGUH72 hypostome, GGU 298506 (WL) ventral view; 16, MGUH 4375 holotype pygidium, St. George Fjord, dorsal view; 17, MGUH 4374 pygidium, Duke of York Bay, northern Southampton Island, dorsal view.

Figs 1–9, 16–17, scale bars = 10 mm; Figs 10–15, scale bars = 5 mm.

PLATE 6

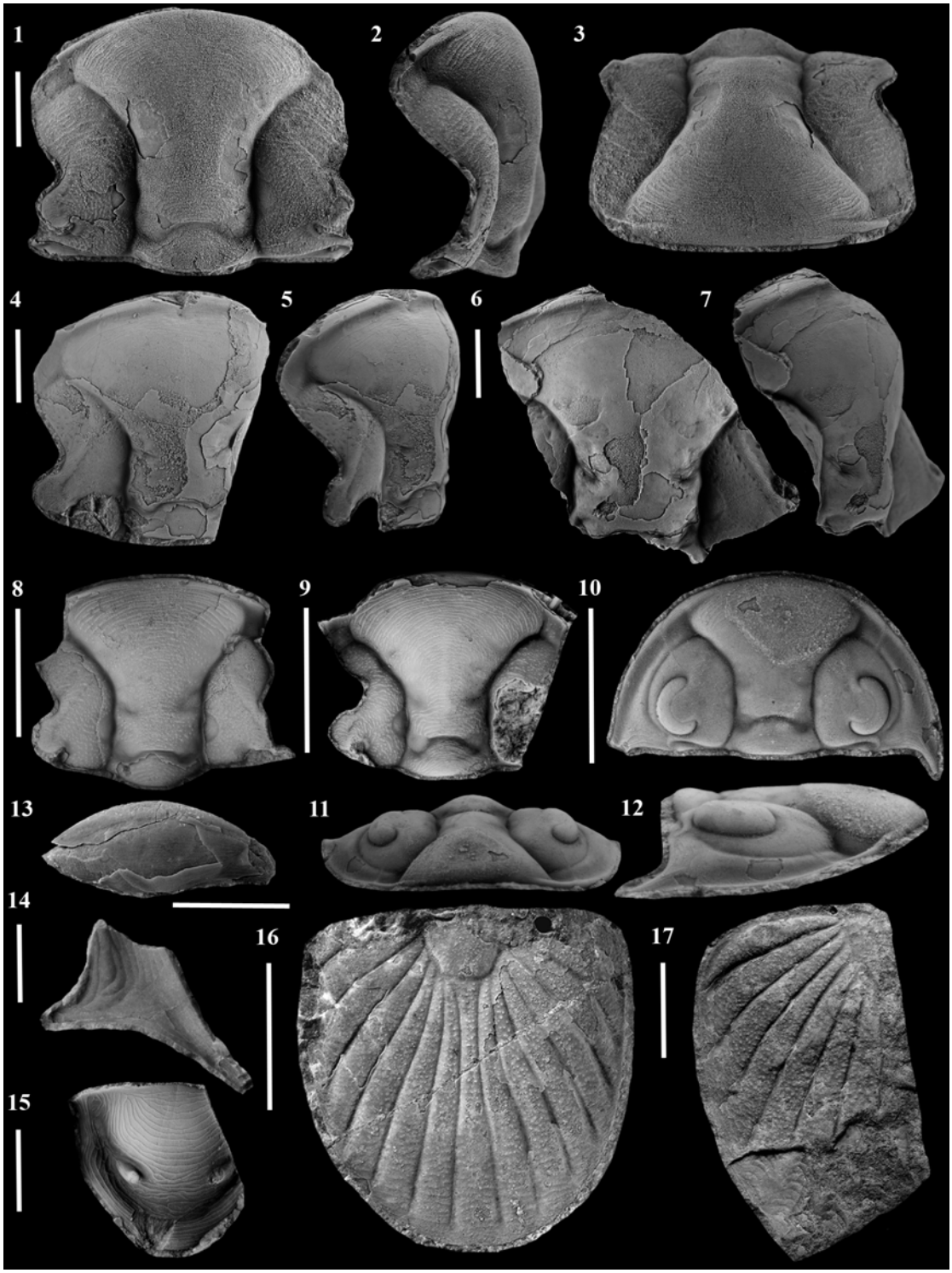

EXPLANATION OF PLATE 7

Figs 1–8. *Periostrix magnifica* (Teichert, 1937), 1–2, MGUH73 pygidium, GGU 301326 (WPL1) 1, dorsal and 2, lateral views; 3, MGUH74 two stacked pygidia, GGU 301318 (WPL1) dorsal view; 4, MGUH75 pygidium, GGU 301318 (WPL1) dorsal view; 5, MGUH76 pygidium, GGU 198834 (WPL2) dorsal view; 6, MGUH77 pygidium (not blackened), GGU 298506 (WL) dorsal view; 7–8, MGUH78 pygidium, GGU 301326 (WPL1) 7, dorsal and 8, lateral views.

Figs 9–14. Genus aff. *Periostrix*, 9–10, MGUH79 cranidium, GGU 225793 (KCL2) 9, dorsal and 10, lateral views; 11, MGUH80 cranidium, GGU 225793 (KCL2) dorsal view; 12, MGUH81 pygidium, GGU 225793 (KCL2) dorsal view; 13–14, MGUH82 pygidium, GGU 225793 (KCL2) 13, dorsal and 14, oblique lateral views.

Figs 15–17. Scutelluid gen. indet. 15, MGUH83 cephalon, GGU 301318 (WPL1) dorsal view; 16, MGUH84 cranidium, GGU 301318 (WPL1) dorsal view; 17, MGUH85 pygidium, GGU 301318 (WPL1) dorsal view.

Figs 1–5, scale bars = 10 mm; Figs 6–17, scale bars = 1 mm.

PLATE 7

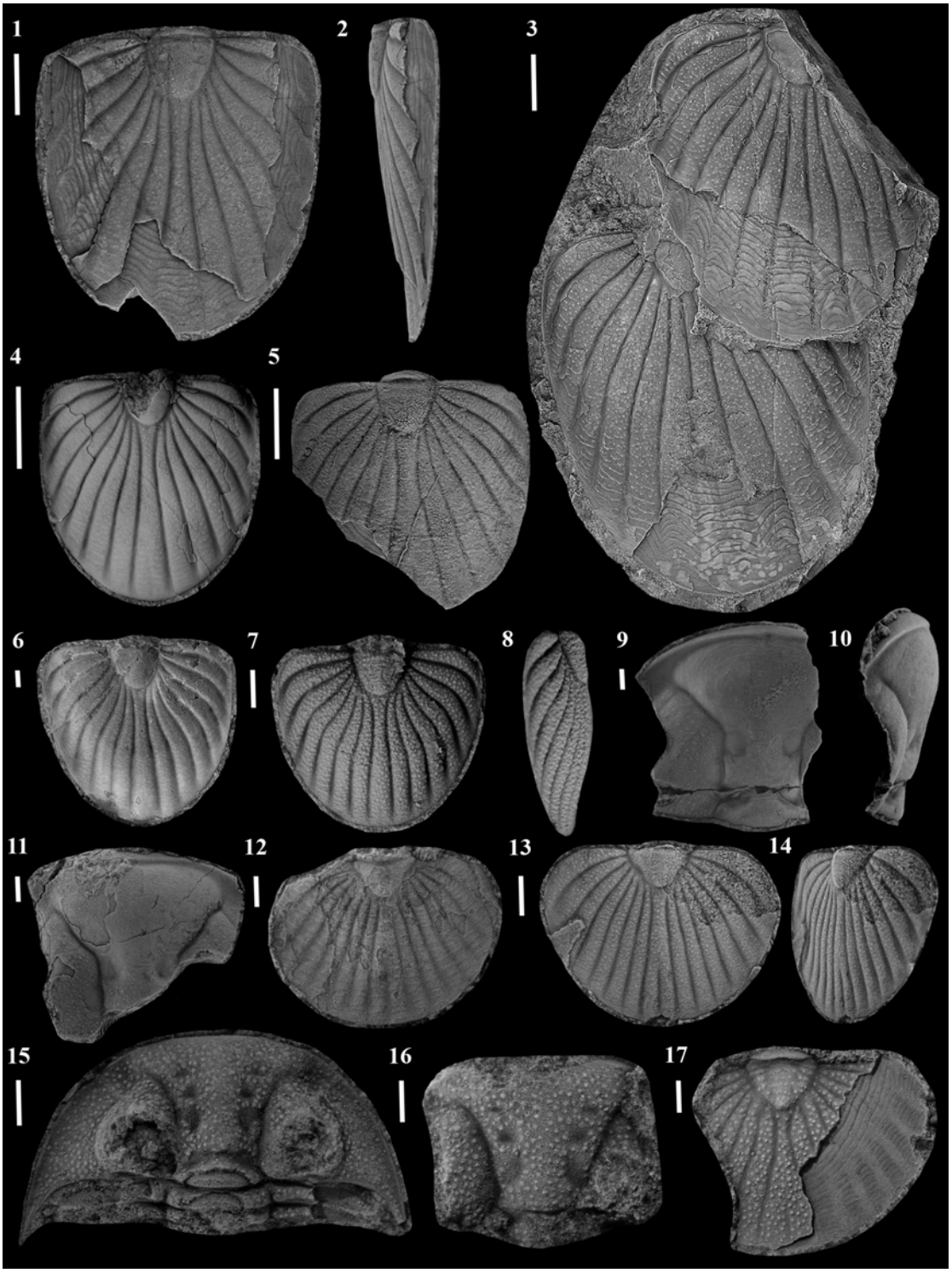

EXPLANATION OF PLATE 8

Figs 1–15. *Cybantyx nebulosus* sp. nov. 1–3, MGUH86 articulated specimen, 1, dorsal view of whole specimen, 2, dorsal view of cephalon, 3, oblique view of whole specimen; 4–5, MGUH87 holotype cephalon, 4, dorsal and 5, lateral views; 6, MGUH88 cephalon, dorsal view (not blackened); 7, MGUH89 cranidium, dorsal view; 8–10, MGUH90 cephalon, 8, dorsal, 9, lateral and 10, anterior views; 11, MGUH91 cephalon, oblique lateral view; 12, MGUH92 cranidium, dorsal view; 13, MGUH93 librigena, dorsal view; 14–15, MGUH94 articulated cephalon and thorax, 14, dorsal and 15, lateral views. All material from GGU 274689 (CPL5).
Figs 1–12, 14–15, scale bars = 10 mm Fig. 13, scale bar = 1 mm.

PLATE 8

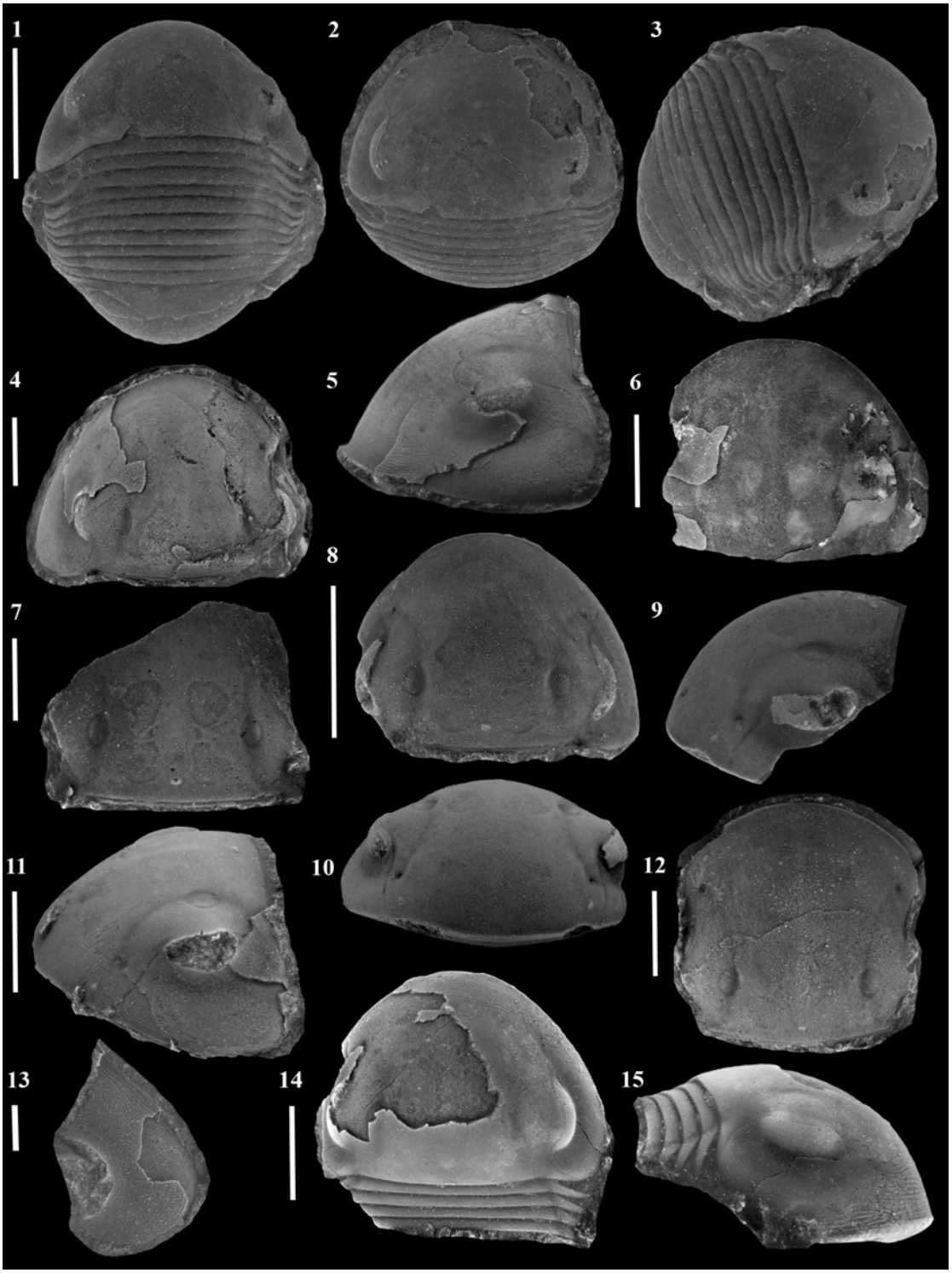

EXPLANATION OF PLATE 9

Figs 1–10. *Cybantyx nebulosus* sp. nov. 1, MGUH95 rostral plate, ventral view; 2, MGUH96 rostral plate, ventral view; 3–4, MGUH97 pygidium, 3, dorsal and 4, lateral views; 5, MGUH98 pygidium, dorsal view; 6–7, MGUH99 pygidium, 6, dorsal and 7, lateral views; 8, MGUH100 pygidium, dorsal view; 9–10, MGUH101 pygidium, 3, dorsal and 4, oblique lateral views. All material from GGU 274689 (CPL5).

Figs 11–16. *Cybantyx* sp. 11–12, MGUH102 cranidium, GGU 301319 (WPL1), 11, dorsal and 12, oblique lateral views; 13, MGUH103 cranidium, GGU 301319 (WPL1), dorsal view; 14, MGUH104 librigena, GGU 301318 (WPL1) dorsal view; 15, MGUH105 pygidium, GGU 301318 (WPL1) dorsal view (not blackened); 16, MGUH106 pygidium, GGU 301319 (WPL1) dorsal view.

Figs 1–2, scale bars = 1 mm Figs 3–16, scale bars = 10 mm.

PLATE 9

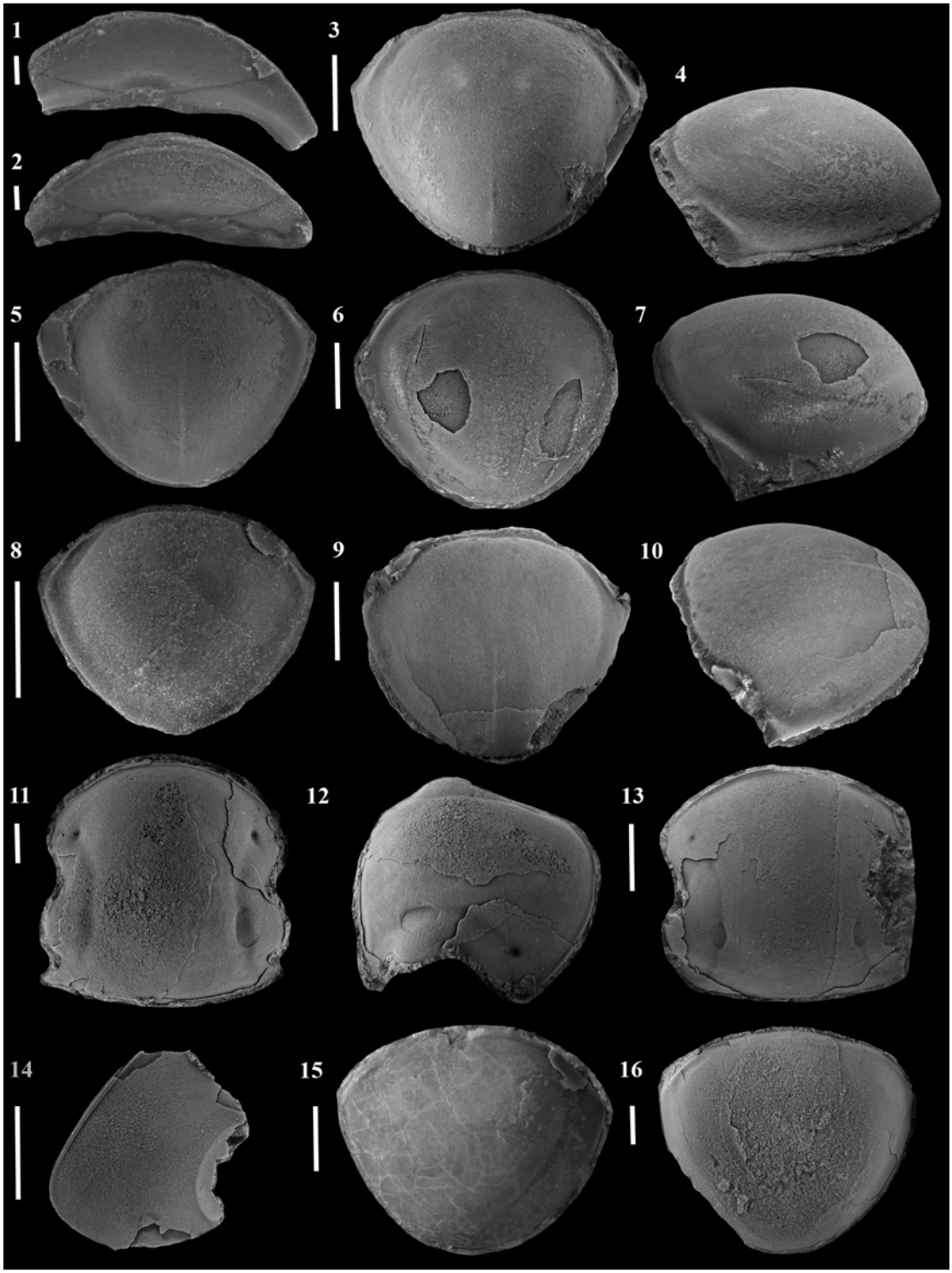

EXPLANATION OF PLATE 10

Figs 1–16. *Lanebestix enalios* gen. et sp. nov. 1–4, MGUH107 holotpe cephalon, 1, dorsal, 2, oblique lateral, 3, anterior and 4, lateral views; 5, MGUH108 cephalon, dorsal view; 6, MGUH109 cephalon, dorsal view; 7–9, MGUH110 cephalon, 7, dorsal view, 8, ventral view of rostral plate and 9, oblique lateral view; 10–11, MGUH111 pygidium, 10, dorsal and 11, oblique lateral views; 12–13, MGUH112 pygidium, 12, dorsal and 13, lateral views; 14, MGUH113 pygidium, dorsal view; 15–16, MGUH114 pygidium, 15, dorsal and 16, lateral views. All material from GGU 275038 (VGL1).

Figs 1–7, 9–16, scale bars = 10 mm Fig. 8, scale bar = 1 mm.

PLATE 10

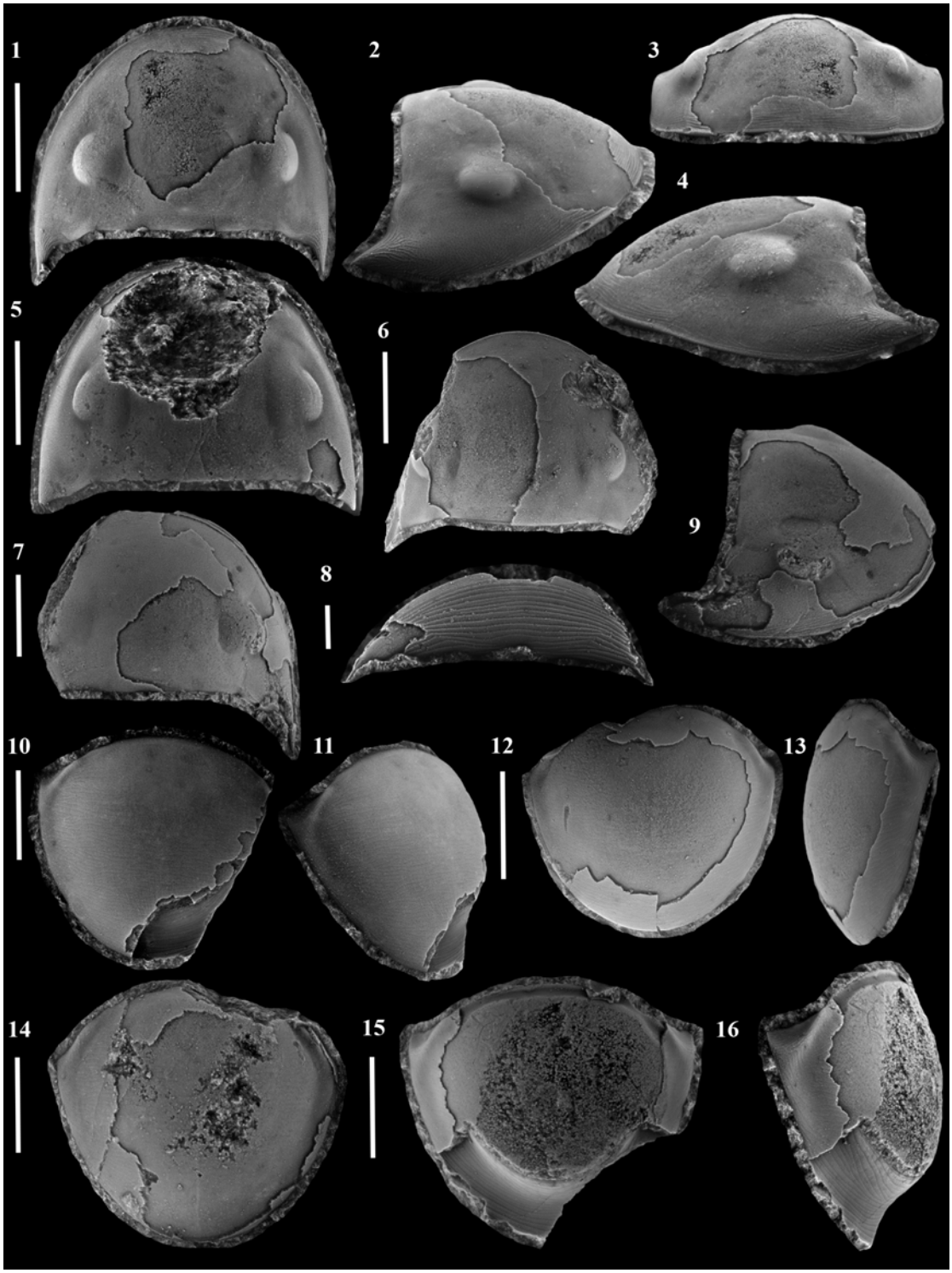

EXPLANATION OF PLATE 11

Figs 1–22. *Ligiscus diana* sp. nov. 1–2, MGUH115 holotype cephalon, GGU 275044 (VGL2) 1, dorsal and 2, lateral views; 3, MGUH116 cephalon, GGU 275044 (VGL2) dorsal view; 4–5, MGUH117 cephalon, GGU 275038 (VGL1) 4, dorsal and 5, oblique lateral views; 6–7, MGUH118 cranidium, GGU 275038 (VGL1) 6, dorsal and 7, oblique lateral views; 8–10, MGUH119 cranidium, GGU 275044 (VGL2) 8, dorsal, 9, anterior and 10, lateral views; 11, MGUH120 cranidium, GGU 275038 (VGL1) dorsal view; 12, MGUH121 cranidium, GGU 275044 (VGL2) dorsal view; 13, MGUH122 librigena, GGU 275044 (VGL2) dorsal view; 14, MGUH123 hypostome, GGU 275044 (VGL2) ventral view; 15–16, MGUH124 pygidium, GGU 275044 (VGL2) 15, dorsal and 16, lateral views; 17–18, MGUH125 pygidium, GGU 275038 (VGL1)17, dorsal and 18, oblique lateral views; 19, MGUH126 pygidium, GGU 275038 (VGL1) dorsal view; 20, MGUH127 pygidium, GGU 275038 (VGL1) dorsal view; 21, MGUH128 pygidium, GGU 275044 (VGL2) dorsal view; 22, MGUH129 pygidium, GGU 275044 (VGL2) dorsal view.

All scale bars = 1 mm.

PLATE 11

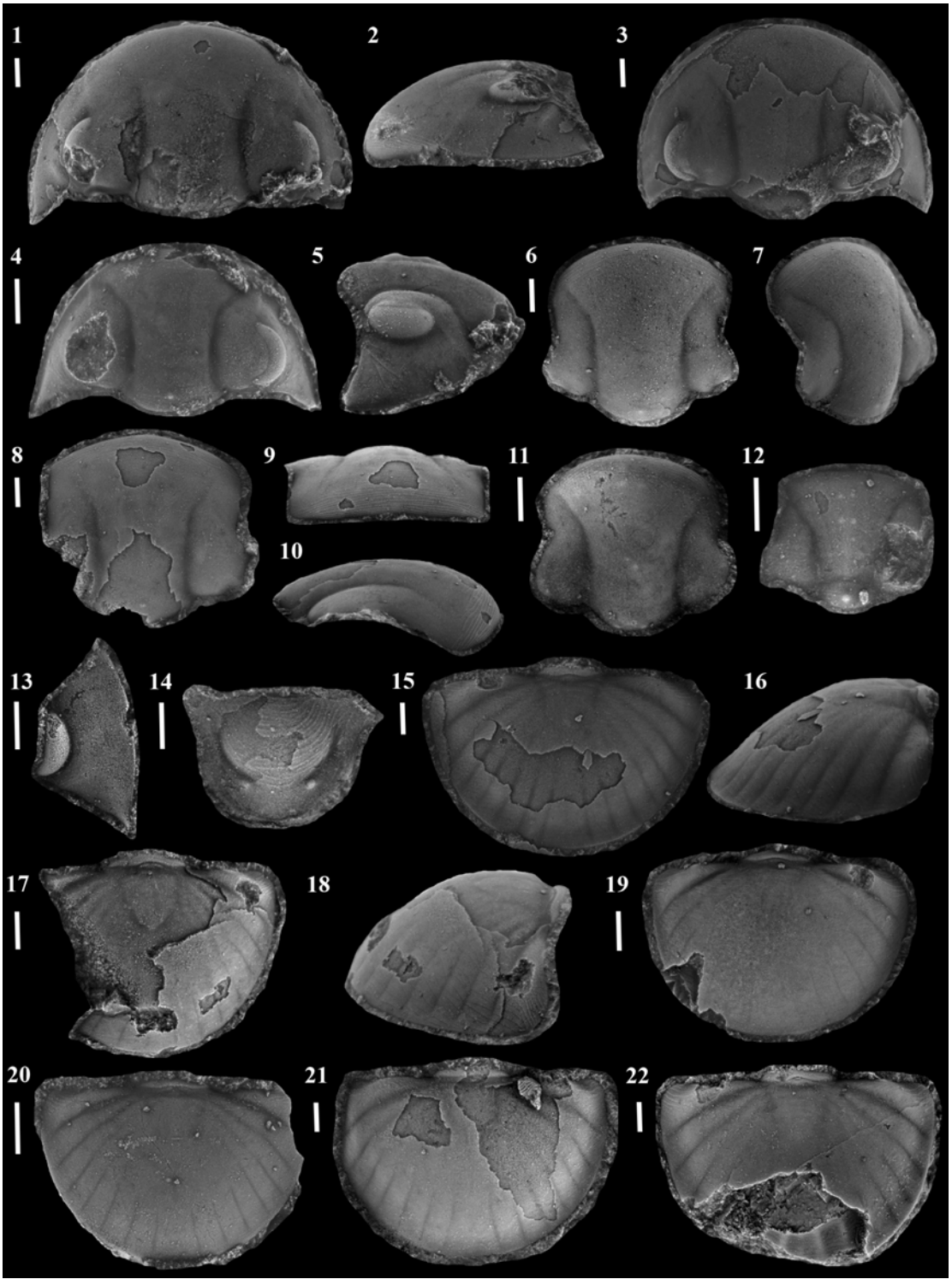

EXPLANATION OF PLATE 12

Figs 1–9. *Liolalax naresi* sp. nov. 1–3, MGUH130 holotype cranidium, 1, dorsal, 2, anterior and 3, lateral views; 4, MGUH131 cranidium, dorsal view; 5, MGUH132 rostral plate, ventral view; 6, MGUH133 pygidium, dorsal view; 7–8, MGUH134 pygidium, 7, dorsal and 8, oblique lateral views; 9, MGUH135 pygidium, dorsal view. All material from GGU 298930 (SNL1).

Figs 10–12. *Liolalax*? sp. 10–12, MGUH136 cephalon, GGU 275015 (KCL1) 10, dorsal, 11, lateral and 12, anterior views.

Figs 13–15. *Stenopareia persica* sp. nov. 13–15, MGUH137 holotype cranidium, GGU 275049 (VGL3) 13, dorsal, 14, lateral and 15, anterior views.

Figs 1–4, 6–15 scale bars = 5 mm; Fig. 5, scale bar = 1 mm.

PLATE 12

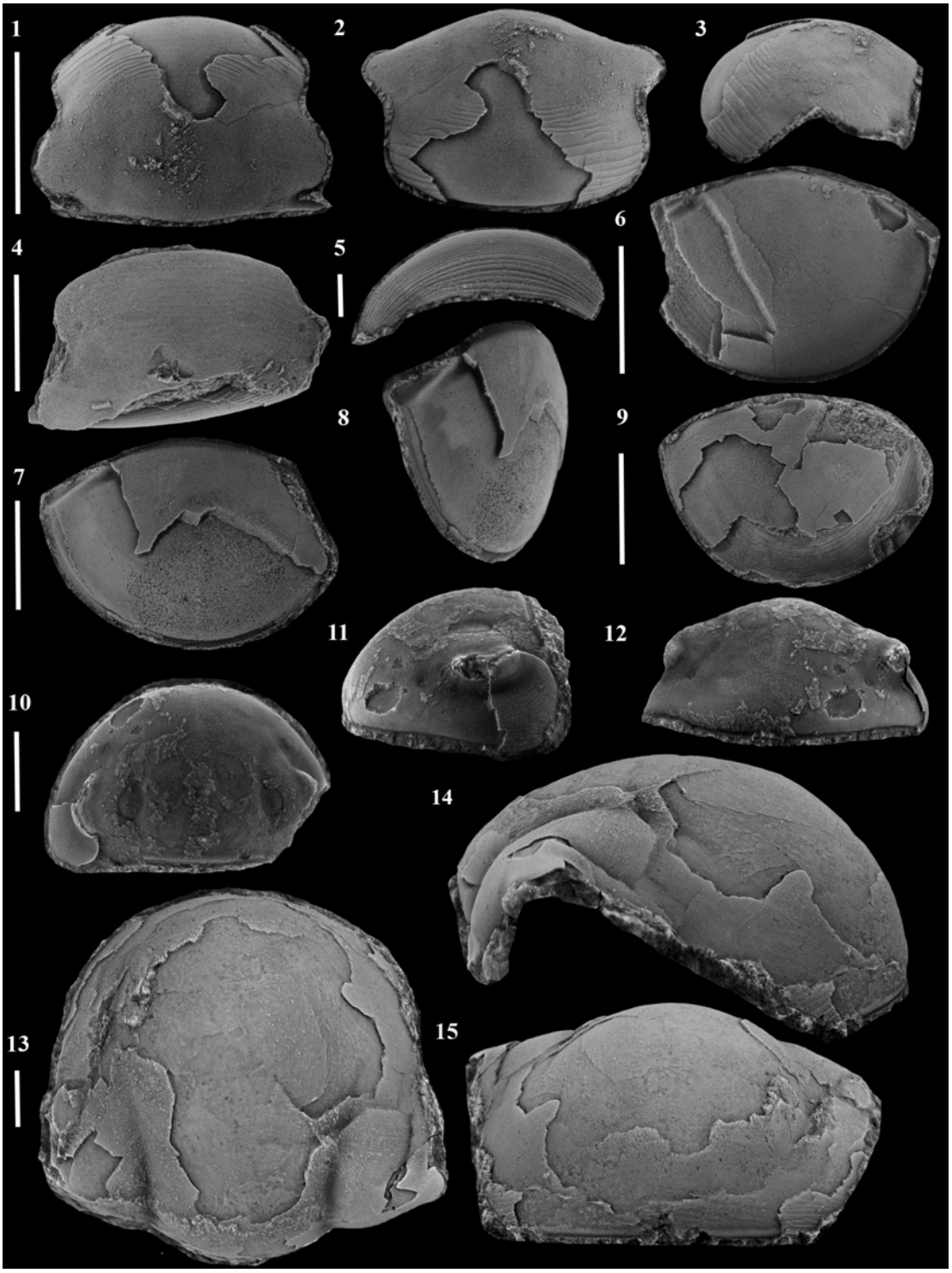

EXPLANATION OF PLATE 13

Figs 1–13. *Stenopareia persica* sp. nov. 1–2, MGUH138 cranidium, GGU 274689 (CPL5) 1, dorsal and 2, lateral views; 3, MGUH139 cranidium, GGU 274689 (CPL5) dorsal view; 4, MGUH140 librigena, GGU 274689 (CPL5) dorsal view; 5–6, MGUH141 librigena, GGU 274689 (CPL5) 5, dorsal and 6, ventral views; 7, MGUH142 rostral plate, GGU 274689 (CPL5) ventral view; 8–9, MGUH143 pygidium, GGU 275038 (VGL1) 8, dorsal and 9, ventral views; 10–11, MGUH144 pygidium, GGU 198136 (CPL2) 10, dorsal and 11, oblique lateral views; 12–13, MGUH145 pygidium, GGU 274689 (CPL5) 12, dorsal and 13, lateral views.
Figs 1–11 scale bars = 10 mm; Figs 12–13, scale bar = 5 mm.

PLATE 13

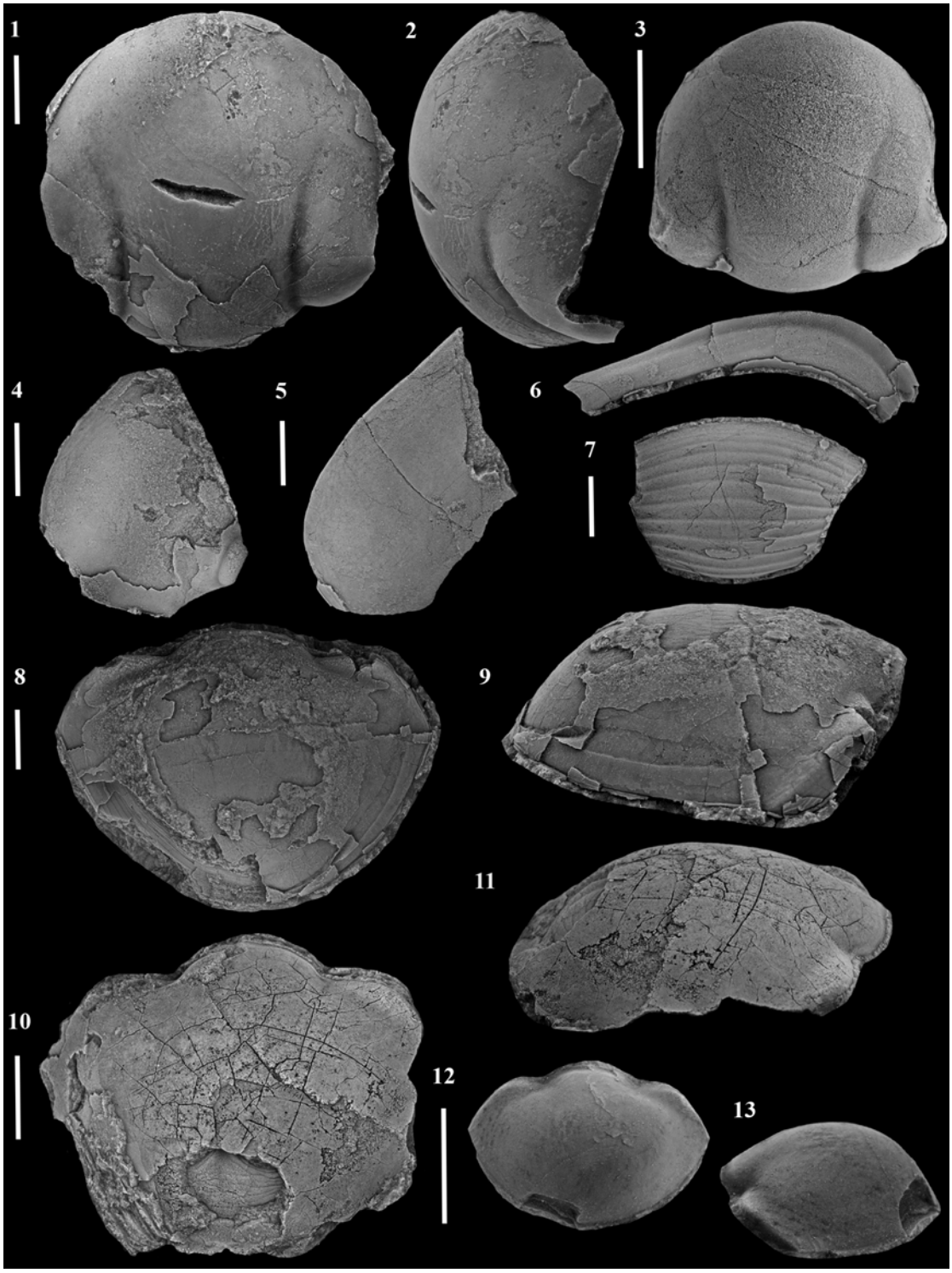

EXPLANATION OF PLATE 14

Figs 1–3. *Stenopareia* cf. *grandis* (Billings, 1859). 1–2, MGUH146 cephalon, GGU 298506 (WL) 1, dorsal and 2, lateral views; 3, MGUH147 pygidium, GGU 301318 (WPL1) dorsal view.

Figs 4–8. *Stenopareia* sp. 4–5, MGUH148 cranidium, 4, dorsal and 5, oblique lateral views; 6–7, MGUH149 pygidium, 6, dorsal and 7, lateral views; 8, MGUH150, pygidium, dorsal view. All material from GGU 275049 (VGL3).

Figs 9–15. *Proetus*? *confluens* sp. nov. 9–11, MGUH151, holotype cephalon, 9, dorsal, 10, oblique lateral and 11, anterior views; 12–13, MGUH152 cephalon, 12, dorsal and 13, lateral views; 14, MGUH153 cranidium, dorsal view; 15, MGUH154 cranidium, dorsal view. All material from GGU 198225 (CPL3).

Figs 1–8 scale bars = 5 mm; Figs 9–15, scale bars = 1 mm.

PLATE 14

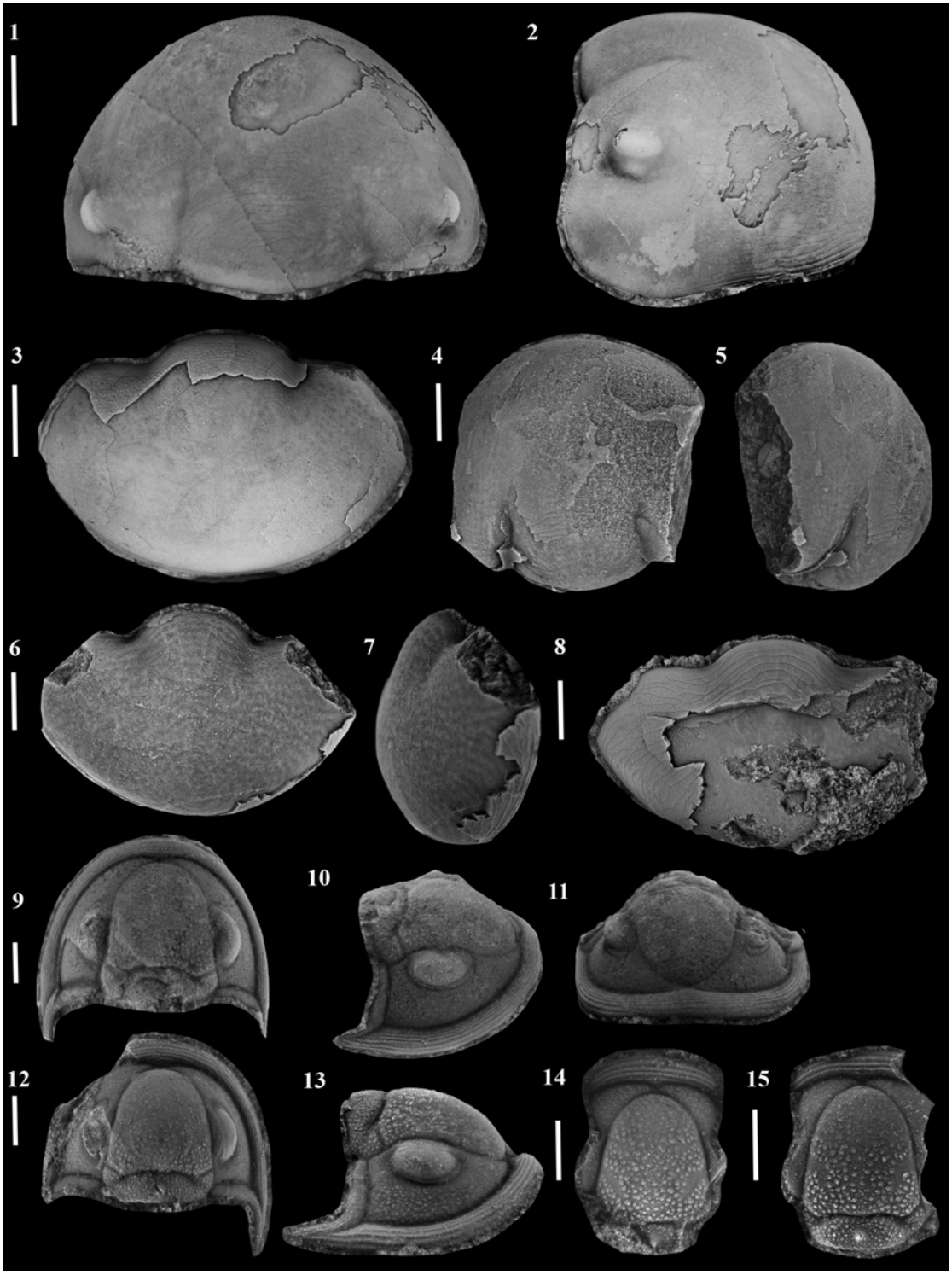

EXPLANATION OF PLATE 15

Figs 1–3. *Proetus*? *confluens* sp. nov. 1–2, MGUH155 articulated pygidium and thorax, 1, dorsal and 2, oblique lateral views. 3, MGUH156 articulated cephalon and thorax, dorsal view. Both specimens from GGU 198225 (CPL3).

Figs 4–8. *Airophrys balios* gen. et sp. nov. 4–6, MGUH157 holotype cranidium, 4, dorsal, 5, oblique lateral and6, anterior views; 7–8, MGUH158 pygidium, 7, dorsal and 8, oblique lateral views. Both specimens from GGU 275038 (VGL1).

Figs 9–13. *Airophrys* sp. 9, MGUH159 cranidium, GGU 198115 (CPL1), dorsal view; 10, MGUH160 cranidium, dorsal view; 11, MGUH161 librigena, dorsal view; 12, MGUH162 librigena, dorsal view; 13, MGUH163 cephalon, dorsal view. All material from GGU 198226 (CPL1).

Figs 14–18. *Cyphoproetus peeli* sp. nov. 14–15, MGUH164 holotype cranidium, GGU 274689 (CPL5), 14, dorsal and 15, lateral views; 16, MGUH165 cranidium, GGU 274689 (CPL5) dorsal view; 17, MGUH166 cranidium, GGU 198219 (CPL2) dorsal view; 18, MGUH167 cranidium, GGU 274689 (CPL5) dorsal view.

Fig. 19. *Cyphoproetus* sp. MGUH168 cranidium, GGU 298924 (SNL2) dorsal view.

All scale bars = 1 mm.

PLATE 15

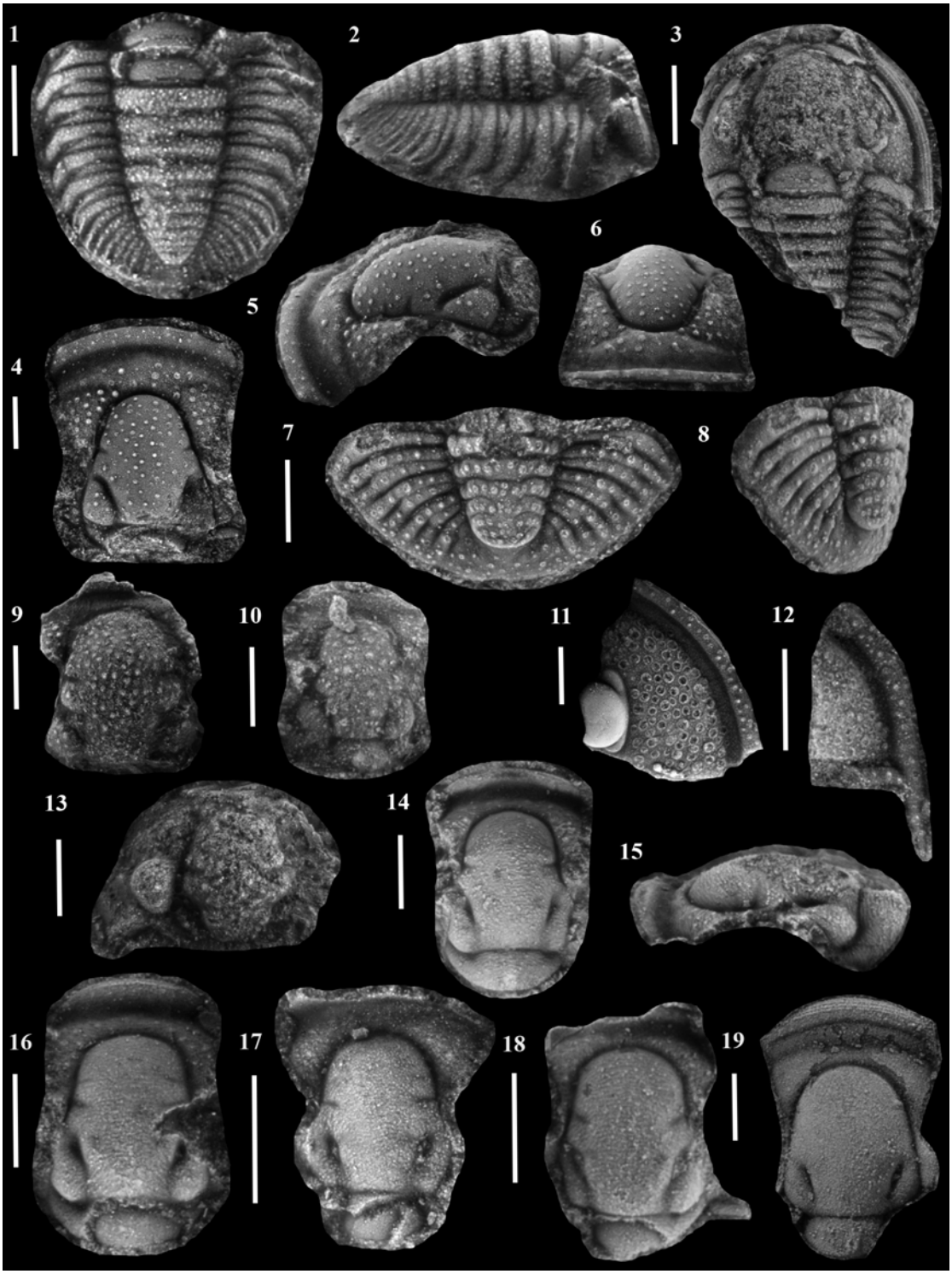

EXPLANATION OF PLATE 16

Figs 1–15. *Owensus arktoperates* gen. et sp. nov. 1–2, MGUH169 holotype articulated specimen, GGU 274689 (CPL5) 1, dorsal and 2, lateral views; 3–5, MGUH170 cephalon, GGU 274689 (CPL5) 3, dorsal, 4, anterior and 5, lateral views; 6, MGUH171 articulated cephalon and thorax, GGU 274689 (CPL5) dorsal view; 7, MGUH172 cranidium, GGU 274654 (CPL4) dorsal view; 8–9, MGUH173 cranidium, GGU 198225 (CPL3) 8, dorsal and 9, lateral views; 10, MGUH174 cephalon, GGU 198188 (CPL2) lateral view; 11, MGUH175 librigena, GGU 274689 (CPL5) dorsal view; 12–13, MGUH176 articulated pygidium and thorax, GGU 274689 (CPL5) 12, dorsal and 13, lateral views; 14–15, MGUH177 articulated pygidium and thorax, GGU 274689 (CPL5) 14, dorsal and 15, oblique lateral views. All scale bars = 1 mm.

PLATE 16

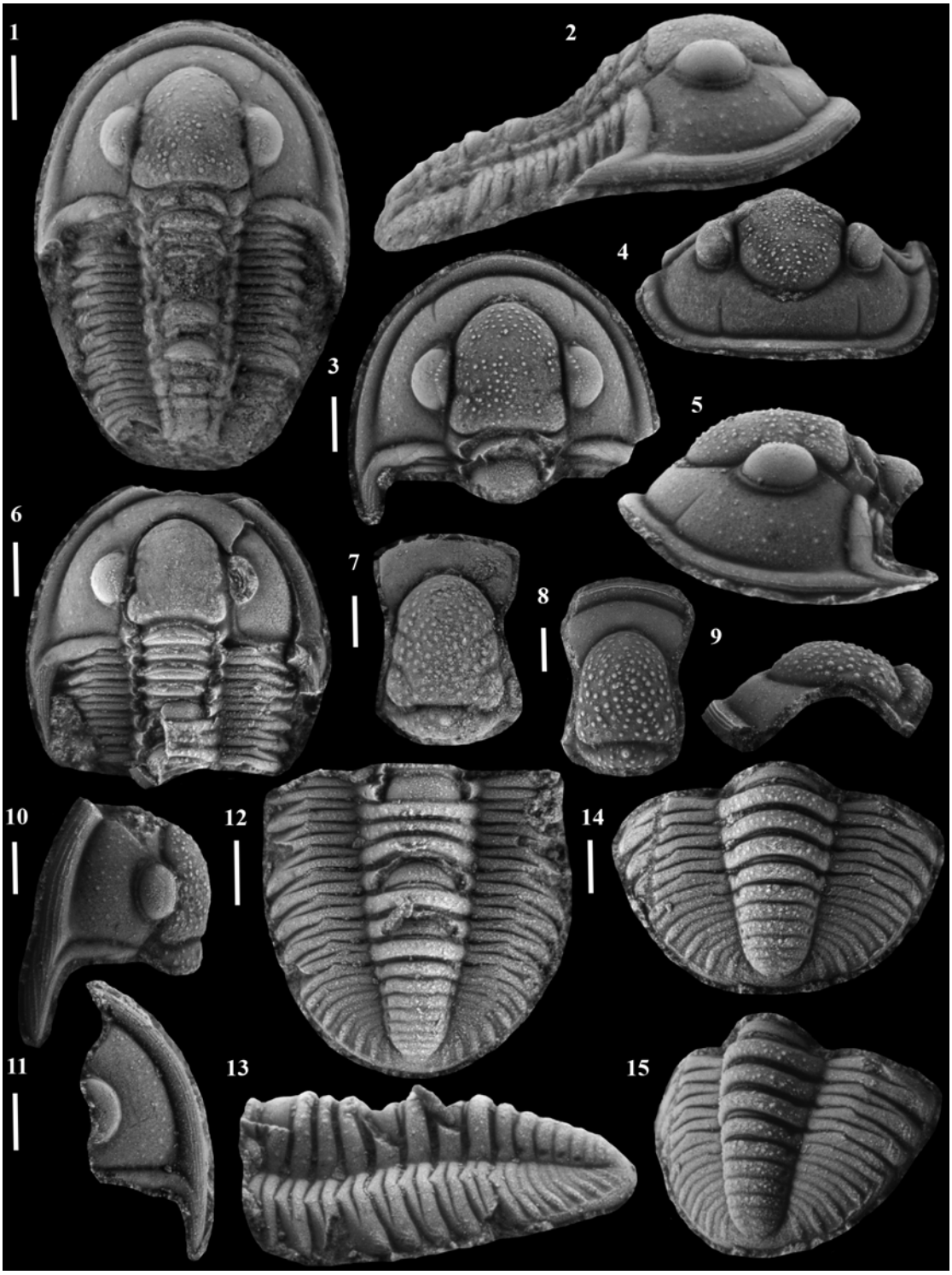

EXPLANATION OF PLATE 17

Figs 1–9 *Astroproetus franklini* sp. nov. 1–2, MGUH178 holotype cephalon, GGU 198226 (CPL1) 1, dorsal and 2, oblique lateral views; 3, MGUH179 cranidium, GGU 274645 (CPL2) dorsal view; 4–5, MGUH180 cephalon, GGU 274645 (CPL2) 4, dorsal and 5, oblique lateral views; 6–7, MGUH181 cephalon, GGU 275038 (VGL1) 6, dorsal and 7, anterior views; 8, MGUH182 librigena, GGU 198226 (CPL1) dorsal view; 9, MGUH183 cranidium, GGU 198226 (CPL1) dorsal view.

Figs 10–12 *Astroproetus* sp. MGUH184 cephalon, GGU 274996 (KCL4) 10, dorsal, 11, anterior and 12, oblique lateral views.

Figs 13–16 *Thebanaspis* sp. 13–14, MGUH185 cranidium, GGU 301326 (WPL1) 13, dorsal and 14, anterior views. 15–16, MGUH186 cranidium, GGU 298506 (WL) 15, dorsal and 16, oblique lateral views.

All scale bars = 1 mm.

PLATE 17

EXPLANATION OF PLATE 18

Figs 1–9. *Winiskia eruga* sp. nov. 1–2, MGUH187 holotype cranidium, GGU 274654 (CPL4) 1, dorsal and 2, oblique lateral views; 3, MGUH188 librigena, GGU 198225 (CPL3); 4–5, MGUH189 thoracic segment, GGU 198225 (CPL3); 6, MGUH190 librigena, GGU 275021 (KCL3); 7, MGUH191 articulated pygidium and partial thorax, GGU 198225 (CPL3) dorsal view; 8–9, MGUH192 pygidium, GGU 198225 (CPL3) 8, dorsal and 9, oblique lateral views.

Figs 10–16. *Winiskia leptomedia* sp. nov. 10–11, MGUH193 holotype cranidium, 10, dorsal and 11, oblique lateral views; 12–13, MGUH194 cranidium, 12, dorsal and 13, lateral views; 14–15, MGUH195 pygidium, 14, dorsal and 15, oblique lateral views; 16, MGUH196 pygidium, dorsal view. All material from GGU 275015 (KCL1).

Figs 17–20. *Winiskia lipopyga* sp. nov. 17–18, MGUH197 holotype pygidium, GGU 274689 (CPL5) 17, dorsal and 18, lateral views; 19, MGUH198 pygidium, GGU 274689 (CPL5) dorsal view; 20, MGUH199 pygidium, GGU 274654 (CPL4) dorsal view.

All scale bars = 5 mm.

PLATE 18

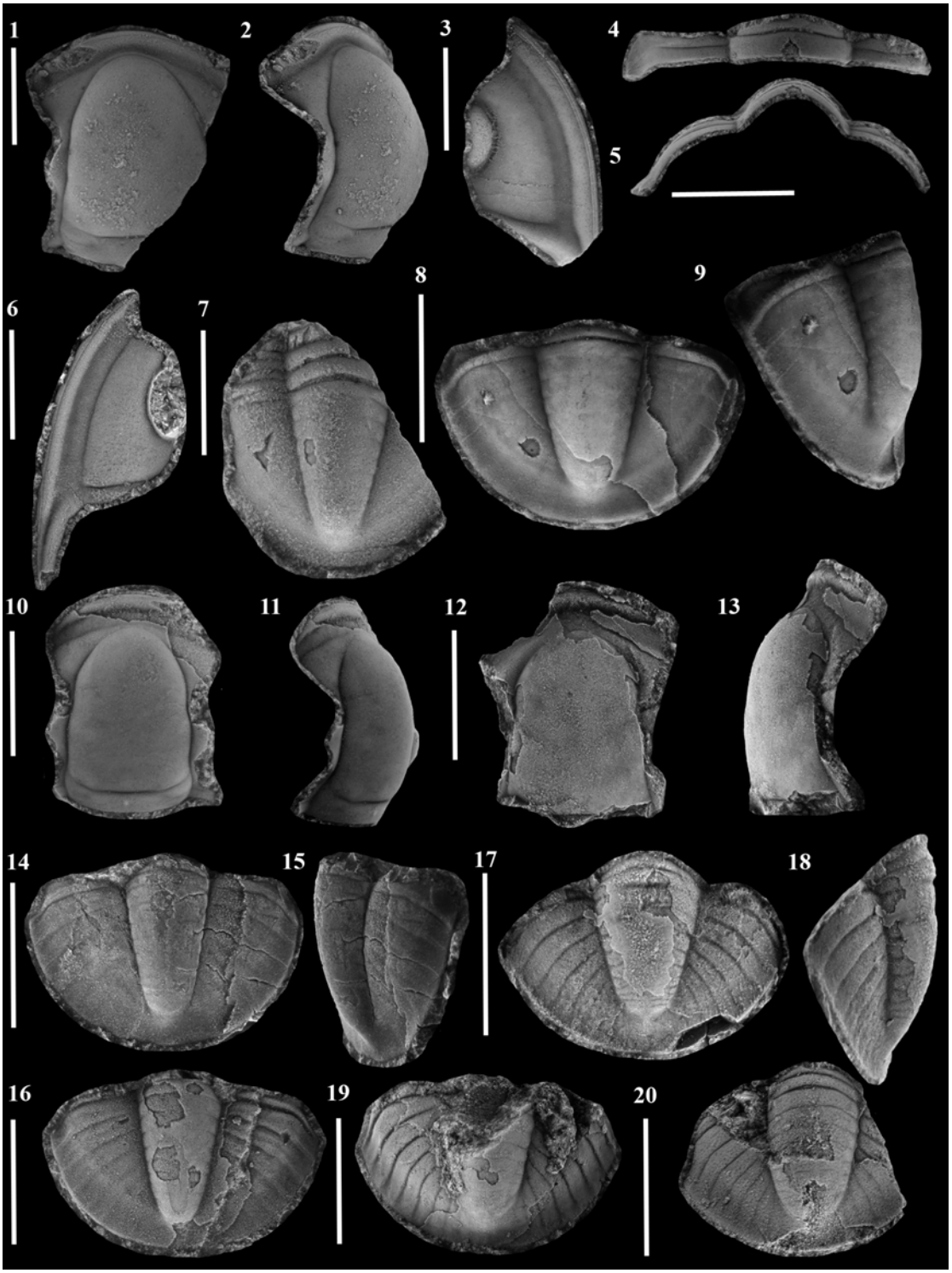

EXPLANATION OF PLATE 19

Figs 1–11. *Winiskia stickta* sp. nov. 1–2, MGUH200 holotype cranidium, GGU 198214 (CPL2) 1, dorsal and 2, lateral views; 3, MGUH201 cranidium, GGU 198200 (CPL2) dorsal view; 4, MGUH202 librigena, GGU 198200 (CPL2) dorsal view; 5–6, MGUH203 hypostome, GGU 198193 (CPL2) 5, dorsal and 6, oblique lateral views; 7–8, MGUH204 pygidium, GGU 198200 (CPL2) 7, dorsal and 8, oblique lateral views; 9, MGUH205 pygidium, GGU 198200 (CPL2) dorsal view; 10, MGUH206 pygidium, GGU 198213 (CPL2) dorsal view; 11, MGUH207 pygidium, GGU198200 (CPL2) dorsal view.

Figs 12–17. *Dalarnepeltis brevifrons* sp. nov. 12–13, MGUH208 holotype cephalon with two articulated thoracic segments, GGU 274654 (CPL4) 12, dorsal and 13, lateral views; 14, MGUH209 pygidium, GGU 198226 (CPL1) dorsal view; 15–16, MGUH210 pygidium, GGU 198226 (CPL1) 15, dorsal and 16, lateral views; 17, MGUH211 pygidium, 274654 (CPL4) dorsal view.

All scale bars = 1 mm.

PLATE 19

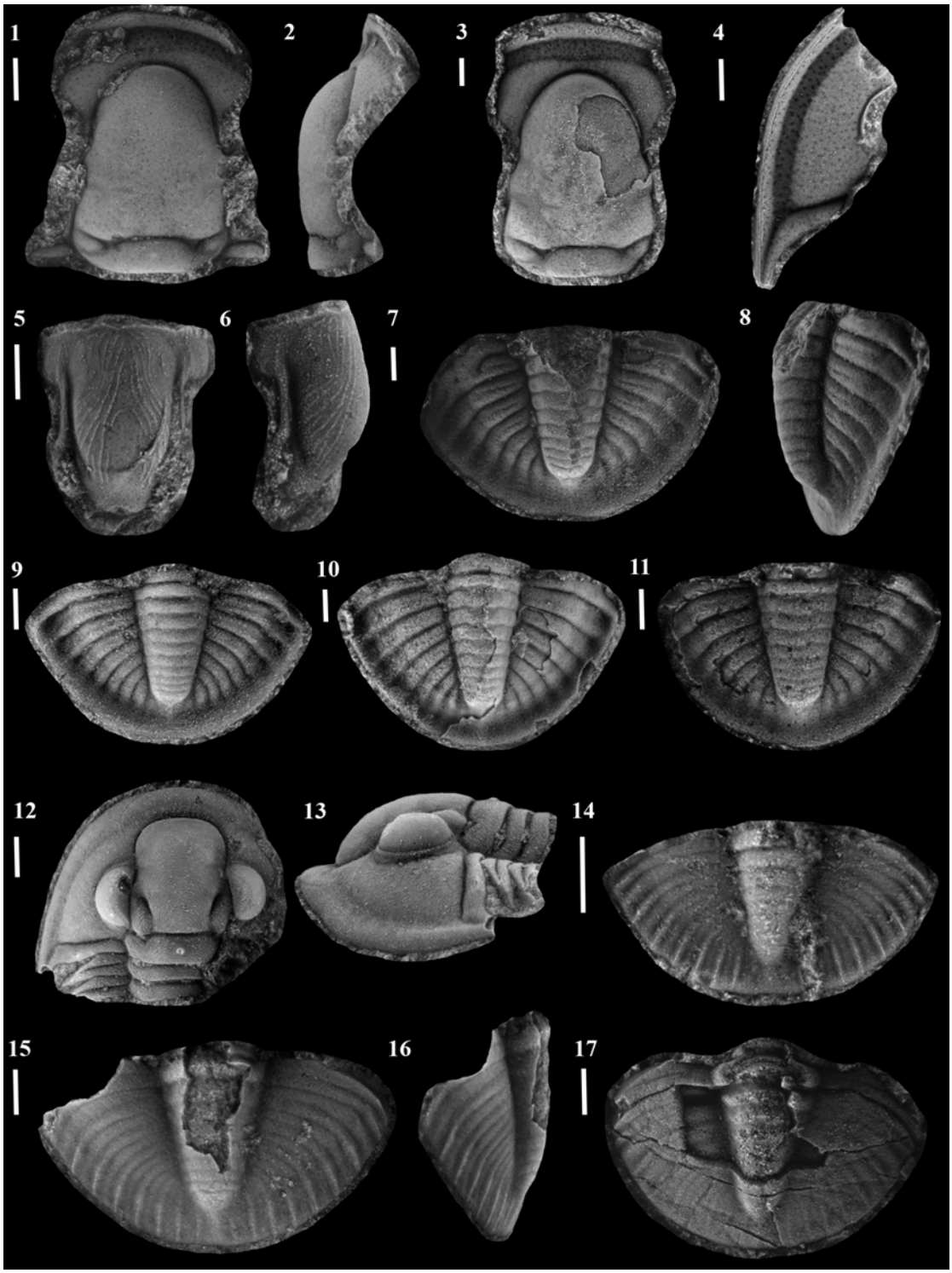

EXPLANATION OF PLATE 20

Figs 1–3.Tropidocoryphine gen. et sp. indet. 1–2, MGUH212 pygidium, GGU 198186 (CPL2) 1, dorsal and 2, oblique lateral views; 3, MGUH213 pygidium, GGU 198201 (CPL2) dorsal view.

Fig. 4. Aulacopleurid cf. *Songkania* Chang, 1974. MGUH214 cephalon, GGU 275038 (VGL1) dorsal view.

Figs 5–7. *Scharyia lobarga* sp. nov. 5–6, MGUH215 holotype pygidium, 5, dorsal and 6, oblique lateral views; 7, MGUH216 pygidium. Both pygidia from GGU 198226 (CPL1).

Figs 8–10. *Scharyia deiropede* sp. nov. 8–9, MGUH217 holotype pygidium, 8, dorsal and 9, lateral views; 10, MGUH218 pygidium, dorsal view. Both pygidia from GGU 198226 (CPL1).

Figs 11–13. *Scharyia unicorna* sp. nov. 11, MGUH219 pygidium, dorsal view; 12–13, MGUH220 holotype pygidium, 12, dorsal and 13, oblique lateral views. Both pygidia from GGU 198226 (CPL1).

Fig. 14. *Radnoria* cf. *Radnoria triquetra* Owens and Thomas, 1975. MGUH221 cranidium, GGU 275038 (VGL1) dorsal view.

Figs 15–17. *Scotoharpes loma* (Lane, 1972). 15–16, MGUH222 cranidium, 15, dorsal and 16, lateral views; 17, MGUH223 cranidium, dorsal view. Both cranidia from GGU 275015 (KCL1).

Figs 1–14, scale bars = 1 mm; Figs 15–17, scale bars = 10 mm.

PLATE 20

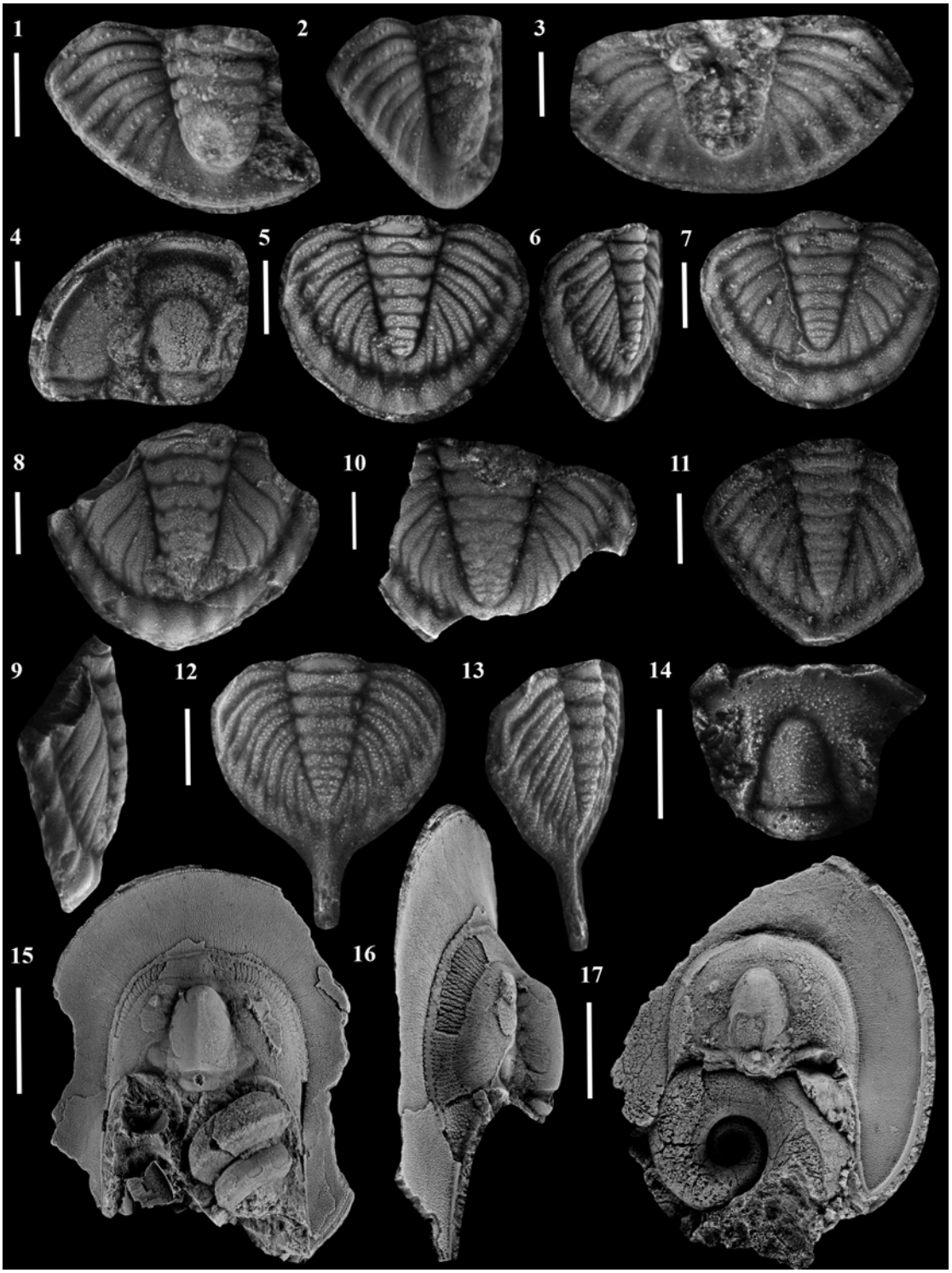

EXPLANATION OF PLATE 21

Figs 1–18. *Cheirurus falcatus* sp. nov. 1–3, MGUH224 cranidium, GGU 198194 (CPL2) 1, dorsal, 2, anterior and 3, lateral views; 4–5, MGUH225 cranidium, GGU 198186 (CPL2) 4, dorsal and 5, lateral views; 6, MGUH226 cephalon, GGU 274774 (KCL5) dorsal view; 7, MGUH227 cranidium, GGU 274689 (CPL5) dorsal view; 8, MGUH228 glabella, GGU 274689 (CPL5) dorsal view; 9–11, MGUH229 cephalon, GGU 274774 (KCL5) 9, dorsal, 10, anterior and 11, oblique lateral views; 12–14, MGUH230 hypostome, GGU 198198 (CPL2) 12, dorsal, 13, lateral and 14, anterior views; 15, MGUH231 hypostome, GGU 274689 (CPL5) dorsal view; 16, MGUH232 hypostome, GGU 274689 (CPL5) dorsal view; 17, MGUH233 thoracic segment, GGU 198198 (CPL2) dorsal view; 18, MGUH234 thoracic segment, GGU 274689 (CPL5) dorsal view.

Figs 1–8, 12–14, 17–18 scale bars = 5 mm; Figs 9–11, 15–16, scale bars = 1 mm.

PLATE 21

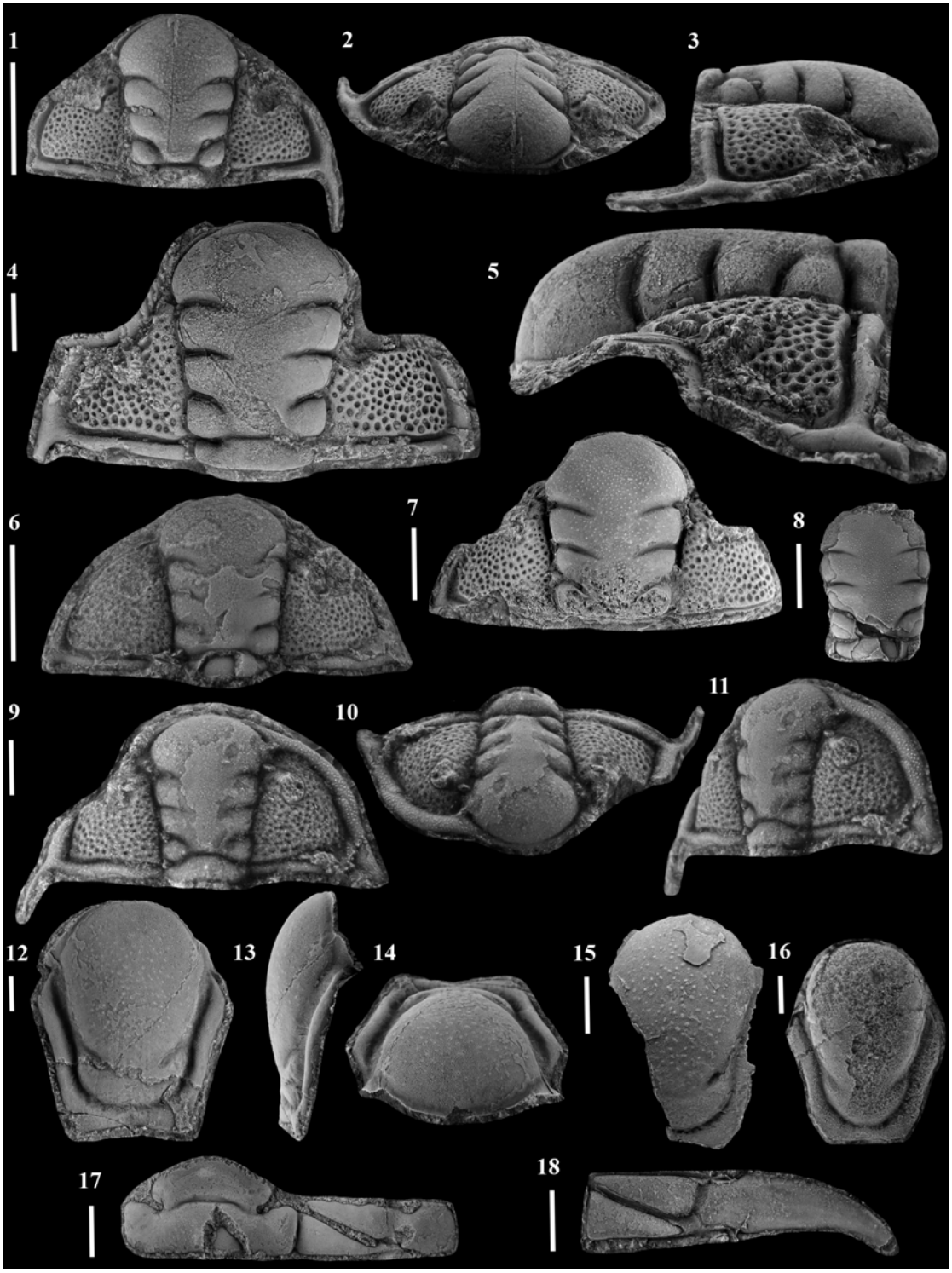

EXPLANATION OF PLATE 22

Figs 1–7. *Cheirurus falcatus* sp. nov. 1–2, MGUH235 holotype pygidium, GGU 274689 (CPL5) 1, dorsal and 2, oblique lateral views; 3–4, MGUH236 pygidium, GGU 198213 (CPL2) 3, dorsal and 4, anterior views; 5, MGUH237 pygidium, GGU 198169 (CPL2) dorsal view; 6–7, MGUH238 pygidium, GGU 274689 (CPL5) 6, dorsal and 7, lateral views.

Figs 8–14. *Proromma*? *parageia* sp. nov. 8–10, MGUH239 holotype cranidium with two articulated thoracic segments, GGU 275038 (VGL1) 8, dorsal, 9, posterior and 10 anterior views; 11, MGUH240 cephalon, GGU 274689 (CPL5) dorsal view; 12–13, MGUH241 cranidium, GGU 275038 (VGL1) 12, dorsal and 13, oblique lateral views; 14, MGUH242 thoracic segment, GGU 275015 (KCL1) dorsal view.

Figs 1–7, scale bars = 5 mm; Figs 8–14, scale bars = 1 mm.

PLATE 22

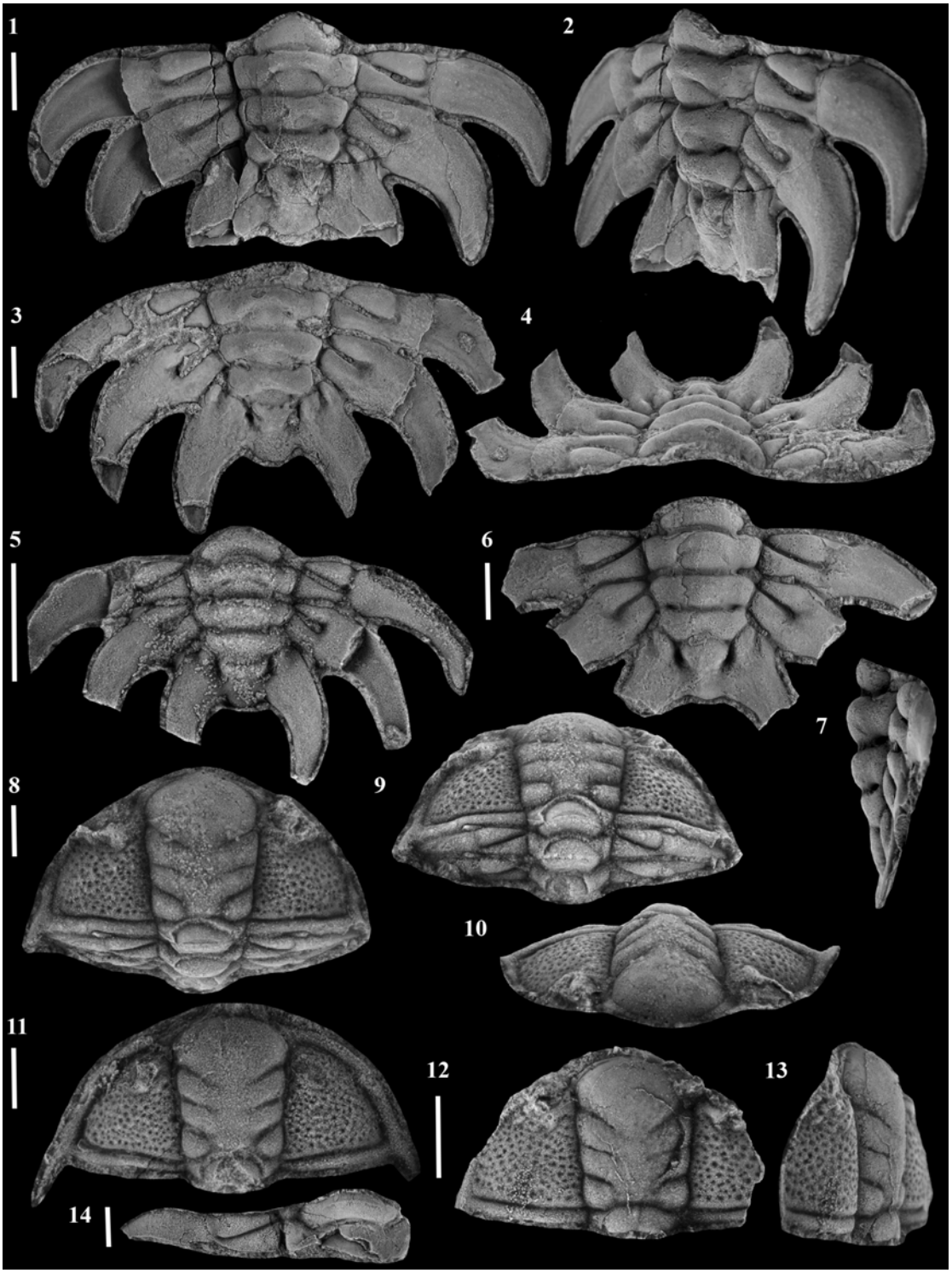

EXPLANATION OF PLATE 23

Figs 1–17 *Radiurus pauli* sp. nov. 1–2, MGUH243 cephalon, GGU 298506 (WL) 1, dorsal and 2, anterior views; 3, MGUH244 cranidium, GGU 298506 (WL) dorsal view; 4–6, MGUH245 cranidium, GGU 298504 (WL) 4, dorsal, 5, lateral and 6, anterior views; 7–8, MGUH246 cranidium (not blackened), GGU 298924 (SNL2) 7, dorsal and 8, anterior views; 9–11, MGUH247 hypostome, GGU 298506 (WL) 9, ventral, 10, anterior and 11, oblique lateral views; 12, MGUH248 pygidium, GGU 298506 (WL), dorsal view; 13, MGUH249 thoracic segment, GGU 298504 (WL), dorsal view; 14, MGUH250 pygidium, GGU 298924 (SNL2), dorsal view; 15–17, MGUH251 holotype pygidium, GGU 298506 (WL), 15, dorsal, 16, oblique lateral and 17, anterior views.

All scale bars = 1 mm.

PLATE 23

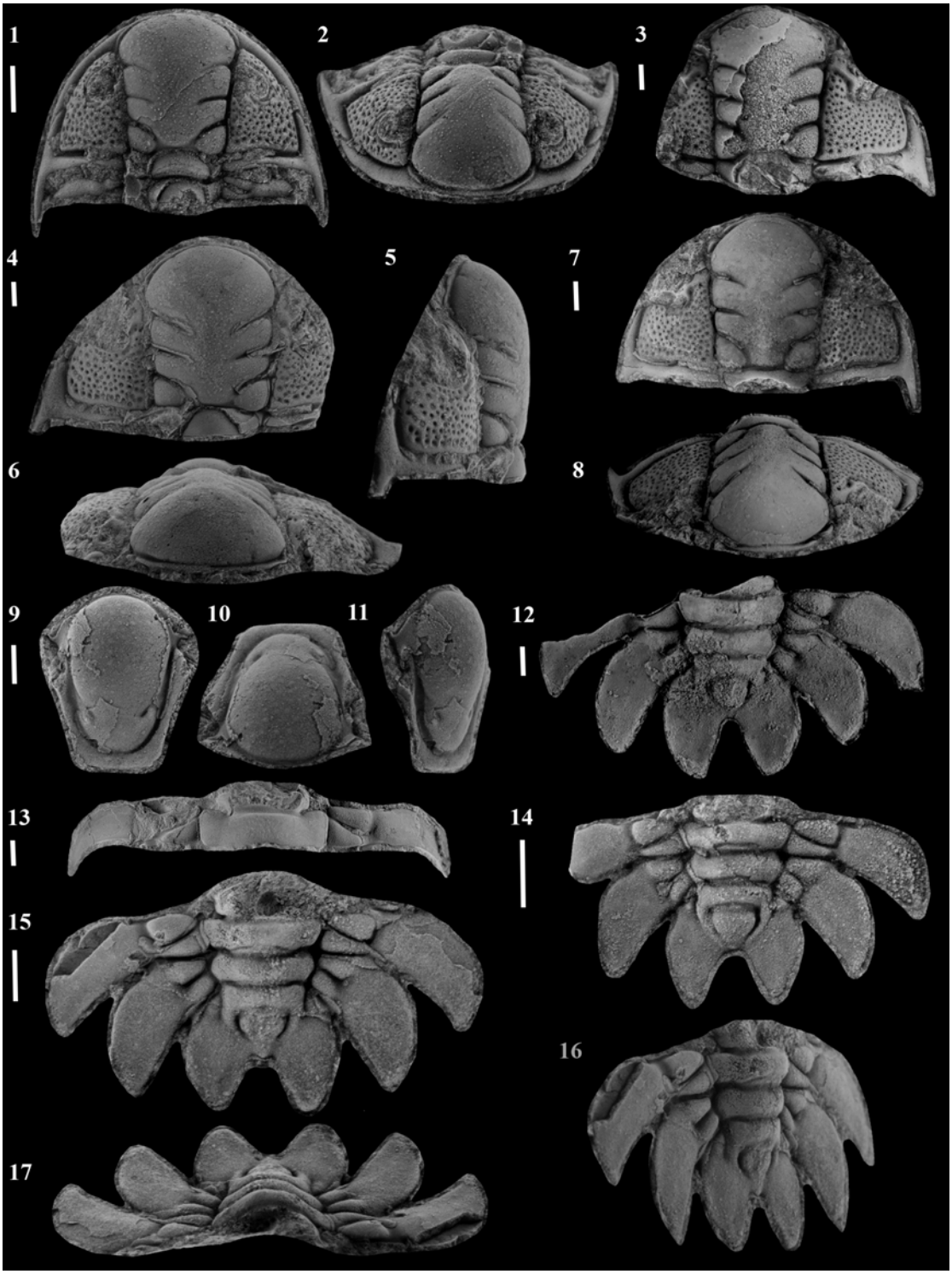

EXPLANATION OF PLATE 24

Figs 1–3. *Hyrokybe pharanx* Lane, 1972. 1–2, MGUH252 cranidium, GGU 274689 (CPL5) 1, dorsal and 2, lateral views; 3, MGUH253 cranidium, GGU 198137 (CPL2) dorsal view.

Figs 4–12. *Hyrokybe*? sp. 4–6, MGUH254 cephalon, GGU 274654 (CPL4) 4, dorsal, 5, anterior and 6, oblique lateral views; 7–9, MGUH255 cranidium, GGU 274689 (CPL5) 7, dorsal, 8, oblique and 9, anterior views; 10, MGUH256 cranidium, GGU 274654 (CPL4) dorsal view; 11–12, MGUH257 cranidium, GGU 274654 (CPL4) 11, dorsal and 12, oblique views

Figs 13–14. Acanthoparyphinae gen. et sp. indet. 1. MGUH258 cephalon, GGU 198226 (CPL1) 13, dorsal and 14, oblique lateral views.

Figs 15–17. Acanthoparyphinae gen. et sp. indet. 2. MGUH259 cranidium, GGU 274689 (CPL5) 15, dorsal, 16, anterior and 17, oblique views.

Figs 1–2 scale bar = 5 mm; Figs 3–17, scale bars = 1 mm.

PLATE 24

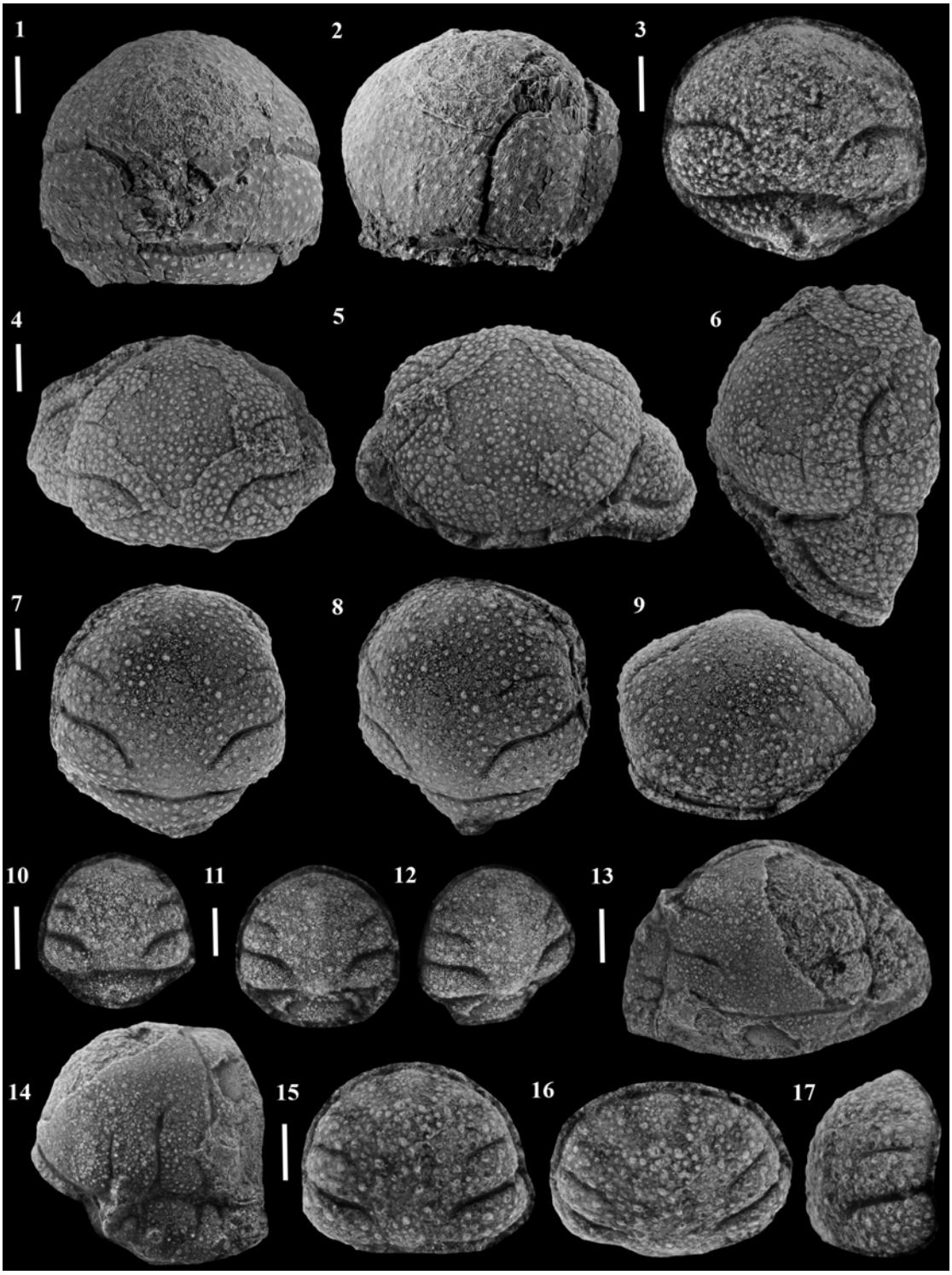

EXPLANATION OF PLATE 25

Figs 1–5. *Distyrax bibullus* sp. nov. 1–3, MGUH260 holotype cephalon, 1, dorsal , 2, oblique and 3, anterior views; 4–5, MGUH261 pygidium, 4, dorsal and 5, oblique lateral views. Both specimens from GGU 275015 (KCL1).

Fig. 6. *Distryax*? sp. MGUH262 cranidium, GGU 274689 (CPL5) dorsal view.

Figs 7–15. *Perryus mikulici* sp. nov. 7–9, MGUH263 holotype cephalon, GGU 275015 (KCL1) 7, dorsal, 8, oblique lateral and 9, anterior views; 10–11, MGUH264 cephalon with articulated thoracic segments, GGU 274689 (CPL5) 10, dorsal and 11, oblique lateral views; 12, MGUH265 cranidium with articulated thoracic segments, GGU 275015 (KCL1) dorsal view; 13, MGUH266 cranidium, GGU 274689 (CPL5) dorsal view; 14, MGUH267 librigena, GGU 274689 (CPL5) dorsal view; 15, MGUH268 cranidium, GGU 274689 (CPL5) dorsal view.

All scale bars = 1 mm.

PLATE 25

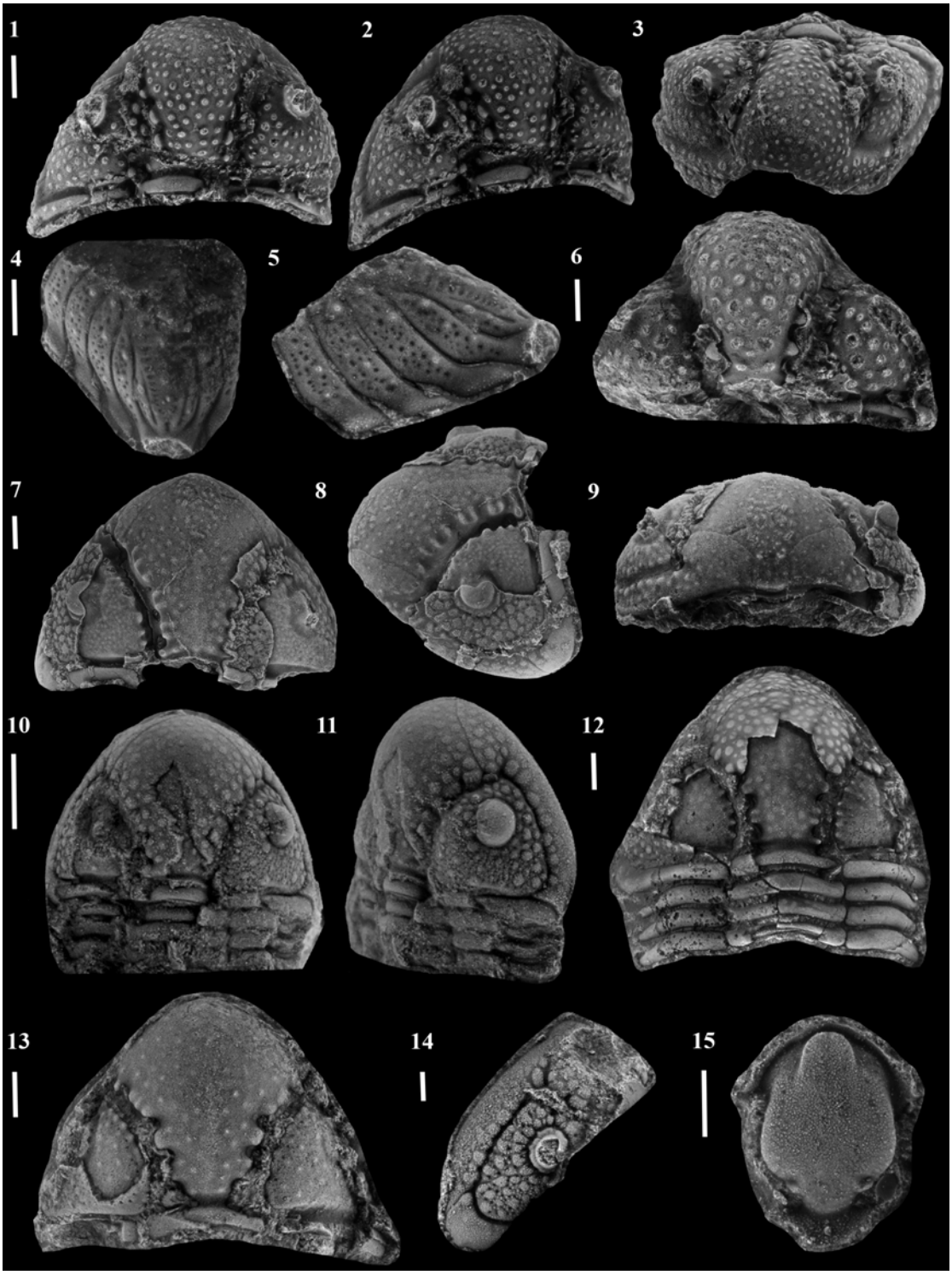

EXPLANATION OF PLATE 26

Figs 1–4. *Perryus mikulici* sp. nov. 1, MGUH269 pygidium, GGU 274689 (CPL5) dorsal view; 2–4 MGUH270 pygidium, GGU 274788 (KCL6) 2, dorsal, 3, lateral and 4, posterior views.

Figs 5–7. *Perryus* cf. *P. palasso* Lane, 1988. 5, MGUH271 cranidium, GGU 298924 (SNL2) dorsal view; 6 MGUH272 pygidium, GGU 298506 (WL) dorsal view; 7 MGUH273 pygidium, GGU 298506 (WL) dorsal view.

Figs 8–12. *Perryus* sp. 1. 8, MGUH274 glabella, GGU 198221 (CPL2) dorsal view; 9–11 MGUH275 cephalon, GGU 198206 (CPL2) 9, dorsal, 10, anterior and 11, oblique lateral views; 12, MGUH276 pygidium, GGU 198214 (CPL2) dorsal view.

Figs 13–17. *Perryus* sp. 2. 13–14, MGUH277 cranidium, 13, dorsal and 14, lateral views; 15, MGUH278 articulated pygidium and thorax, dorsal view; 16–17, MGUH279 pygidium, 16, dorsal and 17, lateral views. All material from GGU 274774 (KCL5).

Figs 18–21. Genus aff. *Perryus*. 18, MGUH280 cranidium, dorsal view; 19–21, MGUH281 cephalon, 19, dorsal, 20, oblique lateral and 21, anterior views. Both specimens from GGU 198225 (CPL3).

All scale bars = 1 mm.

PLATE 26

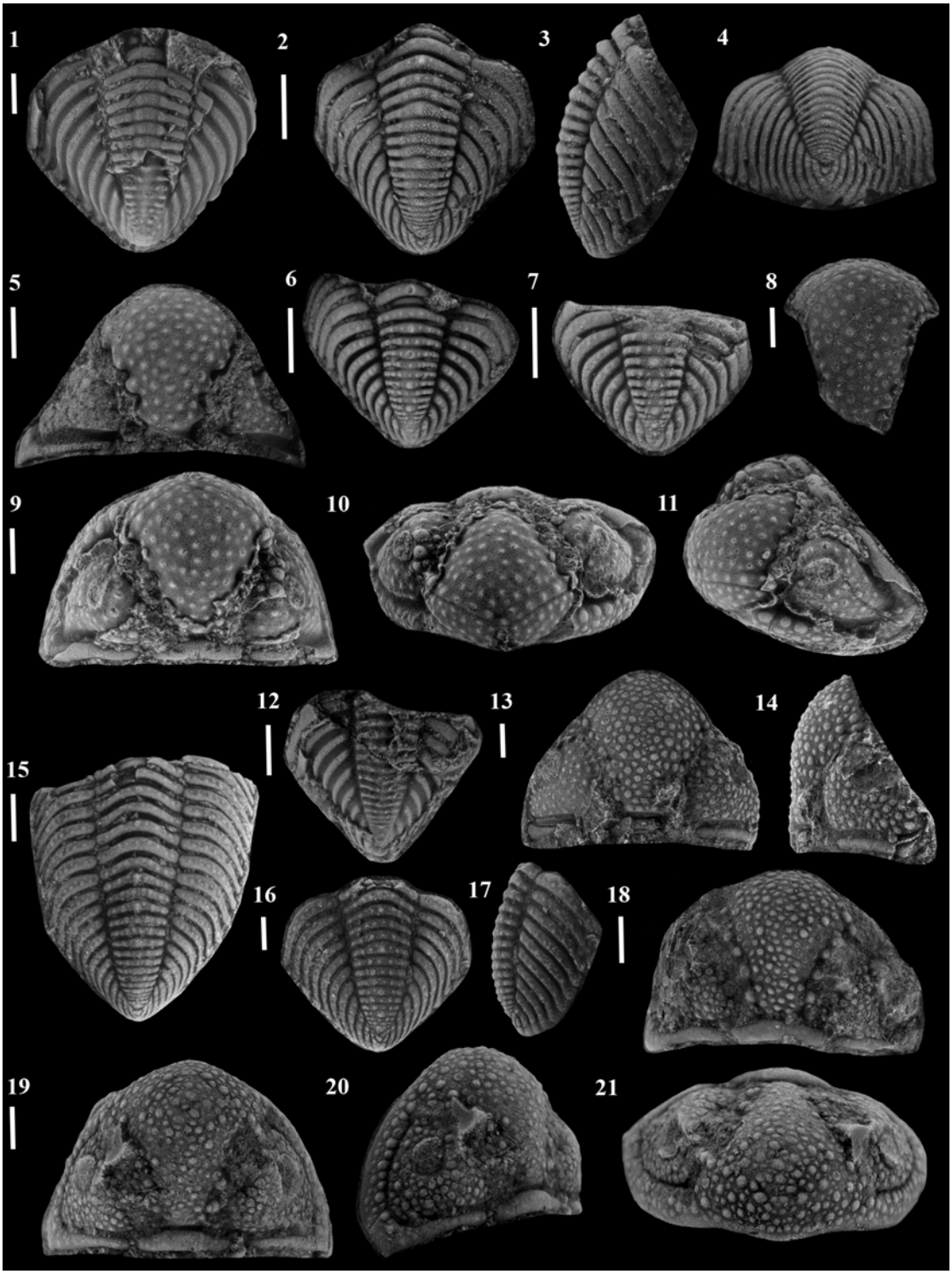

EXPLANATION OF PLATE 27

Figs 1–4. Genus aff. *Perryus*. 1–3, MGUH282 pygidium, 1, dorsal, 2, lateral and 3, posterior views; 4, MGUH283 pygidium, dorsal view. Both specimens from GGU 198225 (CPL3).

Figs 5–11. *variolaris* plexus gen. indet. 1. 5–6, MGUH284 cranidium, GGU 274689 (CPL5) 5, dorsal and 6, oblique lateral views; 7, MGUH285 cranidium, GGU 274996 (KCL4) dorsal view; 8–9, MGUH286 pygidium, GGU 274689 (CPL5) 8, dorsal and 9, oblique views; 10–11, MGUH287 pygidium, GGU 274689 (CPL5) 10, dorsal and 11, oblique views.

Figs 12–20. *variolaris* plexus gen. indet. 2. 12–13, MGUH288 cranidium, 12, dorsal and 13, oblique views; 14, MGUH289 cranidium, dorsal view; 15, MGUH290 glabella, dorsal view; 16, MGUH291 librigena, dorsal view; 17–18, MGUH292 pygidium, 17, dorsal and 18, posterior views; 18–19, MGUH293 pygidium, 19, dorsal and 20, lateral views. All material from GGU 198226 (CPL1).

All scale bars = 1 mm.

PLATE 27

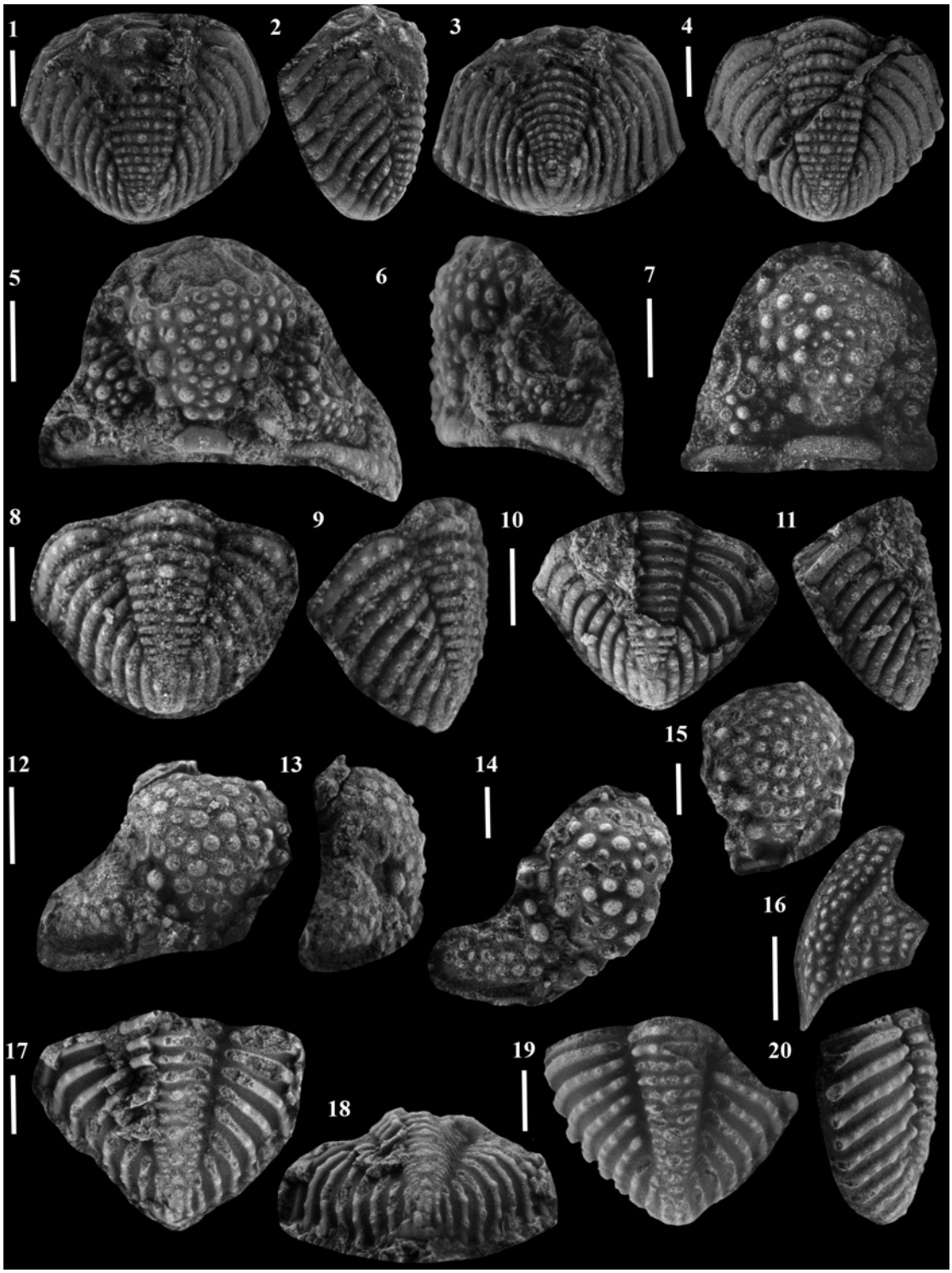

EXPLANATION OF PLATE 28

Figs 1–8. *Calymene* aff. *iladon* Lane and Siveter, 1991. 1–3, MGUH294 cephalon, 1, dorsal, 2, lateral and 3, anterior views; 4, MGUH295 hypostome, ventral view; 5–6, MGUH296 pygidium, 5, dorsal and 6, lateral views; 7–8, MGUH297 pygidium, 7, dorsal and 8, lateral views. All material from GGU 298506 (WL).

Figs 9–18. *Calymene* sp. 9–10, MGUH298 cranidium, GGU 198185 (CPL2) 9, dorsal and 10, lateral views; 11, MGUH299 cranidium with articulated thoracic segments, GGU 198223 (CPL2) dorsal view; 12–13, MGUH300 cranidium, GGU 198223 (CPL2) 12, dorsal and 13, oblique views; 14, MGUH301 pygidium, GGU 198196 (CPL2) dorsal view; 15, MGUH302 pygidium, GGU 198214 (CPL2) dorsal view; 16–18, MGUH303 pygidium with articulated thoracic segments, GGU 198223 (CPL2) 16, dorsal view of pygidium, 17, dorsal view of thoracic segments and 18, oblique lateral view of thoracic segments.

Figs 19–21. *Calymene*? sp. MGUH304 cephalon, GGU 301318 (WPL1) 19, dorsal, 20, oblique lateral and 21, anterior views.

All scale bars = 1 mm.

PLATE 28

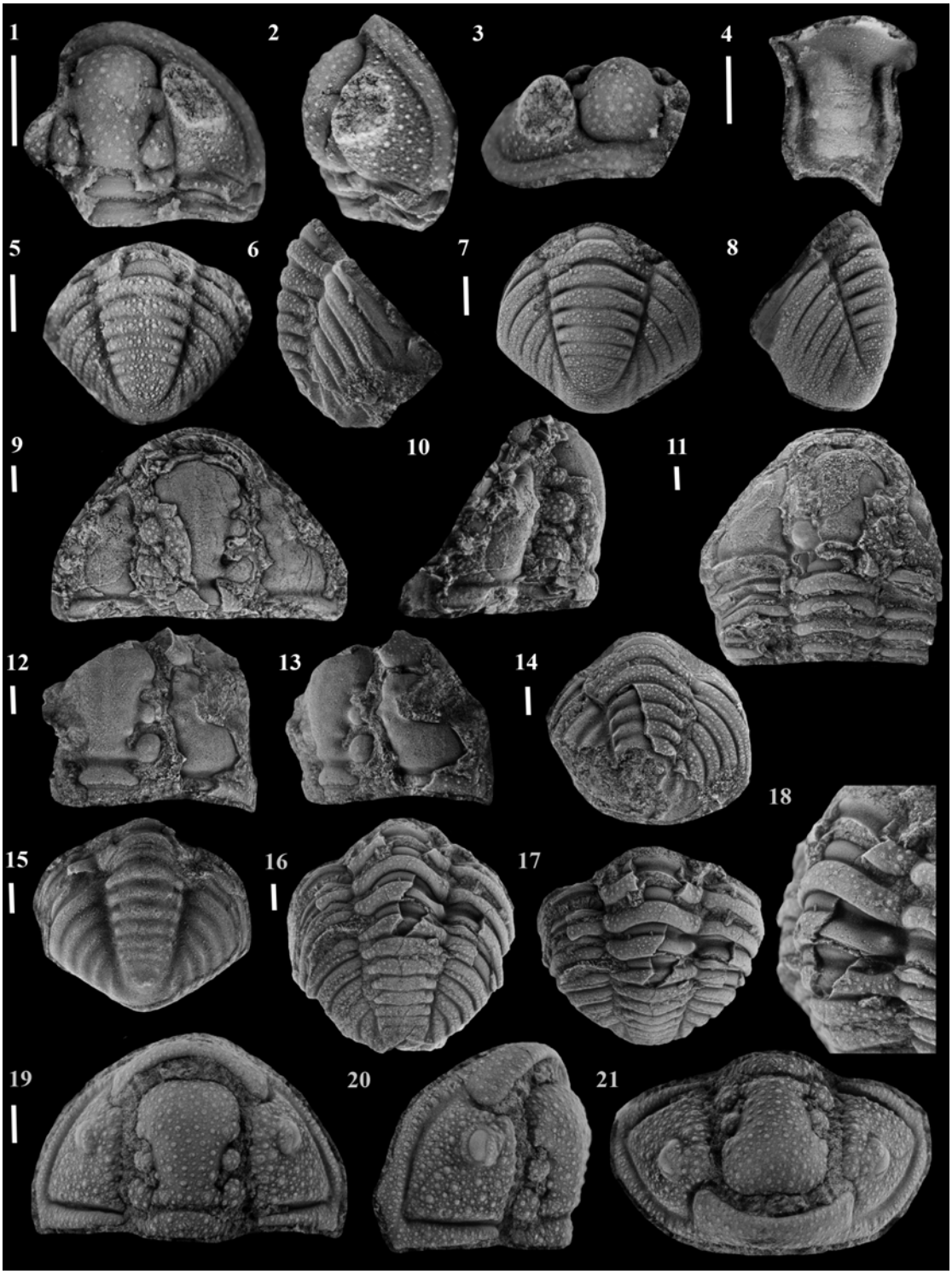

EXPLANATION OF PLATE 29

Figs 1–3. *Acernaspis*? sp. MGUH305 cephalon, GGU 298506 (WL) 1, dorsal view, 2, oblique lateral view and 3, extended view of visual surface.

Figs 4–13. *Dicranogmus pearyi* sp. nov. 4–7, MGUH306 holotype cephalon, 4, dorsal, 5, anterior, 6, lateral and 7, oblique views; 8–9, MGUH307, hypostome, 8, ventral and 9, oblique lateral views; 10, MGUH308, hypostome, ventral view; 11, MGUH309 pygidium, dorsal view; 12–13, MGUH310 pygidium, 12, dorsal and 13, oblique lateral views. All material from GGU 274689 (CPL5).

Figs 14–16. *Dicranogmus mabillardi* sp. nov. 14–15, MGUH311 holotype cranidium, GGU 274654 (CPL4) 14, dorsal and 15, lateral views; 16, MGUH312 cranidium, GGU 198226 (CPL1) dorsal view.

All scale bars = 5 mm.

PLATE 29

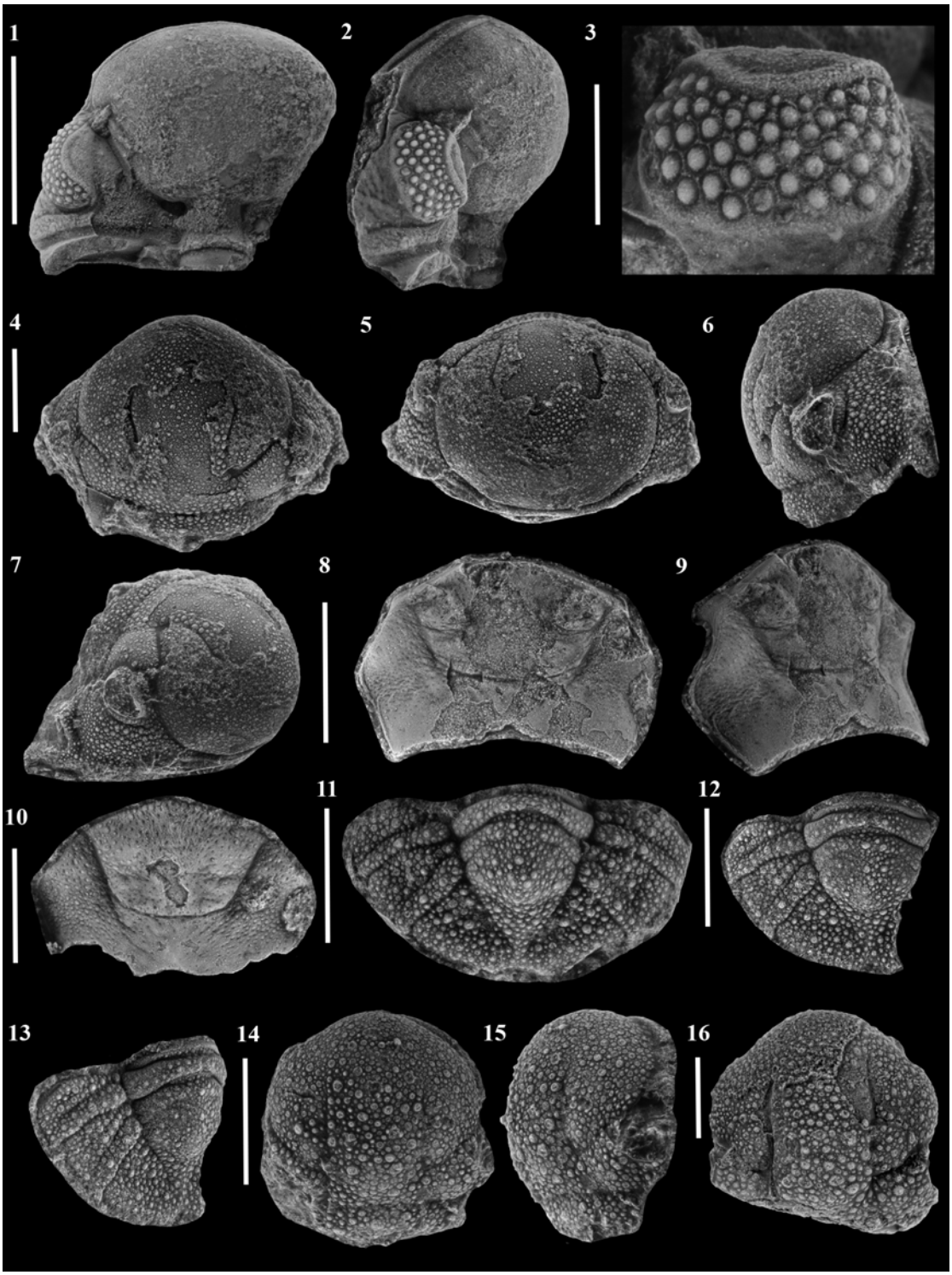

EXPLANATION OF PLATE 30

Figs 1–5. *Dicranogmus mabillardi* sp. nov. 1, MGUH313 hypostome, GGU 198226 (CPL1) ventral view; 2, MGUH314 pygidium, GGU 198137 (CPL2) dorsal view; 3, MGUH315 pygidium, GGU 198226 (CPL1) dorsal view; 4–5, MGUH316 pygidium, GGU 198226 (CPL1) 4, dorsal and 5, lateral views.

Figs 6–8. *Acanthopyge*? sp. 6–7, MGUH317 hypostome, 6, ventral and 7, lateral views; 8, MGUH318 hypostome, ventral view. Both specimens from GGU 274689 (CPL5).

Figs 9–16. *Ceratocephala papilio* sp. nov. 9–10, MGUH319 holotype cranidium, GGU 274689 (CPL5) 9, dorsal and 10, oblique lateral views; 11, MGUH320 cranidium, GGU 274654 (CPL4) dorsal view; 12–13, MGUH321 cranidium, GGU 198226 (CPL1) 12, dorsal and 13, oblique lateral views; 14, MGUH322 cranidium, GGU 275015 (KCL1) dorsal view; 15–16, MGUH323 pygidium, GGU 274689 (CPL5) 15, dorsal and 16, oblique lateral views.

Figs 17–19. *Ceratocephala* sp. 17–18, MGUH324 cephalon, 17, dorsal and 18, oblique lateral views; 19, MGUH325 hypostome, ventral view. Both specimens from GGU 298506 (WL).

All scale bars = 1 mm.

PLATE 30

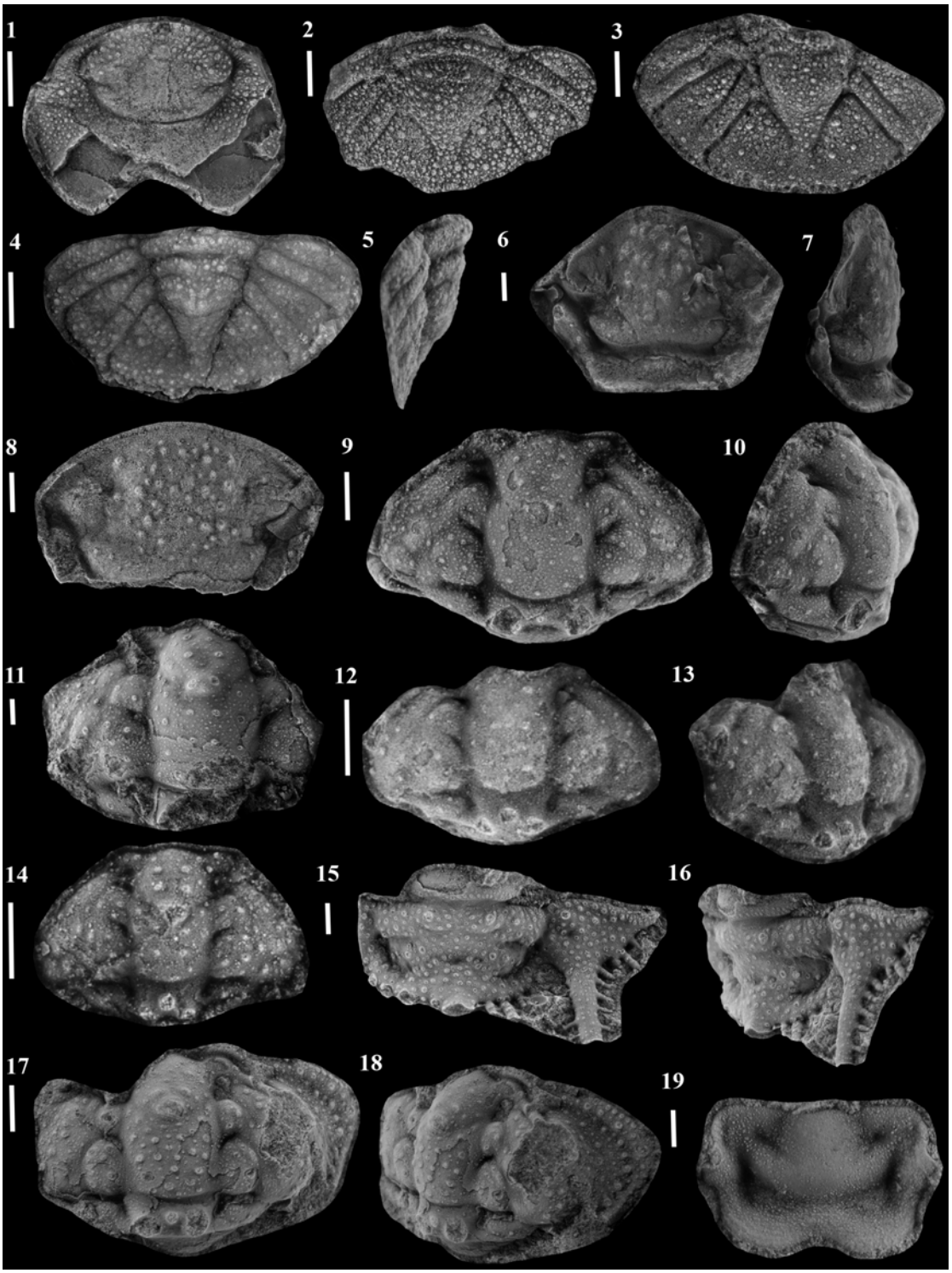

2.4 ALPHA DIVERSITY

Tables 2.1A and B show the distribution of the trilobite taxa described here (as numbers of individuals) across the North Greenland reef belt. A clear faunal distinction can be made between trilobite taxa occurring in western Peary Land and further west, and those occurring in central Peary Land and further east. Only two species; *Scotoharpes loma* and *Perryus mikulici*, occur in reefs from both of these broad areas.

The termination of the reefs by deeper water sediments has been proven to young from east to west across the North Greenland carbonate platform, by limited graptolite evidence (Smith and Rasmussen 2008).This could result in the faunas occurring in the west of North Greenland, being slightly younger than those occurring in the most easterly reefs.

		WEST					EAST
		Locality					
Family	**Taxon**	**WL**	**SNL**	**WPL**	**CPL**	**VGL**	**KCL**
Scutelluidae	*Aboskes anachoretes*	0	0	0	1	0	0
	Ekwanoscutellum agmen	0	0	0	351	7	18
	Jungosulcus emilyae	0	0	0	203	0	0
	Jungosulcus anaphalantos	0	226	0	0	0	0
	Jungosulcus ventricosus	0	0	0	0	25	0
	Meroperix ataphrus	0	0	0	0	1	0
	Opoa limatula	0	0	0	23	0	3
	Opoa sp.	0	0	0	0	0	2
	Periostrix magnifica	99	34	99	0	0	0
	Genus aff. *Periostrix*	0	0	0	0	0	2
	Scutelluid gen. indet.	0	0	2	0	0	0
	Cybantyx nebulosus	0	0	0	127	0	0
	Cybantyx sp.	0	2	14	0	0	0
	Lanebestix enalios	0	0	0	0	11	0
	Ligiscus diana	0	0	0	3	65	1
	Liolalax naresi	0	14	0	0	0	0
	Liolalax? sp.	0	0	0	0	1	1
Illaenidae	*Stenopareia persica* sp. nov.	0	0	0	43	1	0
	Stenopareia cf. *grandis*	5	1	20	0	0	0
	Stenopareia sp.	0	0	0	0	2	0
Proetidae	*Proetus*? *confluens*	0	0	0	12	0	0
	Airophrys balios	0	0	0	0	1	0
	Airophrys sp.	0	0	0	2	0	0
	Cyphoproetus peeli	0	0	0	4	0	0
	Cyphoproetus sp.	0	1	0	0	0	0
	Owensus arktoperates	0	0	0	74	0	0
	Astroproetus franklini	0	0	0	4	1	0
	Astroproetus sp.	0	0	0	0	0	1
	Thebanaspis sp.	1	0	1	0	0	0
	Winiskia eruga	0	0	0	5	0	3
	Winiskia leptomedia	0	0	0	0	0	3
	Winiskia lipopyga	0	0	0	5	0	0
	Winiskia stickta	0	0	0	7	0	0
	Dalarnepeltis brevifrons	0	0	0	5	0	0
	Tropidocoryphine gen. et sp. indet.	0	0	0	2	0	0
Aulacopleuridae	Aulacopleurid cf. *Songkania*	0	0	0	0	1	0
Scharyiidae	*Scharyia lobarga*	0	0	0	7	0	0
	Scharyia deiropede	0	0	0	2	0	0
	Scharyia unicorna	0	0	0	2	0	0
Brachymetopidae	*Radnoria* cf. *Radnoria triquetra*	0	0	0	0	1	0

TABLE 2.1A Distribution of families Scutelluidae, Illaenidae, Proetidae, Aulacopleuridae, Scharyiidae and Brachymetopidae across North Greenland. Numbers given are of trilobite individuals, calculated from the greater of the following groupings: (cephala + cranidia + cephalothoraces) and (pygidia + thoracopygidia).

		WEST					EAST
		Locality					
Family	**Taxon**	**WL**	**SNL**	**WPL**	**CPL**	**VGL**	**KCL**
Harpetidae	*Scotoharpes loma*	2	29	14	9	2	5
Cheiruridae	*Cheirurus falcatus*	0	0	0	52	0	0
	Proromma? *parageia*	0	0	0	2	5	1
	Radiurus pauli	58	15	14	0	0	0
	Hyrokybe pharanx	0	0	0	2	0	0
	Hyrokybe? sp.	0	0	0	7	0	0
	Acanthoparyphinae gen. et sp. indet. 1	0	0	0	1	0	0
	Acanthoparyphinae gen. et sp. indet. 2	0	0	0	1	0	0
Encrinuridae	*Distyrax bibullus*	0	0	0	0	0	1
	Distryax? sp.	0	0	0	1	0	0
	Perryus mikulici	0	0	2	35	0	37
	Perryus cf. *P. palasso*	2	1	0	0	0	0
	Perryus sp. 1	0	0	0	2	0	0
	Perryus sp. 2	0	0	0	0	0	2
	Genus aff. *Perryus*	0	0	0	7	0	0
	variolaris plexus gen. indet. 1	0	0	0	2	0	1
	variolaris plexus gen. indet. 2	0	0	0	21	0	0
Calymenidae	*Calymene* aff. *iladon*	4	0	0	0	0	0
	Calymene sp.	0	0	0	6	0	0
	Calymene? sp.	0	0	1	0	0	0
Phacopidae	*Acernaspis*? sp.	1	0	0	0	0	0
Lichidae	*Dicranogmus pearyi*	0	0	0	13	0	0
	Dicranogmus mabillardi	0	0	0	15	0	0
	Acanthopyge? sp.	0	0	0	2	0	0
Odontopleuridae	*Ceratocephala papilio*	0	0	0	8	0	1
	Ceratocephala sp.	2	0	0	0	0	0

TABLE 2.1B Distribution of families Harpetidae, Cheiruridae, Encrinuridae, Calymenidae, Phacopidae, Lichidae, and Odontopleuridae across North Greenland. Numbers given are of trilobite individuals, calculated from the greater of the following groupings: (cephala + cranidia + cephalothoraces) and (pygidia + thoracopygidia).

2.5 PALAEOBIOGEOGRAPHY

The trilobite faunas from the reefs of North Greenland share close affinities to those described from other northern Laurentian shallow marine environments, which are also Telychian in age. Trilobites from the Telychian–?early Wenlock Attawapiskat Formation from northern Ontario and Northern Manitoba (Norford 1981, Gass and Mikulic 1982, Westrop and Rudkin 1999) occur in pockets within reef lithofacies. Seven of the 15 genera described by Norford (1981) are represented here. Further north Laurentian links are confirmed by a Telychian trilobite fauna described from Alaska by Adrain *et al*. (1995); the seven species identified from the white bioclastic limestone from the Taylor mountains are all congeneric with those here. Chatterton and Ludvigsen (2004) revised and described all known Llandovery trilobites from Anticosti Island, Québec, Canada. They noted that most of the species had restricted stratigraphic ranges and identified six successive faunas. There are some generic affinities with all of the faunal groups identified, however, the material in this present work is most comparable to their *Ekwanoscutellum ekwanensis* fauna from the late Telychian to ?earliest Wenlock Chicotte Formation. Their *Ekwanoscutellum ekwanensis* fauna is predominantly congeneric with that described here, with species of *Ekwanoscutellum, Stenopareia* ?*Distyrax, Hyrokybe* and *Scotoharpes* represented.

CHAPTER THREE

EFFACEMENT IN THE SUBORDER ILLAENINA (TRILOBITA): A CLADISTIC APPROACH TO THE PROBLEMS OF CONVERGENCE

Summary: The morphology of the furrows that plesiomorphically characterize the dorsal exoskeleton of trilobites provides character states that aid interpretation of the relationships between trilobite groups. In some trilobites, these furrows weaken, and may be largely lost. Commonly, this loss of furrows is accompanied by an increase in the width of the axis, and an increase in exoskeleton convexity. The term ‘effacement’ is used to describe this association of character states. The loss of morphological characters presents obvious problems for phylogenetic analysis, and the problem becomes particularly acute when effacement occurs commonly amongst groups of closely related trilobites. This is the case within the Suborder Illaenina. Effaced members of the Illaenina are here analysed cladistically and the polyphyletic nature of effaced taxa is demonstrated. The analysis highlights the problems of ordering based on the choice of outgroup: effacement acts as either an apomorphic or plesiomorphic character state depending on whether or not an effaced taxon is chosen as the outgroup. A clade comprising unambiguous members of the Family Illaenidae is robustly supported when phylogenetic analysis is limited to effaced taxa. This clade is distinguishable from effaced members of the Family Scutelluidae.

3.1 INTRODUCTION

PLESIOMORPHICALLY, the trilobite dorsal exoskeleton is characteristically distinctly furrowed and the patterning of these furrows provides characters that are useful in classifying the animals. Most major groups of trilobites have some representatives in which the furrows weaken, so that the exoskeleton assumes a smoother appearance. This smoothing is one of the characteristic features of the process termed effacement, which is discussed in more detail below. The advantages of effacement to trilobite taxa are not known; it is exhibited by trilobites with widely different overall morphologies, occurring in different environments, and is present in trilobite taxa from the Early Cambrian to the Permian (Fortey and Owens *in* Kaesler 1997).

The loss of recognisable characters presents obvious limitations to any morphologically-based phylogenetic analysis. The effects of effacement are variable, and most notable in the Agnostida, Asaphoidea, Illaenina, and Olenoidea. In some, effacement of the dorsal exoskeleton results in morphological features becoming obscured or removed altogether. There is evidence within certain groups, the Agnostida for example, that the condition of effacement was independently derived in different lineages (Lane and Thomas 1983). This has been considered to be the case within the Illaenina also (Lane and Thomas *in* Thomas 1978; Lane and Thomas 1978; Lane and Thomas 1983), though this view is controversial (see Section 3.3.1). The repeated occurrence of effacement within the Trilobita thus presents itself as a group of convergent character states; a significant phylogenetic problem which requires investigation.

The trilobite Suborder Illaenina Jaanusson *in* Moore, 1959, provides a suitable case study for investigating the effects of effacement on phylogenetic groupings; its

taxa are variably effaced and include some of the most highly effaced of all trilobite taxa. Additionally, although various groupings have been discussed, no phylogenetic consensus exists. As traditional phylogenetic assessments have so far failed to provide agreement concerning the classification within the Illaenina, I here apply cladistic methods for the first time. The purposes are threefold: firstly, to investigate the effects of effacement on cladistic analyses; secondly, to assess the ability of cladistic analyses to recognise independently derived forms with convergent character states, and finally, to recognise individual phylogenetic lineages of effaced taxa within the Illaenina.

The account that follows begins by reviewing the conditions of effacement, and the varying interpretations of phylogeny in the Illaenina. I discuss the possibility of inferring phylogeny from ontogeny, and finally I apply cladistic methods to representatives of the Scutelluidae, Styginidae and Illaenidae, to investigate the effects of effacement.

3.2 EFFACEMENT

Lane and Thomas (1983) recognised effacement as a complex and apomorphic character state and identified three processes which may coexist: reduced distinctness of dorsal furrows, increased exoskeletal convexity, and increase in relative axis width. Effacement is commonly associated with progressive rounding of the genal angle also. The processes may operate together or alone, and as such, the effects of effacement are highly variable.

Within the Illaenina, the most effaced members are termed illaenimorphs, and these are affected by all of the above processes. Illaenimorph taxa are represented by genera such as *Illaenus* (see *Illaenus sarsi* figured by Whittington 1997, figs 7.1–7.6)

and *Cybantyx* (see Text-fig. 3.1F–G, and *Cybantyx anaglyptos* Lane and Thomas *in* Thomas, 1978, pl. 5, figs 1–8, text-fig. 3). These display a convex exoskeleton, wide axis, and very little definition of furrows. The loss of recognisable character states in such highly effaced forms makes their exact phylogenetic relationships among the most poorly understood of all trilobites. There are also examples of partially effaced forms within the Illaenina, typified by the Devoninan scutelluid *Paralejurus* (see *Paralejurus campanifer* figured by Šnajdr 1960, pl. 23, figs 2–14, pl. 24, figs 1–2, pl. 36, fig. 8, text-figs 58–59) and the Silurian scutelluid *Ligiscus* (see Text-fig. 3.1B–E, and *Ligiscus arcanus* Lane and Owens, 1982, pl. 3, figs 4–8, text-fig. 3). These taxa display increased convexity, and a limited loss of definition by furrows. Effacement may affect different parts of the trilobite exoskeleton to different degrees, the cranidia of *Ligiscus* species are more effaced than the pygidia for example (Text-fig. 3.1C, E). Differences in the way that effacement develops have been remarked upon by Fortey and Owens *in* Kaesler (1997). In *Ligiscus*, effacement originates adaxially (Text-fig. 3.1B–E). Effacement may act at any taxonomic level, and intrageneric variation in effacement is common. This is exemplified by different species of the crassiproetine *Winiskia* (Owens 2006, fig. 7) which exhibit varying expression of cephalic and pygidial furrows. The degree of effacement is therefore useful in distinguishing between taxa at specific level in this case. This is not the case at higher taxonomic levels, and Whittington (2000, p. 880) noted that effacement alone should not be used to define a taxon above specific level due to problems of homology. It is clear that the occurrence of this apomorphic character state can effectively mask individual phylogenetic lineages. It is not known how many times effacement has independently evolved within trilobite groups such as the Illaenina, but the discussion below

supports the view that effaced taxa arose independently in the Illaenidae, Scutelluidae and Styginidae.

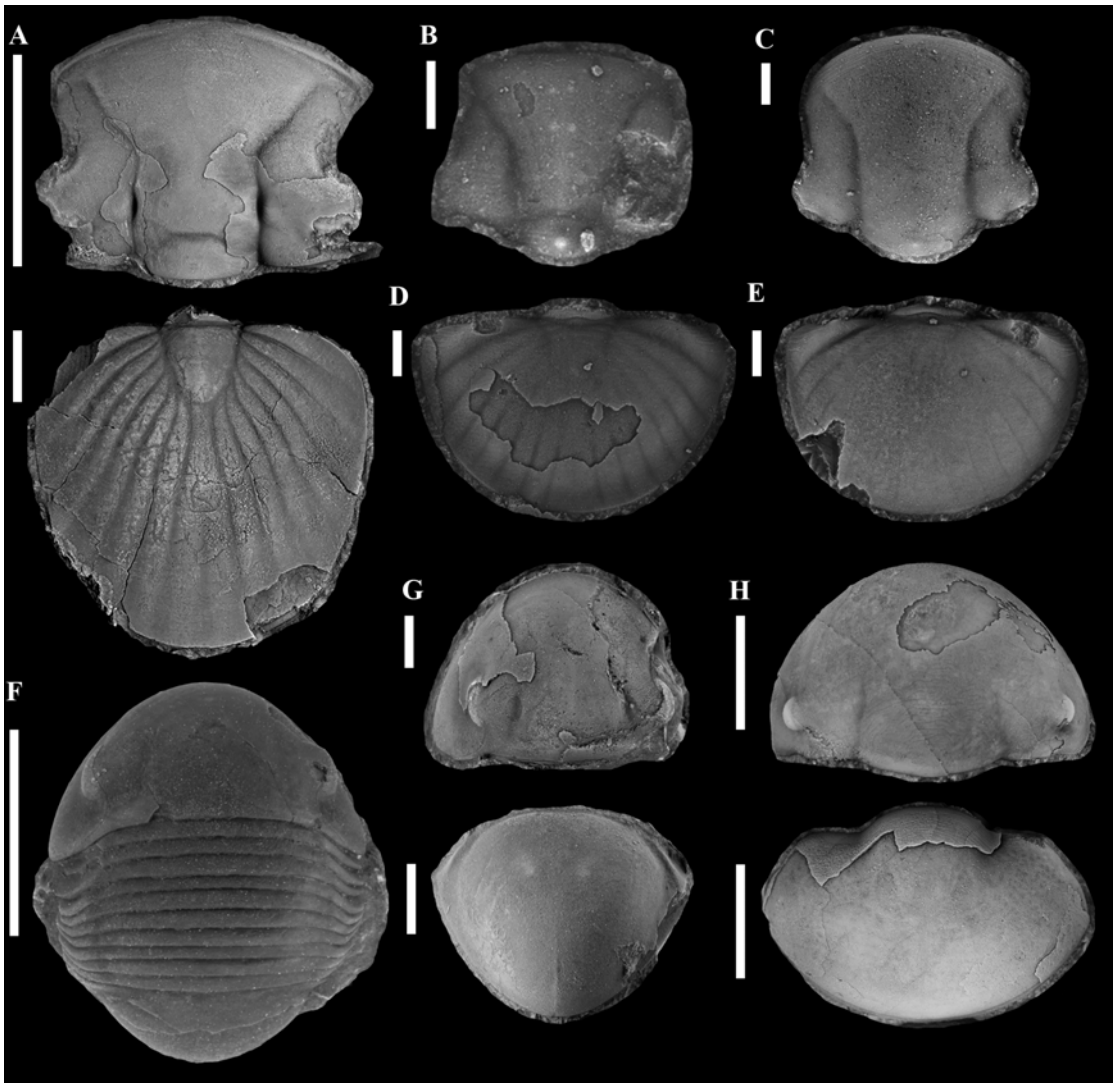

Text-fig. 3.1. Representatives of the Illaenina within the Silurian reefs of North Greenland. **A.** *Ekwanoscutellum*, a scutelluid with some degree of effacement. **B–C.** *Ligiscus*, an illaenimorph with obvious morphological characteristics of scutelluids. **B.** Early holaspis cranidium with impressed occipital furrow and axial furrows intersecting anterior margin. **C.** Late holaspis cranidium with no occipital furrow and axial furrows fading posterior of anterior margin. **D.** Pygidium with impressed axial and interpleural furrows. **E.** Pygidium with shallow axial and interpleural furrows. **F–G.** *Cybantyx*, an Illaenimorph deemed to be an effaced scutelluid by Lane and Thomas *in* Thomas 1978. **H.** *Stenopareia*, an unequivocal illaenid. (A, F–H, scale bars = 10 mm; B–E, scale bars = 1 mm).

3.3 EXISTING PHYLOGENETIC INTERPRETATIONS OF THE ILLAENINA

Lane and Thomas (1983) presented a comprehensive history of classification of the Illaenina. More recent discussions are detailed below. The Suborder as viewed here comprises the families Illaenidae Hupé, 1953, Phillipsinellidae Whittington, 1950, Scutelluidae Richter and Richter, 1955, and Styginidae Vogdes, 1890.

3.3.1 Illaenimorph taxa

The principal debate surrounding the Illaenina remains the placement of the highly effaced illaenimorph taxa. Lane and Thomas *in* Thomas (1978) and Lane and Thomas (1978) were the first to suggest that several taxa previously assigned to the Family Illaenidae, whose taxa are largely characterized by effaced morphologies, actually represented effaced members of the Family Scutelluidae, a group which at the time included no completely effaced forms. They argued that the basic morphology of taxa such as *Bumastus* (see *B. barriensis* figured by Lane and Thomas *in* Thomas 1978, pl. 1, figs 1–7, pl. 2, figs 1–12, pl. 4, fig. 6) was closer to the Scutelluidae, despite the obvious effects of effacement. *Rhaxeros* Lane and Thomas, 1980 (see *R. pollinctrix* Lane and Thomas 1978, p. 1, figs a–l, pl. 2, figs a–g) from the Llandovery/Wenlock of north-east Queensland, shares the following characters with the Scutelluidae: glabella hourglass-shaped, rounded anteriorly and with lateral glabellar muscle impressions; typical scutelluid rostral plate and hypostome; inflated visual surface; opisthoparian cephalon with classic scutelluid course of facial suture; short and narrow (exsag.) posterior section of fixed cheek; palpebral lobe high on the cheek; radially disposed lateral ribs on the pygidium. Lane and Thomas considered that *Rhaxeros* differed most noticeably from the majority of scutelluids, by its high degree of effacement. In discussing the various characters, Lane and Thomas did not clearly

distinguish between synapomorphies and synplesiomorphies, however. Lane and Thomas (1983) further developed their concept of effaced scutelluids, providing a review of the Suborder Scutelluina including a discussion of characters used in classification, and revised classification.

A conflicting argument was presented by Ludvigsen and Chatterton (1980), who suggested that the scutelluids arose from the bumastines (their terminology to include genera such as *Bumastus* and *Rhaxeros*) by changes including the appearance of ribs over the pygidial somites. Although a number of effaced Illaenina occur in the Early Ordovician, the effacement of trilobites is not plesiomorphic, and this interpretation requires the secondary de-effacement of effaced taxa.

Whittington (1997) investigated the phylogenetic applications of thoracic characters of the Illaenidae and Scutelluidae, comparing the morphology of the axial rings of the thorax of species of Illaenidae, to those of *Cybantyx*. The shared lack of the articulating furrow of axial segments dorsally, but instead ventrally represented by a stout ridge, were used to conclude that *C. anaglyptos* is an illaenid. Chatterton and Ludvigsen (2004) regarded this character as a homoplasous feature shared by several effaced trilobite groups, resulting from functional convergence. Whittington (1999, 2000) doubted that the Styginidae (used to include the Styginidae and Scutelluidae) had a common origin with the Illaenidae. The morphological characters used to differentiate between these families were presented in Whittington (1999, p. 419). Some of these characters are directly related to effacement however, for example the presence of pygidial ribs in members of the Scutelluidae, and should not be used alone to differentiate between the families.

3.3.2 The concept of the Styginidae

Prior to 1963, the Styginidae was considered to comprise only *Stygina* Salter, 1853 (see *Stygina latifrons extensa* figured by Whittington 2000, figs 2.1–2.2, 2.6) and some closely related Ordovician genera (Holloway, 2007). Whittington (1963) had first noted the similarities of the Styginidae to the Scutelluidae, and until recently the two families were regarded as synonymous with one another, following Lane and Thomas (1978, 1983). Holloway (2007) revised the genus *Protostygina* Prantl and Přibyl, 1949 (see *Protostygina bohemica* figured by Holloway 2007, figs 1–3) and returned to the concept of the Styginidae as an exclusively Ordovician family of the Illaenina, separate from the Scutelluidae (see Holloway 2007 for a diagnosis of the Styginidae). Within the included genera of Holloway's concept of the Styginidae, is *Harpillaenus* (see *H. arcuatus* figured by Whittington 1963, pl. 20, figs 13, 15–16, pl. 21, text-figs 4 L–N, 5) which is characterised by a highly effaced morphology. *Harpillaenus* was previously considered to be a member of the Illaenidae. The inclusion of this effaced taxon demonstrates the successful separation of what was previously considered a member of the Illaenidae. It is a significant step towards the recognition of different phylogenetic lineages within effaced taxa.

3.4 PHYLOGENY THROUGH ONTOGENY

Ontogenetic forms of closely related trilobite taxa share more similarities with one another than with those of more distantly related taxa (Chatterton *et al.* 1990). The morphological information provided by trilobite larvae can therefore provide important phylogenetic insights. The progressive effacement of certain trilobite taxa through ontogeny has been remarked upon by a number of authors (e.g. Ludvigsen and Chatterton 1980, Fortey and Owens *in* Kaesler 1997, Holloway and Lane 1998,

Webster 2009) and, as Webster (2009) noted, the comparative morphology of ontogenetic stages unaffected by effacement may be of use in resolving the phylogenies of effaced taxa within otherwise non-effaced clades.

Ontogenetic sequences are little known within the Illaenina, but Ludvigsen and Chatterton (1980, fig. 1 and pl. 1) detailed a complete ontogenetic sequence of *Faillaena calva* Chatterton and Ludvigsen , 1976, an effaced member of the Suborder. They remarked on the morphological similarities between the metaprotaspides of *F. calva* and the protaspides of scutelluids. The late meraspis to early holaspis stages of *F. calva* were most comparable with fully mature styginids. The effacement of cephalic and pygidial furrows of *F. calva* that occurs between small and large holaspid stages is prominent. The strong morphological similarity of juvenile specimens of *F. calva* to both scutelluids and styginids suggests a shared common ancestor for these taxa.

Progressive effacement during ontogeny is recognised within other illaenimorph taxa. Smaller specimens of *Excetra* (see *Excetra iotops* Holloway and Lane, 1998, pl. 3, figs 1–19, pl. 4, figs 1–10, 13) exhibit characteristics of scutelluids, including deeper axial furrows, presence of the occipital furrow and a more clearly impressed S1 lateral glabellar muscle impression. Additionally, a new species of *Ligiscus* from the Telychian (Silurian) reefs of North Greenland includes examples of different holaspis ontogenetic stages (Text-fig. 3.1B–E). These show the effacement of what is unequivocally a scutelluid morphology. *Ligiscus* is not only an important example of the gradual effects of effacement through ontogeny, but fully-grown forms show many intermediate characters between non-effaced scutelluids and illaenimorph taxa.

Webster (2009) discussed the ontogeny, systematics and evolution of some effaced Early Cambrian members of the Superfamily Olenelloidea. Taxa such as species of *Peachella* (see *Peachella iddingsi* and *Peachella brevispina* figured by Webster 2009, figs 2–6 and 9–11 respectively) exhibit progressive effacement of their cephala during relatively late stages of ontogeny. Webster (2009) noted that the trend of cephalic effacement during ontogenetic stages mirrors a general stratigraphical and phylogenetic trend. Until more ontogenetic stages are adequately described within the Illaenina, the unequivocal use of pre-effaced morphologies to infer the broader phylogenies is limited. The similarities between early growth stages of illaenimorph taxa and mature scutelluids however, suggest that some illaenimorph taxa belong within the Scutelluidae. These morphological observations are explored in the following phylogenetic analysis.

3.5 PHYLOGENETIC ANALYSIS

Three cladistic analyses were conducted on exemplar members of the Scutelluina, Styginida and Illaenina, to investigate the effects of effacement on the resulting phylogenies. The first two analyses take account of 16 taxa which include effaced, partially effaced and non-effaced morphologies. The third analysis is limited to 11 effaced and partially effaced taxa.

NEXUS Data Editor 0.5.0 (Page 2001) was used for matrix construction, and analyses were conducted using WINCLADA (Nixon 2002) and NONA version 2.0 (Goloboff 1998). In WINCLADA, the heuristic search strategy was used, with 10,000 maximum trees to keep (hold), and 100 replications. The resulting strict consensus trees are presented here. The parsimony ratchet was also applied, with 5 maximum

trees to keep (hold), and 1000 replications. This yielded the same results as the heuristic search strategy. Characters are all unweighted and unordered.

Character coding: As effacement ultimately results in the loss of characters, the number of characters available for analysis of effaced taxa is limited. The characters deemed particularly suitable for analysis are predominantly related to the cephalon. An emphasis is placed on the morphology and relative positions of the lateral glabellar muscle impressions as numerous authors, for example, Stubblefield (1936), Fortey and Owens (1979), and Lane and Thomas (1983), considered that the pattern of glabellar musculature is of fundamental importance when investigating the phylogenies within large groups of trilobites. Ontogenetic, thoracic and ventral characters are not included in the analyses as they are adequately known from only a few illaenimorph taxa. Terminology used follows that of the *Treatise* (Kaesler 1997), except for '*holcos'* (Helbert and Lane *in* Helbert *et al*. 1982); '*cusp'* (Curtis and Lane 1997); '*anterolateral internal pit'*, '*lunette'* and '*omphalus'* (Holloway and Lane 1998).

In total, 30 characters were coded for analyses one and two (Tables 3.1–3.2). For the third analysis, characters specific to non-effaced taxa, such as the presence or absence of palpebral spines, were removed, leaving 25 characters (Tables 3.3–3.4). No uninformative characters are included.

3.5.1 Analysis of effaced and non-effaced taxa

3.5.1.1 Coded taxa

The first two analyses included the following taxa, deemed representative of various subdivisions within the Illaenina. Coded taxa were the type species of the genera concerned whenever possible. The taxa used are listed below:

1) Unequivocal illaenids (*Stenopareia glaber* (Kjerulf, 1865) (see Whittington 1997, figs 8.3, 8.5); *Illaenus sarsi* Jaanusson, 1954).
2) Illaenimorph taxa with obvious morphological characteristics of scutelluids (*Paralejurus campanifer* Hawle and Corda, 1847; *Ligiscus arcanus* Lane and Owens, 1982).
3) Illaenimorph taxa deemed to be effaced scutelluids by Lane and Thomas *in* Thomas (1978) (*Bumastus barriensis* Murchison, 1839; *Cybantyx anaglyptos* Lane and Thomas *in* Thomas, 1978; *Litotix armatus* Lane and Thomas in Thomas, 1978) and *Rhaxeros pollinctrix* (Lane and Thomas, 1978).
4) Illaenimorph taxa described after Thomas and Lane and Thomas (1978) (*Liolalax olibros* Holloway and Lane, 1998; *Excetra iotops* Holloway and Lane, 1998).
5) Scutelluids with some degree of effacement (*Ekwanoscutellum ekwanensis* Přibyl and Vaněk, 1971 (see Norford 1981, fig. 4a, pls 2–4), *Opoa adamsi* Lane, 1972, pl. 59).
6) Non-effaced scutelluids (*Xyoeax eponcus* Holloway, 1996, figs 4–5; *Decoroscutellum haidingeri* Šnajdr, 1960).

3.5.1.2 Outgroup

The analysis was conducted twice using different outgroups, to investigate the effects of having a non-effaced versus an effaced outgroup on the resulting cladograms. The first analysis uses the non-effaced *Perischoclonus capitalis* Raymond, 1925 (see Whittington 1963, pl. 22, pl. 35, figs 10–11, pl. 36, figs 5, 7–8), and the second uses the effaced *Harpillaenus arcuatus* (Billings, 1865). The reasoning behind these choices of outgroup is as follows: firstly, they are both stratigraphically old, occurring in the Middle Ordovician, and secondly they are both members of the Styginidae, an exclusively Ordovician family of the Illaenina. *Perischoclonus* additionally displays many plesiomorphic features.

3.5.1.3 Results

Each analysis produces two trees, and the resulting strict consensus trees are shown in Text-figs 3.2A–B. The strict consensus tree for both analyses have a length of 70 steps, a consistency index of 0.60, and a retention index of 0.75. Homoplasious characters are represented by white circles, and non-homoplasious ones by black circles. Bootstrap analyses using 1000 replications were conducted to assess support at various nodes in the cladograms. The resulting values for these are shown in bold type at the nodes concerned.

Those characters deemed most important in the analyses (those with a CI and RI of 1) are: depth of impression of lateral glabellar muscle impressions S1, S2 and S3 (characters 4–6); connection of lateral glabellar muscle impression S1 to the axial furrow (character 7); impression of cephalic axial furrows (character 11); the presence or absence of an anterolateral internal pit and omphalus (characters 12–13); the presence or absence of a sagittal carina to the glabella (character 14); the presence or

absence of palpebral spines (character 18); cephalic convexity relative to pygidial convexity (character 23); degree of effacement of the radiating ribs on the pygidium (character 25); the presence or absence of a sagittal carina on the pygidium (character 27); the presence or absence of a holcos (character 28); the presence or absence of a posteromedian forward extension of doublure (character 29).

When *Harpillaenus* is used as the outgroup, *Stenopareia* and *Illaenus* form a well constrained group and *Liolalax, Cybantyx* and *Litotix* group together also. The remaining taxa show a general trend of decreasing effacement. When *Perischoclonus* is used as the outgroup, scutelluids exhibiting the least amount of effacement (*Xyoeax* and *Decoroscutellum*) form a well constrained group, and the remaining taxa show a general trend of increasing effacement, with the most effaced taxa separated into two terminal groups, one comprising *Harpillaenus, Stenopareia* and *Illaenus,* and the other comprising *Liolalax, Cybantyx* and *Litotix.* The polarities of both of these analyses are clearly dependent on the degree of effacement exhibited by the outgroup. In both strict consensus trees, this is highlighted by the positions of the styginid taxa (*Harpillaenus* and *Perischoclonus* respectively) which does not make stratigraphical or phylogenetic sense: when not used as the outgroup, they are shown to be amongst the most derived taxa in the analyses. Despite the obvious effects of ordering by effacement, the following groupings are maintained in both analyses: *Stenopareia* + *Illaenus*, *Liolalax* + *Cybantyx* + *Litotix*, *Xyoeax* + *Decoroscutellum*, *Ligiscus* + *Paralejurus.*

Table 3.1. Characters and character states used to analyse effaced and non-effaced taxa.

1. S1 Morphology
   0 Elongate to subquadrate
   1 Kidney-shaped
   2 Subtriangular
   3 Bifurcate
2. S2 morphology
   0 Subcircular-suboval
   1 Transversely elongate
   2 Comma-shaped
3. S3 morphology
   0 Subcircular
   1 Transversely elongate
4. S1 depth of impression
   0 Deeply impressed
   1 Shallow
5. S2 depth of impression
   0 Deeply impressed
   1 Shallow
6. S3 depth of impression
   0 Deeply impressed
   1 Shallow
7. Connection of S1 to axial furrow
   0 S1 connected to axial furrow
   1 S1 isolated from axial furrow
8. Depth of impression of occipital furrow
   0 Visible
   1 Not visible
9. Relative proximity of S1, S2 and S3
   0 S2 roughly equidistant from S1 and S3
   1 S2 much closer to S1 than to S3
   2 S2 closer to S3 than to S1
10. Occipital node
    0 Visible
    1 Not visible
    2 Present as a spine
11. Impression of cephalic axial furrows
    0 Clearly impressed to anterior border or omphalus
    1 Clearly impressed posteriorly of palpebral lobe, but weaker anteriorly
    2 Weak throughout their course
12. Anterolateral internal pit
    0 Absent
    1 Present
13. Omphalus
    0 Absent
    1 Present
14. Sagittal carina to glabella
    0 Absent or extremely faint
    1 Present
15. Cephalic axial furrows divergance point
    0 Do not diverge
    1 Diverge at lunettes
    2 Diverge anteriorly to lunettes
    3 Diverge throughout entire course
16. Lunettes
    0 Large and elongate
    1 Small and circular
17. Anterior border and preglabellar furrow
    0 Present
    1 Absent medially
    2 Absent
18. Palpebral spines
    0 Absent
    1 Present
19. Sagittal length cranidium relative to transverse width across palpebral lobes
    0 Wider than long
    1 Length roughly equal to width
    2 Longer than wide
20. Cranidial convexity
    0 High convexity
    1 Moderate convexity
    2 Low convexity
21. Eye size
    0 Comprising under one quarter total pygidial sagittal length
    1 Comprising over one quarter total pygidial sagittal length
22. Genal spine
    0 Present
    1 Absent
23. Cephalic convexity relative to pygidial convexity
    0 Cephalon much more convex than pygidium
    1 Cephalon and pygidium of roughly equal convexity
24. Maximum length of pygidium relative to maximum width
    0 Pygidium under 50% as long as wide
    1 Pygidium 50-80% as long as wide
    2 Pygidium over 80% as long as wide
25. Radiating ribs on pygidium
    0 Absent
    1 Present but effaced
    2 Present and clear
26. Pygidial axis definition
    0 Only defined anteriorly
    1 Not visible
    2 Visible anteriorly and laterally
27. Sagittal carina to pygidium
    0 Absent
    1 Present
28. Holcos
    0 Very weak or absent
    1 Present and clear
29. Posteromedian forward extension of doublure
    0 Absent
    1 Present
30. Prominant median arch on pygidium
    0 Present
    1 Absent

Taxa	Characters																														
	1	**2**	**3**	**4**	**5**	**6**	**7**	**8**	**9**	**10**	**11**	**12**	**13**	**14**	**15**	**16**	**17**	**18**	**19**	**20**	**21**	**22**	**23**	**24**	**25**	**26**	**27**	**28**	**29**	**30**
Harpillaenus	?	?	?	1	1	1	?	0	?	0	1	0	0	0	0	0	2	0	0	0	0	0	0	0	0	0	0	0	0	1
Perischoclonus	3	1	0	0	0	0	0	0	0	1	0	0	0	0	3	0	0	0	1	2	0	0	1	1	2	2	0	0	0	1
Ligiscus	0	0	1	1	1	1	0	1	1	0	0	0	0	0	2	1	2	0	0	2	1	0	1	1	1	2	0	0	0	1
Cybantyx	0	1	1	1	1	1	1	1	0	0	1	1	1	1	1	0	0	0	0	1	1	1	1	2	0	1	1	1	0	1
Bumastus	1	1	1	1	1	1	1	1	2	0	1	?	0	0	1	0	2	0	0	1	1	1	1	1	0	1	0	0	0	1
Litotix	0	1	1	1	1	1	1	1	2	0	1	1	1	1	1	0	2	0	0	1	1	0	1	1	0	1	1	1	0	1
Liolalax	?	?	?	1	1	1	?	1	?	0	1	1	1	0	1	0	2	0	0	1	1	1	1	1	0	1	0	0	0	1
Rhaxeros	1	0	1	1	1	1	1	1	2	1	0	0	0	0	1	1	1	0	1	1	1	1	1	2	1	1	0	0	0	1
Excetra	1	2	1	1	1	1	1	1	2	1	1	0	0	0	2	0	2	0	1	1	0	1	1	1	0	1	0	0	0	1
Paralejurus	0	0	1	1	1	1	0	0	1	0	0	0	0	0	1	0	0	0	1	1	1	0	1	2	1	2	0	0	0	1
Stenopareia	0	?	0	1	1	1	1	1	0	0	1	0	0	0	0	0	2	0	0	0	0	1	0	1	0	0	0	0	1	0
Illaenus	0	?	0	1	1	1	1	1	2	0	1	0	0	0	0	0	2	0	0	0	0	1	0	1	0	2	0	0	1	0
Ekwanoscutellum	0	0	0	1	1	1	0	0	1	1	0	0	0	0	2	0	1	0	1	2	0	0	1	2	2	2	0	0	0	1
Xyoeax	2	0	1	0	0	0	0	0	0	2	0	0	0	0	3	0	0	1	0	2	0	0	1	1	2	2	0	0	0	1
Opoa	0	0	0	0	1	1	0	0	1	?	0	0	0	0	2	0	0	0	1	2	0	0	1	1	2	2	0	0	0	1
Decoroscutellum	1	0	1	0	0	0	0	0	0	2	0	0	0	0	3	0	0	1	0	2	0	?	1	1	2	2	0	0	0	1

Table 3.2. Matrix of character states used to analyse effaced and non-effaced taxa.

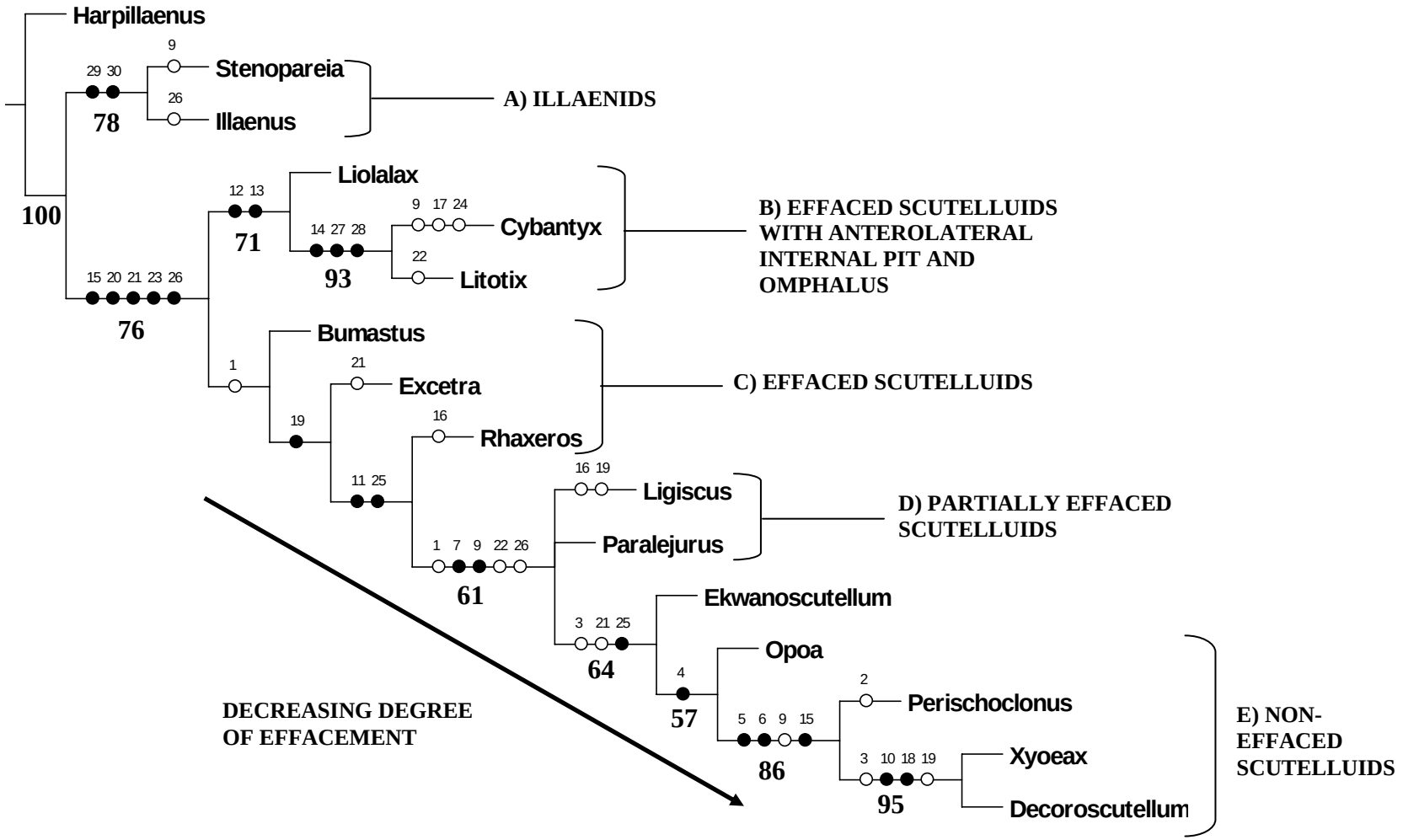

Text-fig. 3.2A. Strict consensus tree of two produced with *Harpillaenus* as outgroup. Length = 70, CI = 0.60, RI = 0.75. Bootstrap values are displayed at their associated nodes in bold type.

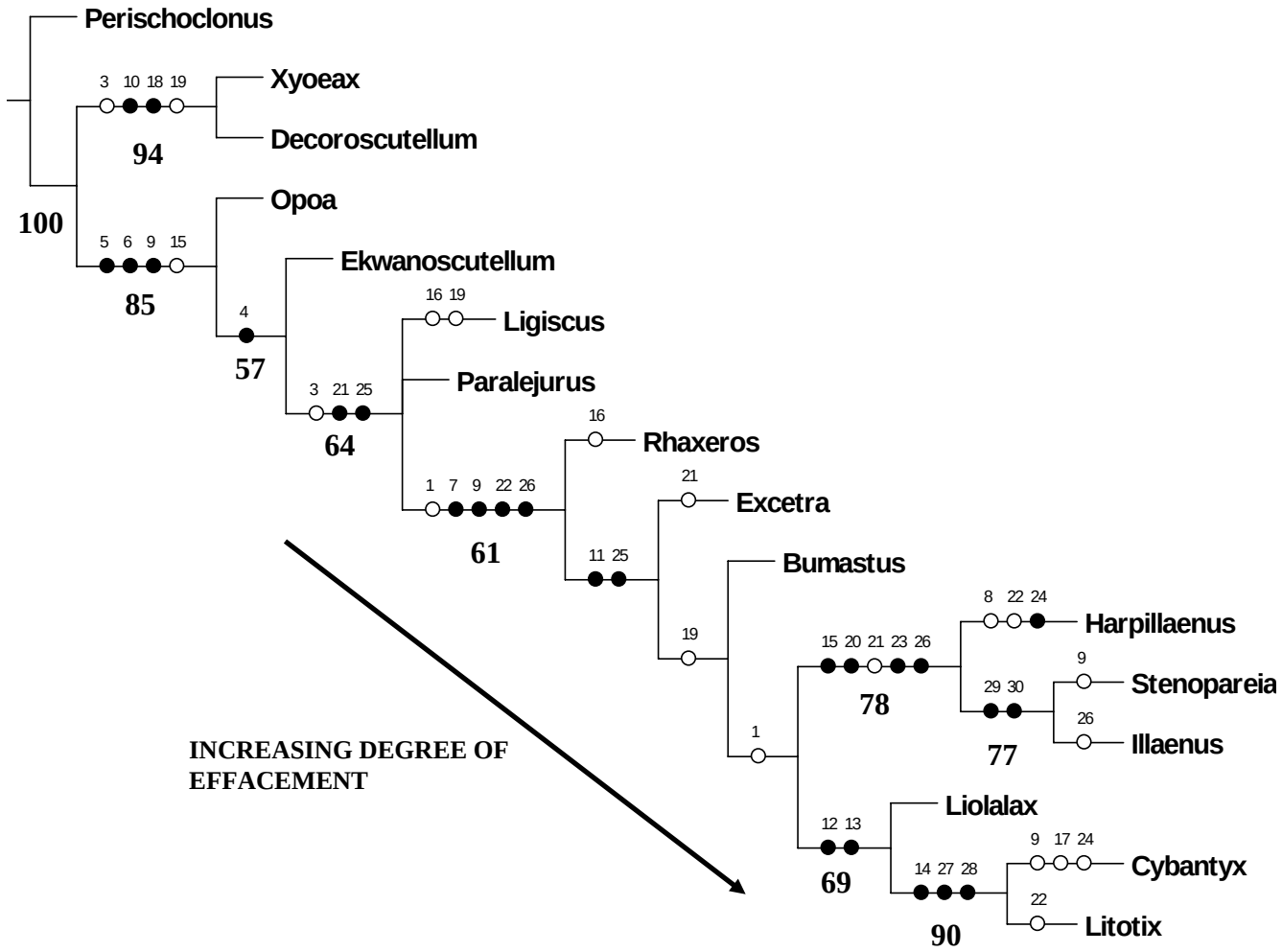

Text-fig. 3.2B. Strict consensus tree of two produced with *Perischoclonus* as outgroup. Length = 70, CI = 0.60, RI = 0.75. Bootstrap values are displayed at their associated nodes in bold type.

3.5.2 Analysis of effaced taxa

3.5.2.1 Coded taxa and outgroup

In order to remove the effects of ordering by the degree of effacement, all non-effaced taxa were removed from the analysis. The following effaced taxa were analysed: *Stenopareia, Illaenus, Paralejurus, Ligiscus,Bumastus, Cybantyx, Litotix, Rhaxeros, Liolalax, Excetra*. *Harpillaenus arcuatus* was chosen as the outgroup for the same reasons as in section 3.5.1.

3.5.2.2 Results

A single most parsimonious tree was produced (Text-fig. 3.3) with a length of 44 steps, a consistency index of 0.70, and a retention index of 0.70. Homoplasious characters are represented by white circles, and non-homoplasious ones by black circles. Bootstrap analyses using 1000 replications were conducted to assess support at various nodes in the cladograms. The resulting values for these are shown in bold type at their nodes.

Those characters deemed most important in the analyses (those with a CI and RI of 1) are: morphology of lateral glabellar muscle impressions S2 and S3 (characters 2–3); connection or isolation of S1 to axial furrow (character 4); depth of impression of cephalic axial furrows (character 8); the presence or absence of an anterolateral internal pit and omphalus (characters 9–10); the presence or absence of a sagittal carina to the glabella (character 11); degree of cranidial convexity (character 15); cephalic convexity relative to pygidial convexity (character 18); degree of effacement of the radiating ribs on the pygidium (character 20); the presence or absence of a holcos (character 23); the presence or absence of a posteromedian forward extension

of doublure (character 24); the presence or absence of a prominent median arch on pygidium (character 25).

The resulting cladogram maintains the same relationships between effaced taxa as the analysis in section 3.5.1, which also uses *Harpillaenus* as the outgroup. The most significant groupings are as follows:

- *Stenopareia* and *Illaenus* form a group distinct from all other taxa, and are united by the presence of a prominent median arch on the pygidium, and a posteromedian forward extension of doublure (characters 24 and 25 respectively).
- *Liolalax, Cybantyx* and *Litotix* are united by the presence of an omphalus and anterolateral internal pit (characters 9 and 10 respectively).
- *Ligiscus* and *Paralejurus* which display morphological characteristics of scutelluids, are closest to *Rhaxeros, Bumastus,* and *Excetra*. The significance of this grouping should be taken with caution; the taxa are not particularly morphologically similar and are perhaps united by the partially effaced nature of their exoskeletons.

Table 3.3. Characters and character states used to analyse effaced taxa.

1. S1 Morphology
   0 Elongate to subquadrate
   1 Kidney-shaped
   2 Subtriangular
   3 Bifurcate
2. S2 morphology
   0 Subcircular-suboval
   1 Transversely elongate
   2 Comma-shaped
3. S3 morphology
   0 Subcircular
   1 Transversely elongate
4. Connection of S1 to axial furrow
   0 S1 connected to axial furrow
   1 S1 isolated from axial furrow
5. Depth of impression of occipital furrow
   0 Visible
   1 Not visible
6. Relative proximity of S1, S2 and S3
   0 S2 roughly equidistant from S1 and S3
   1 S2 much closer to S1 than to S3
   2 S2 closer to S3 than to S1
7. Occipital node
   0 Visible
   1 Not visible
   2 Present as a spine
8. Impression of cephalic axial furrows
   0 Clearly impressed to anterior border or omphalus
   1 Clearly impressed posteriorly of palpebral lobe, but weaker anteriorly
   2 Weak throughout their course
9. Anterolateral internal pit
   0 Absent
   1 Present
10. Omphalus
    0 Absent
    1 Present
11. Sagittal carina to glabella
    0 Absent or extremely faint
    1 Present
12. Cephalic axial furrows divergance point
    0 Do not diverge
    1 Diverge at lunettes
    2 Diverge anteriorly to lunettes
    3 Diverge throughout entire course
13. Lunettes
    0 Large and elongate
    1 Small and circular
14. Sagittal length cranidium relative to transverse width across palpebral lobes
    0 Wider than long
    1 Length roughly equal to width
    2 Longer than wide
15. Cranidial convexity
    0 High convexity
    1 Moderate convexity
    2 Low convexity
16. Eye size
    0 Comprising under one quarter total pygidial sagittal length
    1 Comprising over one quarter total pygidial sagittal length
17. Genal spine
    0 Present
    1 Absent
18. Cephalic convexity relative to pygidial convexity
    0 Cephalon much more convex than pygidium
    1 Cephalon and pygidium of roughly equal convexity
19. Maximum length of pygidium relative to maximum width
    0 Pygidium under 50% as long as wide
    1 Pygidium 50-80% as long as wide
    2 Pygidium over 80% as long as wide
20. Radiating ribs on pygidium
    0 Absent
    1 Present but effaced
    2 Present and clear
21. Pygidial axis definition
    0 Only defined anteriorly
    1 Not visible
    2 Visible anteriorly and laterally
22. Sagittal carina to pygidium
    0 Absent
    1 Present
23. Holcos
    0 Very weak or absent
    1 Present and clear
24. Posteromedian forward extension of doublure
    0 Absent
    1 Present
25. Prominant median arch on pygidium
    0 Present
    1 Absent

Taxa	Characters																								
	1	**2**	**3**	**4**	**5**	**6**	**7**	**8**	**9**	**10**	**11**	**12**	**13**	**14**	**15**	**16**	**17**	**18**	**19**	**20**	**21**	**22**	**23**	**24**	**25**
Harpillaenus	?	?	?	?	0	?	0	1	0	0	0	0	0	0	0	0	0	0	0	0	0	0	0	0	1
Ligiscus	0	0	1	0	1	1	0	0	0	0	0	2	1	0	2	1	0	1	1	1	2	0	0	0	1
Cybantyx	0	1	1	1	1	0	0	1	1	1	1	1	0	0	1	1	1	1	2	0	1	1	1	0	1
Bumastus	1	1	1	1	1	2	0	1	?	0	0	1	0	0	1	1	1	1	1	0	1	0	0	0	1
Litotix	0	1	1	1	1	2	0	1	1	1	1	1	0	0	1	1	0	1	1	0	1	1	1	0	1
Liolalax	?	?	?	?	1	?	0	1	1	1	0	1	0	0	1	1	1	1	1	0	1	0	0	0	1
Rhaxeros	1	0	1	1	1	2	1	0	0	0	0	1	1	1	1	1	1	1	2	1	1	0	0	0	1
Excetra	1	2	1	1	1	2	1	1	0	0	0	2	0	1	1	0	1	1	1	0	1	0	0	0	1
Paralejurus	0	0	1	0	0	1	0	0	0	0	0	1	0	1	1	1	0	1	2	1	2	0	0	0	1
Stenopareia	0	?	0	1	1	0	0	1	0	0	0	0	0	0	0	0	1	0	1	0	0	0	0	1	0
Illaenus	0	?	0	1	1	2	0	1	0	0	0	0	0	0	0	0	1	0	1	0	2	0	0	1	0

Table 3.4. Matrix of character states used to analyse effaced taxa.

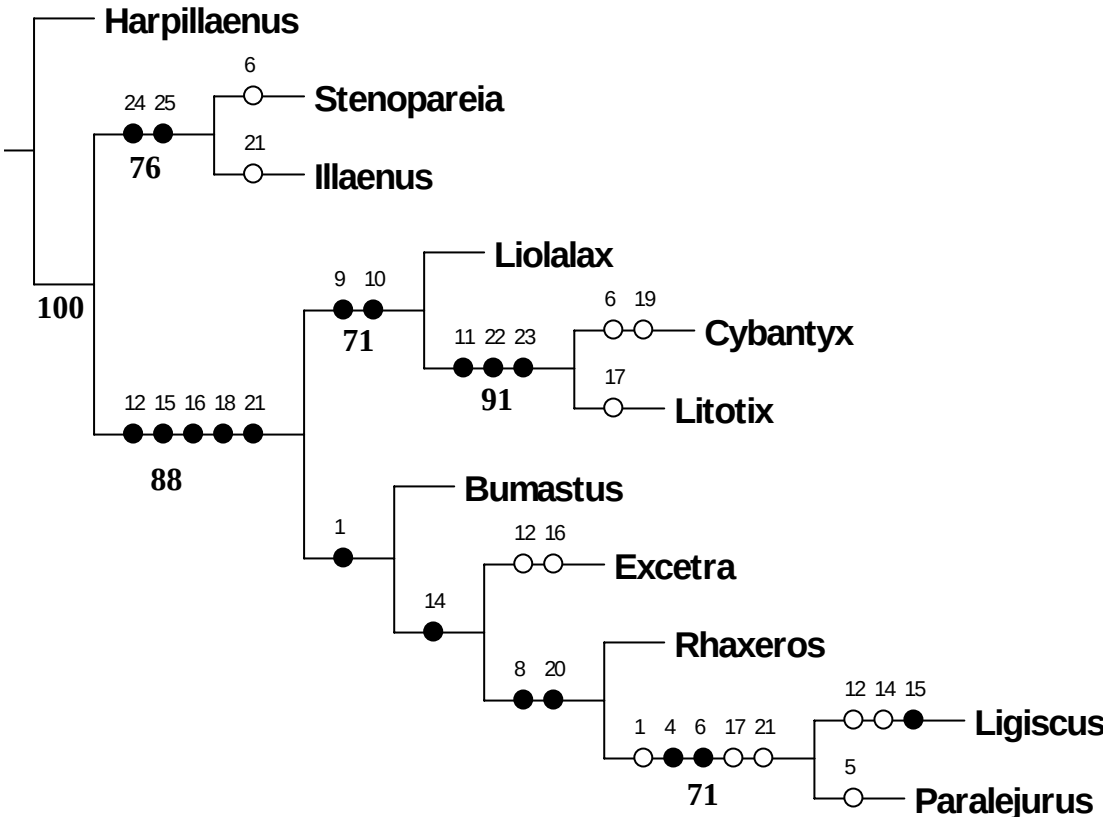

Text-fig. 3.3. The single most parsimonious tree produced through analysis of effaced members of the Illaenina. Length = 44; CI = 0.70; RI = 0.70. Bootstrap values are displayed at their associated nodes in bold type.

3.5.3 Principle Coordinates Analysis (PCO)

The data matrix for the effaced taxa was analysed using the data-analysis software PAST (PAleontological STatistics) (Hammer et al. 2001; Hammer and Harper 2006). Principle coordinates analysis is an ordination method which projects a multivariate dataset into two or three dimensions, enabling visualisation of the distances between data points (Hammer and Harper 2006). A PCO analysis of the data matrix (Table 3.4) used to produce the cladogram shown in Text-fig. 3.4 will thus highlight any discrepancies in the distances between the groups of taxa produced by cladistic analysis. The resulting PCO plot, created using the Euclidean Similarity Index, is shown in Text-fig. 3.4. The PCO plot supports the groups produced by the cladistic analysis, and groups are distinct with no overlap. Axes (coordinates) 1 and 2 (shown) have most control on the distribution of data points. Axis 1 has an eigenvalue of 22.171, accounting for 34% of observed variation, and axis 2 has an eigenvalue of 13.036, accounting for 20% of observed variation. These axes produce the following groupings: *Ligiscus* + *Paralejurus* + *Rhaxeros*, *Cybantyx* + *Litotix* + *Liolalax*, *Bumastus* + *Excetra* and *Illaenus* + *Harpillaenus* + *Stenopareia*. These groups agree well with those produced by the cladistic analysis. However, some relative distances are more obvious: *Rhaxeros* is closer to *Ligiscus* and *Paralejurus* than is implied in the cladogram, and *Harpillaenus* is closer to *Stenopareia*. The remaining axes are not shown. Axis 3 has an eigenvalue of 10.215, accounting for 16% of observed variation. It differs from axes 1 and 2 by showing a greater distance between *Cybantyx* and *Stenopareia* and their respective groups. All other axes each account for fewer than 10% of observed variation.

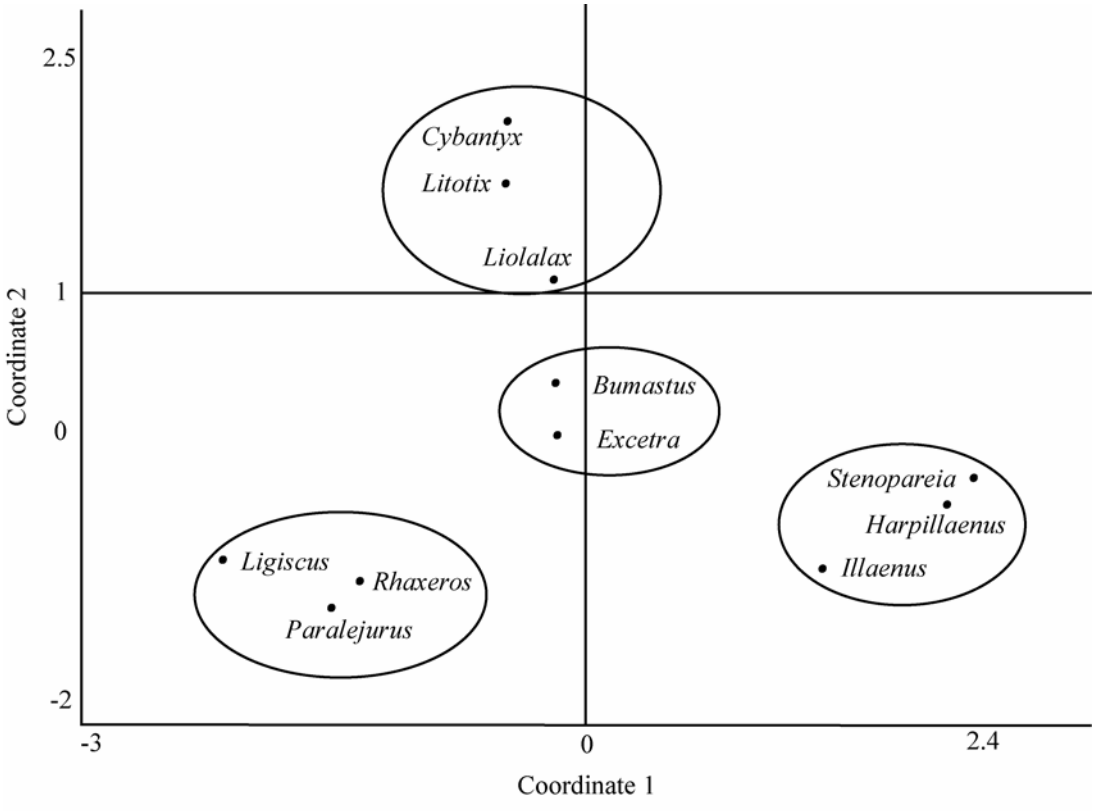

Text-fig. 3.4. Axes (coordinates) one and two of a Principal Coordinates analysis (PCO) of the data matrix shown in Table 3.4.

3.6 CONCLUSIONS

1. Effacement is a complex character state. Cladistic analyses involving effaced and non-effaced members of the Illaenina is controlled largely by the degree of effacement.

2. Trilobites were plesiomorphically non-effaced. Use of an effaced outgroup, however, results in effacement being perceived as a plesiomorphic character state. A non-effaced outgroup results in effacement being perceived as an apomorphic character state, and therefore represents the correct polarity.

3. It is impossible to remove all characters affected by effacement in a phylogenetic analysis. Restricting the analysis to effaced morphologies minimises the effects of effacement on the resulting cladograms.

4. A clade comprising unequivocal members of the Family Illaenidae is robustly supported when phylogenetic analysis is limited to effaced taxa. This suggests that effacement has derived more than once within the Illaenina.

CHAPTER FOUR

TRILOBITE ASSOCIATIONS, TAPHONOMY, LITHOFACIES AND ENVIRONMENTS OF THE SILURIAN REEFS OF NORTH GREENLAND

Summary: Llandovery (Silurian) reefs in North Greenland have yielded extensive collections of remarkably well preserved trilobites dominated by scutelluids. These collections provide a unique opportunity to analyse the reefs and their trilobite faunas in a palaeoenvironmental context, and the study highlights the importance of pre-existing collections, to which further scientific value can be added. Counts of trilobite sclerites from thirteen reef localities are analysed using cluster and correspondence analyses to identify trilobite associations, and taphonomic signatures. Lithofacies analysis additionally aids application of a detailed palaeoenvironmental context. Seven trilobite associations are identified: Scutelluid-Illaenimorph; Scutelluid; Scutelluid-Cheirurid; Scutelluid-Harpetid; Proetid; Encrinurid; Illaenimorph. The number of associations highlights the variable distribution of taxa within the reefs, which is partly a reflection of intense hydrodynamic sorting in reef environments. Trilobites are predominantly associated with a cement-rich microbial lithofacies; it is apparent that microbial processes were the principal contributors to the production of carbonate mud, and played a significant role in development of the Greenland reefs. The observed associations comprise time-averaged event beds in an otherwise low energy and slow sedimentation regime, and possibly result from storm activity remobilising sclerites, and depositing them within depressions and cavity fills within the reef surface. Correspondence analysis reveals two distinct taphonomic signatures within the reef, and transport distance is the primary influence on these. The Proetid

Association is readily separated from the others by its taphonomic attributes, representing the least amount of transport, and suggesting the taxa involved took advantage of the more sheltered niches within the reef. This is the first study of reef-dwelling trilobites to take advantage of multivariate techniques to identify associations and describe their taphonomic attributes. In particular, the effectiveness of correspondence analysis in recognising taphonomic signatures is demonstrated.

4.1 INTRODUCTION

REEFS are sites of major biological productivity, yet remain incompletely understood with respect to the taphonomic controls on their biota. These controls are amongst the most complex of any environment, and their analysis is key to the understanding of reef faunas. Trilobites were both abundant and diverse in the reefs of the Silurian, and their mobile lifestyle and rapid post-mortem disarticulation makes them excellent subjects for taphonomic analysis. As their skeletons comprise sclerites of varying size and shape, patterns produced by hydrodynamic sorting are readily identified (Westrop 1986; Speyer 1987; Mikulic 1990; Westrop and Rudkin 1999). Despite this, few studies have directly evaluated the effects of taphonomy on reef trilobites, the exceptions being those of Mikulic (1979, 1981, 1983, 1990, 1999), Suzuki and Bergström (1999), and Westrop and Rudkin (1999).

The trilobite faunas considered here are from the Telychian (Llandovery, Silurian) reefs of North Greenland (Text-fig. 4.1A). The reef tract, which extends some 850 km along strike, is exposed across North Greenland (Sønderholm and Harland 1989). It represents the first large-scale reef development in the Silurian, and is the most extensive of the late Llandovery reef complexes (Copper and Brunton 1991). The reefs, which can have individual thicknesses of 300 m (Lane and Thomas

1979), have yielded thousands of calcitic trilobite sclerites. These sclerites, as with the reefs themselves, are remarkably well preserved, providing the most significant collections to date from any early Silurian reef locality. Numerous concentrations of Silurian reefs in the Great Lakes area of North America are mainly younger (Wenlock) than those in Greenland. Those reefs and their trilobite faunas are well studied, but have been subject to pervasive dolomitization (Copper and Brunton 1991). The abundance and diversity of trilobite faunas found in Silurian reefs, is however variable. Other Silurian reefs, for example those occurring within the Much Wenlock Limestone Formation in the United Kingdom, have only rare trilobites in the reefs themselves. The highest diversity of trilobite faunas is found associated with reef-flanking sediments and coeval bedded strata (Ray and Thomas 2007).

Trilobite associations denote recurrent assemblages of trilobites of similar taxonomic composition. The term community, in its biological sense, cannot be applied strictly to fossil assemblages as it refers to populations of organisms actually alive at a specific time. This is impossible to establish in the fossil record, where a degree of time averaging is inevitable. The term community is well-established and used extensively in the published literature (e.g. Fortey 1975) however, to denote recurrent groups of trilobites which were thought to have lived together. For this reason, the term community is used here to represent the broader, sometimes long-ranging, associations of trilobites recognised from similar palaeoenvironments.

Fortey (1975) provided the first quantitative study of trilobite communities, based on the Valhallfonna Formation (Ordovician, Spitsbergen), and defined three main community-types whose distribution was related to different palaeoenvironments. These community types were named after either one or two of the dominant trilobite taxa therein. Fortey's Illaenid-Cheirurid Community, which had

a shallow water ‘perhaps reefal’ origin (p. 340), best encompasses the trilobite associations described here. The present study, and others of reef-dwelling trilobites (Lane 1972; Mikulic 1981, 1999; Suzuki and Bergström 1999; Thomas and Lane 1999; Westrop and Rudkin 1999) suggest that, although Palaeozoic reef environments are characterized by a strikingly similar array of recurring trilobite morphotypes, there is much smaller-scale variation within each community. For example, in the associations described here, neither illaenids nor cheirurids comprise the dominant trilobite taxa.

As well as providing a wealth of taxonomic data upon which to study varying associations, the predominantly disarticulated sclerites are ideal for investigating taphonomic attributes of the reef environments. Taphonomic processes can produce preservable signatures or taphonomic signatures that can be used as palaeoenvironmental indicators (Perry and Smithers 2006). This study is the first to utilize the extensive collections of trilobite faunas existing from the reefs of North Greenland, in a combined lithological and taphonomic framework.

The use of these collections in this manner highlights the case that collection-based studies are not, and should not be limited to those of a taxonomic nature. Studies such as those of Olszewski and Erwin (2009) have demonstrated the potential of museum collections to answer topical research questions, despite being collected with different strategies to those which would be employed today. The extensive Cooper and Grant brachiopod collections studied by Olszewski and Erwin (2009) which, like the collections studied here, would not be able to be duplicated now, had previously been the focus of other successful palaeoecological studies (Grant 1971; Erwin 1989; Wood *et al.* 1996). Paterson *et al.* (2007) demonstrated the use of

museum collections to answer taphonomic questions, describing the taphonomy and palaeoecology of the trilobite *Balcoracania dailyi*.

Principally, the purposes of this study are fourfold: firstly, to illustrate the taphonomic value of museum collections; secondly, to add scientific value to pre-existing collections. Although pre-existing field-scale sedimentological observations are lacking, thin section analysis has provided microfacies data which can be interpreted in a palaeoenvironmental context; thirdly, to highlight the importance of intra-environmental taphonomic studies, which enable recognition of fine-scale faunal variation and any ecological structuring, highlight potential collection biases, and determine any fine-scale environmental variability; finally, to show the potential of correspondence analysis in recognizing taphonomic signatures.

A

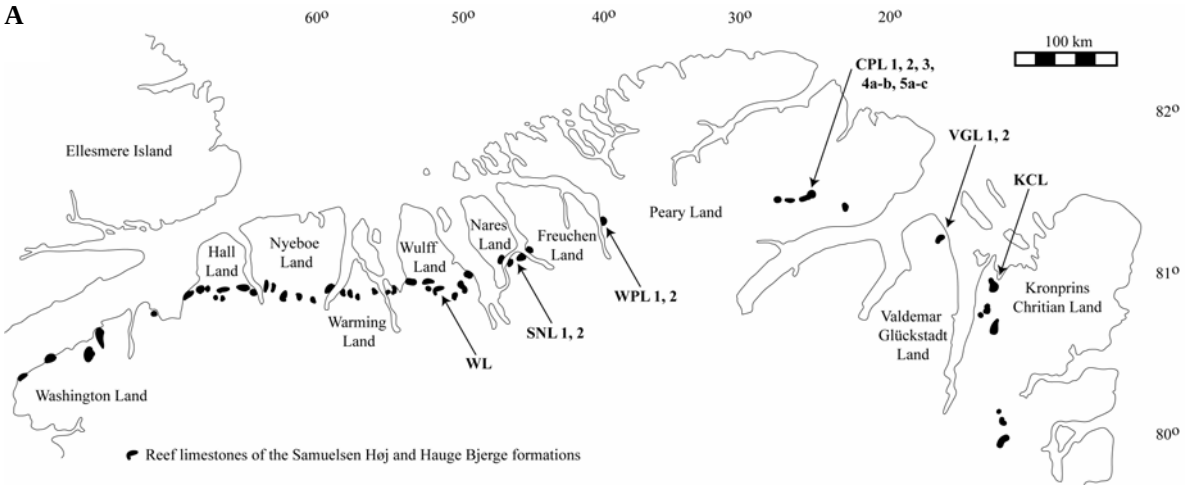

B

Locality	Sample	GGU numbers
Wulff Land	WL	298504–298506
South Nares Land	SNL 1	298930
	SNL 2	298924
Western Peary Land	WPL 1	301314, 301318–9, 301323–6
	WPL 2	198833–6, 198838, 198842–6
Central Peary Land	CPL 1	198115–6, 198226
	CPL 2	198135–198223
	CPL 3	198225
	CPL 4a, b	274654
	CPL 5a, b, c	274689
Valdemar Glückstadt Land	VGL 1	275038
	VGL 2	275044
Kronprins Christian Land	KCL 1	275015

Text-fig. 4.1A. Map of North Greenland showing distribution of Silurian reefs (in black), adapted from Sønderholm & Harland (1989). Sample localities are indicated.

B. Sample information.

4.2 MATERIAL PROCESSING AND DATA COLLECTION

The material on which this study is based was collected during the North Greenland reconnaissance geological mapping programme of the Geological Survey of Greenland (at the time GGU, now merged with DGU to form GEUS) in the 1970s and 1980s. Palaeontological samples were not collected systematically, but were taken from when and where was practicable.

Samples are distinguished by their 'GGU' numbers. Material from Wulff Land was collected from contemporaneous strata between reefs. GGU samples from the same reefs (with identical locality information) were grouped together, unless notably different in composition. The terminology used to denote collections therefore comprises an abbreviated locality, and a number to distinguish between reefs, e.g. WPL1 denotes western Peary Land, reef 1 (Table 4.1B). Likewise, samples which had obvious inter-sample differentiation were treated as separate; CPL4 and CPL5 both comprise distinct associations, each of which was counted separately and so are referred to as CPL4a and b, and CPL5a, b and c. The study was conducted mostly at family level, the term 'Illaenimorph' is the exception, being used to denote any highly effaced taxon (e.g. *Cybantyx*, *Stenopareia*) without implying particular familial affinities.

In total, over 400 kg of rock was available, and this was broken down to an average size of 1cm^2, ensuring that all sizes of trilobite sclerites were available for counting. Trilobite type, sclerite type and degree of fragmentation (if each individual sclerite was under or over 50% complete) were recorded for each sample, and all identifiable sclerites were counted, including thoracic segments. Only samples comprising >50 sclerites, were used. In total, 4287 individual counts were made. Sclerites <25% complete were not counted unless they represented the sole

occurrence of a particular type of trilobite. The percentage of trilobite individuals was calculated from the greater of the following groupings: (cephala + cranidia + cephalothoraces) and (pygidia + thoracopygidia).

All multivariate analyses were conducted using the data-analysis software PAST (PAleontological STatistics) (Hammer *et al.* 2001; Hammer and Harper 2006).

4.3 TRILOBITE ASSOCIATIONS

Scutelluids dominate the Silurian trilobites of North Greenland, comprising over 50% of the faunas studied (Text-fig. 4.2). In order of decreasing abundance, other numerically significant trilobites within the reef facies are: illaenimorphs, cheirurids, encrinurids, and proetids. Harpetids, lichids, odontopleurids, calymenids and phacopids constitute rarer components.

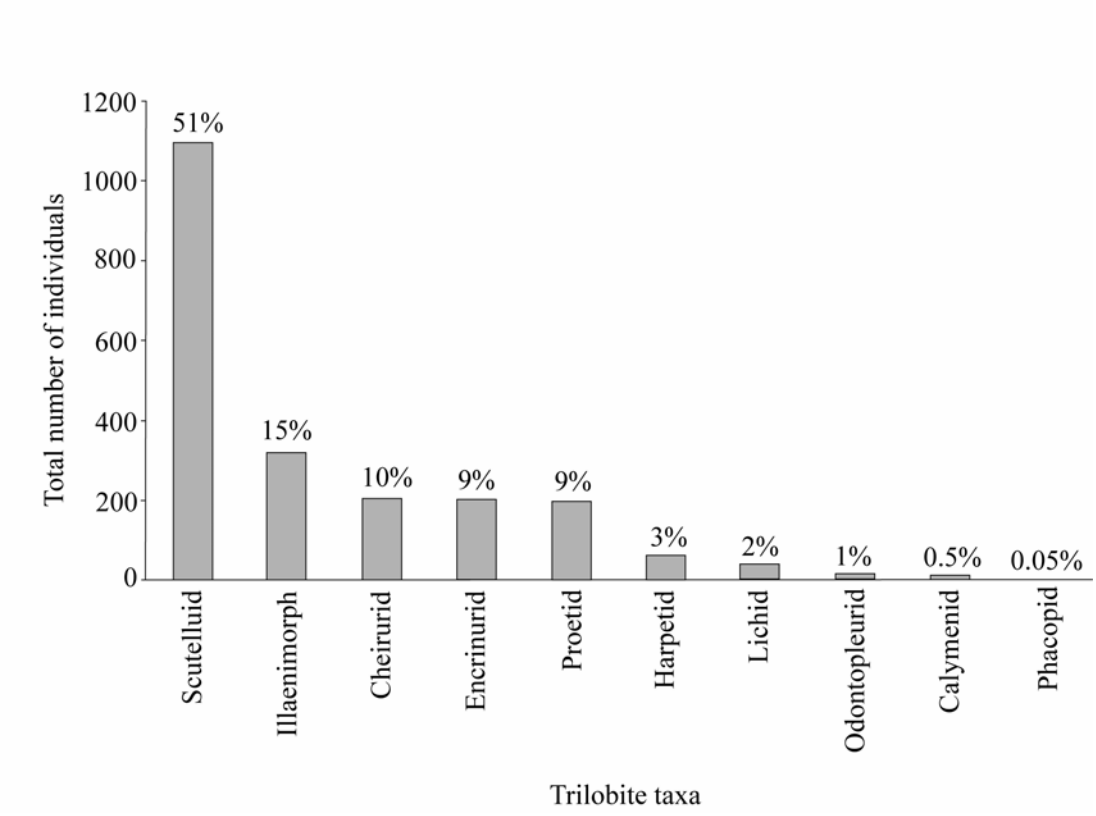

Text-fig. 4.2. Relative abundances of trilobites studied, based on number of trilobite individuals calculated.

4.3.1 Identification of the associations

Hierarchical cluster analysis is an exploratory technique used to identify groups and subgroups in a multivariate dataset (Hammer and Harper 2006). It can be very useful for large, heterogeneous data sets, and there is an extensive literature concerning applications of the technique (Shi 1993). Here, it is used to group reef localities (= samples) according to the trilobites they contain, and therefore provides a means of identifying associations (groups of commonly recurring trilobites).

Before entry into the PAST programme, absolute counts were converted into percentages to remove the effects of sample size (only samples with over 50 individual counts were included). The analysis was run using the paired group algorithm and the chord similarity measure, the latter of which normalises for absolute abundances, to ensure that rarer trilobites are not neglected in the analysis (Hammer and Harper 2006). The resulting dendrogram is shown in Text-fig. 4.3.

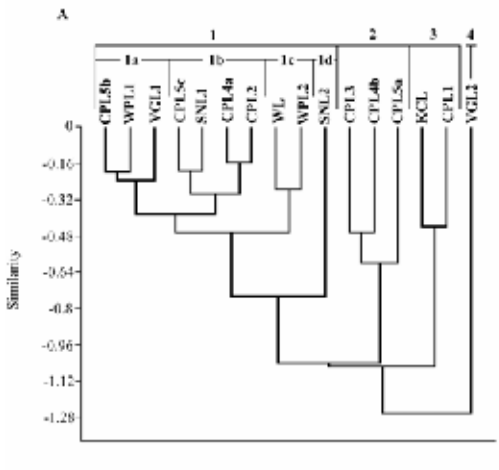

B

			Trilobite taxa/morphotype									
Cluster	Sample	N	Calymenid	Cheirurid	Encrinurid	Harpetid	Illaenimorph	Lichid	Odontopleurid	Proetid	Phacopid	Scotiellid
1a	CPL5b	885	0	8	11	1	**23**	1	0	3	0	53
	WPL1	239	2	16	4	2	**24**	2	0	2	0	**49**
	VGL1	110	0	9	9	3	**32**	0	0	4	0	**43**
1b	CPL5c	553	0	3	3	1	18	2	1	1	0	**71**
	SNL1	433	0	2	2	0	5	3	0	0	0	**88**
	CPL4a	57	0	11	14	0	11	4	4	4	0	**54**
	CPL2	530	3	10	11	0	8	1	1	10	0	**55**
1c	WL	348	2	32	3	1	3	1	1	1	1	**57**
	WPL2	183	0	24	3	14	10	0	0	0	0	**49**
1d	SNL2	108	0	19	0	**36**	4	4	0	2	0	**36**
2	CPL3	94	0	3	**22**	0	6	3	0	36	0	31
	CPL4b	99	0	6	2	0	2	0	10	50	0	30
	CPL5a	275	0	2	6	1	1	1	0	**85**	0	6
3	KCL	147	0	5	**44**	6	6	1	1	9	0	27
	CPL1	105	1	4	**59**	0	7	9	3	8	0	8
4	VGL2	121	0	5	2	0	**91**	2	0	0	0	0

Text-fig. 4.3A. Dendrogram from hierarchical cluster analysis using the paired group algorithm and the chord similarity measure. Samples are clustered according to the trilobites which they contain. 1, 2 and 3 denote superclusters; 4 denotes the non-clustering strand; 1a, 1b, 1c and 1d denote clusters; CPL5b etc. denote sample numbers.

B. Percentage values of trilobites per sample and cluster. Dominant taxa which characterise the clusters are shown in bold.

Three superclusters, and one non-clustering sample are identified. The superclusters are almost equally distinct, as shown by the near trichotomous branching of the dendrogram. Supercluster 1 is the largest, comprising 10 samples, all with a high abundance of scutelluids, and demonstrates the dominance of this trilobite family within the reefs. Within this, four clusters are present: 1a comprises those samples dominated by both scutelluids and illaenimorphs (CPL5b, WPL1, VGL1); 1b comprises samples with over 50% scutelluids (CPL5c, SNL1, CPL4a, CPL2); 1c comprises samples dominated by scutelluids and cheirurids (WL, WPL2); 1d is dominated by scutelluids and harpetids (SNL2). Supercluster 2 comprises samples dominated by proetids (CPL3, CPL4b and CPL5b), and Supercluster 3 comprises the two samples numerically dominated by encrinurids (KCL and CPL1). VGL2 is the non-clustering sample (4), and it is distinct in being the only association to comprise a significantly high proportion (91%) of a single trilobite type; the illaenimorphs. Reef localities in close geographical proximity do not cluster together, and the inter-reef sample from Wulff Land (WL) does not form a distinct association.

ANOSIM (ANalysis Of SIMilarities) is a non-parametric test for difference between groups of multivariate data points (Hammer and Harper 2006). Ivany *et al.* (2009) provided a good summary of the technique and successfully applied it to statistically distinguish faunas from different formations in the Middle Devonian Hamilton Group. Other uses include those by Currano (2009) and Tomašových and Kidwell (2009), to test for differences between groups of samples. ANOSIM was applied to the four superclusters identified here in order to test for significant differences between them. With 5000 permutations, and using chord, Bray-Curtis, Morista and Euclidean distance measures, the test statistic is consistently high (R =

0.92–0.98) and the p value remains <0.005, proving significant differences between groupings and thus supporting the results of the cluster analysis.

4.3.2 Scutelluid-Illaenimorph Association (Cluster 1a)

The Scutelluid-Illaenimorph Association is characterized by a dominance of scutelluids (over 40%), and a significant proportion of illaenimorphs (over 20%). It is recognized from central Peary Land (CPL5b), western Peary Land (WPL1) and Valdemar Glückstadt Land (VGL1). Cheirurids, encrinurids and proetids are also common, with harpetids, lichids and calymenids forming rarer components (Text-fig. 4.3B).

4.3.3 Scutelluid Association (Cluster 1b)

The Scutelluid Association is most closely related to the Scutelluid-Illaenimorph Association, as shown by the dendrogram. It is found in central Peary Land (CPL2, CPL4a, CPL5c) and south Nares Land (SNL2). Scutelluids comprise over half of the total trilobite individuals, and in some layers their pygidia form densely stacked intervals, so comprising 100% of the trilobite fauna locally (Text-fig. 4.4A). Encrinurids, cheirurids, illaenimorphs and proetids are common. Lichids, harpetids, odontopleurids and calymenids are rare (Text-fig. 4.3B).

4.3.4 Scutelluid-Cheirurid Association (Cluster 1c)

Two samples comprise over 40% scutelluids and over 20% cheirurids; that from Wulff Land (WL), and one sample from western Peary Land (WPL2). The sample from Wulff Land was collected from inter-reef facies, but does not significantly differ

from the reef sample from western Peary Land. It is however the only sample to contain a member of the Phacopidae (Text-fig. 4.3B).

4.3.5 Scutelluid-Harpetid Association (Cluster 1d)

One sample from south Nares Land (SNL2) is dominated equally by scutelluids and harpetids. It also includes cheirurids, illaenimorphs, lichids and proetids (Text-fig. 4.3B). This association is the most distinct in Supercluster 1, a reflection of the high percentage of harpetids present (36%).

4.3.6 Proetid Association (Supercluster 2)

The Proetid Association (Text-fig. 4.4B) is identified from three localities in central Peary Land (CPL 3, 4b and 5a). Proetids are dominant, comprising up to 85% of the total fauna. Scutelluids, encrinurids, cheirurids, lichids and illaenimorphs are common, and harpetids rare (Text-fig. 4.3B).

4.3.7 Encrinurid Association (Supercluster 3)

The Encrinurid Association (Text-fig. 4.4C) is identified from Kronprins Christian Land (KCL) and central Peary Land (CPL1). Within this association, encrinurids comprise over 40% of the trilobite fauna. Scutelluids and proetids may also be common (Text-fig. 4.3B).

4.3.8 Illaenimorph Association (Supercluster 4)

A near monospecific illaenimorph association is recognized from Valdemar Glückstadt Land (VGL2). *Ligiscus* (Text-fig. 4.4D) is the only illaenimorph identified

and comprises 91% of the total trilobite fauna; other components are cheirurids, encrinurids and lichids (Text-fig. 4.3B).

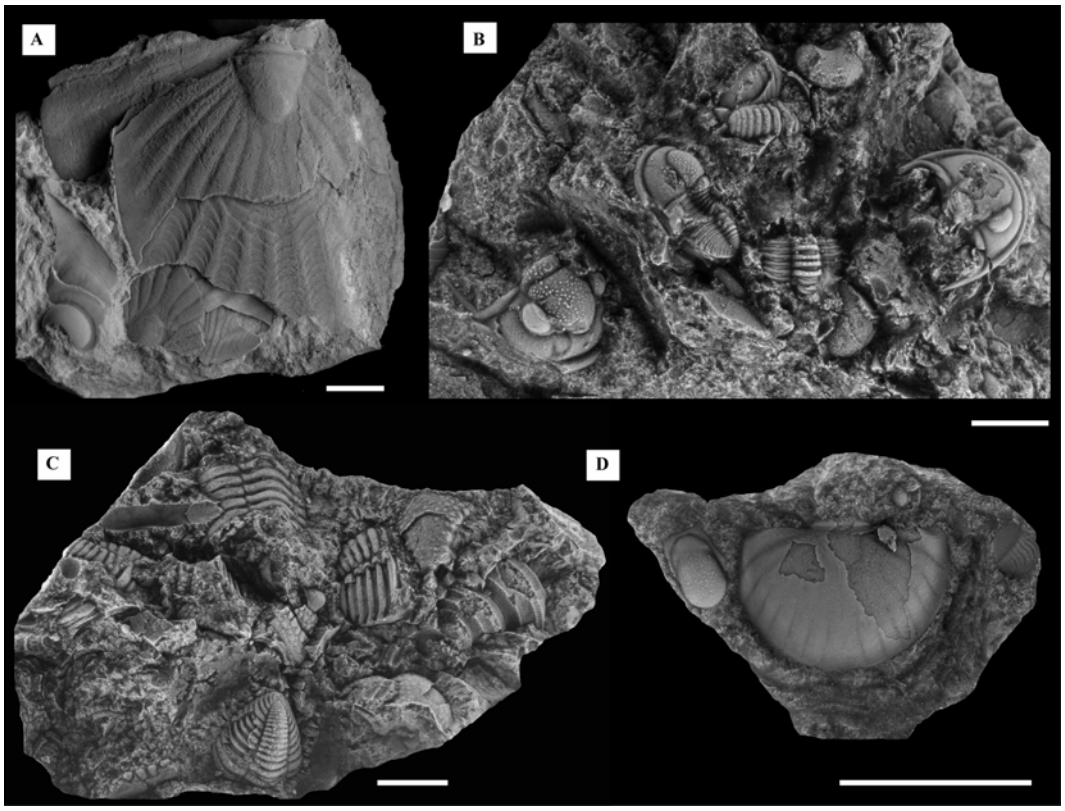

Text-fig. 4.4. Examples of some of the trilobites comprising the associations. **A.** Scutelluid pygidia and free cheek, typical of associations in Supercluster 1 (Sample CPL2, GGU 198186). **B.** Proetid cephala, thorax, pygidium and an articulated specimen, characteristic of Supercluster 2, the Proetid Association (Sample CPL5, GGU 274689). **C.** Encrinurid Association (Supercluster 3) comprising disarticulated elements of the encrinurid *Perryus* (Sample KCL, GGU 275015). **D.** Illaenimorph Association (Supercluster 4) comprising *Ligiscus* pygidium and cheirurid hypostome (Sample VGL2, GGU 275044). Scale bars = 1 cm.

4.4 LITHOFACIES DESCRIPTIONS

Three different lithofacies are recognised, which are readily distinguished in hand specimen. Cement-rich microbial boundstones predominate, and these, together with subordinate crinoidal grainstones, yield trilobite faunas. Minor coral boundstones are also present.

4.4.1 Cement-rich microbial lithofacies

Trilobites occur most commonly in a cement-rich microbial lithofacies. It is identified from all of the localities, and is dominated by non-ferroan calcite spar and microspar, and microbially precipitated micrite. In hand specimen, it is light grey to light olive grey in colour, weathering pale yellowish brown to greyish orange. In thin section, the lithofacies contains fabrics detailed below, reflecting both the microbial nature of micrite precipitation and the effects of diagenesis. These can hamper interpretation of original fabrics at the time of deposition. The lithofacies is characterised by varying amounts of spar, microspar and micrite, with a relatively low abundance of bioclasts.

4.4.1.1 Micrite

Micrite commonly has a clotted texture (Text-fig. 4.5A), indicative of a microbial origin (either forming clots of bacteria or cementing peloids). Locally, filaments of *Girvanella* are preserved (Text-fig. 4.5B), and rare *Renalcis*. In places, the micrite is clearly organically bound, and can occur as discrete laminae (Text-fig. 4.5C). The micrite present may be termed automicrite (Wolf 1965) interpreted as forming *in situ*, in this case by microbial activity.

4.4.1.2 Peloids

The term peloid denotes a grain composed of micro- or cryptocrystalline carbonate, which may form in a number of different ways (Flügel 2004). The peloids here are rounded and vary considerably in size and shape (Text-fig. 4.5D). They occur either as layers within the sediment (locally as distinct laminae), or are found 'floating' within calcite cement. Rounded peloids associated with laminated and clotted fabrics are thought to form *in situ* through biochemical precipitation triggered by microbes (Flügel 2004). Peloids such as these have been regarded as cement by some authors (Macintyre 1984, 1985; Sun and Wright 1998). Flügel (2004) noted that potential microbial peloids are widespread in ancient reefs. *In situ* precipitation has been recorded from Holocene reefs (Lighty 1985) also, and Reitner and Neuweiler (1995) described the occurrence of small-scale peloids which grew in organic mucilages, found in microcavities off Lizard Island, Great Barrier Reef.

4.4.1.3 Intraclasts

Micritic intraclasts, locally with a filamentous microstructure indicating microbial precipitation, are locally present (Text-fig. 4.5E). They are irregularly shaped, but mostly rounded. Angular intraclasts are found directly above some algal laminae, representing rip-up clasts and suggesting there was sufficient time for reworking (Text-fig. 4.6C).

4.4.1.4 Bioclasts

In order of relative abundance, bioclasts present are: ostracods and brachiopods (articulated), trilobites, crinoid ossicles (often with syntaxial overgrowths), bryozoans, gastropods, cephalopods, oncoids, and machaeridians. Additionally, indeterminate

‘shelly fragments’ are present. Bioclasts locally display geopetal fills, and thus prove useful way-up indicators. They are associated both with micritic areas, and with cement.

4.4.1.5 Micritization

Micritization related to microboring is widespread ranging from discrete micrite envelopes to commonplace micritisation of the entire grain (Text-fig. 4.5F). Some envelopes may represent biofilm calcification (Perry 1999). Complete micritization of grains may account for a proportion of the ‘intraclasts’ present, and partial micritization may give the appearance of geopetal fills in places.

4.4.1.6 Synsedimentary cemented cavities

Synsedimentary cemented cavities are categorized according to their morphology into stromatactis, zebra cavities/fabric/rock, and reticulated cavities, the nomenclature following the morphology of the cavities and not their inferred mechanisms of formation. Examples of the three morphologies are present, and all comprise turbid, radiaxial and syntaxial fibrous cement. Radiaxial fibrous cement is volumetrically the most important cement in many Palaeozoic and Mesozoic reef limestones (Flügel 2004). Schmid *et al.* (2001) summarised the general criteria for defining stromatactis as follows: sparitic structures embedded in micrite-dominated carbonate; flat to undulose smooth lower surface; digitate upper surface; internal sediment present; sparitic areas forming a three-dimensional network. Only a small number of cavities found in this facies have the correct morphology to be attributed to true stromatactis, and these are generally under 1 cm thick (Text-fig. 4.6A, B). Other morphologies present include a laminoid fenestral system comprising banding of micrite-rich layers

(clotted or peloidal), radiaxial fibrous cement, and clear cement. These are the zebra cavities first described by Emmons *et al.* (1927) and subsequently by Fischer (1964). Individual layers are up to 5 mm thick and are more laterally continuous than stromatactis structures. The undulating form of the laminae, accompanied by obvious microbially bound fabrics, lends support to a mechanism of formation through the superposition of microbial mats (Pratt 1982). The remaining synsedimentary cemented cavities may be termed reticulated cavities. These describe a complex form of cavity composed of disconnected masses of micrite around which fibrous cement is precipitated (Monty 1995).

Regardless of morphology, the processes underlying the formation of synsedimentary cemented cavities are not fully understood. A synsedimentary origin of these structures is confirmed here, by the identification of turbid first-generation cements (Text-fig. 4.6D), and by the inclusion of peloids and microbial laminae with associated microborings and rip-up clasts within cemented areas (Text-fig. 4.6C). Early marine lithification would have been required to maintain the steep slopes of the Greenland reefs. Pratt (1982) interpreted stromatactis cavities as being formed by binding of locally derived mud and bioclasts by cyanobacteria. Binding was followed by sporadic episodes of rapid sedimentation leaving unbound sediment which was then winnowed out, promoting synsedimentary cementation, and thereby forming stromatactis cavities.

4.4.1.7 Fenestrae

Fenestra is a term used to describe any kind of cavity or infilled cavity in a rock or unconsolidated sediment which is not of an intergranular nature (Demicco and Hardie 1994). Here, it is used to describe laminoid patches of clear, equant cement,

associated with microbially precipitated micrite and peloids (Text-fig. 4.6E). The fenestrae clearly have a different origin to other cavity structures in the facies since they are filled with a diagenetically later cement (Text-fig. 4.6E). This fabric has been related to degassing and shrinkage of microbial mats (Monty 1995).

4.4.1.8 Neomorphic sparite

Neomorphism as defined by Folk (1965) refers to the transformation of minerals taking place in the presence of water, including the processes of replacement, inversion, and recrystallization. Here, neomorphism is identified by the presence of irregularly sized and shaped (anhedral to subhedral) crystals with curved edges, intimately associated with micrite (Text-fig. 4.6C). Micrite floating within spar and recrystallised bioclasts, locally as ghosts or just as micritic envelopes, and the presence of microspar are common neomorphic fabrics (Flügel 2004). Neomorphism has clearly reduced the amount of micrite in the lithofacies. The process is localised, differentially affecting layers within the sediment.

4.4.2 Crinoidal Grainstone Lithofacies

Although occurring variably in the cement-rich microbial facies, crinoids form a true crinoidal grainstone only at locality CPL1, which yields an Encrinurid Association fauna. In hand specimen the lithofacies is pale light grey, weathering light olive grey, and is readily identified by its friable nature. In thin section, it includes synsedimentary cements as found in the cement-rich microbial facies, and is dominated by crinoid fragments (single colunmals), commonly displaying micrite envelopes (Text-fig. 4.7A) and syntaxial overgrowths. Microbial intraclasts, trilobites, corals, cephalopods, bryozoans, brachiopods, ostracods and dasyclad algae are also

present, but are not common. Fracture porosity and lesser dissolution porosity are present. Grainstones with a high proportion of cortoids (grains with micrite envelopes: Flügel 1982), are characteristic of constant water action at or above wave base, and are often associated with patch reefs (Flügel 2004).

4.4.3 Coral boundstone Lithofacies

A small amount of this facies formed part of the collections (Locality CPL2). It does not contain trilobites, so only a brief treatment is necessary here. Hand specimens reveal a cemented cellular structure. In thin section, the tubular structures of the boundstone are micritised (Text-fig. 4.7B). The specimens are identified as the tabulate coral *Multisolenia* (Heldur Nestor and Mari-Ann Motus, pers. comm.).

4.4.4 Diagenesis

Study of the diagenesis undergone by the above lithofacies is essential to understand the controls on the fabrics observed at the present day, the timing of lithification, and the origination of the observed cements. Cement stratigraphy is best determined by cathodoluminescence. The technique allows interpretation of zoning in cements in terms of burial history and the nature of diagenetic pore waters (Boggs and Krinsley 2006). Study of both turbid and equant cements have identified at least three main generations:

4.4.4.1 First generation cements

The first generation non-ferroan calcite cement is turbid and has a dull brown, non-uniform luminescence with bright microdolomite specks indicating the presence of original high magnesium calcite (Text-figs 4.7C, D).

4.4.4.2 Later generation cements

Equant non-ferroan calcite cement, lacking inclusions overlies the first generation turbid cements (Text-figs 4.6D; 4.7C, D), and occurs elsewhere between clotted micrite (Text-figs 5A–D) and within bioclasts (Text-fig. 4.7B), as fenestrae (Text-fig. 4.6E), and as fracture infills (Text-fig. 4.7E). It locally displays a geopetal fabric. Cathodoluminescence reveals two main generations: dog-tooth spar with alternating non-luminescent and thin rims of brightly luminescent cement is pre-compactional, and is followed by more subtly zoned moderately luminescent generations (Text-figs 4.7C, D).

4.4.4.3 Diagenetic history

The timing of cementation relative to other principle diagenetic events is summarized in Text-fig. 4.8. Micritization of grains and first generation cements represent marine diagenesis. Burial diagenesis includes neomorphism and later generation cements. Additionally, brittle fracture is indicated by non-ferroan calcite filled veins (Text-fig. 4.7E). Veins are up to 1 mm thick, exhibit a drusy fill, and offset sedimentary features. At least two generations are identified. Chemical compaction is represented by stylolitization along compositional boundaries. Stylolites are predominantly peaked high amplitude forms and locally bituminous. Dolomite is rare, particularly in samples from central Peary Land, Valdemar Glückstadt Land and Kronprins Christian Land. It overlies all other cements.

The final diagenetic event is the formation of crusts on exposed surfaces by significantly later vadose zone precipitation (Ian Fairchild, pers. comm.) (Text-fig. 4.7F). This locally effects preservation of the trilobite faunas and is visible in hand specimen.

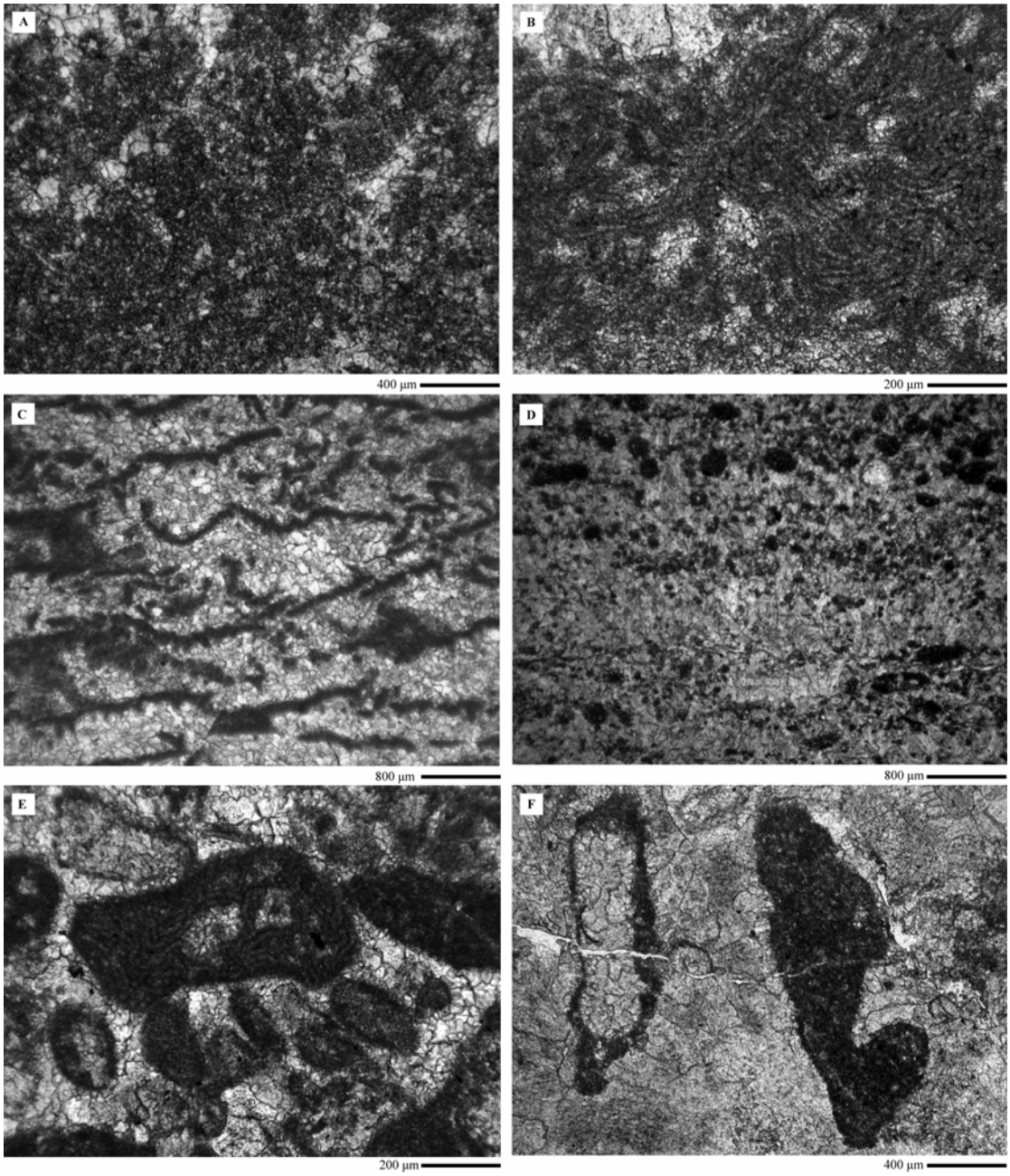

Text-fig. 4.5. Elements of the cement-rich microbial facies in unstained thin sections. **A.** Clotted micrite (Sample CPL2, GGU 198221). **B.** Well preserved filaments of *Girvanella* (Sample CPL2, GGU 198137). **C.** Filamentous micrite (Sample CPL1, GGU 198226). **D.** Laminated peloids, note their rounded form and variation in size and shape (Sample CPL2, GGU 198169). **E.** Intraclasts or micritised grains with *Girvanella* filaments preserved (Sample CPL2, GGU 198139). **F.** Variable micritization of grains. The grain on the left has a fairly uniform micrite envelope, whereas the grain on the right has been completely micrtitised (Sample CPL2, GGU 198137).

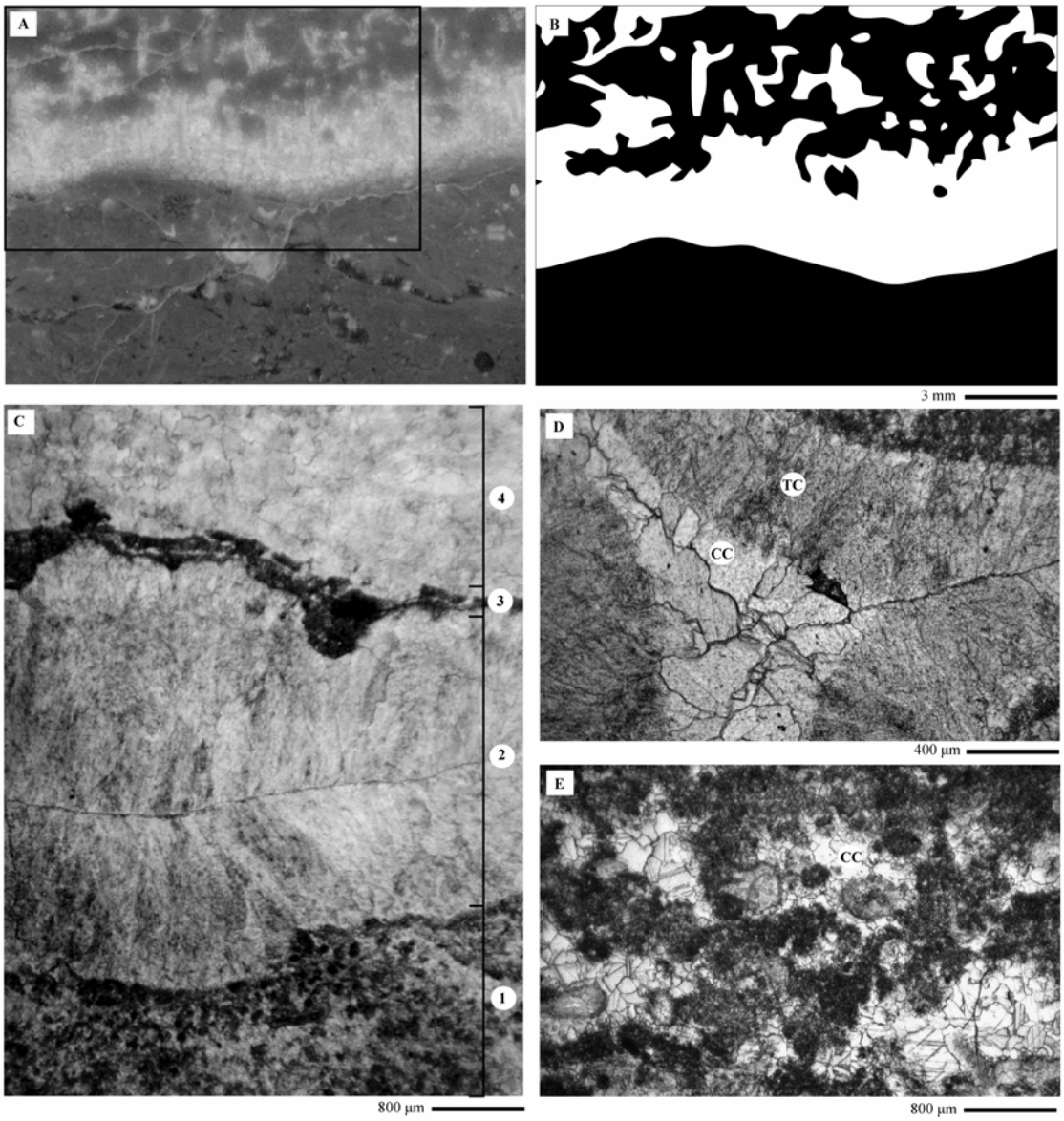

Text-fig. 4.6. Cementation of the reef limestones in hand specimen **(A–B)** and unstained thin sections **(C–E)**. **A.** Calcite-cemented cavities. **B.** Tracing of boxed area of A: the smoothly undulose lower surface and digitate top of the cavities indicate a form approaching true stromatactis (Sample CPL2, GGU 198136). **C.** Thin section demonstrating the variable nature of sedimentation: 1) Peloids 'floating' in calcite spar; 2) Fibrous cements of syn-sedimentary infilled cavity; 3) Microbored surface, indicated by micrite, with rip-up clasts directly above; 4) Neomorphic spar (Sample CPL3, GGU 274654). **D.** Cavity infill with first generation turbid cements (TC) and later clear, equant spar (CC). (Sample CPL2, GGU 198221) **E.** Fenestral fabric. Peloids associated with diagenetically later clear, equant spar (CC) (Sample CPL2, GGU 198169).

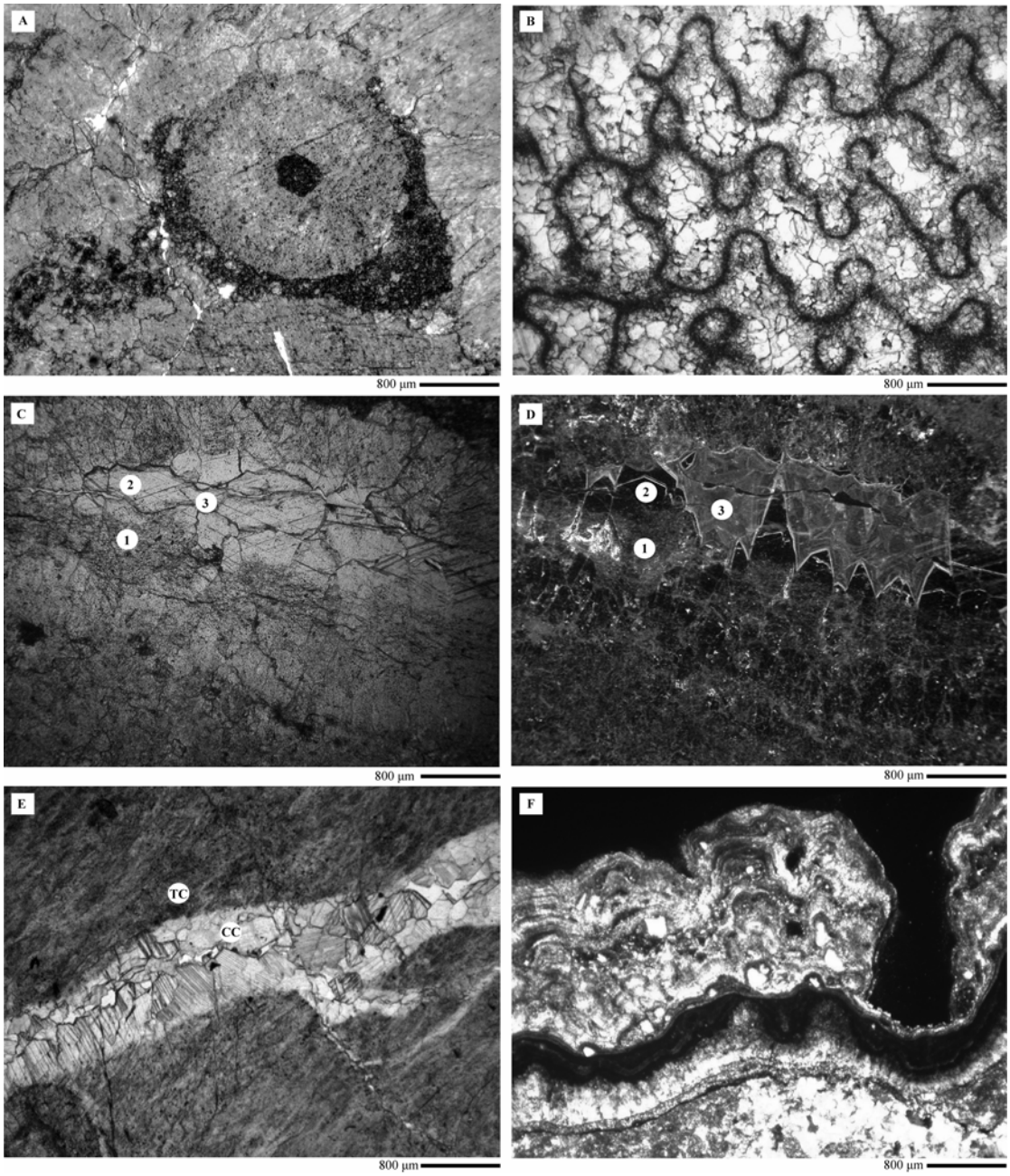

Text-fig. 4.7. Examples of the crinoidal grainstone and coral boundstone lithofacies **(A–B)** and diagenetic features **(C–F)**. Unstained thin sections. **A.** Crinoidal grainstone lithofacies showing micritised crinoid columnal (Sample CPL1, GGU 198226). **B.** Coral boundstone lithofacies comprising *Multisolenia* (Sample CPL2, GGU 198169). **C, D.** View of calcite cemented cavity in plain light (C), and with cathodoluminesce (D). At least three cement generations are obvious: 1) Early fibrous cement with dull luminescence. 2) Later, clear, non-luminescent dogtooth cement with bands of bright luminescence. 3) Subtly zoned moderate luminescent spar to dark burial cement (coarse mosaic) (Sample CPL2, GGU 198200).

E. Clear-cemented fracture (CC) cross-cutting early turbid calcite spar (TC) (Sample CPL1, GGU 198226). **F.** Vadose zone crust coating specimen (Sample CPL2, GGU 198201).

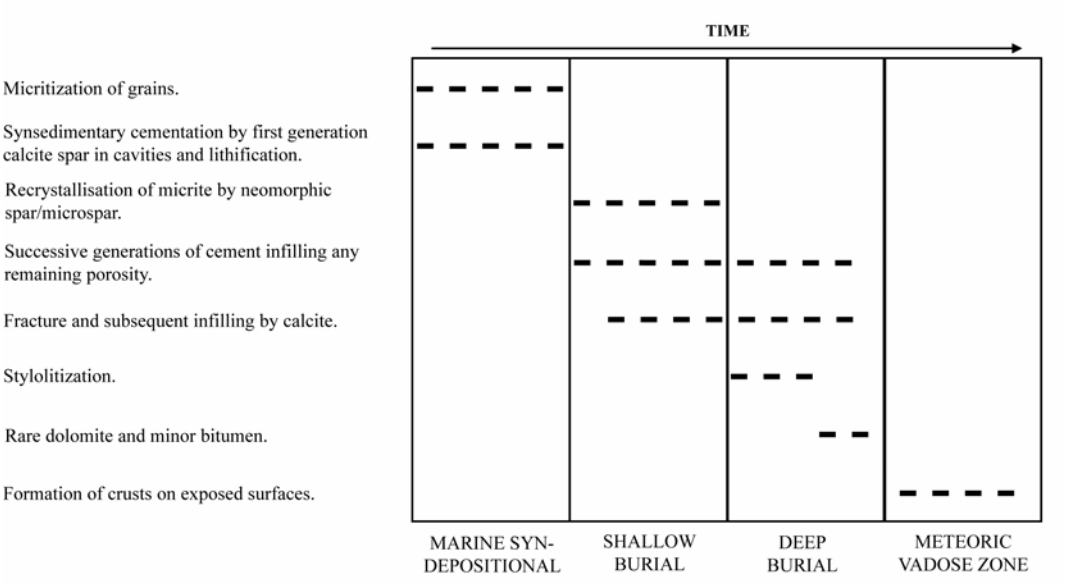

Text-fig. 4.8. Summary diagenetic history of the reef lithofacies.

4.4.5 Interpretations

The presence of microbially precipitated micrite, accompanied by disarticulated bioclasts is indicative of deposition between storm and fair–weather wave base. *Girvanella* (cyanobacterium) is not restricted to shallow waters (Lucas 1979, Riding 1992, Monty 1995), however its occurrence does suggest formation well within the photic zone, as optimum growth conditions would have been in well-lit areas (Ratcliffe 1988). The presence of abundant micritic intraclasts and fenestral fabrics are consistent with very shallow carbonate platform deposits (Webb 2001).

The crinoidal grainstone lithofacies represents the highest energy environment, as indicated by the lack of micrite, accompanied by fragmentation of large crinoid ossicles. The cement-rich microbial lithofacies is indicative of a lower energy regime, and extensive early cementation suggests a slower rate of

sedimentation. Sedimentation was clearly variable, alternating layers of micrite, cement, neomorphosed boundstones and laminated peloids are present. These layers are locally demarcated by prominent surfaces which may be micritised, micro-bored and reworked suggesting a significant time gap between them (Text-fig. 4.6B). This is supported by the diagenetic history which indicates syn-sedimentary cementation which would have added stability to the reef. The cement-rich lithofacies is interpreted as representing cavity fills, between areas of coral boundstones.

This study suggests that the role of microbial processes in the formation of the Silurian reefs of North Greenland has been underestimated previously; it is apparent that they were the principal contributors to the production of carbonate mud.

4.5 TAPHONOMY

All trilobite associations are dominated by disarticulated sclerites with limited fragmentation, and with significant disparity in numbers between the various sclerite types. Speyer (1991) noted that the presence of disarticulated trilobite remains indicated periods of exposure, which are associated with surface scavenging and/or current agitation. A low percentage of partially articulated and complete, compared with disarticulated sclerites, is therefore indicative of some degree of reworking (Paterson *et al*. 2007). Sclerite fragmentation is consistently low (excluding thoracic segments, over 80% of sclerites are over 50% complete), and there are no obvious signs of abrasion. The sclerites therefore lack the effects of agitation in high energy environments Speyer (1991). A degree of time averaging is certain in such taphonomic settings, and as such the samples represent within-habitat, time-averaged assemblages (Kidwell 1993).

4.5.1 Multivariate analysis of sclerite counts

Hydrodynamic sorting preferentially concentrates sclerites of a similar morphology together. This could in part reflect the preferential preservation of more resistant elements (i.e. the loss of thoracic segments and other less resistant sclerites). Measuring individual sclerites to provide information on size sorting is inhibited by their densely packed nature, however, the type of sclerite (pygidium, cephalon etc.) is easily recognisable and these counts indicate any preferential occurrence of certain sclerite types through shape sorting. The counts also highlight any differences in the degree of articulation between samples.

Counts of sclerite type can therefore be analysed to determine any variation in taphonomic attributes between the samples (taphonomic signatures) which can in turn be compared with the associations already identified. Relative proportions of the following sclerite types per sample were put into the PAST programme: complete + partially articulated; cephala + cranidia; free cheeks; hypostomes; pygidia (Text-fig. 4.9B).

4.5.1.1 Cluster analysis

As with the cluster analysis used to identify the trilobite associations, the paired group algorithm and chord distance measure were employed to produce a dendrogram (Text-fig. 4.9A). ANOSIM was then used to test for robustness of the analysis, and with 5000 permutations, and chord, Bray-Curtis, Morista and Euclidean distance measures, the p value remained <0.05.

Using the relative proportions of sclerite types which they contain, three superclusters are recognised, the first of which is divisible into two clusters. Superclusters 1 and 2 comprise the Encrinurid, Scutelluid, Scutelluid-Illaenimorph,

Scutelluid-Cheirurid, Scutelluid-Harpetid and Illaenimorph associations. These associations are all dominated by either cranidia + cephala (Supercluster 1) or pygidia (Supercluster 2) and this is independent of association–type. Supercluster 3 comprises all 3 examples of the Proetid Association. The distinguishing taphonomic features of this association are a higher proportion of complete and partially articulated specimens (average 9%) and free cheeks (average 31%).

4.5.1.2 Correspondence analysis

Correspondence analysis is an ordination technique, projecting a multivariate dataset into 2 or 3 dimensions so as to visualise trends and groupings (Hammer and Harper 2006). The technique has been applied to identify taxonomic associations (Olszewski and Erwin 2009) and biofacies (Olszewski and Patzkowsky 2001). Herkat (2007) used correspondence analysis to identify palaeontological associations and the system tracts linked to them.

In a taphonomic context, correspondence analysis has been applied to compare the frequencies of bone types in different Pleistocene bony assemblages, collected by different agents (Arribas and Palmqvist 1998), and to study differential representations of skeletal elements in different Plio-Pleistocene depositional environments (Alemseged 2003).

Correspondence analysis of the same data supports the groupings of the cluster analysis, and reveals two main axes which control the distribution of the data (Text-fig. 4.9C). Axis 1 accounts for 62% of observed variation, and separates the Proetid Association from all others. It is controlled by the relative abundances of complete and partially articulated specimens, and of free cheeks, factors relating to degree of articulation and thus transport distance: Axis 1 therefore represents transportation

distance primarily. In principle, repeated exhumation and transport could result in total transport distances significantly exceeding the size of the reef. Axis 2 accounts for 21% of observed variation, and separates cluster 1a from 1b. It is largely controlled by the relative proportions of cephala + cranidia and pygidia. This is an effect of hydrodynamic sorting and reflects the ability of different associations to be dominated by different sclerite types. Axes 3 and 4 are not shown: Axis 3 accounts for 11% of observed variation, and separates samples WL and KCL from all other samples. These two samples are the only ones to comprise 5% or over of both hypostomes and complete and partially articulated specimens. Axis 4 accounts for only 6% of observed variation.

4.5.1.3 Taphonomic signature 1

Superclusters 1 and 2 define the first taphonomic signature. In these samples, sclerites are dominated by either cranidia and cephala, or pygidia, with under 10% of any other sclerite type (Text-figs 4.9B, Di, ii). Typically under 5% of sclerites are either partially or completely articulated (Text-figs 4.9B, Di, ii). Sclerites commonly occur as discrete layers within the sediment, where they are nestled on top of one another in densely stacked patterns in both convex-up and convex-down orientations (Text-fig. 4.10). The exception to this is shown by sample CPL1, where sclerites are dispersed within the sediment and display no obvious stacking. This sample is the only one to occur in a crinoidal grainstone facies (Section 4.4.2).

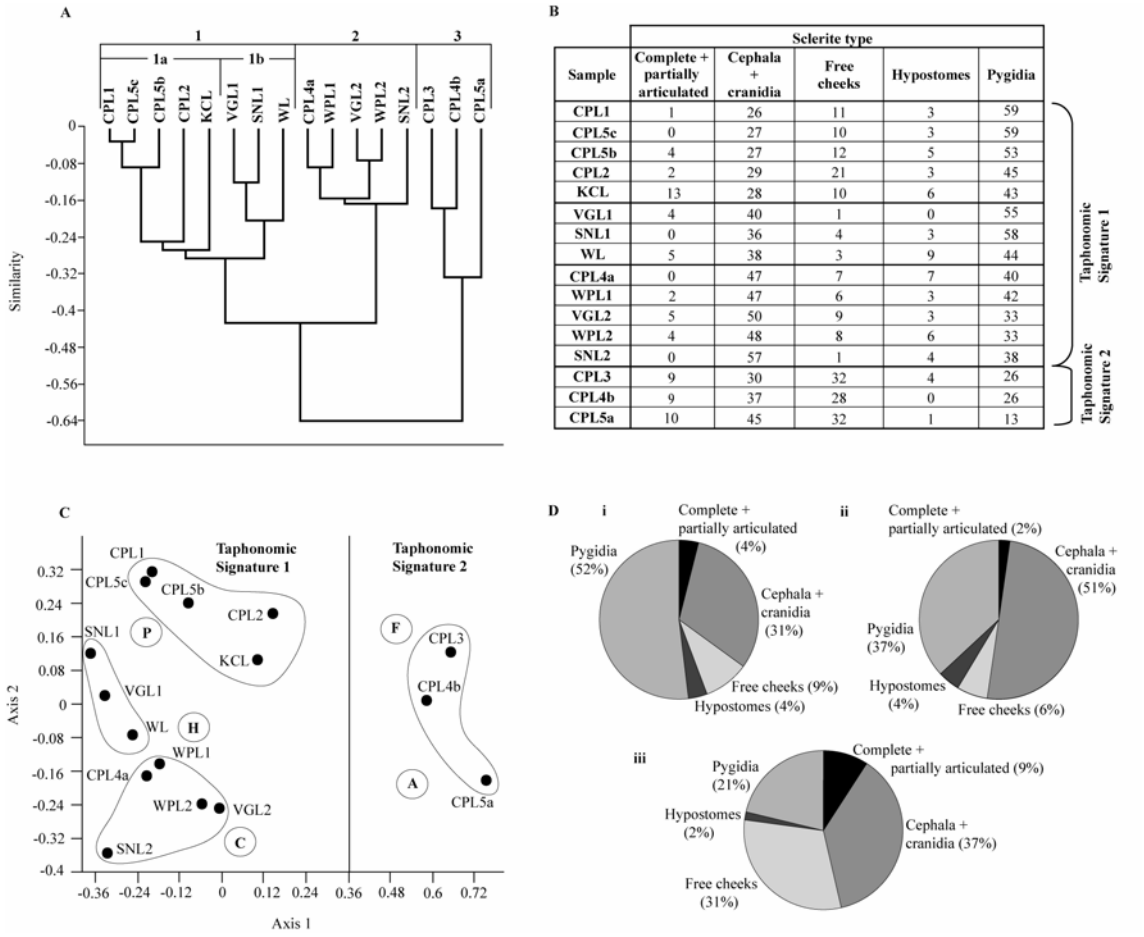

Text-fig. 4.9A. Dendrogram from hierarchical cluster analysis using the paired group algorithm and the chord similarity measure. Samples are clustered according to the sclerites types which they contain. **B.** Percentage values of sclerite types per sample and cluster. **C.** Correspondence analysis of trilobite type per sample. Abbreviations as follows: P = pygidia; H = hypostomes; C = cephala + cranidia; F = free cheeks; A= complete + partially articulated. **D.** Pie charts showing average proportions of sclerite types for: i, Supercluster 1 (Taphonomic signature 1); ii, Supercluster 2 (Taphonomic signature 1); iii, Supercluster 3 (Taphonomic signature 2).

Interpretation

Sclerites occurring as densely stacked patterns with a convex-down orientation, are suggestive of passive settling of sclerites in areas of reduced energy conditions, whereas a predominantly convex-up orientation suggests reorientation due to surface currents (Speyer and Brett 1986; Speyer 1987, 1991; Lask 1993; Mikulic 1979, 1990). Way-up information in the samples here, is restricted to the presence of geopetal fills, or shelter porosity; both of which are rarely observable in hand specimen. It is clear however, that both orientations are present, demonstrating at least some inversion by currents.

The scutelluid pygidia provide a low convexity but elongated morphology which would be easily aligned when placed in a directional current. Two slabs with >10 scutelluid pygidia were identified from the inter-reef sample from Wulff Land. This sample does not significantly differ from those from reef localities; it is taxonomically similar to a reef sample from central Peary Land (WPL2, Text-fig. 4.3) and comprises a cement-rich microbial lithofacies. The slabs were designated an arbitrary north, the angle from this to the anterior midpoint of the pygidial axis was measured, and rose diagrams constructed (Text-fig. 4.10). These samples are too small to test statistically, but appear to represent different directional trends which may reflect differences in their formation. Speyer (1991) noted that disarticulated skeletons with no preferred orientation suggest either rapid, mass deposition, or long-term accumulations in low-energy environments.

The lack of stacking patterns in CPL1 may be a reflection of the taxonomic composition of the sample (Text-fig. 4.3B). Stacking patterns are most commonly displayed by scutelluids and illaenimorphs, due to their smoothly curved

morphologies, and are therefore not observed in samples which contain a low abundance of these taxa/morphotypes.

4.5.1.4 Taphonomic signature 2

Samples included here are dominated by cephala and cranidia, with 9–10% partially or completely articulated specimens (Text-fig. 4.9B), and a relatively high proportion of free cheeks (average 31%; Text-fig. 4.9D). A degree of sorting is apparent; hypostomes are significantly under-represented, and there is up to 32% disparity between cephala/cranidia and pygidia (Text-fig. 4.9B). Trilobite sclerites are found clustered within the sediment.

Interpretation

The relatively high percentage of free cheeks, despite them having a different size and shape from all other sclerite types, is suggestive of limited transport. Complete specimens are predominantly outstretched (Text-fig. 4.4B), suggesting rapid burial.

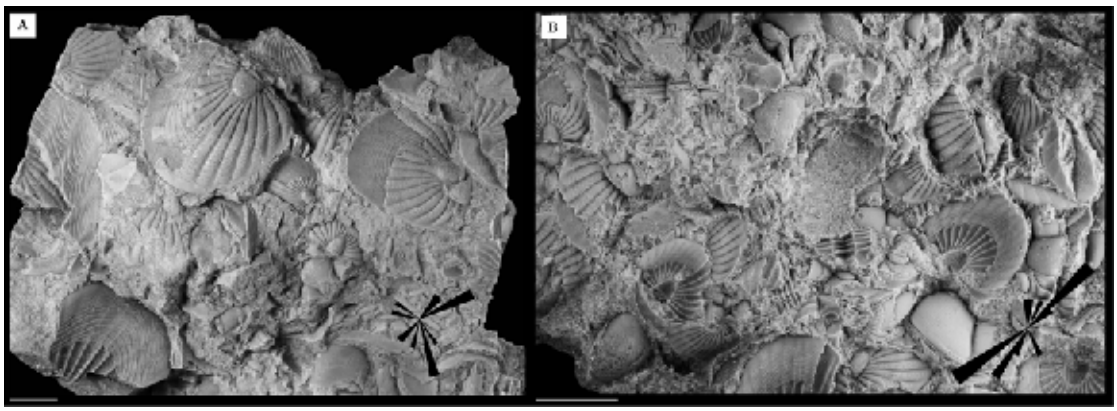

Text-fig. 4.10. Slabs of stacked scutelluid sclerites and their resulting rose diagrams. Sample WL (inter-reef facies, Wulff Land). **A.** GGU 298506. **B.** GGU 298504. Scale bars = 10 mm.

4.6 DISCUSSION AND COMPARISON

4.6.1 Trilobite associations of the cement-rich microbial lithofacies

A model to explain the processes behind formation of these associations is shown in Text-fig. 4.11. The reef trilobites from across North Greenland are predominantly found within a cement-rich microbial lithofacies which implies low energy and slow sedimentation rates, interpreted as representing depressions and cavity fills within the reef surface. Cavities/depressions/fissures are characteristic of reef environments, and provide a means of producing accumulations of trilobites as concentrations or 'pockets'. Mikulic (1979, 1981, 1983, 1990, 1999) conducted flume experiments and studied the distribution of trilobite sclerites in Wenlock-Ludlow reefs from the Great Lakes–Upper Mississippi Valley region of North America, which are characterized by similar morphotypes (illaenids, scutelluids, and lichids) to those found in North Greenland. He recognised the densely stacked concentrations of trilobite sclerites, with some sclerite types under-represented, as forming by selective current transport of trilobite exuviae into depressions or current shadow zones behind objects.

Here, the trilobites associated with a cement-rich microbial lithofacies are found as discrete layers within the sediment, representing event beds. Sclerites were thus transported and concentrated periodically, possibly by storm activity increasing currents along the reef surface and remobilising sclerites. These currents served also to invert a proportion of sclerites. Surface currents and bioerosion may have led to the destruction of some less resistant sclerites, and there does appear to be some preferential preservation of more resistant sclerites, for example, members of the Subfamily Acanthoparyphinae are characterized by almost spherical cranidia, and smaller less convex pygidia. No acanthoparyphine pygidia were found, despite 50

cephala and cranidia being identified from various samples. The same disparity could be produced by sorting, however. Suzuki and Bergström's study of the trilobite taphonomy and ecology of the Upper Ordovician reefs of the Boda Limestone (1999) suggested the selective entrapment of smaller particles by microbial mats, and this could certainly have aided segregation of such sclerite types. As the sclerites were transported, they were subject to increased sorting and disarticulation, and this is the principle taphonomic control on the associations. Mikulic (1979) observed the rapid nature of disarticulation of arthropods during transportation, and it is clear that the transportation distances within the Greenland reefs were not great; sclerites lack the abrasion and fragmented nature of sclerites subject to long-distance transport.

Particular similarities with the trilobite associations from the North Greenland reefs are found in associations from the coeval Attawapiskat Formation, Northern Ontario (Norford 1981, Westrop and Rudkin 1999). There, Westrop and Rudkin (1999) identified a monospecific to low diversity *Ekwanoscutellum* Association reminiscent of the Scutelluid Association described here, and a more diverse *Stenopareia-Meroperix* Association similar to the Scutelluid-Illaenimorph Association. There are also clear taphonomic similarities between Attawapiskat and Greenland as pygidia are commonly stacked, and hydrodynamic sorting results in significant disparities between sclerite types. The phenomenon of hydrodynamic sorting, and the stacking of flat scutelluid pygidia is observed too in the Upper Ordovician Boda Limestone (Suzuki snd Bergström 1999), the Silurian of North America (Mikulic 1979, 1981, 1999), the Pragian Koněprusy reef (Šnajdr 1960, pl. 12) and in the Hamar Lagdad Lower Emsian pinnacle mudmounds from southern Morocco (Alberti 1981, fig. 8, Feist 2001, Chatterton *et al*. 2003).

The Proetid Association is distinguished from all others not only by its taxonomic composition (all other associations comprise <10% proetids, compared to these samples where proetids are the dominant trilobite type), but also by its taphonomic signature. The increased prevalence of articulated material is significant, accompanied by a relatively high proportion of free cheeks, and this association is considered to represent the most *in situ* type. As the cement-rich microbial lithofacies in which the Proetid Association is found also yields faunas belonging to the other associations – with less articulated material and a greater disparity of sclerite types – the difference in taphonomic attributes is interpreted as being due to amount of transport, and not differing environmental conditions at the site of deposition. It is likely that proetids inhabited more sheltered environments within the reef and therefore had a smaller transportation potential. Owens (1979, 1990) had suggested the visitation of cavities/crevices by proetids to moult, from studies at Kallholn, and the Carboniferous of Britain respectively. Suzuki and Bergström (1999) suggested that proetids visited cavities in the Upper Ordovician reefs of Dalarna, Sweden, in order to moult and/or hide. Furthermore, partly articulated and disarticulated parts of proetids were documented from a single fissure fill in the Lower Devonian reef at Hamar Laghdad, Morocco (Chatterton *et al*. 2003). These genera were either rare or absent in other trilobite-filled fissures. They suggested that trilobite sclerites found in reef fissures entered in different ways, with live trilobites intending to moult or hide with subsequent movement and winnowing of sclerites out of the cavities mostly during storms, and secondly, with post-mortem transport of trilobite sclerites into fissures.

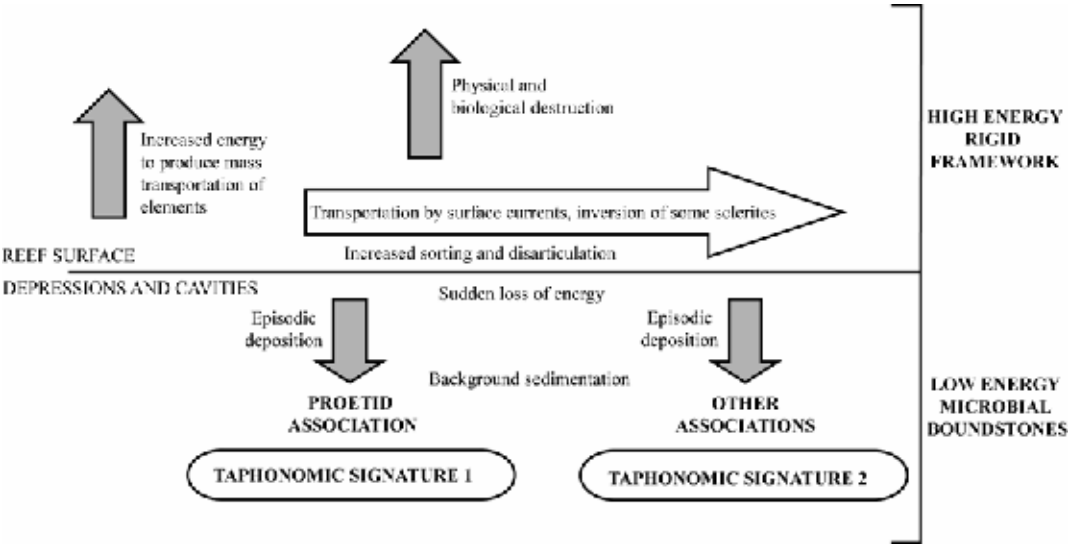

Text-fig. 4.11. Model for sediment transport and resulting trilobite associations within the reefs.

4.6.2. Encrinurid Association found within crinoidal grainstone lithofacies

The Encrinurid Association identified from central Peary Land (CPL 1) displays the greatest disparity of sclerite types, suggesting that this association has been most strongly influenced by hydrodynamic sorting and transported the greatest distance. This is the only association to be found in a true crinoidal grainstone lithofacies which represents the highest energy facies, indicated by the lack of micrite (other than that precipitated microbially), suggesting that mud was winnowed out above fair-weather wave-base. The complete absence of partially articulated and complete specimens supports this. The presence of clean grainstones suggests that the Encrinurid Association could be related to flank beds. It is probable that this material was derived from the reef core, given that the same species of encrinurids are described from the core facies (CPL2) which could have formed part of the same reef as CPL1.

4.7. CONCLUSIONS

1) Trilobite morphotypes are unevenly distributed throughout the reefs, despite being predominantly associated with a single lithofacies. Recurring groups of trilobite families/morphotypes are readily clustered into seven associations. This highlights the high probability of sampling bias when studying reef environments.
2) All associations are reworked and to a degree time averaged.
3) Trilobite sclerite types are also distributed unevenly, and their occurrence is determined primarily by amount of transport.
4) As different associations are found in a cement-rich microbial lithofacies, this suggests that it is taphonomic processes which vary, and not the environment of deposition. The trilobite associations occur in event beds which do not represent the background sedimentation within the reef.
5) Application of correspondence analysis to counts of sclerite types provide the most effective means of understanding taphonomic mechanisms, and successfully separates the controls on taphonomic groupings, with two distinct taphonomic signatures recognised. These are not separated by lithofacies.
6) Differences in transportation show that there was some segregation of morphotypes within the reefs. Proetids were more closely associated with cavities.

CHAPTER FIVE

CONCLUSIONS

THE Silurian reefs of North Greenland comprise abundant and diverse trilobite faunas belonging to the previously defined and long-ranging ‘Illaenid-Cheirurid Community’. Taxonomic study of the trilobite faunas (Chapter 2) reveals a high number of new taxa. Thirty six named species are described, of which 32 are new. Additionally, 30 taxa are described under open nomenclature. In total, 32 genera are represented, of which six are new. The high number of new trilobite taxa described reflects the prior lack of sampling of Silurian reef trilobite faunas of the region. The faunas are most comparable with those described from similar shallow marine environments from other Telychian Laurentian localities. The Telychian to ?early Wenlock Attawapiskat Formation fauna from northern Ontario and Northern Manitoba described by Norford (1981) comprises 15 genera, seven of which are described here. Additionally, a Telychian trilobite fauna described from the Taylor Mountains, Alaska, by Adrain *et al*. (1995) contains seven species congeneric with the North Greenland taxa. Most of the species in the *Ekwanoscutellum ekwanensis* fauna from the late Telychian to ?earliest Wenlock Chicotte Formation in Anticosti Island, Québec, Canada described by Chatterton and Ludvigsen (2004) are congeneric with forms described here. Study of taxa from different reef localities across North Greenland has revealed a degree of segregation of species across the reef belt. It is likely that this uneven distribution is age-related, possibly reflecting the gradual foundering of the carbonate platform from east to west.

Members of the Suborder Illaenina dominate the reef faunas; in order of decreasing abundance, cheirurids, encrinurids, and proetids are other numerically significant trilobites within the reef facies. Harpetids, lichids, odontopleurids, calymenids and phacopids are rarer components. The phylogenetic relationships of the Illaenidae are particularly controversial, as many representatives have lost recognisable characters of the carapace due to the process of effacement. Cladistic analyses of representative members of the Illaenidae are presented in Chapter 3. When both effaced and non-effaced taxa are included in the same cladistic analysis, coded genera grouped according to the degree of effacement they exhibit. This demonstrates the control of effacement on the resulting cladograms, masking phylogenetic lineages. Analysis limited to effaced taxa however, supports the separation of effaced members of the Scutelluidae from unequivical members of the Illaenidae, demonstrating the polyphyletic nature of effacement.

In Chapter 4, counts of trilobite sclerites from thirteen different reef localities were analysed by cluster analysis to group reef localities according to the trilobites they contain. This technique identified trilobite associations, groups of commonly recurring trilobites. The relative proportions of different types of sclerite (cephalon, pygidium etc.) and degree of articulation within samples, were analysed by cluster and correspondence analysis to identify any between-sample variation in taphonomic signatures. Seven trilobite associations are recognised: the Scutelluid-Illaenimorph, Scutelluid, Scutelluid-Cheirurid, Scutelluid-Harpetid, Proetid, Encrinurid, and Illaenimorph associations. The identification of these highlights the uneven distribution of trilobite morphotypes throughout the reefs. This variability results partly from intense hydrodynamic sorting in reef environments, with two distinct taphonomic signatures identified. The first signature includes samples whose sclerites

occur commonly as discrete layers within the sediment, and are dominated by either cranidia and cephala, or pygidia, and have less than 5% of sclerites either partially or completely articulated. The second signature includes samples where sclerites are found clustered within the sediment. These samples are dominated by cephala and cranidia, with 9–10% partially or completely articulated specimens, and a relatively high proportion of free cheeks. This taphonomic signature is represented only by the Proetid Association and represents the least amount of transport, suggesting that these particular taxa took advantage of the more sheltered niches within the reef. There was therefore some segregation of morphotypes within these environments.

The trilobites are predominantly associated with a cement-rich microbial lithofacies. Crinoidal grainstone and coral boundstone lithofacies are also represented. The crinoidal grainstone lithofacies represents the highest energy environment, and the cement-rich microbial lithofacies indicates a lower energy regime, with extensive early cementation suggesting a slower rate of sedimentation. The cement-rich lithofacies is interpreted as representing cavity fills, between areas of coral boundstones. It is apparent from the high abundance of microbial-precipitated micrite, that microbial processes were the principal contributors to the production of carbonate mud present. These processes therefore played a significant role in development of the North Greenland reefs.

The trilobite associations were deposited between storm- and fair-weather wave base. They are reworked, and to a degree are time averaged. Deposition of the sclerites occurred as event beds in an otherwise low energy and slow sedimentation regime. It is possible that storm activity remobilising sclerites, subsequently depositing them within depressions and cavity fills within the reef surface. The associations do not represent the background sedimentation within the reef.

REFERENCES

ADRAIN, J. M. 1998. Systematics of the Acanthoparyphinae (Trilobita), with species from the Silurian of Arctic Canada. *Journal of Paleontology*, **72**, 698–718.

— 2003. Validity and composition of the Silurian trilobite genera *Borealarges* and *Dicranogmus*, with new species from the Canadian Arctic. *Canadian Journal of Earth Sciences*, **40**, 749–763.

— and CHATTERTON, B. D. E. 1993. A new rorringtoniid trilobite from the Ludlow of Arctic Canada. *Canadian Journal of Earth Sciences*, **30**, 1634–1643.

—, CHATTERTON, B. D. E. and BLODGETT, R. B. 1995. Silurian trilobites from Southwestern Alaska. *Journal of Paleontology*, **69**, 723–726.

— and EDGECOMBE, G. D. 1995. *Balizoma* and the new genera *Aegrotocatellus* and *Perirehaedulus*: encrinurid trilobites from the Douro Formation (Ludlow) of Arctic Canada. *Journal of Paleontology*, **69**, 736–752.

— and **—** 1997. Silurian (Wenlock) calymenid trilobites from the Cape Phillips Formation, central Canadian Arctic. *Journal of Paleontology*, **71**, 657–682.

— and FORTEY, R. A. 1997. Ordovician trilobites from the Tourmakeady Limestone, western Ireland. *Bulletin of the Natural History Museum, Geology Series*, **53**, 79–115.

— and KLOC, G. J. 1997. Lower Devonian aulacopleuriodean trilobites from Oklahoma. *Journal of Paleontology*, **71**, 703–712.

— and TETREAULT, D. K. 2005. The brachymetopid *Radnoria* in the Silurian (Wenlock) of New York State and Arctic Canada. *Canadian Journal of Earth Sciences*, **42**, 2087–2096.

ALBERTI, G. K. B. 1967. Neue obersilurische sowie unter- und mitteldevonische Trilobiten aus Marokko, Deutschland und einigen anderen europäischen Gebieten. 2. *Senckenbergiana lethaea*, **48**, 481–509, pl. 1.

— 1969. Trilobiten des jüngeren Siluriums sowie des Unter- und Mitteldevons. I. Mit Beiträgen zur Silur-Devon-Stratigraphie einiger Gebiete Marokkos und Oberfrankens. *Abhandlungen der Senckenbergischen Naturforschenden Gesellschaft*, **520**, 1–692, 52 pls.

— 1981. Scutelluidae (Trilobita) aus dem Unter-Devon des Hamar Laghdad (Tafilalt, SE-Marokko) und das Alter der 'mud mounds' (Ober-Zlichovium bis tiefstes Dalejum). *Senckenbergiana Lethaea*, **62**, 193–204.

ALEMSEGED, Z. 2003. An integrated approach to taphonomy and faunal change in the Shungura Formation (Ethiopia) and its implication for hominid evolution. *Journal of Human Evolution*, **44**, 451–478.

ALDRIDGE, R. J. 1979. An upper Llandovery conodont fauna from Peary Land, eastern North Greenland. *Rapports Grønlands Geologiske Undersøgelse*, **91**, 7–23.

ANGELIN, N. P. 1854. *Palaeontologia Scandinavica. I. Crustacea formationis transitionis*. Fascicule, 2, Lipsiae, 21–92, pls 25–41. Lund.

ARMSTRONG, H. A. 1990. Conodonts from the Upper Ordovician–lower Silurian Carbonate Platform of North Greenland. *Bulletin Grønlands Geologiske Undersøgelse*, **159**, 151 pp.

ARRIBAS, A. and PALMQVIST, P. 1998. Taphonomy and palaeoecology of an assemblage of large mammals: Hyaenid activity in the Lower Pleistocene site at Venta Micena (Orce, Guadix-Baza Basin, Granada, Spain. *Geobios*, **31**, 3–47.

BARRANDE, J. 1846a. *Notice préliminaire sur le Systême Silurien et les trilobites de Bohême*. vi + 97 pp. Leipsic.

— 1846b. *Nouveaux trilobites. Supplément à la notice préliminaire sur le Systême Silurien et les trilobites de Bohême.* 40 pp. Prague.

— 1850. [Bohemian trilobites] *Berichte über die Mittheilungen von Freunden der Naturwissenschaften in Wien.* **7**, 4–7, 2 text-figs (unnumbered). Wien.

— 1852. *Systême Silurien du centre de la Bohême. 1ère partie: Recherches paléontologiques. Vol. 1. Crustacés: Trilobites.* xxx + 935 pp., 51 pls. Prague and Paris.

— 1868. R*éapparition du genre* Arethusina *Barr.* 1–29, 1 pl. Prague and Paris.

— 1872. *Systême Silurien du centre de la Bohême. 1ère partie: Recherches paléontologiques. Supplément au vol.* 1. *Trilobites, Crustacés divers et Poissons.* xxx + 647 pp., 35 pls. Prague and Paris.

BARTON, D. C. 1916. A revision of the Cheirurinae, with notes on their evolution. *Washington University Studies, Scientific Series*, **3**, 101–152.

BATHURST, R. G. C. 1980. Stromatactis - origin related to submarine-cemented crusts in Paleozoic mud mounds. *Geology*, **8**, 131–134.

BEGG, J. L. 1939. Some new species of Proetidae and Otarionidae from the Ashgillian of Girvan. *Geological Magazine*, **76**, 372–82, pl. 6.

BEYRICH, E. 1845. *Ueber einige böhmischen Trilobiten.* 47 pp., 1 pl. Berlin.

BILLINGS, E. 1859. Description of some new species of trilobites from the Lower and Middle Silurian rocks of Canada. *Canadian Naturalist and Geologist*, **4**, p. 367–383.

— 1860. Description of some new species of trilobites from the Lower and Middle Silurian rocks of Canada. *Canadian Naturalist and Geologist*, **5**, 49–73.

— 1865. Palaeozoic fossils, vol. 1. *Geological Survey of Canada*, Montreal, 1–426.

BOGGS, S. and KRINSLEY, J. 2006. *Application of cathodoluminescence imaging to the study of sedimentary rocks.* Cambridge University Press, Cambridge, 176 pp.

BOURQUE, P.-A. and GIGNAC, H. 1983. Sponge-constructed Stromatactis mud-mounds, Silurian of Gaspe, Quebec. *Journal of Sedimentary Petrology*, **53**, 521–532.

BRONGNIART, A. 1822. Les Trilobites, pp. 1–65, pls 1–4. *In* BRONGNIART, A., and DESMAREST, A. G. 1822. *Histoire naturelle des crustacés fossiles*. 154 pp., 11 pls. Paris.

BRUTON, D. L. 1966. A revision of the Swedish Ordovician Odontopleuridae (Trilobita). *Bulletin of the Geological Institution of the University of Uppsala*, **43**, 1–44.

BURMEISTER, H. 1843. *Die Organisation der Trilobiten, aus ihren lebenden Verwandten entwickelt; nebst einer systematischen Uebersicht aller zeither beschriebenen Arten*. 147 pp., 6 pls. Berlin.

CAMPBELL, K. S. W. 1967. Trilobites of the Henryhouse Formation (Silurian) in Oklahoma. *Oklahoma Geological Survey, Bulletin*, **115**, 68 pp., 19 pls.

— 1977. Trilobites of the Haragan, Bois d'Arc and Frisco formations (early Devonian) Arbuckle Mountains Region, Oklahoma. *Oklahoma Geological Survey, Bulletin*, **123**, vi + 227 pp.

CHANG, W.–T. 1974. Silurian trilobites. 173–187. *In* EDITORIAL BOARD OF NANJING INSTITUTE OF GEOLOGY AND PALAEONTOLOGY, ACADEMICA SINICA (ed.). *A handbook of stratigraphy and palaeontology of southwest China*. Academica Sinica, Academic and Science Press, Beijing, iii + 454 pp. [in Chinese]

CHATTERTON, B. D. E. 1971. Taxonomy and ontogeny of Siluro-Devonian trilobites from Yass, New South Wales. *Palaeontographica, A*, **137**, 108 pp.

— and CAMPBELL, K. S. W. 1980. Silurian trilobites from near Canberra and some related forms from Yass. *Palaeontographica, A,* **167**, 77–119, pls 1–16.

—, COLLINS, D. H. and LUDVIGSEN, R. 2003. Cryptic behaviour in trilobites: Cambrian and Silurian examples from Canada, and other related occurrences. *Special Papers in Palaeontology*, **70**, 157–173.

—, EDGECOMBE, G. D., WAISFELD, B. G. and VACCARI, N. E. 1998. Ontogeny and systematics of Toernquistiidae (Trilobita, Proetida) from the Ordovician of the Argentine Precordillera. *Journal of Paleontology*, **72**, 273–303.

— and LUDVIGSEN, R. 1976. Silicified Middle Ordovician trilobites from the South Nahanni River area, District of Mackenzie, Canada. *Palaeontographica, A,* **154**, 1–106.

— and **—** 2004. Silurian trilobites of Anticosti Island, Québec, Canada. *Palaeontographica Canadia*, **22**, 264pp, 85 pls.

—. and PERRY, D. G. 1983. Silicified Silurian odontopleurid trilobites from the Mackenzie Mountains. *Palaeontographica Canadiana*, **1**, 1–127, 36 pls.

— and **—** 1984. Silurian cheirurid trilobites from the Mackenzie Mountains, northwestern Canada. *Palaeontographica, A*, **184**, 1–78.

—, SIVETER, D. J., EDGECOMBE, G. D. and HUNT, A. S. 1990. Larvae and relationships of the Calymenina (Trilobita). *Journal of Paleontology*, **64**, 255–277.

CHLUPÁČ, I. 1987. Ecostratigraphy of Silurian trilobite associations of the Barrandian area, Czechoslovakia. *Newsletters in Stratigraphy*, **17**, 169–86.

CHRISTIE, R. L. and PEEL, J. S. 1977.Cambrian-Silurian stratigraphy of Børglum Elv, Peary Land, eastern North Greenland. *Rapport Grønlands Geologiske Undersøgelse*, **82**, 1–48.

CURTIS, N. J. and LANE, P. D. 1997. The Llandovery trilobites of England and Wales. *Palaeontographical Society Monograph*, **151**, 1–50, 3 pls.

— and **—** 1998. The Llandovery trilobites of England and Wales. Part 2. *Palaeontographical Society Monograph*, **152**, 51–101.

COCKS, L. R. M. and TORSVIK, T .H. 2002. Earth geography from 500 to 400 million years ago: a faunal and palaeomagnetic review. *Journal of the Geological Society of London*, **159**, 631–644.

COPPER, P. and BRUNTON, F. 1991. A global review of Silurian reefs. *Special Papers in Palaeontology*, **44**, 225–259.

CURRANO, E. D. 2009. Patchiness and long-term change in early Eocene insect feeding damage. *Paleobiology*, **35**, 484–498.

DALMAN, J. W. 1827. Om palaederna, eller de så kallade trilobiterna. *K. svenska Vetensk-Akad. Handl.* (for 1826), 113–52, 226–94, 6 pls.

DAWES, P.R. 1971. The North Greenland fold belt and environs. *Meddelelser Dansk Geologiske Forening*, **20**, 197–239.

— 1976. Precambrian to Tertiary of northern Greenland. 248–303. *In* ESCHER, A and WATT, W.S. (eds) *Geology of Greenland*, Geological Survey of Greenland, Copenhagen.

DEMICCO, R. V. and HARDIE, L. A. 1994. *Sedimentary structures and early diagenetic features of shallow marine carbonate deposits*. SEPM Atlas Series 1, 265 pp.

DESMAREST, A. G. 1817. In *Nouveau Dictionnaire d'Histoire Naturelle*. (2nd Edition), **5**, 49–50.

DUPONT, E. 1881. Sur l'origine des calcaires Dévoniens en Belgique. *Bulletin de l'Académie royale des Sciences de Belgique*, **3**, 264–280**.**

— 1882. Les îles coralliennes de Roly et de Philippeville. *Bulletin du Musée Royal d'Histoire Naturelle de Belgique*, **1**, 89–160.

EDGECOMBE, G. D and CHATTERTON, B. D. E. 1992. Early Silurian (Llandovery) encrinurine trilobites from the Mackenzie Mountains, Canada. *Journal of Paleontology*, **66**, 52–74.

— and **—** 1993. Silurian (Wenlock-Ludlow) encrinurine trilobites from the Mackenzie Mountains, Canada, and related species. *Palaeontolographica, A*, **229**, 75–112.

— and RAMSKÖLD, L. 1996. The "*Encrinurus" variolaris* plexus (Trilobita, Silurian): relationships of Llandovery species. *Geobios*, **29**, 209–233.

— and SHERWIN, L. 2001. Early Silurian (Llandovery) trilobites from the Cotton Formation, near Forbes, New South Wales, *Alcheringa*, **25**, 87–105.

EMMONS, S. F., IRVING, J. D. and LOUGHLIN, G. F. 1927. Geology and ore deposits in Leadville mining district, Canada. *United States Geological Survey Professional Paper*, **148**, 368.

ERBEN, H. K. 1951. Beitrag zur Gleiderung der Gattung *Proetus* Stein, 1831 (Trilobitae). Neues Jahrbuch fuer Geologie und Palaeontologie. *Abhandlungen*, **94**, 5–48.

ERWIN, D. H. 1989. Regional paleoecology of Permian gastropod genera, south-western United States and the end-Permian mass extinction. *Palaios*, **4**, 424–438.

FEIST, R. 2001. *Clustered trilobite assemblages formed under shelter: case studies of paleoecological behaviour*. Abstracts of the Third International Symposium of Trilobites and their Relatives, Oxford, 2001, p. 12.

FISCHER, A. G. 1964. The lower cyclotherm in the Alpine Triassic. *Kansas Geological Survey Bulletin*, **169**, 107–149.

FLÜGEL, E. 1982. Evolution of Triassic reefs: current concepts and problems. *Facies,* **6**, 297–328.

— 2004. *Microfacies of carbonate rocks: analysis, interpretation and application.* Springer, Heidelberg, 976 pp.

FOLK, R. L. 1965. Some aspects of recrystallization in ancient limestones. *In* PRAY, C. L. and MURRAY, R. C. (eds.) *Dolomitization and limestone diagenesis.* Society of Economic Paleontologists and Mineralogists Special Publication 13, pp. 14–48.

FORTEY, R. A. 1975. Early Ordovician trilobite communities. *Fossils and Strata*, **4**, 331–352.

— and COCKS, L.R.M. 2003. Palaeontological evidence bearing on global Ordovician-Silurian continental reconstructions. *Earth Science Reviews*, **61**, 245–307.

— and OWENS, R. M. 1975. Proetida: a new order of trilobites. *Fossils and Strata*, **4**, 227–239.

— and **—** 1979. Enrolment in the classification of trilobites. *Lethaia*, **12**, 219–226.

FRITZ, M. A. 1964. ?*Scutellum regale* sp. nov. Fritz from the Silurian of the Hudson Bay area. *Proceedings of the Geological Association of Canada*, **15**, 91–97.

GASS, K, C. and MIKULIC, D. G. 1982. Observations on the Attawapiskat Formation (Silurian) trilobites of Ontario, with description of a new encrinurine. *Canadian Journal of Earth Sciences*, **19**, 589–596.

GOLOBOFF, P.A. 1998. NONA, version 2.0. Software available online at: http://www.cladistics.com

GRANT, R. E. 1971. *Brachiopods in the Permian reef environment of West Texas.* First North American Paleontological Convention, Proceedings (1969), Part J, 1444–1481.

HALL, J. 1852. Containing descriptions of the organic remains of the lower middle division of the New York System (equivalent in part to the Middle Silurian rocks of Europe). *New York State Geological Survey, Palaeontology New York,* **2**, viii + 362 pp., 85 pls.

— 1863. Notice of some new species of fossils from a locality of the Niagara group in Indiana, with a list of identified species from the same place. *Transactions of the Albany Institute*, author's preprint, 1–34. Republished in *Transactions of the Albany Institute* (1864a) **4,** 195–228.

— 1864b. Account of some new or little-known species of fossils from rocks of the age of the Niagara Group. *Report of the New York State Museum of Natural History*, **18**, 1–48, 1 pl.

— 1867. *Report of the New York State Museum of Natural History*, **20**, 305–401, pls 10–23 (Republication, with additions, of Hall 1864b).

— 1870. Descriptions of new or little known species of fossils from rocks of the age of the Niagara Group. *Report of the New York State Museum of Natural History*, **20** (revised edition), 347–447, 25 pls.

— 1879. The fauna of the Niagara Group, in central Indiana. *Report of the New York State Museum of Natural History*, **28**, 99–199, pls 3–34.

HAMMER, Ø. and HARPER, D. A. T. 2006. *Paleontological data analysis.* Blackwell, Oxford, 351 pp.

—, **—** and RYAN, P. D. 2001. PAST: Palaeontological Statistics software package for education and data analysis. *Palaeontologia Electronica*, **4**, 9 pp.

HARRINGTON, H. J. and LEANZA, A. F. 1957. Ordovician trilobites of Argentina. *Special publications of the Department of Geology, University of Kansas*, **1**, 1–276, 140 figs.

HARPER, D. A. T., MACNIOCAILL, C. and WILLIAMS, S. H. 1996. The palaeogeography of Early Ordovician Iapetus terranes: an integration of faunal and palaeomagnetic constraints. *Palaeogeography, Palaeoclimatology, Palaeoecology,* **121**, 297–312.

HAWLE, I. and CORDA, A. J. C. 1847. *Prodrom einer Monographie der böhmischen Trilobiten*. Prague, 176 pp., 7 pls.

HEDSTRÖM, H. 1923. Contributions to the fossil fauna of Gotland. I. *Sveriges Geologiska Undersökning, C,* **316**, 1–25, 5 pls.

HELBERT, G. J., LANE, P. D., OWENS, R. M., SIVETER, D. J. and THOMAS, A. T. 1982. Lower Silurian trilobites from the Oslo region. 129–148. *In* WORSLEY, D. (ed.) *International Union of Geological Sciences Subcomission on Silurian Stratigraphy. Field meeting, Oslo region, 1982.* Palaeontological contributions from the University of Oslo, **278**, Paleontologisk Museum, Oslo, 175 pp.

HERKAT, M. 2007. Application of correspondence analysis to palaeobathymetric reconstruction of Cenomanian and Turonian (Cretaceous) rocks of Eastern Algeria. *Palaeogeography, Palaeoclimatology, Palaeoecology,* **254**, 583–605.

HIGGINS, A. K., INESON, J. R., PEEL, J. S., SURLYK, F. and SØNDERHOLM, M. 1991. The Franklinian Basin in North Greenland. *Bulletin Grønlands Geologiske Undersøgelse*, **160**, 71–139.

HOLLOWAY, D. J. 1980. Middle Silurian trilobites from Arkansas and Oklahoma, U.S.A. *Palaeontolographica, A,* **170**, 1–85.

— 1994. Early Silurian trilobites from the Broken River area, North Queensland. *Memoirs of the Museum of Victoria*, **54**, 243–269.

— 1996. New Early Devonian Styginid trilobites from Victoria, Australia, with revision of some spinose styginids. *Journal of Paleontology,* **70**, 428–438.

— 2007. The trilobite *Protostygina* and the composition of the Styginidae, with two new genera. *Paläontologische Zeitschrift*, **81**, 1–16.

— and LANE, P. D. 1998. Effaced styginid trilobites from the Silurian of New South Wales. *Palaeontology*, **41**, 853–896.

— and **—** 1999. A replacement name for the trilobite *Lalax* Holloway and Lane *non* Hamilton. *Palaeontology*, **42**, p. 375.

HOLM, G. 1882. De svenska arterna af Trilobitslägtet *Illaenus* (Dalman). *Bihang till Konglungen Svenska Vetenskaps-Akademiens Handlingar*, **7**, i–xiv + 1–148, 6 pls.

— 1886. Revision der ostbaltischen silurischen Trilobiten. Abhandlung III. Die Ostbaltischen Illaeniden. *Mémoirs de Impériale des Sciences de St Pétersbourg*, **33**, 1–173, 12 pls.

HOWELL, B. F. and SANFORD, J. T. 1946. Trilobites from the Silurian Irondequoit formation of New York. *Wagner Free Institute of Science, Bulletin*, **21**, 5–10, 1 pl.

HOWELLS, Y. 1982. Scottish Silurian trilobites. *Palaeontographical Society Monograph*, **135**, 1–76, 15 pls.

HUPÉ, P. 1953. Classe de trilobites. *In* PIVETEAU, J. (ed.). *Traité de paleontologié*, **3**, 44–246, 140 text-figs.

HURST, J. M. 1980. Palaeogeographic and stratigraphic differentiation of Silurian carbonate buildups and biostromes of North Greenland. *The American Association of Petroleum Geologists Bulletin*, **64**, 527**–**548.

— 1984. Upper Ordovician and Silurian carbonate shelf stratigraphy, facies and evolution, eastern North Greenland. *Bulletin Grønlands Geologiske Undersøgelse*, **148**, 1–70.

— and SURLYK, F. 1982. Stratigraphy of the Silurian turbidite sequence of North Greenland. *Bulletin Grønlands Geologiske Undersøgelse*, **145**, 121 pp.

IVANOVA, O., OWENS, R. M., KIM, I. and POPOV, L. E. 2009. Late Silurian trilobites from the Nuratau and Turkestan ranges, Uzbekistan and Tajikistan. *Geobios,* **42**, 715–737.

IVANY, L. C., BRETT, C. E., WALL, H. L. B., WALL, P. D. and HANDLEY, J. C. 2009. Relative taxonomic and ecologic stability in Devonian marine faunas of New York State: a test of coordinated stasis. *Paleobiology,* **35**, 499–524.

JAANUSSON, V. 1954. Zur morphologie und taxonomie der Illaeniden. *Arkiv for Mineralogi och Geologi*, **1**, 545–583, 3 pls.

JELL, P. A. and ADRAIN, J. M. 2003. Available generic names for trilobites. *Memoirs of the Queensland Museum*, **48**, 331–553.

KAESLER, R. L. (ed.) 1997. *Treatise on invertebrate paleontology. Part O. Arthropoda 1. Trilobita, revised*. Geological Society of America, Boulder, Colorado and University of Kansas Press, Lawrence, Kansas. xxiv + 530 pp.

KEGEL, W. 1927. Über obersilurische Trilobiten aus dem Harz und dem Rheinischen Schiefergebirge. *Jahrbuch der Preussischen Geologischen landesanstalt und Bergakademie zu Berlin*, **48**, 616–647, pls 31–32.

KIDWELL, S. M. 1993. Patterns of time-averaging in the shallow marine fossil record. *In* KIDWELL, S. M. and BEHRENSMEYER, A. K. (eds.) *Taphonomic approaches to time resolution in fossil assemblages.* Short Courses in Palaeontology, **6**, pp. 275–300.

KJERULF, R. 1865. Veiviser ved geologisker Excursioner I Christiania Omegn. *Universitets-program seminar,* **2**, 43 pp.

LAMONT, A. 1948. Scottish dragons. *Quarry Managers' Journal*, **31**, 531–535.

LANE, P. D. 1971. British Cheiruridae (Trilobita). *Palaeontographical Society Monograph*, **125**, 1–95, 16 pls.

— 1972. New trilobites from the Silurian of north-east Greenland, with a note on trilobite faunas in pure limestones. *Palaeontology*, **15**, 336–364.

— 1979. Llandovery trilobites from Washington Land, North Greenland. *Bulletin Grønlands Geologiske Undersøgelse*, **131**, 1–37, 6 pls.

— 1984. Silurian trilobites from Hall Land and Nyeboe Land, western North Greenland. *Rapports Grønlands Geologiske Undersøgelse*, **121**, 51–73, 4 pls.

— 1988. Silurian trilobites from Peary Land, central North Greenland. *Rapports Grønlands Geologiske Undersøgelse*, **137**, 93–117.

— and OWENS, R. M. 1982. Silurian trilobites from Kap Schuchert, Washington Land, western North Greenland. *Rapports Grønlands Geologiske Undersøgelse*, **107**, 41–69, pls 1–5.

— and SIVETER, D. J. 1991. A Silurian trilobite fauna dominated by *Calymene* from Kap Tyson, Hall Land, western North Greenland. *Rapports Grønlands Geologiske Undersøgelse*, **150**, 5–14, 2 pls.

— and THOMAS, A. T. 1978. Silurian trilobites from NE Queensland and the classification of effaced trilobites. *Geological Magazine*, **115**, 351–358.

— and **—** 1979. Silurian carbonate mounds in Peary Land, north Greenland. *Rapports Grønlands Geologiske Undersøgelse*, **88**, 51–54.

— and **—** 1983. A review of the trilobite suborder Scutelluinae. *In* BRIGGS, D. E. G. and LANE, P. D. (eds). *Trilobites and other early arthropods*. Papers in honour of Professor H. B. Whittington. F. R. S. Special Papers in Palaeontology, **30**, 141-160.

LASK, P. B. 1993. The hydrodynamic behaviour of sclerites from *Flexicalymene meeki*. *Palaios*, **8**, 219–225.

LIGHTY, R. G. 1985. Preservation of internal reef porosity and diagenetic sealing of submerged early Holocene Barrier Reef, southeast Florida shelf. *In*

SCHNEIDERMANN, N. and HARRIS, P. M. (eds.) *Carbonate cements.* Society of Economic Paleontologists and Mineralogists Special Publication, **36**, pp. 123–151.

LINDSTRÖM, G. 1885. Förteckning på Gotlands Siluriska Crustacéer. *Öfversigt af Konglungen Vetenskaps Akademiens Förhandlingar Stockholm*, **6**, 37–100, pls 12–16.

LUCAS, K. J. 1979. The effects of marine microphytes on carbonate substrata. *SEM*, **11**, 447–456.

LUDVIGSEN, R. 1979. Fossils of Ontario, Part 1: The Trilobites. *Royal Ontario Museum, Life Sciences Miscellaneous Publications*, 1–96.

— and CHATTERTON, B. D. E. 1980. The ontogeny of *Failleana* and the origin of the Bumastinae (Trilobita). *Geological Magazine*, **117**, 471–478.

— and TRIPP, R. P. 1990. Silurian trilobites from the northern Yukon Territory. *Royal Ontario Museum, Life Sciences Contributions*, **153**, 1–59.

LÜTKE, F. 1990. Contributions to a phylogenetical classification of the subfamily Proetinae Salter, 1864 (Trilobita). *Senckenbergiana lethaea*, **71**, 1–83.

MABILLARD, J. E. 1980. Silurian carbonate mounds of south-east Peary Land, eastern North Greenland. *Rapports Grønlands Geologiske Undersøgelse*, **99**, 57–60.

MACINTYRE, I. G. 1984. Extensive submarine lithification in a cave in the Belize barrier reef platform. *Journal of Sedimentary Petrology*, **54**, 221–235.

— 1985. Submarine cements - the peloidal question. *In* SCHNEIDERMANN, N. and HARRIS, P. M. (eds.) *Carbonate cements.* Society of Economic Paleontologists and Mineralogists Special Publication, **36**, pp. 109–116.

MACNIOCAILL, C., VAN DER PLUIJM, B.A. and VAN DER VOO, R. 1997. Ordovician paleogeography and the evolution of the Iapetus Ocean. *Geology*, **25**, 159–162.

MÄNNIL, R. 1982a. Wenlock and late Silurian trilobite associations of the east Baltic area and their stratigraphical value. 63–70. *In* KALJO, D. and KLAAMANN, E. (eds) *Ecostratigraphy of the East Baltic Silurian,* Academy of Sciences of the Estonian S. S. R., Tallinn.

— 1982b. Trilobite communities (Wenlock, East Baltic). 51–62. *In* KALJO, D. L. and KLAAMANN, E. (eds) *Communities and biozones in the Baltic Silurian,* Academy of Sciences of the Estonian S. S. R., Tallinn.

MAYR, U., 1976. Middle Silurian reefs in southern Peary Land, North Greenland. *Bulletin of Canadian Petroleum Geology*, **24**, 440–449.

MIKULIC, D. G. 1979. *The paleoecology of Silurian trilobites with a section of the Silurian stratigraphy of southeastern Wisconsin*. Unpublished Ph.D. dissertation, Oregon State University, Corvallis, 864 pp.

— 1981. Trilobites in Palaeozoic carbonate buildups. *Lethaia,* **14**, 45–56.

— 1983. *Hydrodynamic control of localized trilobite and cephalopod accumulations in Silurian carbonate buildups.* Geological Society of America 96th Annual Meeting, Abstracts with programs, **15**, p. 644.

— 1990. The arthropod fossil record: biologic and taphonomic controls on its composition. *In* CULVER, S. J. (ed.) *Arthropod Paleobiology: Short courses in Paleontology,* **3**, pp. 1–23.

— 1999. Silurian trilobite associations in North America. 793–798. *In* BOUCOT, A. J. and LAWSON, J. D. (eds) *Paleocommunities: A case study from the Silurian and Lower Devonian*. Cambridge University Press.

MONTY, C. L. V. 1995. The rise and nature of carbonate mud-mounds: an introductory actualistic approach, in: MONTY, C. L. V., BOSENCE, D. W. J., BRIDGES, P. H. and PRATT, B. R. (eds.) *Carbonate mud-mounds: their origin and*

evolution. Special Publication of the International Association of Sedimentologists, **23**, Blackwell, pp. 11–48.

MOORE, R. C. 1959. *Treatise on invertebrate paleontology. Part O. Arthropoda 1.* Geological Society of America, Boulder, Colorado and University of Kansas Press, Lawrence, Kansas. xix + 560 pp.

MURCHISON, R. I. 1839. *The Silurian System, founded on geological researches in the counties of Salop, Hereford, Radnor, Montgomery, Caermarthen, Brecon, Pembroke, Monmouth, Gloucester, Worcester and Stafford; with descriptions of the coalfields and overlying formations*, xxxii + 768 pp., 37 pls. London.

— 1854. *Siluria. The history of the oldestv known rocks containing organic remains, with a brief sketch of the distribution of gold over the Earth, x*vi + 523 pp., 37 pls. London.

— 1859. *Siluria. The history of the oldest known rocks and their foundations, with a brief sketch of the distribution of gold over the Earth.* 3rd edition, x + 592 pp., 41 pls.

— 1867. *Siluria. A history of the oldest rocks in the British Isles and other countries; with sketches of the origin and distribution of native gold, the general succession of geological formations, and the changes of the Earth's surface.* 4th Edition, xviii + 566 pp., 41 pls.

— 1872. *Siluria. A history of the oldest rocks in the British Isles and other countries; with sketches of the origin and distribution of native gold, the general succession of geological formations, and the changes of the Earth's surface.* 5th Edition, xviii + 566 pp., 41 pls.

NIXON, K.C. 2002. Winclada, version 1.00.08. Software available online at: http://www.cladistics.com

NORFORD, B. S. 1973. Lower Silurian species of the trilobite *Scotoharpes* from Canada and Northwestern Greenland. *Geological Survey of Canada, Bulletin*, **479**, 13–47.

— 1981. The trilobite fauna of the Attawapiskat Formation, northern Ontario and northern Manitoba. *Geological Survey of Canada, Bulletin*, **327**, 1–37.

— 1994. Biostratigraphy and trilobite fauna of the Lower Silurian Tegart Formation, southeastern British Columbia. *Geological Survey of Canada, Bulletin*, **479**, 13–47.

NORTHROP, S. A. 1939. Paleontology and stratigraphy of the Silurian rocks of the Port Daniel-Black Cape region, Gaspé. *Geological Society of America, Special Paper*, **21**, 1–302.

OGG, J. G., OGG, G. and GRADSTEIN. 2008. *The concise geologic time scale*. Cambridge.

OLSZEWSKI, T. D. and ERWIN, D. H. 2009. Change and stability in Permian brachiopod communities from western Texas. *Palaios*, **24**, 27–40.

— and PATZKOWSKY, M. E. 2001. Measuring recurrence of marine biotic gradients: A case study from the Pennsylvanian-Permian Midcontinent. *Palaios*, **16**, 444–460.

ÖPIK, A. A. 1937. Trilobiten aus Estland. *Acta et Commentationes Universitatis Tartuensis, A*, **32**, 1–163.

ORMISTON, A. R. 1967. Lower and middle Devonian trilobites of the Canadian Arctic Islands. *Bulletin of the Geological Survey of Canada*, **153**, 1–148, 17 pls.

OSMÓLSKA, H. 1957. Trilobites from the Couvinian of Wydryszów (Holy Cross Mountains, Poland). *Acta Palaeontologica Polonica*, **2**, 53–77, 3 pls.

— 1970. Revision of non-cyrtosymbolinid trilobites from the Tournaisian-Namurian of Eurasia. *Palaeontologica Polonica*, **23**, 1–165, 22 pls.

OVER, D. J. and CHATTERTON, B. D. E. 1987. Silurian conodonts from the southern Mackenzie Mountains, Northwest Territories, Canada. *Geologica et Paleontologica*, **21**, 1–49.

OWEN, A. W. 1981. The Ashgill trilobites of the Oslo Region, Norway. *Palaeontogrphica, A,* **175**, 1–88, 17 pls.

OWENS, R. M. 1973*a*. British Ordovician and Silurian Proetidae (Trilobita). *Palaeontographical Society Monograph*, **127**, 1–98, 15 pls.

— 1973*b*. Ordovician Proetidae (Trilobita) from Scandinavia. *Norsk Geologisk Tidsskrift*, **53**, 117–81.

— 1974. The affinities of the trilobite genus *Scharyia*, with a description of two new species. *Palaeontology*, **17**, 685–697.

— 1979. The trilobite genera *Panarchaeogonus* Öpik, *Isbergia* Warburg and *Cyamops* gen. nov. from the Ordovician of Balto-Scandia and the British Isles. *Norsk Geologisk Tidsskrift,* **58**, 199–219.

— 1990. Carboniferous trilobites: the beginning of the end. *Geology Today,* May-June 1990, 96–100.

— 2006. The proetid trilobite *Hedstroemia* and related Ordovician to Carboniferous taxa. 119–143. *In* BASSETT, M. G. and DEISLER, V. K. (eds). *Studies in Palaeozoic palaeontology*. National Museum of Wales Geological Series No. 25, Cardiff.

— and FORTEY, R. A. 2009. Silicified Upper Ordovician trilobites from Pai-Khoi, Arctic Russia. *Palaeontology*, **52**, 1209-1220, 2 pls.

— and HAMMANN, W. 1990. Proetide trilobites from the Cystoid Limestone (Ashgill) of NW Spain, and the suprageneric classification of related forms. *Paläontologische Zeitschrift*, **64**, 221–244.

— and THOMAS, A. T. 1975. *Radnoria*, a new Silurian proetacean trilobite, and the origins of the Brachymetopidae. *Palaeontology*, **18**, 809–822, pls 95–96.

PAGE, R. D. M. 2001. Nexus Data Editor, version 0.5.0. Software available online at: http://taxonomy.zoology.gla.ac.uk/rod/ NDE/nde.html

PATERSON, J. R., JAGO, J. B., BROCK, G. A. and GEHLING, J. G. 2007. Taphonomy and palaeoecology of the emuellid trilobite *Balcoracania dailyi* (early Cambrian, South Australia). *Palaeogeography, Palaeoclimatology, Palaeoecology*, **249**, 302–321.

PEEL, J. S. and SØNDERHOLM, M. (eds). 1991. Sedimentary basins of North Greenland. *Bulletin Grønlands Geologiske Undersøgelse*, **160**, 164 pp.

PENG, S. 1990. Trilobites from the Panjiazui Formation and the Madaoyu Formation in Jiangnan Slope Belt. *Beringeria*, **2**, 55–171.

PERRY, C. T. 1999. Biofilm-related calcification, sediment trapping and constructive micrite envelopes: a criterion of ancient grass-bed environments? *Sedimentology*, **46**, 33–46.

— and SMITHERS, S. G. 2006. Taphonomic signatures of turbid-zone reef development: Examples from Paluma Shoals and Lugger Shoal, inshore central Great Barrier Reef, Australia. *Palaeogeography, Palaeoclimatology, Palaeoecology*, **242**, 1–20.

PERRY, D. G. and CHATTERTON, B. D. E. 1977. Silurian (Wenlockian) trilobites from Baille-Hamilton Island, Canadian Arctic Archipelgo. *Canadian Journal of Earth Sciences*, **14**, 285–317.

PHLEGER, F. B. 1936. Lichadian trilobites. *Journal of Paleontology*. **10**, 593–615.

PILLET. J. 1972. Les trilobites du Dévonien inferieur et du Dévonien moyen du Sud-Est du Massif Amoricain. *Mémoire du Société d' étude scientifique de l'Anjou*, **1**, 1–307, 64 pls.

POULSEN, C. 1934. The Silurian faunas of North Greenland, I. The fauna of the Cape Schuchert Formation. *Meddeleser om Grønland*, **72**, 1–47.

PRANTL, F. and PŘIBYL, A. 1949. O nových nebo málo známých trilobitech českého ordoviku. *Rozpravy České Akademie Věd a Umění, Třida 2*, **58**, 1–22.

— and **—** 1951. A revision of the Bohemian representatives of the Family Otarionidae R. and E. Richter (Trilobitae). *Sborník Státního geologického ústavu Československé Republiky, oddíl paleontologicky*, **17** (for 1950), 353–512. [in Czech and English, with Russian summary]

PRATT, B. R. 1982. Stromatolitic framework of carbonate mud mounds. *Journal of Sedimentary Petrology*, **52**, 1203–1227.

PŘIBYL, A. 1946a. Příspěvek k poznání českých Proetidů. *Rozpravy České akademie věd a umění, tř. 2*, [Notes on the recognition of the Bohemian Proetidae]. **55**, 1–37. Prague.

— 1946b. O několika nových trilobitových rodech z českého siluru a devonu. *Příroda*, **38**, 89–95, 7 figs.

— and VANĚK, J. 1971. Studie über die famille Scutelluida Richter et Richter (Trilobita) und ihre phyllogenetische Entwicklung. *Acta Universitatis Carolinae, Geologica*, **4**, 361–394.

— and **—** 1978. Studie zu einigen neuen trilobiten der Proetidae-familie. *Acta Universitatis Carolinae, Geologica*, **1–2**, 163–182.

RAMSKÖLD, L. 1983. Silurian cheirurid triloites from Gotland. *Palaeontology*, **26**, 175–210, pls 19–28.

— 1984. Silurian odontopleurid trilobites from Gotland. *Palaeontology*, **27**, 239–264, pls. 26–31.

— 1986. Silurian encrinurid trilobites from Gotland and Dalarna, Sweden. *Palaeontology*, **29**, 527–575.

RATCLIFFE, K. T. 1988. Oncoids as environmental indicators in the Much Wenlock Limestone Formation of the English Midlands. *Journal of the Geological Society London*, **145**, 117–124.

RAY, D. C. and THOMAS, A. T. 2007. Carbonate depositional environments, sequence stratigraphy and exceptional skeletal preservation in the Much Wenlock Limestone Formation (Silurian) of Dudley, England. *Palaeontology*, **50**, 197–222.

RAYMOND, P. E. 1916. New and old Silurian trilobites from south-eastern Wisconsin, with notes on the genera of the Illaenidae. *Bulletin of the Museum of Comparative Zoology, Harvard*, **60**, 1–41.

— 1925. Some trilobites of the lower Middle Ordovician of eastern North America. *Bulletin of the Museum of Comparative Zoology at Harvard College*, **67**, 1–180.

REED, F. R. C. 1902. Notes on the genus *Lichas. Quarterly Journal of the Geological Society, London*, **58**, 59–82.

— 1931. The Lower Palaeozoic trilobites of Girvan. Supplement No 2. *Palaeontographical Society Monograph*, 1–30.

— 1935. The Lower Palaeozoic trilobites of Girvan. Supplement No 3. *Palaeontographical Society Monograph*, **89**, 1–64, 4 pls.

—1941. A new genus of trilobites and other fossils from Girvan. *Geological Magazine*, **78**, 268–78, pl. 5.

REITNER, J. and NEUWEILER, F. C. 1995. Mud mounds: a polygenetic spectrum of fine-grained carbonate buildups. *Facies*, **32**, 1–70.

RICHTER, R. and RICHTER, E. 1925. Unterlagen zur Fossilium Catalogus, Trilobita II. *Senckenbergiana*, **7**, 126.

— and **—** 1949. Die Trilobiten der Erbach-Zone (Kulm) im Rheinischen Schiefergebirge und im Harze. I. Die Gattung *Phillibole*. *Senckenbergiana*, **30**, 63–94.

— and **—** 1955. Scutelluidae n. n. (Tril.) durch 'kleine Änderung' eines Familien-Namens wegen Homonymie. *Senckenbergiana lethaea,* **36**, 291–293.

RIDING, R. 1992. Temporal variation in calcification in marine cyanobacteria. *Journal of the Geological Society London,* **149**, 979–989.

SALTER, J. W. 1848. *In* PHILLIPS, J. and SALTER, J. W. Palaeontological appendix to Professor John Phillips' memoir on the Malvern Hills, compared with the Palaeozoic districts of Abberley, and c. *Memoirs of the Geological Survey of the United Kingdom*, **2**, viii–xiv + 331–386, pls 4–30.

— 1849. Figures and descriptions illustrative of British organic remains. *Memoirs of the Geological Survey of the United Kingdom*, decade 2, vi + 10 pls.

— 1853. Figures and descriptions illustrative of British organic remains. *Memoirs of the Geological Survey of the United Kingdom*, decade 7, 10 pls.

— 1857. On two Silurian species of *Acidaspis*, from Shropshire. *Quarterly Journal of the Geological Society of London*, **13**, 210–211, pl. 6, figs 15–17.

— 1864a. Figures and descriptions illustrative of British organic remains. *Memoirs of the Geological Survey of the United Kingdom*, decade 11, 9 pls.

— 1864b–1883. A monograph of the British trilobites from the Cambrian, Silurian and Devonian formations. *Palaeontographical Society Monographs*, **1** 1864, 1–80, pls 1–6; **2**, 1865, 81–128, pls 7–14; **3**, 1866, 129–176, pls 15–25; **4**, 1867, 177–214, 25–30; **5**, 1883, 215–224.

— 1868. *Homalonotus johannis* (Salter) (A local and rare species of trilobite from Usk, Monmouthshire). *Transactions of the Woolhope Naturalists Field Club,* 241–2, fossil sketch 5.

SANDFORD, A.C. and HOLLOWAY, D.J. 2006. Early Silurian phacopide trilobites from central Victoria. *Australia Memoirs of Museum Victoria,* **63**, 215–255.

SAVAGE, T. E. and VAN TUYL, F. M. 1919. Geololgy and stratigraphy of the area of Paleozoic rocks in the vicinity of Hudson and James Bays. *Geological Society of America, Bulletin*, **30**, 339–377.

SCHMID, D. U., REINHOLD, R. L. and NOSE, N. 2001. Growth dynamics and ecology of Upper Jurassic mounds, with comparisons to Mid-Palaeozoic mounds. *Sedimentary Geology*, **145**, 343–376.

SCOTESE, C. R. 2002. http://www.scotese.com (PALEOMAP website).

— and MCKERROW, W. S. 1990. Revised world maps and introduction. 1–21. *In* MCKERROW, W. S. and SCOTESE, C. R. (eds) *Palaeozoic Palaeogeography and Biogeography*. Geological Society of London Memoir, **12**.

SHI, G. R. 1993. Multivariate data analysis in palaeoecology and Palaeobiology – a review. *Palaeogeography, Palaeoclimatology, Palaeoecology,* **105**, 199–234.

SHIRLEY, J. 1933. A redescription of the known British Silurian species of *Calymene* (s.l.). *Memoirs and Proceedings of the Manchester Literary and Philosophical Society*, **77**, 5–67.

SIVETER, D. J. 1985. The type species of *Calymene* (Trilobita) from the Silurian of Dudley, England. *Palaeontology*, **28,** 783–792.

SMITH, M. P., RASMUSSEN, J. A., HIGGINS, A. K. and LESLIE, A. G. 2004. Lower Palaeozoic stratigraphy of the East Greenland Caledonides. *Geological Survey of Denmark and Greenland Bulletin*, **6**, 5–28.

— and RASMUSSEN, J. A. 2008. Cambrian-Silurian development of the Laurentian margin of the Iapetus Ocean in Greenland and related areas. 137–167. *In* HIGGINS, A. K., GILOTTI, J. A. and SMITH, M. P. (eds) *The Greenland Caledonides: evolution of the northeast margin of Laurentia.* Geological Society of America Memoir, **202**.

ŠNAJDR, M. 1958. Trilobiti českého středního kambria [The Trilobites of the Middle Cambrian of Bohemia]. *Rozpravy Ústředního ústavu geologického,* **24**, 1–236 [Czech], 237–280 [English], 46 pls.

— 1960. Studie o čeledi Scutelluidae (Trilobitae) [A study of the family Scutelluidae (Trilobita)]. *Rozpravy Ústředního ústavu geologického,* **26**, 1–221 [Czech], 223–265 [English], 36 pls.

— 1977. New genera of Proetidae (Trilobita) from the Barrandian, Bohemia. *Věstník Ústředního ústavu geologického*, **52**, 293–297 [in Czech].

— 1978. The Llandoverian trilobites from Hskov (Barrandian area). *Sbornik geologickych ved, Palaeontologie*, **21**, 7–47.

— 1980. Bohemian Silurian and Devonian Proetidae (Trilobita). *Rozpravy Ústředního Ústavu Geologického*, **45**, 1–324, 64 pls [in Czech].

SØNDERHOLM, M. and HARLAND, T. L. 1989. Franklinian reef belt, Silurian, North Greenland. 263–270. *In* GELDSETZER, H. H. J., JAMES, N. P. and TEBBUTT, G. E. (eds) *Reefs, Canada and adjacent areas.* Canadian Society of Petroleum Geologists Memoir, **13**.

—, —, DUE, P. H., JØRGENSEN, L. N., PEEL, J. S. 1987. Lithostratigraphy and depositional history of Upper Ordovician–Silurian shelf carbonates in central and western North Greenland. *Rapports Grønlands Geologiske Undersøgelse*, **133**, 27–40.

SPEYER, S.E., 1987. Comparative taphonomy and paleoecology of trilobite lagerstätten. Alcheringa 11, 205–232.

— 1991. Trilobite taphonomy: a basis for comparative studies of arthropod preservation, functional anatomy and behaviour. *In* DONOVAN, S. K. (ed.) *The processes of fossilization.* Belhaven Press, London, pp. 194–219.

— and BRETT, C. E. 1986. Trilobite taphonomy and Middle Devonian taphofacies. *Palaios,* **1**, 312–327.

STEININGER, J. 1831. Observations sur les fossiles du Calcaire intermédiare de l'Eifel. *Mémoirs de Societé géologique de la France,* **1**, 331–71, pls 21–23.

STRUSZ, D. L. 1980. The Encrinuridae and related trilobite families, with a description of Silurian species from southestern Australia. *Palaeontographica, A,* **168**, 1–68.

STUBBLEFIELD, C. J. 1936. Cephalic sutures and their bearing on current classifications of trilobites. *Biological Review,* **11**, 407–440.

SUN, S. Q. and WRIGHT, V. P. 1998. Controls on reservoir quality of an Upper Jurassic reef mound in the Palmers Wood field area, Weald basin, south England. *American Association of Petrolium Geology Bulletin,* **82**, 497–515.

SUZUKI, Y. and BERGSTRÖM, J. 1999. Trilobite taphonomy and ecology in Upper Ordovician carbonate build-ups in Dalarna, Sweden. *Lethaia*, **32**, 159–172.

SWINNERTON, H. H. 1915. Suggestions for a revised classification of trilobites. *Geological Magazine*, **6**, 487–496, 538–545.

TEICHERT, C. 1937. Ordovician and Silurian faunas from Arctic Canada. Report of the fifth Thule Expedition 1921-24, The Danish expedition to Arctic North America in charge of Knud Rasmussen, Vol. I, No. 5. *Gyldendalske Boghandel, Nordisk Forlag*, 24 pls. Copenhagen.

TEXTORIS, D. A. and CAROZZI, A. V. 1964. Petrography and evolution of Niagaran (Silurian) reefs. Indiana. *American Association of Petroleum Geology Bulletin,* **48**, 397–426.

THOMAS, A. T. 1978. British Wenlock trilobites. *Palaeontographical Society Monograph*, **1**, 1–56, 14 pls.

— 1979. Trilobite associations in the British Wenlock. 447–451. *In* HARRIS, A. L., HOLLAND, C. H. and LEAKE, B. E. (eds) *The Caledonides of the British Isles – Reviewed*. Geological Society of London.

— 1981. British Wenlock trilobites. Part 2. *Palaeontographical Society Monograph*, **134**, 57–99.

— 1994. Silurian trilobites from the G. B. Schley Fjord region, eastern Peary Land, North Greenland. *Rapports Grønlands Geologiske Undersøgelse,* **164**, 29**–**35.

— and HOLLOWAY, D. J. 1988. Classification and phylogeny of the trilobite order Lichida. *Philosophical Transactions of the Royal Society of London,* **321**, 179–262.

— and LANE, P. D., 1999. Trilobite assemblages of the North Atlantic region. 444–457. *In* BOUCOT, A. J., LAWSON, J. D. (eds) *Paleocommunities: A case study from the Silurian and Lower Devonian*. Cambridge University Press.

TOMAŠOVÝCH, A. and KIDWELL, S. M. 2009. Preservation of spatial and environmental gradients by death assemblages. *Paleobiology*, **35**, 119–145.

TORSVIK, T. H., SMETHURST, M. A., MEERT, J. G., VAN DER VOO, R., MCKERROW, W. S., BRASIER, M. D., STUART, B. A. and WALDERHAUG, H. J. 1996. Continental break-up and collision in the Neoproterozoic and Palaeozoic – a tale of Baltica and Laurentia. *Earth Science Reviews,* **40**, 229–258.

VOGDES, A. W. 1890. A bibliography of the Paleozoic crustacea from 1698 to 1889. *Bulletin of the U.S. geological Survey*, **63**, 1–177.

WARBURG, E. 1925. The trilobites of the Leptaena Limestone in Dalarne. *Bulletin of the Geological Institution of the University of Uppsala,* **17**, 1–446, 11 pls.

WARDER, J. A. 1838. New trilobites. *American Journal of Earth Science,* **34**, 377–380.

WEBB, G. E. 2001. Biologically induced carbonate precipitation in reefs through time. *In* STANLEY, G. (ed.) *The History and Sedimentology of Ancient Reef Systems.* Topics in Geobiology, **17**. New York, Kluwer Academic/Plenum Publishers, pp. 159–203.

WEBSTER, M. 2009. Ontogeny, systematics, and evolution of the effaced Early Cambrian trilobites *Peachella* Walcott, 1910 and *Eopeachella* new genus (Olenelloidea). *Journal of Paleontology*, **83**, 197–218.

WELLER, S. 1907. The paleontology of the Niagaran Limestone in the Chicago area. The Trilobita. *Bulletin of Chicago Academic Science*, **4**, 163–128, pls 16–25.

WESTROP, S. R. 1986. Taphonomic versus ecologic controls on taxonomic relative abundance patterns in tempestites. *Lethaia*, **19**, 123–132.

— and RUDKIN, D. M. 1999. Trilobite taphonomy of a Silurian reef: Attawapiskat Formation, Northern Ontario. *Palaios*, **14**, 389–397.

WHITEAVES, J. F. 1904. Preliminary list of fossils from the Silurian (Upper Silurian) rocks of the Ekwan River, and Sutton Mill Lakes, Keewatin, collected by D. B. Dowling in 1901, with description of such species as appear to be new. *Geological Survey of Canada, Annual Report,* **14**, p. 38F–59F.

— 1906. The fossils of the Silurian (Upper Silurian) rocks of the Keewatin, Manitoba, the north eastern shore of Lake Winnipegosis, and the lower Saskatchewan River. *Geological Survey of Canada, Palaeozoic Fossils*, **3**, 243–298.

WHITFIELD, R. P. 1882. Palaeontology; in Geology of Wisconsin. *Wisconsin Geological Survey*, **4**, p. 161–363.

— 1999. Siluro-Devonian Scutelluinae (Trilobita) from the Czech Republic: morphology and classification. *Journal of paleontology*, **73**, 414–430.

— and CAMPBELL, K. S. W. 1967. Silicified Silurian trilobites from Maine. *Bulletin of Comparative Zoology at Harvard College*, **135**, 447–482.

— and EVITT, W. R. 1954. Silicified Middle Ordovician trilobites. *Memoirs of the Geological Society of America*, **59**, 1–137, 33 pls.

WHITTINGTON, H. B. 1950. Sixteen Ordovician genotype trilobites. *Journal of Paleontology*, **24**, 531–565, pls. 68–75.

— 1963. Middle Ordovician trilobites from Lower Head, Western Newfoundland. *Bulletin of the Museum of Comparative Anatomy, Harvard*, **129**, 1–118.

— 1997. Illaenidae (Trilobita): Morphology of thorax, classification, and mode of life. *Journal of Paleontology*, **71**, 878–896.

— 1999. Siluro-Devonian Scutelluinae (Trilobita) from the Czech republic: morphology and classification. *Journal of Paleontology*, **73**, 414–430.

— 2000. *Stygina, Eobronteus* (Ordovician Styginidae, Trilobita): morphology, classification, and affinities of Illaenidae. *Journal of Paleontology*, **74**, 879–8.

WOLF, K. H. 1965. Littoral environments, indicated by open-space structures in algal limestones. *Palaeogeography, Palaeoclimatology, Palaeoecology*, **1**, 183–223.

WOOD, R. A., DICKSON, J. A. D. and KIRKLAND, B. L. 1996. New observations on the ecology of the Permian Capitan Reef, Texas and New Mexico. *Palaeontology*, **39**, 733–762.